[This blank, unnumbered page will be the back of your front cover]

Technical Report Document Page

1. Report No.	2. Government Accession No.	3. Recipient's Catalog No.
4. Title and Subtitle Improved Load Rating Procedures for Deteriorated Unstiffened Steel Beam Ends Deliverable 1: Identification of common unstiffened steel beam-end corrosion topologies		5. Report Date August, 2021 6. Performing Organization Code
7. Author(s) Aidan Provost, Anderson Pires, George Tzortzinis, Simos Gerasimidis, Sergio Brena		8. Performing Organization Report No.
9. Performing Organization Name and Address University of Massachusetts Amherst UMass Transportation Center 130 Natural Resources Way Amherst, MA 01003		10. Work Unit No. (TRAIS) 11. Contract or Grant No.
12. Sponsoring Agency Name and Address New England Transportation Consortium		13. Type of Report and Period 14. Sponsoring Agency Code n/a
15. Supplementary Notes		
16. Abstract This report contains the information regarding the first task of an ongoing project aiming to enhance load rating methods for assessing corroded unstiffened beam ends for the six New England States. The first task of the project aims to collect and compile the information provided by DOTs within New England. Within this task, based on reports provided by the DOTs, the most common corrosion patterns were identified. From the information collected, the research team was able to carefully identify trends and patterns in the data, which allowed the research team to determine the most common scenarios of corrosion encountered in bridges within New England States.		
17. Key Word	18. Distribution Statement	

19. Security Classif. (of this report)	20. Security Classif. (of this page)	21. No. of	22. Price
unclassified	unclassified		n/a

This page left blank intentionally.

Improved Load Rating Procedures for Deteriorated Unstiffened Steel Beam Ends

Deliverable 1: Identification of common unstiffened steel beam-end corrosion topologies

Prepared By:

Aidan Provost
Graduate Researcher
aqprovost@umass.edu

Anderson Pires
Graduate Researcher
avpires@umass.edu

George Tzortzinis
Graduate Researcher
gtzortzinis@umass.edu

Simos Gerasimidis, Ph.D.
Principal Investigator
sgerasimidis@umass.edu

Sergio Breña, Ph.D.
Co-Principal Investigator
brena@umass.edu

University of Massachusetts Amherst,
130 Natural Resources Way, Amherst, MA 01003

Prepared For:
New England Transportation Consortium
August 2021

This page left blank intentionally.

Disclaimer

This page left blank intentionally.

Table of Contents

This page left blank intentionally.

List of Figures

This page left blank intentionally.

List of Tables

This page left blank intentionally.

1. Introduction

Across the world, and the United States in particular, the transportation network is utilized to transport people and goods efficiently and effectively. When considering transportation systems, these encapsulate roads, bridges, tunnels and even waterways. Thus, transportation systems are an imperative and foundational network of our society and our world.

While transportation systems serve most of the nations' population, [1] points out that 7.5% of the bridges in the U.S. are structurally deficient. In absolute terms, this means that roughly 46,000 bridges in the U.S. need constant attention and/or repairs. This number is only expected to grow in the coming years, as our nation's infrastructure continues to age and deteriorate.

When considering steel bridges, corrosion represents a major source of deterioration particularly in coastal regions or in areas where deicing chemicals are used and may result in the loss of serviceability of affected bridges. Corrosion can occur anywhere on the steel bridge beams, but the area of interest for this study is the beam end. Beam ends are critical to the structural system, as damage to them significantly reduces the capacity of the whole beam. In extreme cases, corrosion can lead to the failure or closing of a bridge. For this reason, determining an estimate of remaining capacity via laboratory tests of the beams and structural system is a crucial task. Conducting these tests ultimately help us understand and assure the safety of other bridge systems. Additionally, corrosion can often cause irregular patterns, thus causing more challenges in the construction of models that predict the remaining capacity of damaged beams ([2]-[22]).

Corrosion is a pressing issue in the New England region specifically. With harsh precipitation and winter temperatures, chemical use is necessary for de-icing roads and bridge structures. As a result of this process, inspectors have been observing increasing corrosion due to de-icing chemicals and water. This project aims to develop tools which can more accurately estimate the remaining capacity of corroded beams in the New England region than those currently available to engineers. To achieve this, the project was divided into 6 tasks, summarized in Table 1:

Table 1: Project Tasks

Task #	Description of work
Task 1	Identify common unstiffened beam-end corrosion topologies
Task 2	Review of existing structures
Task 3	Laboratory testing
Task 4	Calculate and validate/update the new load rating procedures
Task 5	Draft final report, presentation
Task 6	Final report

This report exclusively covers the first task of the project, which is divided into 3 sub-tasks, described in Table 2 below. In general, this first task aims to collect and compile the information provided by state Departments of Transportation (DOTs) of the New England region. Within this task, based on reports provided by the DOTs, the most common shapes and locations of corrosion were identified in bridge beam ends. From the information collected, the research team was able to carefully search for trends and patterns in the data, which gave the team the opportunity to determine the most common scenarios of corrosion.

Table 2: The Sub-tasks of Identifying common unstiffened beam-end corrosion topologies

Sub-task #	Description of work
Task 1.1.	**Collection of Bridge Inspection Reports** Management of a vast quantity of bridge inspection reports provided by the DOTs. Task 1.1 consists of defining a new way to describe the corrosion phenomenon by grouping similar cases. Each group presents several parameters that can fully describe the corrosion.
Task 1.2.	**Summarize Data into Excel Spreadsheets** The data collected in Task 1.1 is to be summarized into Excel spreadsheets, which allows the research team to efficiently store the data from each beam end reported in the bridge inspection reports.
Task 1.3.	**Postprocess Summarized Data** Perform the post-processing of data stored into the Excel spreadsheets in MATLAB. Besides, statistical analysis shall be performed, aiming to detect trends and patterns in the reported data.

1.1. Data Collection

The database available for this project was provided by Departments of Transportation of all states from the New England region. As each state has its own method of reporting data, the specific inspection report processes of each state are discussed in the following section. It is important to note in this data collection process that the project focuses on the corrosion of beam ends whose bridge superstructures NBI ratings were less or equal 5.

1.1.1. Format of data received from the Connecticut Department of Transportation (CTDOT) Inspection reports

According to [23], there are two types of inspection reports for bridge structures in the State of Connecticut: (i) Routine Inspections and (ii) In-depth inspections. Routine inspections are conducted on a biennial basis and aim to identify critical problems or deficiencies so corrections can be made before the structure presents hazards to the public.

For this project, only routine inspections were provided and considered to evaluate corrosion patterns and damage in the bridge beams. Figure 1 depicts an example of a report from CTDOT.

Form: BRI-19, Rev. 2/15
Inspection type: Routine
Inspection Date: 5/21/2019
Inspected by: Infrastructure Engineers

:Bridge No 05158

Town: WASHINGTON
Carried: TUNNEL ROAD
Crossed: SHEPAUG RIVER
Inventory Route: Non-NHS

STRUCTURE INVENTORY & APPRAISAL

INSPECTION

Structurally Deficient	Y	**Functionally Obsolete**	N
Sufficiency Rating	56.6		
(90) Inspection Date	05/21/2019	**(91) Frequency**	24
Indepth Insp	No	**Proposed next Indepth Year**	
Deck Survey Date		**Class**	01
Access	22 - 30-40 ft.reach required	**Flagman**	0

	Frequency	Date	Type
Fracture			
Underwater			
Special			

IDENTIFICATION

Bridge Name	05158
Town Code - Name	79720 - WASHINGTON
(5) Inventory Route	
(A) Record Type	1: Route carried "on" the structure
(B) Signing Prefix	5 - CITY STREET
(C) Level of Service	0 - NONE OF THE BELOW
(D) Route Number.	00000
(E) Dir Suffix	0 - NOT APPLICABLE
(6A) Featured Intersected	SHEPAUG RIVER
(6B) Critical Facility Indicator	
(7) Facility Carried	TUNNEL ROAD
(9) Location	100 FT S OF CHURCH HILL R
(11) Mile Post	0 Miles
(16) Latitude	41 Deg. 37 Min. 18.26 Sec.
(17) Longitude	-73 Deg. 19 Min. 32.62 Sec.
(98) Border Bridge	
(A) State Code	(B) Percent Responsibility %
(C) Border Town Name	
(99) Border Bridge Structure No.	

STRUCTURE TYPE & MATERIALS

(43) Structure Type, Main	
A) Material	3 - Steel
B) Design Type	02 - Stringer/Multi-beam or Girder
(44) Structure Type, Approach	
A) Material	0 - Other
B) Design Type	00 - Other
(45) Number of Spans, Main Unit	003
(46) Number of Approach Spans	0000
(107) Deck Structure Type	1 - Concrete Cast-in-Place
(108) Wearing Surface/Protection Systems	
A) Type of Wearing Surface	6 - Bituminous
B) Type of Membrane	0 - None
C) Type of Deck Protection	0 - None
Substructure	
A) Material	2 - CONCRETE
B) Design Type	2 - STUB ABUTMENT
Paint	
Type	3 - Non-Lead Paint
Year	1956
Comment	Based on visual inspection.

GEOMETRIC DATA

(48) Length of Maximum Span	36 ft.
(49) Structure Length	112 ft.
(50) Curb or Sidewalk Widths	
A) Left	0 ft. 9 in.
B) Right	0 ft. 9 in.
(51) Bridge Roadway Width Curb to Curb	22 ft. 0 in.
(52) Deck Width, Out to Out	25 ft. 6 in.
(32) Approach Roadway Width	24 ft.

Figure 1: Sample of a report provided by CTDOT

Routine inspection reports, in general, are divided into the 11 following sections:

1. Report cover
2. Table of contents
3. Report title page
4. Location map
5. Structure inventory and appraisal (BRI-19)
6. Inventory routes under structure (BRI-25)
7. Inspection Data (BRI-18)

8. National bridge elements
9. Fracture critical data (BRI-12)
10. Sketches
11. Pictures

The first three sections present general information about the report and the bridge structure (e.g., identification number, date of report, company responsible for the inspection report). The "*Location map*" section describes the bridge location, including its latitude and longitude. The "*Structure inventory and appraisal (BRI-19)*" section presents a summary of the NBI ratings, which are imperative to scope of this work. The section "*Inventory routes under structure (BRI-25)*" summarizes information about the route under the bridge. It is important to note that in case the structure is above water, this section is not considered or presented in the inspection report.

The section "*Inspection data (BRI-18)*" denotes specific details and data from the field inspection. This section is of major interest to the project because many reports include comments about the condition of the structure, field measurements, bridge component conditions, and often the corresponding NBI ratings.

The table depicted in section "*National bridge elements*" is required by FHWA [24]. For this reason, all reports present a similar table. Such a table summarizes the condition of several components of the bridge.

The section "*Fracture Critical Data (BRI-12)*" aims to report all fractures encountered in the bridge. Finally, the sections "*Sketches*" and "*Pictures*" report visual information, which complements the notes presented in the "*Inspection data*" section. It is worthwhile pointing out that all pictures are labeled. Often, inspection notes reference pictures so a reader or inspector can fully understand what is being described in the notes.

Much of the corrosion information gathered to meet the goals of this task was found by compiling the notes of Inspection data, sketches, and the pictures. Figure 2 below depicts a corrosion scenario described by a sketch and by a photograph presented in an inspection report from the State of Connecticut.

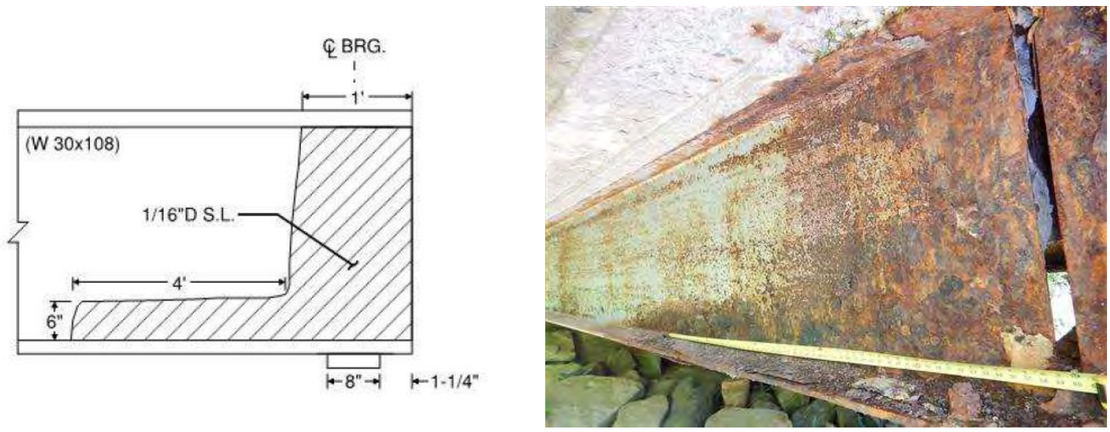

Figure 2: Sketch (Left) and Photography (Right) of corrosion damage

1.1.2. Format of data received from the Maine Department of Transportation (MaineDOT) Inspection reports

Similarly to the State of Connecticut, there are four types of reports collected from the State of Maine (MaineDOT): (i) Routine inspections, (ii) Special inspections, (iii) Underwater inspections, and (iv) Fracture Critical inspections. The routine inspections are conducted on a regular basis, special inspections are conducted on demand, and underwater inspections are often conducted on a 60 month cycle. Fracture Critical inspections are conducted on a 24 month cycle.

The inspection reports from MaineDOT are, in general, organized into the following 5 sections:

1. Report cover
2. National bridge inventory
3. Inspection notes report
4. Element inspection
5. Photos

The "*report cover*" provides general information about the bridge structure and the report. For instance, name and ID of the bridge, as well as the type of inspection can be found in this section. In the section "*National bridge inventory*", shown in Figure 3, the report summarizes the NBI ratings for several items of the bridge. These ratings are of interest to the evaluation of corrosion patterns and severity of damage.

The section "Element inspection" consists of a table which summarizes the condition of several components of the bridge and is required by FHWA. The "*Inspection notes report*" section of the report provides comments and field measurements based on the inspection. Lastly, the section "*Photos*" depicts several photographic records of the bridge under inspection.

Unfortunately, not all reports include field measurements in their reports. This can cause difficulty in the assessment of the impact caused by corrosion. Additionally, the photographs documented include labels but are not referenced in the field notes, which poses a challenge in identifying each part of the structure.

With the goal of increasing the available corrosion damage data for the project, the load ratings were provided by the MaineDOT. Via the load rating data, more information about corrosion is provided and were ultimately used to determine the beam type of each bridge. It was feasible to estimate the section loss in bridge beams by compiling information from the documents provided by MaineDOT.

National Bridge Inventory

Status: 1 - SD   Bridge Name: KENNEDY   Sufficiency Rating: 49.1

Inspections

(90) INSPECTION DATE	& (91) DESIGNATED INSPECTION FREQUENCY	24	04/18/2019
(92) CRITICAL FEATURE INSPECTION	& (93) CFI DATE		
(92A) FRACTURE CRITICAL DETAIL		N	
(92B) UNDERWATER INSPECTION		N	
(92C) OTHER SPECIAL INSPECTION		N	

Identification

(1) STATE CODE	231 - Maine
(8) STRUCTURE NUMBER	0394
(5) INVENTORY ROUTE	
(5A) RECORD TYPE	1: Route carried "on" the structure
(5B) ROUTE SIGNING PREFIX	5 - CITY STREET
(5C) DESIGNATED LEVEL OF SERVICE	0 - None
(5) INVENTORY ROUTE	0
(5) INVENTORY ROUTE	0 - NOT APPLICABLE
(2) HIGHWAY AGENCY DISTRICT	03 - Western
(3) COUNTY CODE	007 Franklin
(4) PLACE CODE	81300
(6) FEATURES INTERSECTED	HOUGHTON BROOK
(7) FACILITY CARRIED	TEMPLE RD
(9) LOCATION	0.8 MI E RTE 156
(11) MILEPOINT	1.300
(12) BASE HIGHWAY NETWORK	Inventory Route is not on the Base Network
(13) LRS INVENTORY ROUTE, SUBROUTE	
(13A) LRS INVENTORY ROUTE	0000701105
(13B) SUBROUTE NUMBER	00
(16) LATITUDE	44.70501
(17) LONGITUDE	-70.39612
(98A) BORDER BRIDGE CODE	
(98B) PERCENT RESPONSIBILITY	0
(99) BORDER BRIDGE STRUCT NO.	

Structure Type and Material

(43) STRUCTURE TYPE, MAIN	
(43A) KIND OF MATERIAL/DESIGN	3 - Steel
(43B) TYPE OF DESIGN/CONSTR	02 - Stringer/Multi-beam or Girder
(44) STRUCTURE TYPE, APPROACH SPANS	
(44A) KIND OF MATERIAL/DESIGN	0 - Other
(44B) TYPE OF DESIGN/CONSTRUCTION	00 - Other
(45) NUMBER OF SPANS IN MAIN UNIT	1
(46) NUMBER OF APPROACH SPANS	0
(107) DECK STRUCTURE TYPE	8 - Wood or Timber
(108) WEARING SURFACE/PROTECTIVE SYSTEMS	
(108A) WEARING SURFACE	7 - Wood or Timber
(108B) DECK MEMBRANE	0 - None
(108C) DECK PROTECTION	0 - None

Age of Service

(27) YEAR BUILT	1990
(106) YEAR RECONSTRUCTED	2010
(42) TYPE OF SERVICE	
(42A) TYPE OF SERVICE ON BRIDGE	1 - Highway
(42B) TYPE OF SERVICE UNDER BRIDGE	5 - Waterway
(28) LANES	
(28A) LANES ON THE STRUCTURE	01
(28B) LANES UNDER THE STRUCTURE	00
(29) AVERAGE DAILY TRAFFIC	64
(30) YEAR OF AVERAGE DAILY TRAFFIC	2016
(109) AVERAGE DAILY TRUCK TRAFFIC	5
(19) BYPASS DETOUR LENGTH	100

Figure 3: Sample of report provided by Maine DOT

1.1.3. Format of data received from the Massachusetts Department of Transportation (MassDOT) Inspection reports

The inspection reports from MassDOT can be sub-divided in eight types:

i. Routine: This report aims to provide information on the overall condition of the bridge.
ii. Special member: This report provides information regarding a specific element of the bridge.
iii. Combination of routine and special member: This report culminates information on the overall condition of the bridge and specific elements.
iv. Closed/Rehabilitation: This report has a primary focused on the traffic safety of a closed bridge.
v. Other: This report primarily focuses on documenting special events (for example floods or repairs).
vi. Underwater: This report documents the conditions of the bed of the water feature and the bridge structure.
vii. Freeze-Thaw: This report documents the conditions of the exposed concrete
viii. Fracture Critical: This report documents fracture critical members and elements of the structure and their condition

Although the reports from MassDOT are not formally divided into different sections, each inspection report follows the same structure:

1. NBI Ratings
2. Inspection notes
3. Photos
4. National Bridge Element inspection

The first section, "NBI ratings" displays the ratings of several NBI items and general information about the bridge. This includes but is not limited to the structure's name, location, structural system, and deck type. Figure 5 depicts the first page of a MassDOT bridge inspection report.

The "inspection notes" section consists of written information about the elements of the bridge structure. Often, imperative information and measurements, such as corrosion data, can be found in this section. Additionally, this section contains details regarding bridge elements and defects that were detected during the inspection.

The "Photos" section contains several pictures from the bridge inspection, which often include a detailed description. Additionally, the inspection notes reference the photographs often, aiming to illustrate what is being described by text. The combination of sketches, photos and inspection notes represent the major source of corrosion data. Figure 4 depicts an example of a sketch and a picture illustrating corrosion damage taken from the records of MassDOT.

Finally, the last section, "National Bridge Element inspection", presents the table requested by FHWA [24].

Figure 4 : The same beam, as was described by sketch (left) and by photograph (right). Adopted from W46010-3RY-DOT-NBI (district 5, City of Wrentham)

MASSACHUSETTS DEPARTMENT OF TRANSPORTATION PAGE 1 OF 29

2-DIST	B.I.N.	STRUCTURES INSPECTION FIELD REPORT	BR. DEPT. NO.
05	AF0	**ROUTINE INSPECTION**	K-01-010

CITY/TOWN	8.-STRUCTURE NO.	11-Kilo. POINT	41-STATUS	90-ROUTINE INSP. DATE
KINGSTON	K01010-AF0-DOT-NBI	028.871	A:OPEN	FEB 19, 2016

07-FACILITY CARRIED	MEMORIAL NAME/LOCAL NAME	27-YR BUILT	106-YR REBUILT	YR REHAB'D (NON 106)
ST 3 PILGRIM HWY	GRAND ARMY	1955	1979	0000

06-FEATURES INTERSECTED	26-FUNCTIONAL CLASS	DIST. BRIDGE INSPECTION ENGINEER
HWY LANDING RD	Freeway/Expressway	G. Simpson

43-STRUCTURE TYPE	22-OWNER	21-MAINTAINER	TEAM LEADER
402 : Steel continuous Stringer/Girder	State Highway Agency	State Highway Agency	W. Ferry

107-DECK TYPE	WEATHER	TEMP. (air)	TEAM MEMBERS
1 : Concrete Cast-in-Place	SUNNY	4°C	M. SILVIA, M. MARSHALL

ITEM 58 — *DECK* — 6

DECK		DEF
1.Wearing surface	7	-
2.Deck Condition	6	-
3.Stay in place forms	6	-
4.Curbs	N	-
5.Median	H	-
6.Sidewalks	N	-
7.Parapets	7	-
8.Railing	N	-
9.Anti Missile Fence	N	-
10.Drainage System	N	-
11.Lighting Standards	N	-
12.Utilities	N	-
13.Deck Joints	4	S-A
14.	N	-
15.	N	-
16.	N	-

CURB REVEAL (In millimeters)	E	W
	N	N

APPROACHES		DEF
a. Appr. pavement condition	7	-
b. Appr. Roadway Settlement	7	-
c. Appr. Sidewalk Settlement	N	-
d.	N	-

OVERHEAD SIGNS (Attached to bridge) (Y/N) N

		DEF
a. Condition of Welds	N	-
b. Condition of Bolts	N	-
c. Condition of Signs	N	-

ITEM 59 — *SUPERSTRUCTURE* — 5

SUPERSTRUCTURE		DEF
1.Stringers	N	-
2.Floorbeams	N	-
3.Floor System Bracing	N	-
4.Girders or Beams	5	S-P
5.Trusses - General	N	-
a. Upper Chords	N	-
b. Lower Chords	N	-
c. Web Members	N	-
d. Lateral Bracing	N	-
e. Sway Bracings	N	-
f. Portals	N	-
g. End Posts	N	-
6.Pin & Hangers	N	-
7.Conn Plt's, Gussets & Angles	7	-
8.Cover Plates	N	-
9.Bearing Devices	6	M-P
10.Diaphragms/Cross Frames	7	-
11.Rivets & Bolts	7	-
12.Welds	7	-
13.Member Alignment	6	-
14.Paint/Coating	4	S-A
15.	N	-

Year Painted 1979

COLLISION DAMAGE: *Please explain*
None X) Minor ( ) Moderate ( ) Severe ( )

LOAD DEFLECTION: *Please explain*
None) Minor (X) Moderate ( ) Severe ( )

LOAD VIBRATION: *Please explain*
None) Minor (X) Moderate ( ) Severe ( )

Any Fracture Critical Member: (Y/N) N

Any Cracks: (Y/N) N

ITEM 60 — *SUBSTRUCTURE* — 7

SUBSTRUCTURE	Dive	Cur		DEF
1. Abutments			7	
a. Pedestals	N	N		-
b. Bridge Seats	N	7		S-P
c. Backwalls	N	6		M-P
d. Breastwalls	N	7		-
e. Wingwalls	N	7		-
f. Slope Paving/Rip-Rap	N	6		M-P
g. Pointing	N	N		-
h. Footings	N	H		-
i. Piles	N	H		-
j. Scour	N	N		-
k. Settlement	N	7		-
l.	N	N		-
m.	N	N		-
2. Piers or Bents			7	
a. Pedestals	N	N		-
b. Caps	N	7		-
c. Columns	N	7		-
d. Stems/Webs/Pierwalls	N	N		-
e. Pointing	N	N		-
f. Footing	N	H		-
g. Piles	N	H		-
h. Scour	N	N		-
i. Settlement	N	7		-
j.	N	N		-
k.	N	N		-
3. Pile Bents			N	
a. Pile Caps	N	N		-
b. Piles	N	N		-
c. Diagonal Bracing	N	N		-
d. Horizontal Bracing	N	N		-
e. Fasteners	N	N		-

UNDERMINING (Y/N) If YES please explain N

COLLISION DAMAGE:
None X) Minor ( ) Moderate ( ) Severe ( )

SCOUR: Please explain
None X) Minor ( ) Moderate ( ) Severe ( )

I-60 (Dive Report): N *I-60 (This Report):* 7

93B-U/W (DIVE) Insp 00/00/0000

X=UNKNOWN N=NOT APPLICABLE H=HIDDEN/INACCESSIBLE R=REMOVED

RTN(1)7-96

Figure 5: Sample of report provided by MassDOT

1.1.4. Format of data received from New Hampshire Department of Transportation (NHDOT) Inspection reports

The NHDOT Bridge Inspection Manual [25] divides their inspections and reports into 7 types:

i. Routine Inspections (Regular inspection or NBIS inspection): Conducted to compare the current condition of the bridge with the previously documented condition.
ii. Inventory inspections: Consists of the first inspection performed on the bridge. It aims to collect information regarding size, location, structural and functional conditions.
iii. In-Depth inspections: Provides detailed reports, using hands-on techniques. In-depth reports can be requested for specific parts of the structure.
iv. Fracture Critical Member inspections: Utilizes hands-on techniques with non-destructive tests to provide detailed reports regarding fracture critical members.
v. Special inspections: Used to evaluate load posted bridges, inspect bridges that are out of service, monitor suspected or known deficiencies, or assess bridge or bridge members following a natural or manmade emergency.
vi. Underwater (Diving) inspections: Utilized to determine the condition of the portions of the bridge which cannot be inspected visually.
vii. Damage inspections: Aims to check whether the bridge is safe to remain open after damaged was caused by environmental effects and/or human actions.

Although there are no formal sections in the reports from NHDOT, all the reports have the same layout with 5 sections as follows:

1. Report cover
2. Element details
3. Bridge and inspection notes
4. Inspection history

The section “report cover” comprises two pages and contain all the general information about the bridge. All information pertaining to identification (for instance, NBI number of the bridge), the NBI condition of elements, dimensions and structure type can be found in this section. Figure 6 depicts an excerpt of a report cover from NHDOT.

New Hampshire Department of Transportation

Bridge Inspection Report

NBI Structure Number: 004401700013500

Existing Bridge Section
Bureau of Bridge Design

Chester 170/135

Date of Inspection: 11/10/2020
Date Report Sent: 12/29/2020
Owner: Municipality
Bridge Inspection Group: D-Team
Bridge Maintenance Crew: OTHER

HANSON ROAD
over
EXETER RIVER

Recommended Postings:

Weight: **E-2** ☑ Weight Sign OK

SIGNS IN PLACE. 11/10/20

Width: **Not Required** ☑ Width Sign OK

Primary Height Sign Recommendation: *None*
Optional Centerline Height Sign Rec: *None*

Clearances: (Feet) Over: 99.99 Under: 0.00 Route: 99.99

☑ Height Sign OK

Condition:

Red List Status: Municipal Redlist
Deck: 4 Poor
Superstructure: 5 Fair
Substructure: 5 Fair
Culvert: N N/A (NBI)
Sufficiency Rating: 49.5 %

Bridge Rail: Substandard
Rail Transition: Substandard
Bridge Approach Rail: Substandard
Approach Rail Ends: Substandard

Bridge Dimensions:

Length Maximum Span: 26.0 ft
Left Curb/Sidewalk Width: 0.0 ft
Width Curb to Curb: 26.0 ft
Approach Roadway Width: (W/Shoulders) 22.0 ft

Structure Type and Materials:

Number of Main Spans: 1
Number of Approach Spans: 0

Main Span Material and Design Type
Steel/Stringer/Girder

NH Bridge Type: IB-C (I Beams w/ Concrete Deck)
Deck Type: Concrete-Cast-in-Place
Wearing Surface: Bituminous
Membrane: Unknown
Deck Protection: None
Curb Reveal: Not Measured
Plan Location: unknown
Total Bridge Length: 31.0 ft
Right Curb/Sidewalk Width: 0.0 ft
Total Bridge Width: 28.0 ft
Median: No median
Bridge Skew: 0.00 °
Year Built/Rebuilt: 1932

NHDOT 008 Inspection
Chester 170/135
Printed on: 12/30/2020 5:47:16 AM
Page 1 of 5

Figure 6: Sample of report provided by NHDOT

The "element details" section contains a table where the elements of the bridge are discussed individually. Corrosion data can most often be found in this section of the report. It is imperative to note that there is great variability among reports pertaining to the data presented in this table. For example, not all bridge reports present the same items in the table. More specifically to the scope of this project, there are reports which contain corrosion information while others do not.

The “Element states” section presents the table required by FHWA [24]. This table summarizes the condition of several bridge components. The section “Bridge and inspection notes” describes the observed flaws found during present and past inspections in the bridge structure.

Lastly, the section “Inspection history” includes a table depicting the history of the NBI rating of bridge elements. This does not include every bridge element. This table is helpful in identifying the condition in time for given bridge elements. Additionally, this table can give insight into repairs done on a given bridge component.

It is crucial to note that a “photos” section was not provided in the reports but was reported in a separate file by NHDOT. Every photograph was labeled, but they are often not referenced in the text. While photos from the inspections are provided, no sketches regarding corrosion damage are found on the photographic records. Figure 7 depicts an example of corrosion damage taken from the records of a bridge from NHDOT.

Figure 7: Example of corrosion damage taken from the records of a bridge from NHDOT

1.1.5. Format of data received from Rhode Island Department of Transportation (RIDOT) Inspection reports

According to the RIDOT Bridge Inspection Manual [26], the RIDOT conducts 8 types of inspections and reports:

i. Inventory: Consists of the first inspection of the bridge, right after it is entered into the bridge file. The purpose of such a report is to provide the required inventory information of the original structure type, size, location as well as to document its structural and functional conditions.
ii. Routine: Conducted in a time interval no greater than 24 months and serves to assess if all service requirements are satisfied.
iii. Damage: Consists of an unscheduled inspection which evaluates the structural damage caused to the bridge by environmental effects and/or human actions.
iv. In-depth: Provides detailed assessment of the condition of the bridge or bridge elements.

v. Fracture critical: Details the condition of fracture critical members, i.e., members under tension which fracture could cause the structure to collapse partially or entirely.

vi. Underwater: Used to determine the condition of the underwater portion of the bridge substructure and the surrounding channel.

vii. Interim (Special) and miscellaneous: Conducted either in bridges which can no longer support the minimum live loads, closed bridges, or bridges which have gone through a flood event or bridges located on a public roadway that has suspected or known deterioration on one or more of its members.

viii. Non-NBI inspections: Aim to classify the non-NBI bridge into a similar type of bridge presented in the NBI. Once the classification is done, the NBI procedure for the classified type of bridge must be used.

While the sections of the reports are not explicitly denoted, RIDOT follows a structured template. To clearly discuss the reports, the following 5 sections are considered:

1. Identification, structure inventory and appraisal
2. Bridge notes
3. Inspection notes
4. Element inspection
5. Element notes

The “Identification, structure inventory and appraisal” section consists of the first and second pages of the reports. Here, general information about the bridge is reported (e.g., identification and location) and several NBI items discussing many bridge elements are summarized. Additionally, the reports from RIDOT discuss and present the historical records of some NBI ratings. Figure 8 depicts the first page of a report provided by RIDOT.

In the section “Bridge notes”, many details about the procedure during the inspection was provided. This includes but is not limited to the equipment required, whether local police were present, and the labeling or layout of the bridge beams. In the section “Inspection notes”, one can find general information about the crew responsible for the inspection, the temperature, and additional comments about NBI ratings.

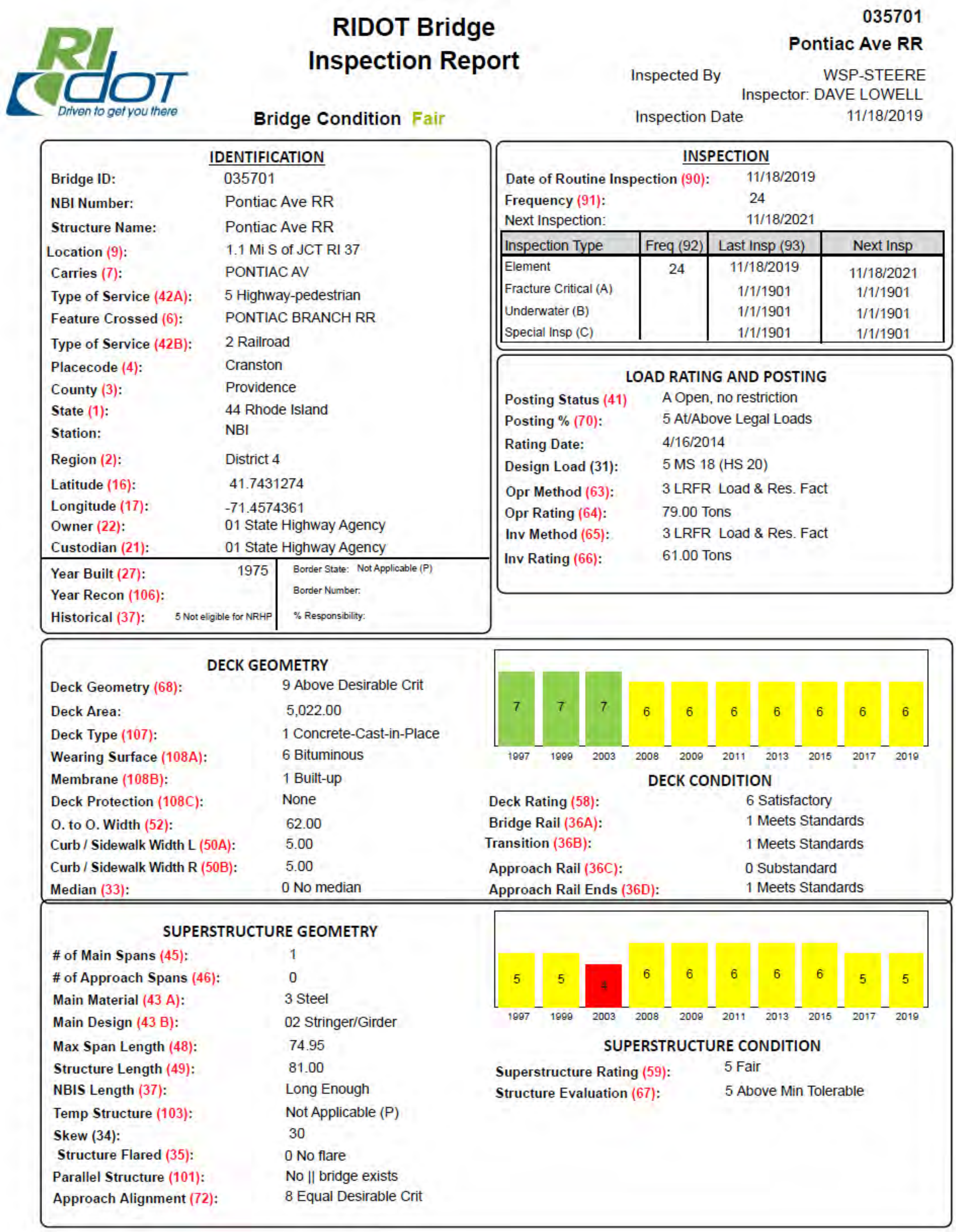

RI DOT — Driven to get you there

RIDOT Bridge Inspection Report

035701
Pontiac Ave RR

Inspected By: WSP-STEERE
Inspector: DAVE LOWELL
Inspection Date: 11/18/2019

Bridge Condition: Fair

IDENTIFICATION

Bridge ID:	035701
NBI Number:	Pontiac Ave RR
Structure Name:	Pontiac Ave RR
Location (9):	1.1 Mi S of JCT RI 37
Carries (7):	PONTIAC AV
Type of Service (42A):	5 Highway-pedestrian
Feature Crossed (6):	PONTIAC BRANCH RR
Type of Service (42B):	2 Railroad
Placecode (4):	Cranston
County (3):	Providence
State (1):	44 Rhode Island
Station:	NBI
Region (2):	District 4
Latitude (16):	41.7431274
Longitude (17):	-71.4574361
Owner (22):	01 State Highway Agency
Custodian (21):	01 State Highway Agency
Year Built (27):	1975
Year Recon (106):	
Historical (37):	5 Not eligible for NRHP
Border State:	Not Applicable (P)
Border Number:	
% Responsibility:	

INSPECTION

Date of Routine Inspection (90): 11/18/2019
Frequency (91): 24
Next Inspection: 11/18/2021

Inspection Type	Freq (92)	Last Insp (93)	Next Insp
Element	24	11/18/2019	11/18/2021
Fracture Critical (A)		1/1/1901	1/1/1901
Underwater (B)		1/1/1901	1/1/1901
Special Insp (C)		1/1/1901	1/1/1901

LOAD RATING AND POSTING

Posting Status (41)	A Open, no restriction
Posting % (70):	5 At/Above Legal Loads
Rating Date:	4/16/2014
Design Load (31):	5 MS 18 (HS 20)
Opr Method (63):	3 LRFR Load & Res. Fact
Opr Rating (64):	79.00 Tons
Inv Method (65):	3 LRFR Load & Res. Fact
Inv Rating (66):	61.00 Tons

DECK GEOMETRY

Deck Geometry (68):	9 Above Desirable Crit
Deck Area:	5,022.00
Deck Type (107):	1 Concrete-Cast-in-Place
Wearing Surface (108A):	6 Bituminous
Membrane (108B):	1 Built-up
Deck Protection (108C):	None
O. to O. Width (52):	62.00
Curb / Sidewalk Width L (50A):	5.00
Curb / Sidewalk Width R (50B):	5.00
Median (33):	0 No median

DECK CONDITION

Deck Rating (58):	6 Satisfactory
Bridge Rail (36A):	1 Meets Standards
Transition (36B):	1 Meets Standards
Approach Rail (36C):	0 Substandard
Approach Rail Ends (36D):	1 Meets Standards

SUPERSTRUCTURE GEOMETRY

# of Main Spans (45):	1
# of Approach Spans (46):	0
Main Material (43 A):	3 Steel
Main Design (43 B):	02 Stringer/Girder
Max Span Length (48):	74.95
Structure Length (49):	81.00
NBIS Length (37):	Long Enough
Temp Structure (103):	Not Applicable (P)
Skew (34):	30
Structure Flared (35):	0 No flare
Parallel Structure (101):	No || bridge exists
Approach Alignment (72):	8 Equal Desirable Crit

SUPERSTRUCTURE CONDITION

Superstructure Rating (59):	5 Fair
Structure Evaluation (67):	5 Above Min Tolerable

Figure 8: Front page of a typical routine inspection report provided by RIDOT

The section "Element inspection" presents the table required by FHWA [24], which summarizes the condition of several components of the bridge. Lastly, in the section "*Element notes*", detailed information and field measurements for distinct elements of the bridge are provided. In general, the corrosion damage and information is found in this section.

While the RIDOT reports do not present a section containing photos, all reports provided are accompanied with photographical records. The photographs are labeled with comments and measurements provided, as depicted in Figure 9. For some reports and bridges, more documentation on corrosion damage was provided. Among the outstanding documents, section loss calculations and corrosion damage sketches were provided.

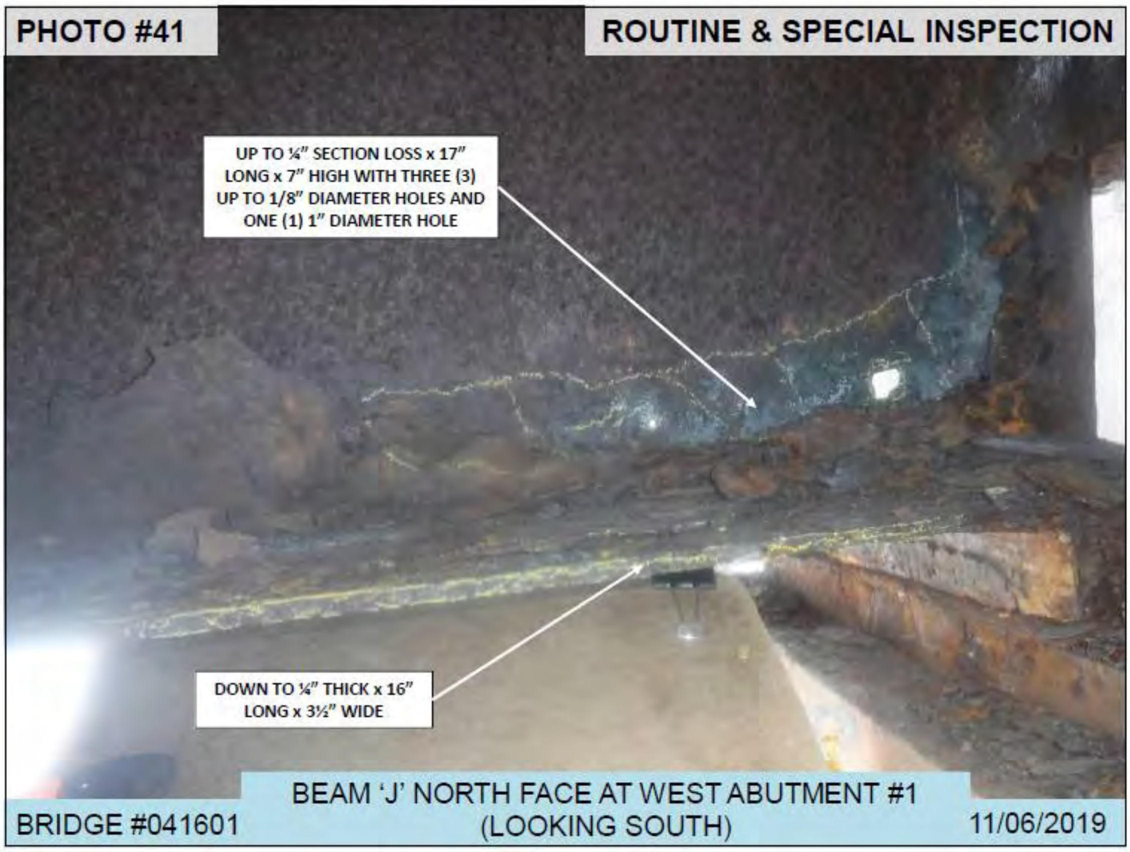

Figure 9: An example of picture provided by RIDOT

1.1.6. Format of data received from Vermont's Agency of Transportation (VTrans) Inspection reports

The VTrans Bridge Inspection Manual [27] indicates the existence of three types of reports:

i. Routine Inspections: Conducted in a regular basis by VTrans
ii. Special inspections: Required in situations when special equipment is needed during inspections.
iii. Underwater inspections: Aim to check the underwater elements of the bridge and the condition of foundations.

The inspection reports from VTrans consist of a table which sections are, in general, the elements of the bridge that are to be analyzed. The reports are organized in the following 7 sections:

1. Approach
2. Deck
3. Superstructure

4. Substructure
5. Piers
6. Channel
7. Summary

VTrans bridge inspection reports do not contain a cover but present general information about the bridge and the inspection report. This is given in a header on the first page of the report. Figure 11 depicts an example of a first page of a VTrans report.

The section "Approach" contains information about the condition of the settlement, erosion on abutments, and the condition of the rails. The section following "Approach" is denoted as "Deck", where information about the asphalt, joints and drains can be found.

The next section refers to the "Superstructure". Most of the information regarding corrosion can be found in this section, making it crucial to this project. Additionally, this section often contains comments on the condition of the floor beams, and the painting of the beams.

The following section is the "Substructure" and discusses its elements, such as abutments and wingwalls. The last two element sections of the report discuss the condition of the "Piers" and "Channels" of the bridge structure. Lastly, there is a "Summary" section in which an overview about the bridge is provided along with NBI ratings.

The reports do not depict photographic records, as this type of data can be found for all bridges in the VTrans web-portal. Not all pictures are labeled, and the text does not often reference the photographs. No sketches regarding corrosion are provided along with the photographs or the inspection reports. Figure 10 depicts an example of photo which can be found in VTrans web-portal.

Figure 10: Example of photo of a buckled beam found in VTrans web-portal

State of Vermont Bridge Inspection Form

Date: 04/20/20 **Route:** C3081 **Bridge #:** 42 **District:** 7

Town: Barnet **Bridge Type:** Single Span Rolled Beam

Crossing: South Peacham Brook **Inspectors:** MJK MJ

Approach ~

Rail: Galv. Standard Steel Beam **and** Type Condition

Posts: Galv. Standard Steel I Beam **and** Type Condition

Some areas of impact damage with couple post are twisted and bent back

Settlement: Minor

Erosion: Minor

Deck ~

Wearing Surface: Asphalt Condition Other -

Litter with cracking and potholes with 10" +/_ of cover of asphalt and gravel

Curb: Concrete Condition

Pavement is flush with top of curbing so unable to view facing

Sidewalks: N/A

Rail: Galv. Standard Steel Beam **and** Type Condition

Galv beam retroffited years ago with heavy duty C channels 2 tier.

Posts: A588 Standard Steel I Beam **and** Type Condition

Heavy duty I beams attach to longitudinal I beams that have heavy rusting and holes through webbing in places. Downstream side post and rail pushed back

Figure 11: Sample of report provided by VTrans

1.2. Variability and Quality of Data

A first observation from all the inspection reports is that there is variability among the reports from different states in terms of the quantity of information provided and the structure of how information is reported. This finding is expected, as different states have been inspecting bridges differently and according to their needs and goals. It should be noted however, that with this variability, the reports from all states still meet the minimum requirements of NBI reporting.

The most noticeable differences between the inspection reports can be found when we consider the following two groups: MaineDOT, NHDOT and VTrans in Group 1 and RIDOT, MassDOT and CTDOT in Group 2. The Northern New England States (Group 1) have inspection reports which rarely provide sketches where the Southern New England States (Group 2) often provide sketches and photographs. Another related important note is that several reports from Group 1, in which corrosion information is provided in a generic form, are the result of a visual inspection. For this reason, there are no detailed measurements or thickness losses provided in the report. It is imperative to note that the methods of Group 2 were developed over time and had performed inspection methods much like those of Group 1 until nearly recently. Figure 12, Figure 13 and Figure 14 depict examples of corrosion information provided by the DOT's of the Northern States (Group 1).

Superstructure **NBI Item 59: 5**

Downstream exterior girder has steel delamination of top flange and light section loss near web.
7 of 10 girders in good condition with paint which is generally intact. The other 3 have paint freckling and flaking. Noticeable light section loss at web/flange interface scattered along girders. All bearings have major to complete paint loss with moderate surface rust.

Figure 12: Example of corrosion information (Adapted from bridge *0854,* Maine)

Stringers: Rolled Beams and < > Varying amounts of rust scale throughout out. The exterior beams and abutment 1 beam end of beam 4 have heavy rust scale. The fascia beams have significant section loss and small perforations could soon occur. The upstream fascia beam has a small area in the web near abutment 2 w/ 1" perforations.

Figure 13: Example of inspection notes (Adapted from *BENNINGTON-BR22-19OCT2*, Vermont)

107	Steel Open Girder/Beam	I-BEAMS
		LIGHT SECTION LOSS AT ENDS OF BEAMS.
└ 515	Steel Protective Coating	PAINT PEELING IN AREAS.
└ 1000	Corrosion	LIGHT SECTION LOSS AT ENDS OF BEAMS.

Figure 14: Example of inspection notes (Adapted from *Andover 125-129*, New Hampshire)

The generic description of corrosion data and the lack of cross referencing to the pictures pose a challenge for the compilation and identification of corrosion patterns and the condition of the beams.

While there is visual inspection, many reports from the Southern New England States (Group 2) provide sketches regarding corrosion information. It is important to note that many of these sketches are not to scale and are depicted in Figure 15, Figure 16 and Figure 17.

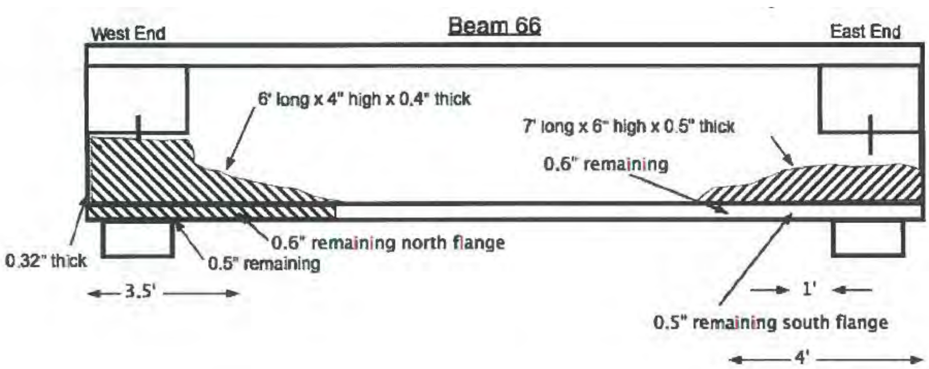

Figure 15: Typical inspection report sketch not in scale. Adapted from N19059-101-DOT-NBI (Northampton, MA)

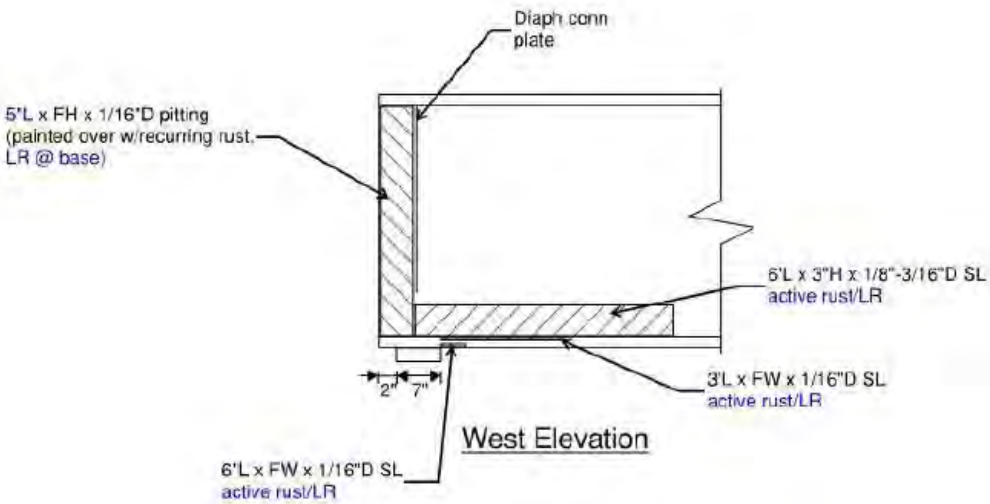

Figure 16: Typical inspection report sketch (not to scale). Adapted from Br. #00297 (Plainfield, CT)

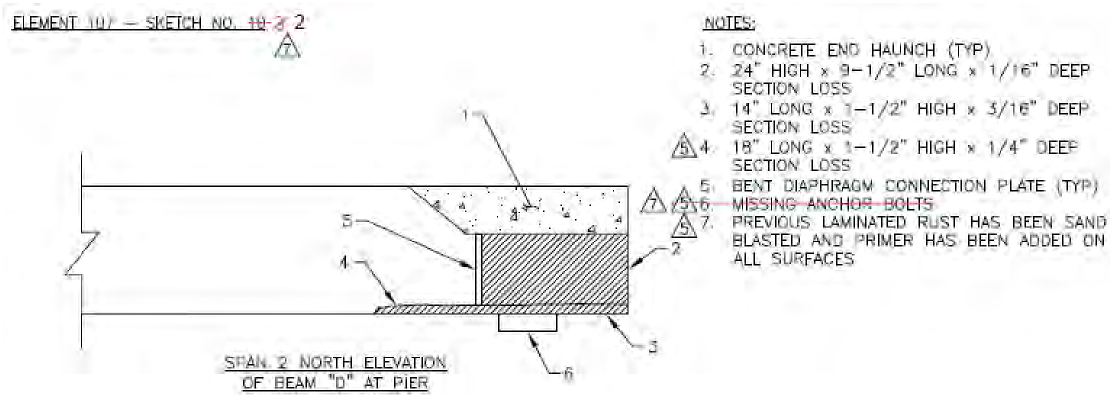

Figure 17: Typical inspection report sketch not to scale (*Adapted from Br. #042501, RI*)

The reports from all states that contain information about corrosion most often include a single data point of web thickness measurement. This is a gross simplification of the corrosion region since it is likely that web thickness will vary within a corroded region of the beam. The corrosion damage is considered uniform within the corroded region, and the given measurement is assumed to be the maximum thickness loss. The sparsity of thickness measurements is critical to note and consider here, as the average thickness of the beam is an important parameter of capacity load equations. Figure 18, Figure 19, and Figure 20 show the variation in how some of the New England states report this critical section loss parameter. The inspection reports from Massachusetts, Connecticut, and Rhode Island are where diagrams like these can be found.

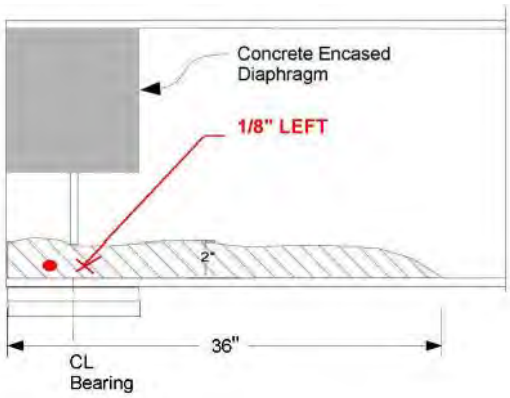

Figure 18: **Corroded area described by only one thickness value. Adapted from W46010-3RY-DOT-NBI (Wrentham, MA)**

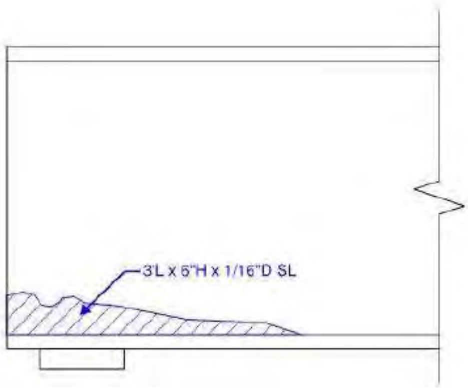

Figure 19: **Corroded area described by only one thickness value. Adapted from bridge 00501 (Killingly, CT)**

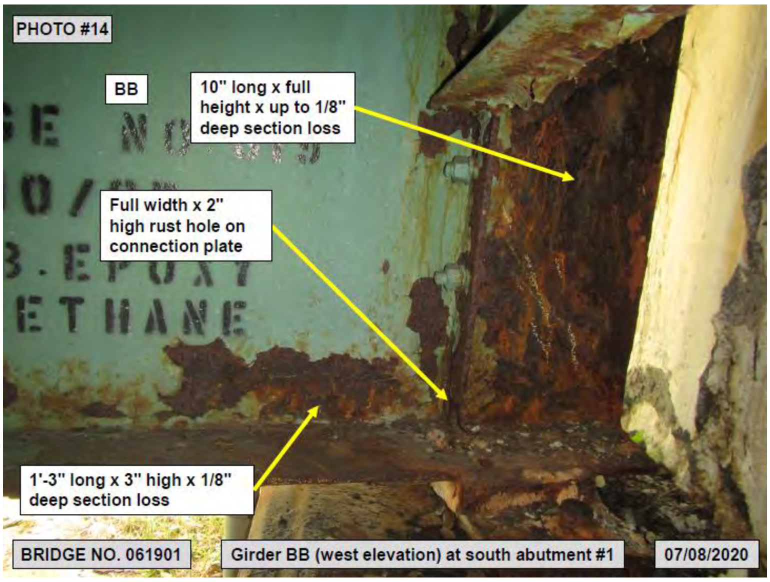

Figure 20: **Corroded areas described by only one thickness value. Adapted from bridge 061901(RI)**

There are also cases, where multiple thickness measurements are provided in an effort of the inspector to provide higher accuracy as Figure 21. It is worthwhile to note that the thickness measurement and its variation throughout the corroded region are important parameters needed when assessing the load capacity of the beams.

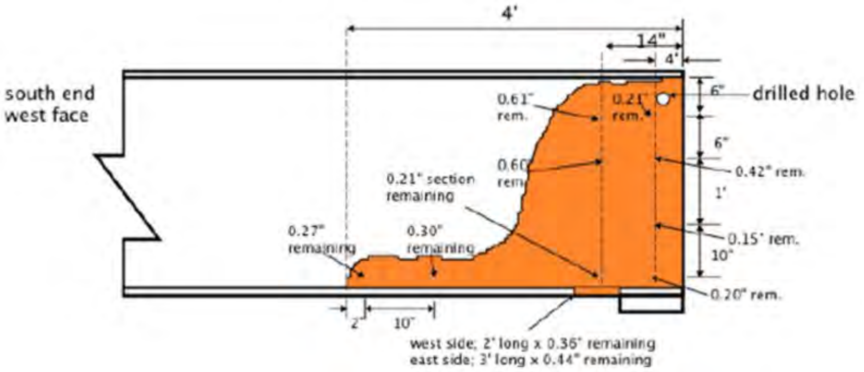

Figure 21: **Corroded area described by multiple thickness loss values. Sketch adopted from H08003-18J-MUN-NBI (District 2, Town of Hardwick)**

There are sketches that provide an interval of section loss over a particular area. While this interval is depicted in a given area, they do not often indicate where the maximum and minimum loss occurs, as depicted in Figure 22.

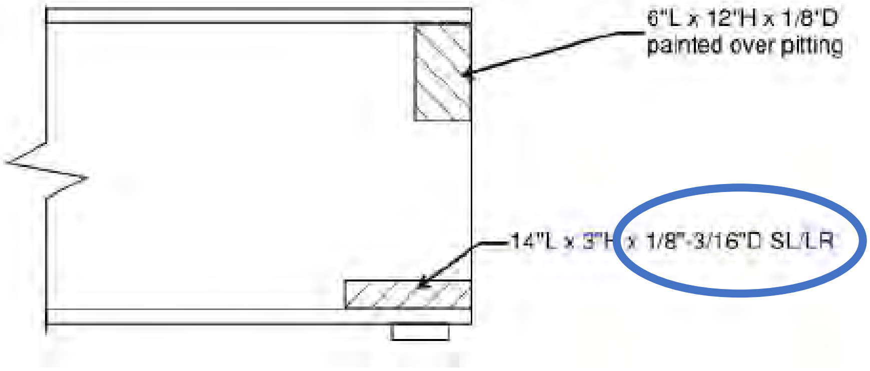

Figure 22: **No indication of where the section loss occurs. Adapted from Br. #00297 (Plainfield, CT)**

While they provide incredible insight to the beam end condition, sketches are often not enough to accurately describe corroded beam ends. For this reason, it is important that a report depicts a coherent combination of sketches, photographs, and written descriptions regarding the phenomenon. In some cases, there are times where reporting is not accurate, i.e., when the description and the sketches/pictures do not match. Additionally, some pictures do not have labels nor captions, which hinders the understanding of the records. This usually happens to simplify and to generalize a condition. An example of this could be that the area of section loss is described as a rectangle, but the real pictures depict another pattern. In many cases, this simplification is used for 100% material loss, leading to overestimation of the phenomenon.

As a general note, the reports typically from the Northern New England States (Group 1), lack information regarding the type of beams used in the construction of the bridge structure. This information is imperative to this work, as it provides a basis to understand the current conditions of the beams being analyzed relative to a control point or, original data.

1.3. Amount of Data

Figure 23 presents the amount of inspection reports each state in the New England Region provided for this research work. In summary, our team received a total of 553 inspection reports. However, some reports were from the same bridge in a different time or inspection interval. As a result, our team was able to create a database of 515 total bridges across the six New England states.

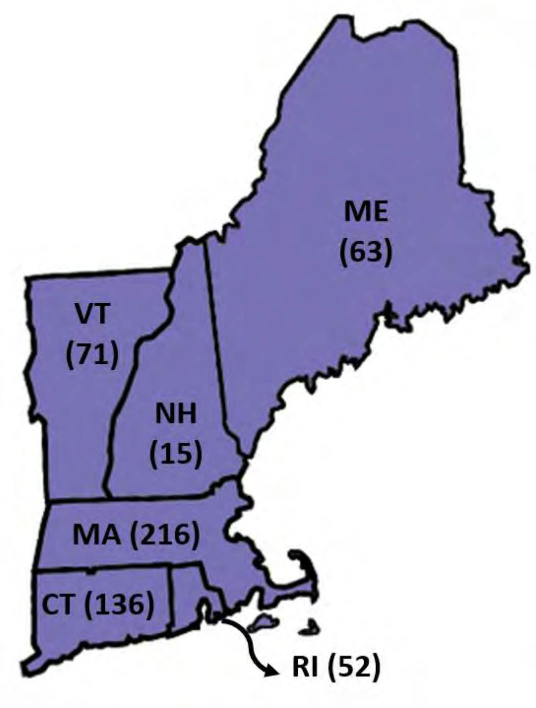

Figure 23: Summary of reports provided by each state

1.4. Preliminary filtering of the data

As discussed above, not all the provided reports were used in the final bridge database of this research work. Some of them included but were not limited to reports describing other types of bridges (e.g., concrete bridges) and reports in which no corrosion information was provided. These bridges and reports could not be used in the database generated because they are out of the scope of the current work. As a result of this, the inspection reports needed to be sorted and compiled. Table 3 summarizes the number of reports used to create the current database.

Table 3: Preliminary Sorting of Inspection reports

State	All	Summarized	Stiffeners	Previous Reports (In time)	No data/No corrosion/Other type of damage	Other type of bridge	Too corroded
Connecticut	136	55	83	1	18	5	--
Maine	63	32	7	1	31	--	--
Massachusetts	216	93	30	33	36	23	1
New Hampshire	15	13	--	--	2	--	--
Rhode Island	52	13	37	--	8	1	--
Vermont	71	19	0	3	48	1	--
Total	553	225	157	38	143	30	1

Table 3 includes the detailed numbers of the reports used from each state. The first column shows the number of all reports provided from each state. The second column details how many reports were summarized and effectively contributed to our database. The third column isolates inspection reports of bridges with stiffened beams; these reports were disregarded due to this type of beam being out of the scope of this project. The fourth column of Table 3 identifies reports which describe the evolution of the corrosion phenomenon in time. For example, many of the reports describe the same bridge at different time intervals. Although it is important to observe the evolution of corrosion, and possibly develop prediction tools, these reports were removed from post-processing as only the current (latest) condition of these bridges was accounted for. The fifth column of Table 3 shows the inspection reports which did not provide corrosion. There was a single report, which described a bridge with extreme corrosion, which the research team decided should be removed from further post-processing.

As a result, from the 553 reports provided by the states, 225 reports were summarized. From the summarized reports, our team was able to obtain data for 1,723 beam ends. The amount of information collected is considered a rich source of data, from which the research team can draw conclusions regarding deterioration of unstiffened beam ends due to corrosion.

1.5. Corrosion Patterns

Building on a recently completed research project in MA, the research team identified six primary web corrosion patterns and six web hole patterns to classify the damage in bridge beam ends. These patterns were generated based on the most common types of corrosion identified in the beam ends of the reports provided by MassDOT, as discussed in [28].

In this project, the corrosion patterns identified previously were used. The existing patterns allowed our team to describe more than 95% of the new data available in the reports for this project. With this large percentage of beams that could be described by existing patterns, our team decided that no new corrosion type needed to be created. This observation is not surprising because the source of corrosion in all states is similar: salt-laden water leaking through bridge expansion joints located at beam ends.

The goal of creating the corrosion patterns is to simplify and classify the extensive data available. This type of corrosion classification allowed our team to describe and group cases that were similar. As a result, we were able to summarize the data into Excel spreadsheets and efficiently extract conclusions from the data available via MATLAB. Furthermore, this classification allowed building analytical models that included the most common corrosion patterns to conduct parametric analyses of beams containing these patterns.

Table 4 through Table 9 describe the web corrosion patterns. These tables provide a label for the pattern, a diagram, a real inspection report example, and a brief description.

Table 4: Web corrosion pattern W1

Pattern name	Pattern shape	Example from an inspection report
W1	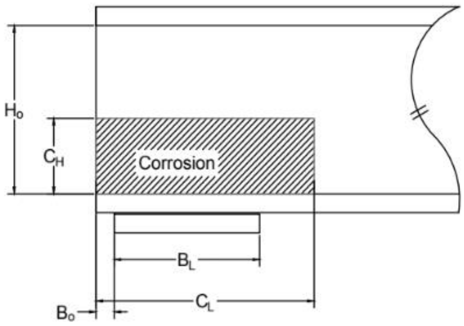	 Adopted from H-23-011-1UQ-DOT-NBI (District 3, Town of Hopkinton)
	<u>Short description:</u> W1 is a rectangular shape corrosion pattern which appears at the beam end above the bearing. The dimensions of the damaged area are C_H for the depth of the damaged area and C_L for the length. B_L is the bearing width and B_o is the length of the free end of the beam beyond the bearing. The photograph on the right shows a case of W1 for which the C_H is equal to the depth of the beam web H_o.	

Table 5: Web corrosion pattern W2

Pattern name	Pattern shape	Indicative example from an inspection report
W2	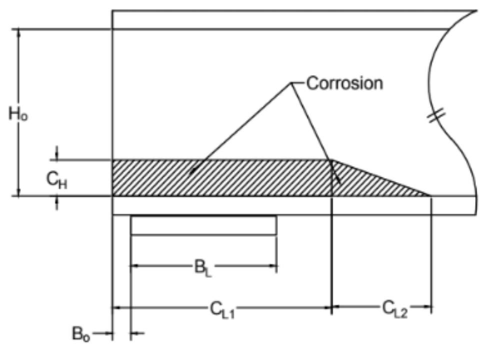	 Adopted from N-06-015-3WR-DOT-NBI (District 5, Town of New Bedford)
	Short description: W2 is similar to W1 with the addition of a triangular shaped corrosion area at the end of the rectangular shape. For W2, C_H is the depth of the damaged area, while C_{L1} is the length of the rectangular part of the corrosion. C_{L2} is the length of the triangular damage. B_L is the bearing width and B_o is the length of the free end of the beam beyond the bearing. The photograph on the right shows a typical case of W2.	

Table 6: Web corrosion pattern W3

Pattern name	Pattern shape	Indicative example from an inspection report
W3	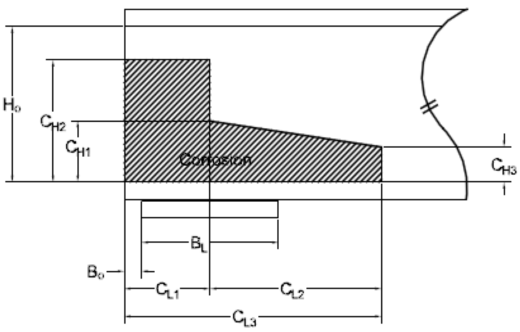	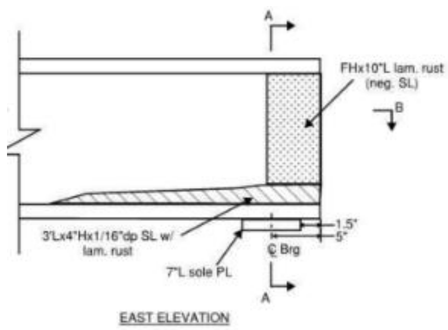 Adapted from Bridge 00162, Girder G1, Span 2, Pier 2 West Haven, Connecticut
	Short description: W3 is a more complex shape than W1 and W2. It can be described by the three areas as shown at the sketch above (left). For W3, the depth of the corroded area is described using C_{H1}, C_{H2} and C_{H3}. Similarly, C_{L1} and C_{L2} are used to provide the length of the corroded area. B_L is the bearing width and B_o is the length of the free end of the beam beyond the bearing. The photograph on the right shows a typical case of W3.	

Table 7: Web corrosion pattern W4

<table>
<tr><th>Pattern name</th><th>Pattern shape</th><th>Indicative example from an inspection report</th></tr>
<tr><td rowspan="2">W4</td><td>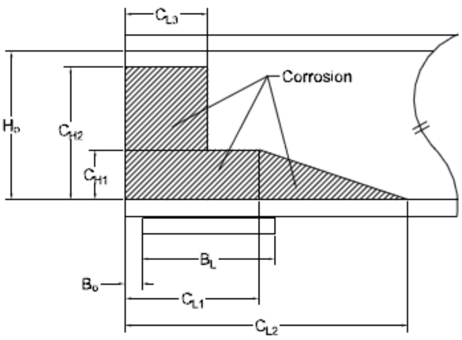
</td><td>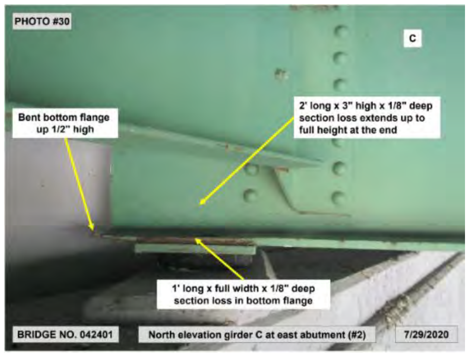

Adapted from Bridge 042401, Girder C, Abutment 2
New London Ave, Rhode Island</td></tr>
<tr><td colspan="2"><u>Short description:</u> W4 is a slight modification of W3 to include the bottom left rectangular shape. The depth of the corroded area is described using C_{H1} and C_{H2}. Similarly, C_{L1}, C_{L2} and C_{L3} are used to provide the length of the corroded area. B_L is the bearing width and B_o is the length of the free end of the beam beyond the bearing. The photograph on the right shows a typical case of W4.</td></tr>
</table>

Table 8: Web corrosion pattern W5

<table>
<tr><th>Pattern name</th><th>Pattern shape</th><th>Indicative example from an inspection report</th></tr>
<tr><td rowspan="2">W5</td><td>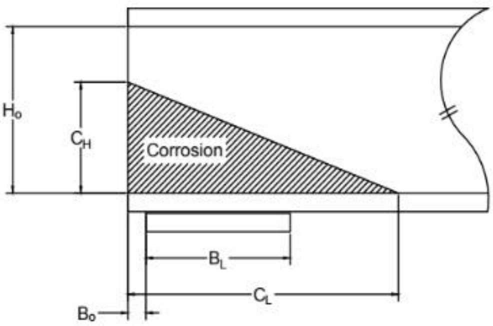
</td><td>
Adapted from W-05-024-0T4-MUN-NBI
(District 2, Town of Ware)</td></tr>
<tr><td colspan="2"><u>Short description:</u> W5 is a simple triangular shape corroded area described by C_H which is the height of the triangle and C_L which is the length of the triangle. B_L is the bearing width and B_o is the length of the free end of the beam beyond the bearing. The photograph on the right shows a typical case of W5.</td></tr>
</table>

Table 9: Web corrosion pattern W6.

Pattern name	Pattern shape	Indicative example from an inspection report
W6	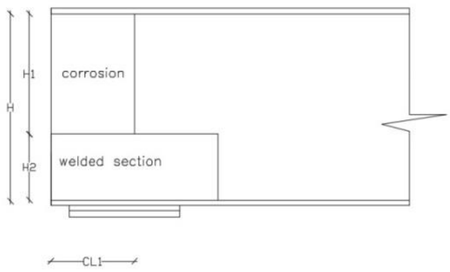	 Adapted from N-19-064-10C-DOT-NBI (District 2, City of Northampton, Massachusetts)
	Short description: W6 is a rare case but it is included here for the sake of completeness. It involves a plate at the bottom side of the web. The corrosion extends above the welded section as shown in the graph above (left). For this case, H_1 is the height of the corroded area, C_{L1} is the length of the corroded area, and H_2 is the height of the welded plate. The photograph on the right shows a typical case of W6.	

Much like the web corrosion patterns, no new web hole corrosion patterns were created as the existing patterns described more than 95% of the beam ends. Table 11: Web hole pattern M2 through

Table **13** depict the web hole corrosion patterns considered. These tables provide a label for the pattern, a diagram, a real inspection report example, and a brief description.

Table 10: Web hole pattern M1

Pattern name	Hole shape	Indicative example from an inspection report
M1	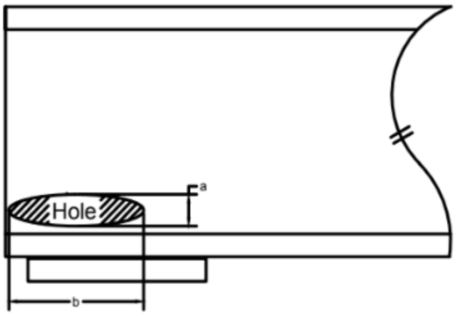	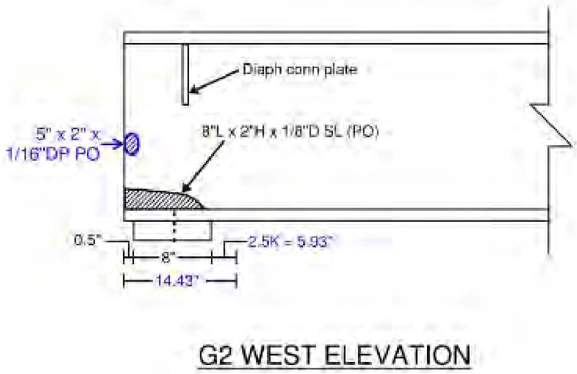 Adapted from Bridge 00636, Girder 2, Span 2, Pier 2 Middletown, Connecticut
	Short description: M1 is a case where a hole appears at the lower part of the web and extends longitudinally over the bearing. For this case, a is the height of the hole and b is the length of the hole. The photograph on the right shows a typical case of M1.	

Table 11: Web hole pattern M2

Pattern name	Hole shape	Indicative example from an inspection report
M2	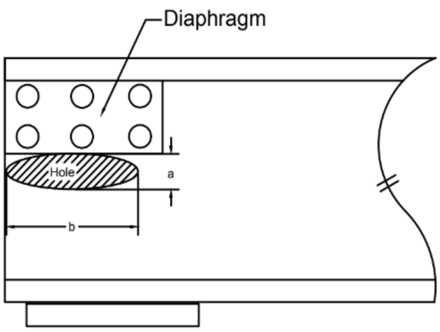	 Adapted from S-24-017-14K-DOT-634 (District 2, City of Springfield, Massachusetts)
	Short description: M2 is a case where the beams have a diaphragm and the hole appears just below the diaphragm. For this case, a is the height of the hole and b is the length of the hole. The photograph on the right shows a typical case of M2.	

Table 12: Web hole pattern M3

<table>
<tr><th>Pattern name</th><th>Hole shape</th><th>Indicative example from an inspection report</th></tr>
<tr><td rowspan="2">M3</td><td>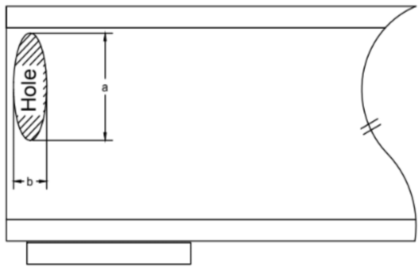
</td><td>
Adapted from F-04-017-23N-DOT-634
(District 3, City of Fitchburg, Massachusetts)</td></tr>
<tr><td colspan="2"><u>Short description:</u> M3 is a case where a hole appears at the top part of the beam. For this case, a is the height of the hole and b is the length of the hole. The photograph on the right shows a typical case of M3.</td></tr>
</table>

Table 13: Web hole pattern M4

<table>
<tr><th>Pattern name</th><th>Hole shape</th><th>Indicative example from an inspection report</th></tr>
<tr><td rowspan="2">M4</td><td>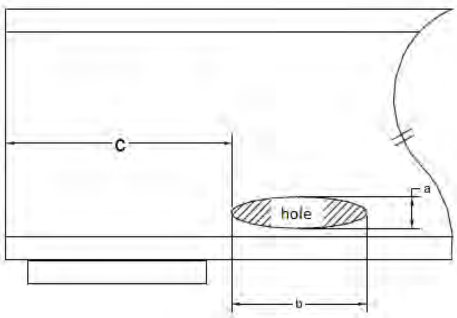
</td><td>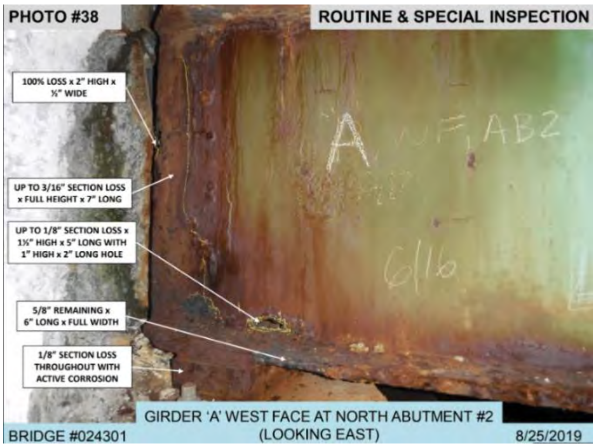

Adapted from Bridge 024301, Girder A West Face, North Abutment 2
Lafayette RR, Rhode Island</td></tr>
<tr><td colspan="2"><u>Short description:</u> M4 is a case where a hole appears away from the bearing at the lower part of the beam. For this case, a is the height of the hole, b is the length of the hole, and c is the distance of the end of the hole from the end of the beam. The photograph on the right shows a typical case of M4.</td></tr>
</table>

It is worthwhile mentioning that the beam ends usually present a combination of corrosion web patterns and web hole patterns. Additionally, the same beam end can present more than a single web hole pattern. The three following combinations of web hole patterns were considered in this project: M1+M2, M1+M3, and M2+M4.

Flange Corrosion

The reports from each state often describe the flange corrosion by measuring only the length of the phenomenon and the thickness loss. As a result, there is the underlying assumption that corrosion is uniform across the width of the flanges. Although this is a rough assumption, this is recurring when dealing with corrosion. For instance, a similar assumption is made when the thickness loss is uniform in the corroded area.

Therefore, to summarize the flange corrosion, no pattern was created. Instead, the length and thickness loss were recorded. In case the report did not show any information regarding flange corrosion, no corrosion was considered in the flanges.

2. Organization of Data and Post-Processing

2.1. Organizing Data

To work with the extensive amount of available data, the corrosion information from the reports was organized into Excel spreadsheets. The usage of Excel allows one to easily organize the phenomenon by using the parameters defined for each corrosion pattern. Once the data was organized, our team was able to run a MATLAB code which provides efficiency in post-processing the data available in the reports.

Figure 24 depicts the top of the spreadsheet, which includes general information for the bridge, such as name, location, construction year, and so on.

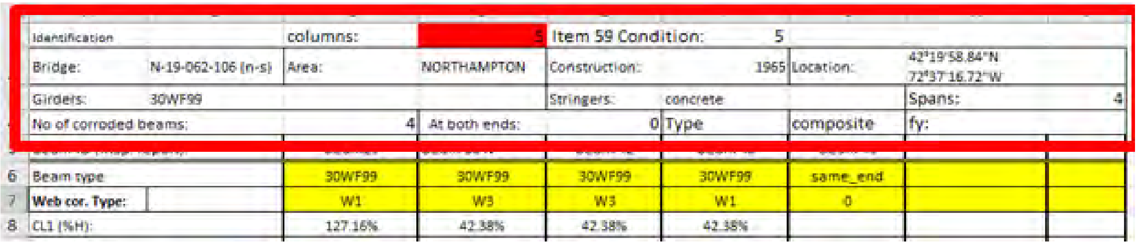

Identification		columns:	5	Item 59 Condition:	5			
Bridge:	N-19-062-106 (n-s)	Area:	NORTHAMPTON	Construction:	1965	Location:	42°19'58.84"N 72°37'16.72"W	
Girders:	30WF99			Stringers:	concrete		Spans:	4
No of corroded beams:		4	At both ends:	0	Type	composite	fy:	
6 Beam type		30WF99	30WF99	30WF99	30WF99	same_end		
7 Web cor. Type:		W1	W3	W3	W1	0		
8 CL1 (%H):		127.16%	42.38%	42.38%	42.38%			

Figure 24: Bridge identification and general information isolated at the top of the spreadsheet.

Every bridge is described by a sheet in an Excel file. This allows for many bridges to be placed into a single file. Each corroded beam end is described by a single column with cells which contain general information regarding the beams. This allowed the team to compile each beam end from a given bridge into one sheet. Thus, in a single Excel file we were able to gather all the beam ends from each bridge from every state. However, to maintain organization and to avoid errors, our team decided to separate Excel files by state. Excel files varied between Group 1 and Group 2 and was dependent on the amount of corrosion data that was presented for a given beam end.

By describing each corroded beam end within a column, we accurately consider each unique beam end case. Figure 25 depicts the whole column in which the corrosion data of each beam end is summarized.

The first section of the spreadsheet describes the web corrosion pattern (lines 7-13 in Figure 25). The first field that must be filled concerns the beam type, (shadowed area A, in Figure 25). Then, in part B (lines 8-13 and 18-20) the corrosion shape is described using one of the six defined corrosion patterns, the corresponding dimensions are normalized with the height H_0, where $H_0 = H\text{-}2t_f$, and the web thickness loss is reported as well, where H is the depth of the beam and t_f the flange thickness.

The second part of the spreadsheet involves the hole patterns. In Part C, if a web hole exists, it is classified according to the hole patterns discussed earlier in the report. In case hole dimensions are given, they are normalized the same way as web corrosion lengths. In Part D, the diaphragm and signs of buckling are reported with “yes” or “no”.

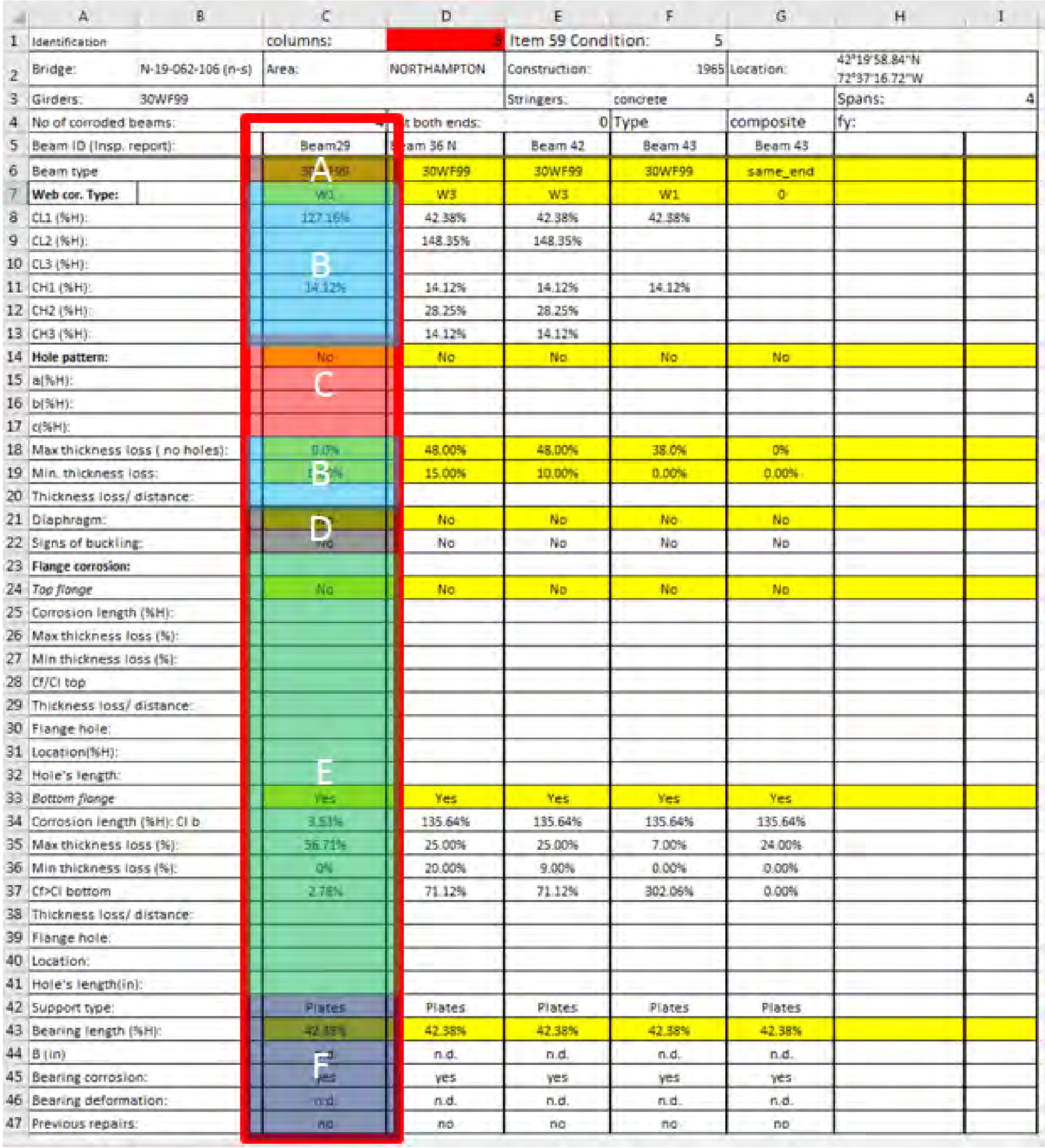

	A	B	C	D	E	F	G	H	I
1	Identification		columns:	5	Item 59 Condition:	5			
2	Bridge:	N-19-062-106 (n-s)	Area:	NORTHAMPTON	Construction:	1965	Location:	42°19'58.84"N 72°37'16.72"W	
3	Girders:	30WF99			Stringers:	concrete		Spans:	4
4	No of corroded beams:		[illegible]	t both ends:	0	Type	composite	fy:	
5	Beam ID (Insp. report):		Beam29	am 36 N	Beam 42	Beam 43	Beam 43		
6	Beam type		[illegible]	30WF99	30WF99	30WF99	same_end		
7	Web cor. Type:		W1	W3	W3	W1	0		
8	CL1 (%H):		127.16%	42.38%	42.38%	42.38%			
9	CL2 (%H):			148.35%	148.35%				
10	CL3 (%H):								
11	CH1 (%H):		14.12%	14.12%	14.12%	14.12%			
12	CH2 (%H):			28.25%	28.25%				
13	CH3 (%H):			14.12%	14.12%				
14	Hole pattern:		No	No	No	No	No		
15	a(%H):								
16	b(%H):								
17	c(%H):								
18	Max thickness loss (no holes):		0.0%	48.00%	48.00%	38.0%	0%		
19	Min. thickness loss:		[illegible]	15.00%	10.00%	0.00%	0.00%		
20	Thickness loss/ distance:								
21	Diaphragm:		[illegible]	No	No	No	No		
22	Signs of buckling:		No	No	No	No	No		
23	Flange corrosion:								
24	Top flange		No	No	No	No	No		
25	Corrosion length (%H):								
26	Max thickness loss (%):								
27	Min thickness loss (%):								
28	Cf/Cl top								
29	Thickness loss/ distance:								
30	Flange hole:								
31	Location(%H):								
32	Hole's length:								
33	Bottom flange		Yes	Yes	Yes	Yes	Yes		
34	Corrosion length (%H): Cl b		3.51%	135.64%	135.64%	135.64%	135.64%		
35	Max thickness loss (%):		56.71%	25.00%	25.00%	7.00%	24.00%		
36	Min thickness loss (%):		0%	20.00%	9.00%	0.00%	0.00%		
37	Cf>Cl bottom		2.78%	71.12%	71.12%	302.06%	0.00%		
38	Thickness loss/ distance:								
39	Flange hole:								
40	Location:								
41	Hole's length(in):								
42	Support type:		Plates	Plates	Plates	Plates	Plates		
43	Bearing length (%H):		42.38%	42.38%	42.38%	42.38%	42.38%		
44	B (in)		[illegible]	n.d.	n.d.	n.d.	n.d.		
45	Bearing corrosion:		yes	yes	yes	yes	yes		
46	Bearing deformation:		n.d.	n.d.	n.d.	n.d.	n.d.		
47	Previous repairs:		no	no	no	no	no		

Figure 25: Spreadsheet designed to organize corrosion data

Part E is dedicated to flange corrosion identification. The corrosion length and the thickness loss are reported. It is critical to note that thickness loss considers both sides of a given beam end and its corrosion. Additionally, in a case with a hole present, its position and length are reported. Finally, in Part F, the condition of the bearing is described, if any information is available.

2.2. MATLAB script

Once all the available data was organized into Excel spreadsheets, we could assume that the information from all beam ends is stored in the same shape. Using this information, a MATLAB script was created to post-process the data stored in the spreadsheets.

The MATLAB script used in this project was first developed in the previous project and was updated to be utilized here. Upon running, the code looks for the existence of diaphragm in the beam ends. Further, the code accounted for the patterns of each beam end stores the parameters written in the spreadsheet into MATLAB matrices. From this, our team could assess the maximum length, maximum height, etc., for each pattern.

2.3. Results

Following the post-processing of the data from the reports provided, our team could determine, for instance, the most common patterns, or the extreme cases of corrosion. Some of the states studied in this project have a significantly greater amount of recorded beam-ends than others. Additionally, in some cases, it was not possible to determine the corrosion pattern from every state. In response to this, results were presented by state, rather than as a region. This was adopted to avoid bias in the results and to provide useful data by state.

Additionally, with the division of results by states, the results were further divided into two categories; to address structures that had diaphragms and structures that did not. It is imperative to distinguish that a structure was considered to have "diaphragms" for either concrete diaphragms or for cases in which the connection plate of the metallic diaphragm occupied a significant area of the web, as depicted in Figure 26.

Figure 26: To the left is P-01-005 (Massachusetts) and the right structure is 042401 (Rhode Island)

2.3.1. Connecticut

2.3.1.1. General Metrics

Following the methodology explained above, our research team was able to compile information of 369 beams ends without diaphragm from the reports provided by CTDOT. It is important to note that beam ends without corrosion are not considered in this count. To help with the understating of the behavior of corrosion and extract more meaningful results, patterns W1 and W2 were grouped, as well as patterns W3 and W4. By doing this, the research team was able to easily distinguish the relevant web corrosion patterns and relevant hole patterns. Table 14 and Table 15 depict the results obtained by grouping the corrosion patterns of beams with and without diaphragm.

Table 14: Beam end categorization metrics for beam ends without a diaphragm system

	Number	No Hole	M1	M2	M3	M4	M1 and M2	M1 and M3	M2 and M4
W1 and W2	243	236	3	0	2	3	0	1	0
W3 and W4	50	45	3	0	2	0	0	1	0
W5	26	26	0	0	0	0	0	0	0
W6	2	2	0	0	0	0	0	0	0
Total	321	309	6	0	4	3	0	2	0

Table 15: Beam end categorization metrics for beam ends with a diaphragm system

	Number	No Hole	M1	M2	M3	M4	M1 and M2	M1 and M3	M2 and M4
W1 and W2	36	33	1	1	0	0	0	0	0
W3 and W4	10	9	1	0	0	0	0	0	0
W5	2	2	0	0	0	0	0	0	0
W6	0	0	0	0	0	0	0	0	0
Total	48	44	2	1	0	0	0	0	0

2.3.1.2. Final Corrosion patterns

From the data shown above, it becomes clear that the majority of beam end deterioration does not include holes. Additionally, it is also clear that the W1, W2, W3 and W4 patterns are present in a large majority of the beam ends. It is important to note that although patterns W1 and W2 and W3 and W4 were grouped together, these patterns were separately analyzed. Further results of isolated patterns can be found in the Appendix section of this report.

Based on Table 14 and Table 15, the research group was able to determine the most dominant cases of corrosion, which are shaded in green in Table 16 and

Table 17. On the other hand, cases shaded in red were disregarded, as they were very sparse in number.

Table 16: Dominant cases for beams without a diaphragm system

	Number	No Hole	M1	M2	M3	M4	M1 and M2	M1 and M3	M2 and M4
W1 and W2	243	236	3	0	2	3	0	1	0
W3 and W4	50	45	3	0	2	0	0	1	0
W5	26	26	0	0	0	0	0	0	0
W6	2	2	0	0	0	0	0	0	0

Total	321	309	6	0	4	3	0	2	0

Table 17: Dominant cases for beams with diaphragm

	Number	No Hole	M1	M2	M3	M4	M1 and M2	M1 and M3	M2 and M4
W1 and W2	36	33	1	1	0	0	0	0	0
W3 and W4	10	9	1	0	0	0	0	0	0
W5	2	2	0	0	0	0	0	0	0
W6	0	0	0	0	0	0	0	0	0
Total	48	44	2	1	0	0	0	0	0

2.3.1.3. Beams ends without a diaphragm system

2.3.1.3.1. W1 and W2

Based on the 317 appearances of W1 and W2 without a diaphragm system, our team was able to determine the most common cases regarding web and flange corrosion for both patterns and the most common interaction between the parameters of a pattern. Table 18, Table 19, and Table 20 depict the most common trends observed in the compiled data. The graphs which allowed the team to observe these behaviors are found in the Appendix of this report.

Table 18: Final corrosion patterns for W1 and W2 without holes (beam ends without diaphragm) - CTDOT

Auxiliary Sketch

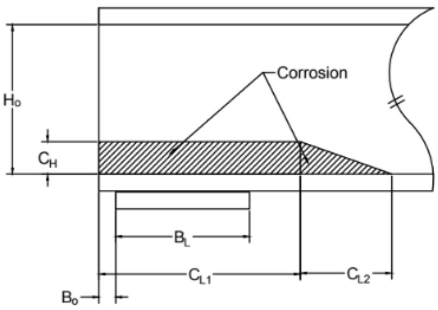

Description | Pattern W1

Case A

$$\mathbf{0 < CH_1 < 0.4H_0,\ 0 < CL_1 < 2.5H_0}$$

$$\mathbf{0 < \frac{t_{loss}}{t_{web}} \leq 0.4}$$

$$\mathbf{1 \leq \frac{C_f}{C_l} \leq 3, \text{ with } 0.1 \leq \frac{t_{loss}}{t_{flange}} \leq 0.7}$$

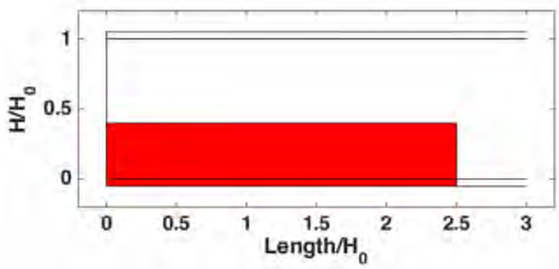

Case B

$$\mathbf{0 < CH_1 < 1H_0,\ 0 < CL_1 < 1H_0}$$

$$\mathbf{0 < \frac{t_{loss}}{t_{web}} \leq 0.4}$$

$1 \leq \frac{C_f}{C_l} \leq 2.5$, with $\frac{t_{loss}}{t_{flange}}$ $taking\ values\ of\ 0.2,\ 0.4,\ 0.6,\ 1$	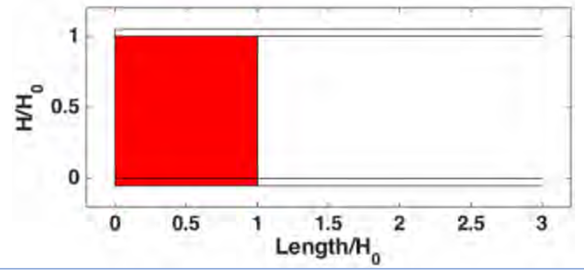

2.3.1.3.2. W3 and W4

Table 19 : Final corrosion patterns for W3 and W4 without holes (beam ends without diaphragm) - CTDOT

Auxiliary Sketch	
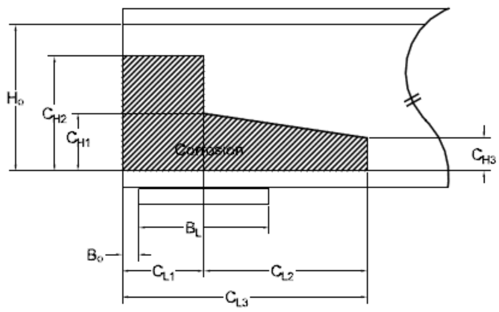	
Description	Pattern W3
Case A $0 < CH_1 < 0.4H_0, 0 < CH_2 < 1H_0, 0 < CH_3 < 0.4H_0, 0 < CL_1 < 1H_0, 0 < CL_2 < 1.5H_0, 0 < CL_3 < 2.5H_0$ $0 < \frac{t_{loss}}{t_{web}} \leq 0.4$ $0 < \frac{C_f}{H_0} \leq 0.4$, with $0 < \frac{t_{loss}}{t_{flange}} \leq 0.4$	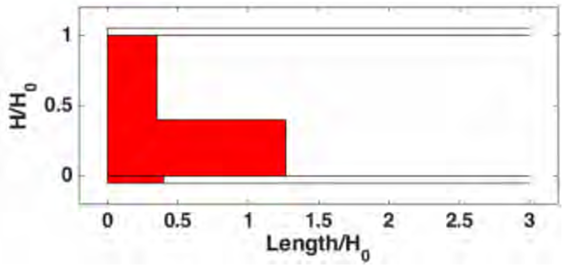

2.3.1.3.3. W5

Table 20: Final corrosion patterns for W5 without holes (beam ends without diaphragm) - CTDOT

Auxiliary Sketch	
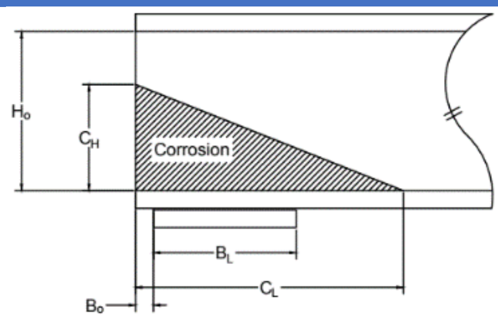	
Description	Pattern W5
Case A $0 < CH_1 < 0.2H_0, 0.4H_0 < CL_1 < 1.5H_0$	

$$0.1 \leq \frac{t_{loss}}{t_{web}} \leq 0.5$$ $$0 < \frac{C_f}{H_0} \leq 1.5, \text{ with } 0 < \frac{t_{loss}}{t_{flange}} \leq 0.4$$	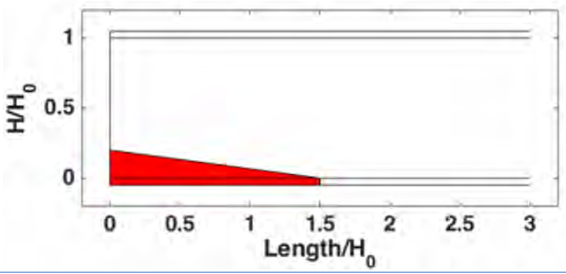

2.3.1.4. Beam ends with a diaphragm system

2.3.1.4.1. W1 and W2

The goal of this section of the report is to describe the interaction between the parameters of the corrosion patterns. To meet this goal, the main trends in patterns W1 and W2 were observed. As commented in the previous sections, patterns W1 and W2 were grouped, as W1 can be expressed from W2 pattern if CL2 is zero.

The existence of the diaphragm makes the understanding of the corrosion problem more difficult, due to the inability to predict the diaphragms' location placement. For this reason, in this section, only observed cases of corrosion are plotted.

From the results, it was observed that beam ends with a diaphragm have two main trends. It was found that in both cases, CL2 is equal to 0. Additionally, the corrosion height was found either to be the full height or up to 40% of H0, as depicted in Table 21.

Table 21: Final corrosion patterns for W1 and W2 without holes (beam ends with diaphragm) - CTDOT

Auxiliary Sketch	
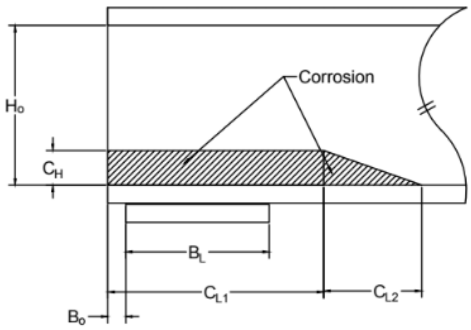	
Description	Pattern W1
Case A (Report 01807, CT, Span 1, G4, Pier 1) $\mathbf{0.1H_0 < CH_1 < 0.3H_0, 0 < CL_1 < 2.5H_0}$ $\mathbf{0 < \frac{t_{loss}}{t_{web}} \leq 0.3}$ $\mathbf{1 \leq \frac{C_f}{C_l} \leq 3, \text{with } 0.1 \leq \frac{t_{loss}}{t_{flange}} \leq 0.4}$	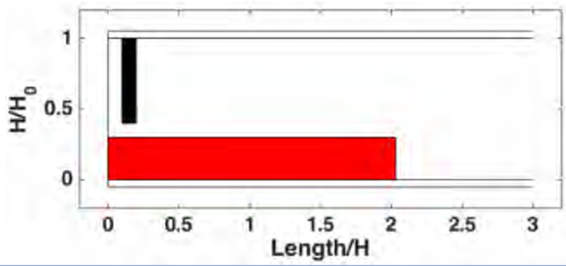
Case B (0 **1732, CT, Span 3, G6, Pier 2)** $\mathbf{0 < CH_1 < 1H_0, 0.2H_0 < CL_1 < 0.4H_0}$ $\mathbf{0.2 \leq \frac{t_{loss}}{t_{web}} \leq 0.4}$ $\mathbf{0 < \frac{C_f}{C_l} \leq 1, \text{with}}$ $\mathbf{\frac{t_{loss}}{t_{flange}} takes\ values\ of\ 0.2, 0.4}$	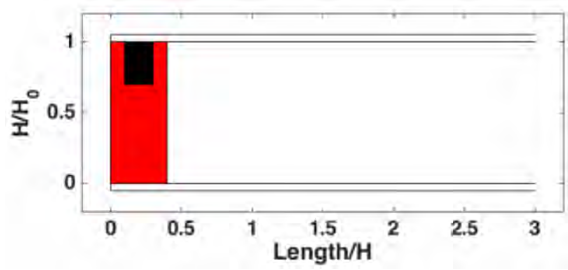

2.3.1.4.2. W3 and W4

Table 22: Final corrosion patterns for W3 and W4 without holes (beam ends with diaphragm) - CTDOT

<table>
<tr><th colspan="2">Auxiliary Sketch</th></tr>
<tr><td colspan="2">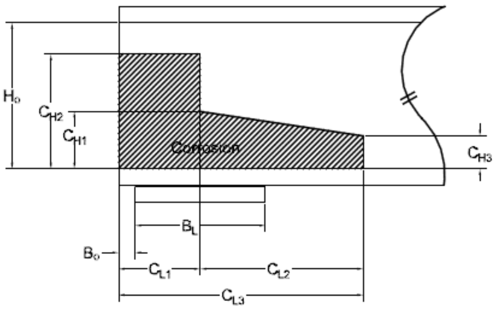
</td></tr>
<tr><td>Description</td><td>Pattern W3</td></tr>
<tr><td>Case A (00281, CT, Span 2, G1, Pier 2, East El)

$$0 < CH_1 < 0.2H_0, 0 < CH_2 < 1H_0, 0 < CH_3 < 0.2H_0, 0.2H_0 < CL_1 < 0.4H_0, 0 < CL_2 < 2H_0, 0.5H_0 < CL_3 < 2.5H_0$$
$$0.1 \leq \frac{t_{loss}}{t_{web}} \leq 0.3$$
$$0 < \frac{C_f}{H_0} \leq 1, \text{with } 0 < \frac{t_{loss}}{t_{flange}} \leq 0.2$$</td><td>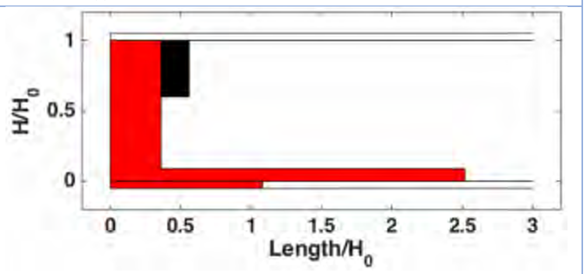
</td></tr>
</table>

2.3.2. Maine

As discussed in the previous sections, the bridge inspection reports did not provide enough documentation to allow the research team to match the corrosion patterns to the existing beams. For this reason, it was not possible to account for the most common corrosion topologies. The results the research team was able to obtain from the documentation provided by MaineDOT can be found in the Appendix section of this report.

2.3.3. Massachusetts

2.3.3.1. General Metrics

Following the two stage post-processing described above, the 808 beam ends were categorized to all the patterns. It must be mentioned that out of the 808, 69 beam ends had no corrosion. Therefore, from this point on there will be 739 beam ends as the total number in the following tables. At this stage, it was decided to group some of the patterns together: W1 with W2, W3 with W4. A further distinction between beam ends with and without diaphragm was also realized. The categorization metrics are shown in Table 23 and Table 24 for all the 739 beam ends.

Table 23: Beam end categorization metrics for beam ends with a diaphragm system

Beam ends with diaphragm									
	Number	**No Hole**	**M1**	**M2**	**M3**	**M4**	**M1 and M2**	**M1 and M3**	**M2 and M4**
W1 and W2	268	235	13	13	5	2	1	0	0
W3 and W4	176	125	35	8	6	2	9	4	1
W5	9	9	0	0	0	0	0	0	0
W6	0	0	0	0	0	0	0	0	0
Total	453	369	48	21	11	4	10	4	1

Table 24 : Beam end categorization metrics or beam ends without a diaphragm system

Beam ends without diaphragm									
	Number	**No Hole**	**M1**	**M2**	**M3**	**M4**	**M1 and M2**	**M1 and M3**	**M2 and M4**
W1 and W2	171	154	13	1	3	0	0	3	0
W3 and W4	96	78	14	0	3	1	0	4	0
W5	17	13	3	1	0	0	0	0	0
W6	2	2	0	0	0	0	0	0	0
Total	286	247	30	2	6	1	0	7	0

From the data shown above, it becomes clear that most of the beam end deterioration does not include holes. In addition, it is also very clear that many beam ends belong to W1, W2, W3 and W4 patterns. Table 25 shows the same categorization according to different districts.

Table 25: Distribution of beam ends according to district

	Total	District 1	District 2	District 3	District 4	District 5
W1	380	2	79	31	9	259
W2	59	4	4	0	2	49
W3	216	7	60	72	20	57
W4	56	1	7	4	0	44
W5	26	3	4	3	0	16
W6	2	0	2	0	0	0

2.3.3.2. Final Corrosion patterns

As mentioned above, the pattern W1 is merged with W2 and pattern W3 is merged with W4. W1 can be expressed from W2 pattern if CL_2 is set to zero. This allowed us to group W1 and W2 into one case which can be carried through the post-processing; there are 3 extreme scenarios identified. It is imperative to note that both the W1 and W2 patterns were examined separately.

Similarly, W3 and W4 can be expressed as a W3 pattern with $Cl_3(W4)=Cl_1$ and $C_{H1}=C_{H3}$. Based on this merge, the cases which were selected as "more dominant" are shown in green in the following two tables. The cases which have a red shade were disregarded as they were very few. In total, the green cases consist of the 91% of all the cases of corroded beam ends which is considered an adequate threshold. The data were divided in 2 main categories, beams ends with diaphragm and without. The dimensions of the pattern are normalized with the height H_0, where $H_0 = H - 2t_f$. It should be mentioned that the final corrosion patterns for the top flange are considered intact, because only at 19 out of 732 beam ends top flange deterioration was reported.

Table 26: Metrics for beam ends with a diaphragm after the merging

Beam ends with diaphragm									
	Frequency	**No Hole**	**M1**	**M2**	**M3**	**M4**	**M1 and M2**	**M1 and M3**	**M2 and M4**
W1 and W2	268	235	13	13	5	2	1	0	0
W3 and W4	176	125	35	8	6	2	9	4	1
W5	9	9	0	0	0	0	0	0	0
W6	0	0	0	0	0	0	0	0	0
Total	453	369	48	21	11	4	10	4	1

Table 27: Metrics for beam ends without a diaphragm after the merging

Beam ends without diaphragm									
	Frequency	No Hole	M1	M2	M3	M4	M1 and M2	M1 and M3	M2 and M4
W1 and W2	171	154	13	1	3	0	0	3	0
W3 and W4	96	78	14	0	3	1	0	4	0
W5	17	13	3	1	0	0	0	0	0
W6	2	2	0	0	0	0	0	0	0
Total	286	247	30	2	6	1	0	7	0

2.3.3.3. Beam ends without a diaphragm system

2.3.3.3.1. W1 and W2

Table 28: Final corrosion patterns for W1 and W2 without holes (beam ends without a diaphragm) - MassDOT

Description	W1 and W2 pattern
Helpful sketch	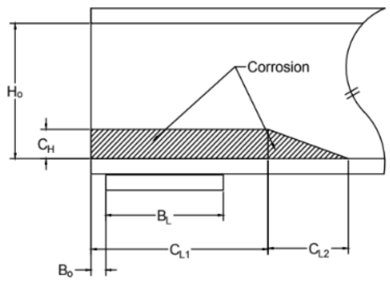
Case A: $0 < CH_1 \le 0.3H_o$, $0< CL_1 \le 1.5H_o$ and $\frac{t_{loss}}{t_{web}}$ *takes values of* {0.2, 0.4, 0.6, 0.8} $1 \le \frac{C_f}{C_l} \le 2$, with $\frac{t_{loss}}{t_{flange}}$ *taking values of* {0.2, 0.4, 0.6, 0.8}	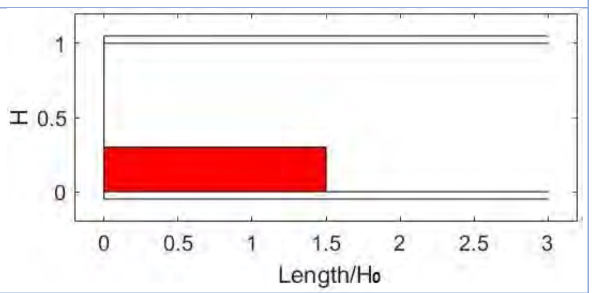
Case B: $CH_1 = H_o$, $0 < CL_1 \le 1.5H_o$ and $\frac{t_{loss}}{t_{web}}$ *takes values of* {0.2, 0.8} $1 \le \frac{C_f}{C_l} \le 2$, with $\frac{t_{loss}}{t_{flange}}$ *taking values of* {0.45, 0.65}	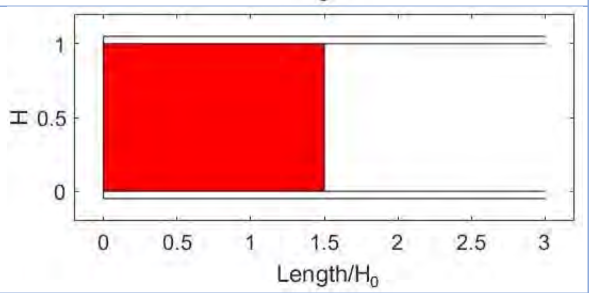

Case C: $\boldsymbol{CH_1 = H_o,\quad 0 < CL_1 \leq 0.5H_o}$ and $\boldsymbol{\frac{t_{loss}}{t_{web}}\, takes\ values}$ **{0.2,0.8}** $\boldsymbol{1 \leq \frac{C_f}{C_l} \leq 2}$, with $\boldsymbol{\frac{t_{loss}}{t_{flange}}\, taking\ values\ of}$ $\{\boldsymbol{0.45, 0.65}\}$	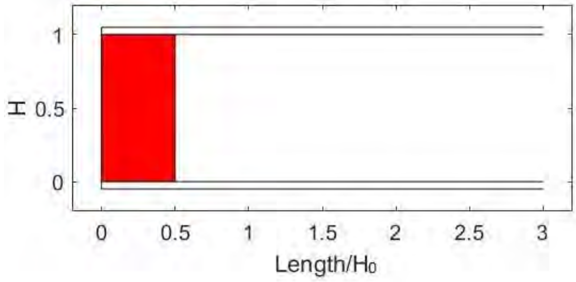

2.3.3.3.2. M1 hole pattern

Table 29: Final corrosion patterns for W1 and W2 with holes (beam ends without a diaphragm) - MassDOT

Description	W1 and W2 pattern
Helpful sketches	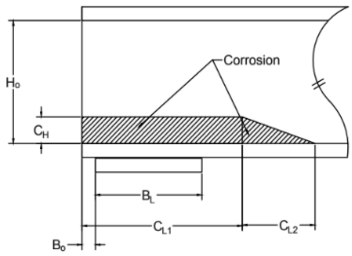 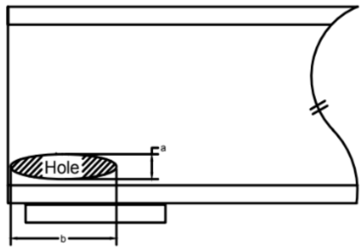
<u>The extreme scenario is projected on the W1 and W2 Case C:</u> The extreme hole scenario was found on W2, with a=0.15 and b=0.5.	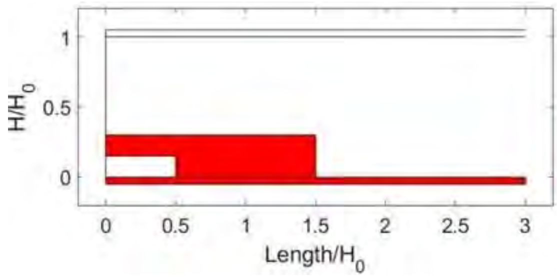

2.3.3.3.3. W3 and W4

Table 30: Final corrosion patterns for W3 and W4 without holes (beam ends without a diaphragm) - MassDOT

Description	W3 and W4 pattern
Helpful sketch	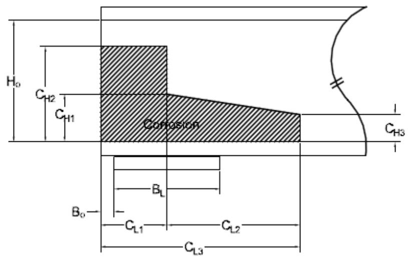
<u>The extreme scenario is:</u> $\mathbf{0 < CH_1 \leq 0.35H_o,\ 0 < CH_3 \leq 0.35H_o}$ $\mathbf{0.05H_o < CL_1 \leq 0.7H_o, 0.5H_o < CL_3 \leq 2.3H_o}$ $\frac{t_{loss}}{t_{web}}$ **taking values of** $\{0.1,0.2,0.3,0.4,0.5,0.6,0.7,0.8\}$ $\frac{C_f}{C_{L3}} = 1$, with $\frac{t_{loss}}{t_{flange}}$ **taking values of** $\{0.4, 0.6, 0.8\}$	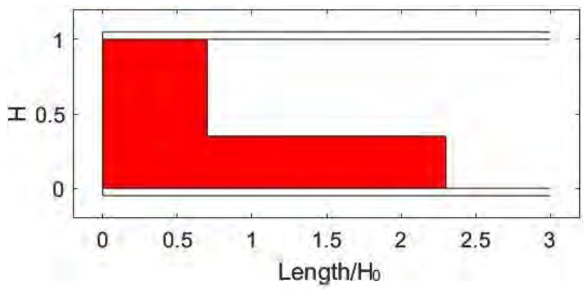

2.3.3.3.4. M1 hole pattern

Table 31: Final corrosion patterns for W3 and W4 with holes (beam ends without a diaphragm) - MassDOT

<table>
<tr><th>Description</th><th>W3 and W4 pattern</th></tr>
<tr><td colspan="2">Helpful sketches
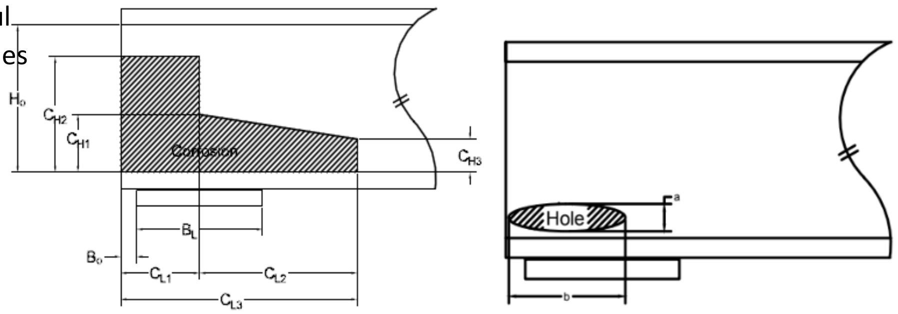
</td></tr>
<tr><td><u>The extreme scenario is:</u>
Holes seem to be mainly thin and long across the web, with the extreme case a=0.21H₀ and b=0.63H₀.</td><td>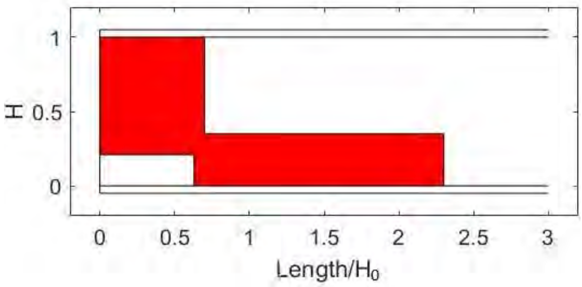
</td></tr>
</table>

2.3.3.3.5. W5

Table 32: Final corrosion patterns for W5 without holes (beam ends without a diaphragm) - MassDOT

<table>
<tr><th>Description</th><th>W5 pattern</th></tr>
<tr><td colspan="2">Helpful sketch
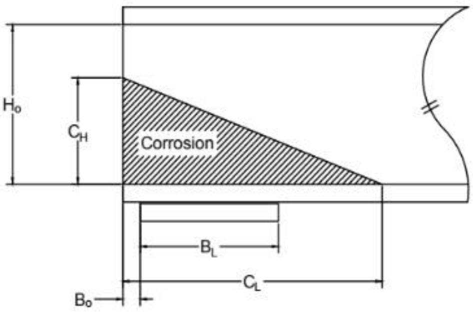
</td></tr>
<tr><td><u>The extreme scenario is:</u>
$0.15H_o \leq CH_1 \leq 1H_o,\ 0 < CL_1 \leq 0.35H_o$
$\frac{t_{loss}}{t_{web}}$ takes values of {0.2,0.5}, $1 \leq \frac{C_f}{C_{L3}} \leq 1.8$, with
$\frac{t_{loss}}{t_{flange}}$ taking values of {0.1, 0.8}</td><td>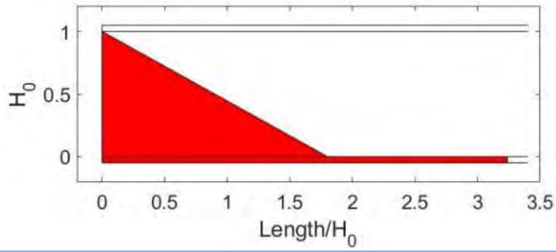
</td></tr>
</table>

2.3.3.4. Beam ends with diaphragm

2.3.3.4.1. W1 and W2

Table 33: Final corrosion patterns for W1 and W2 without holes (beam ends with a diaphragm) - MassDOT

Description	W1 and W2 pattern
Helpful sketch	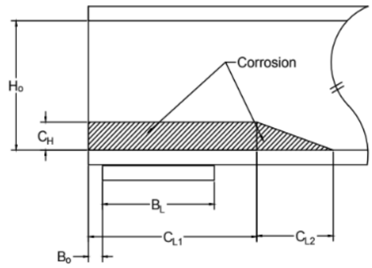
Case A: 0< $CL_1 \le 0.35H_o$, $\frac{t_{loss}}{t_{web}}$ *tkaing values of* {0.2,0.4,0.6,0.8} Flange: $0.15 < \frac{t_{loss}}{t_{flange}} \le 0.45$, 1≤ $\frac{Cf}{Cl} \le 1.7$	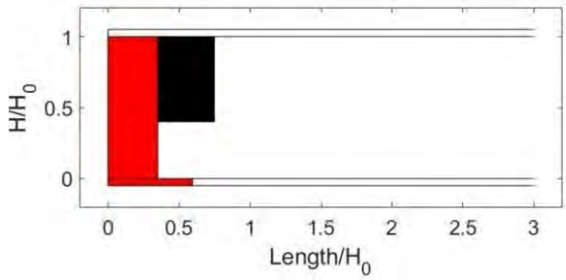
Case B: $0 < CL_1 \le 2.5H_o$, $\frac{t_{loss}}{t_{web}}$ *taking values of* $\{0.2, 0.4, 0.6, 0.8\}$ Flange:0≤ $\frac{Cf}{Cl} \le 1$, $\frac{t_{loss}}{t_{flange}}$ *taking values of* $\{0.2, 0.4, 0.6, 0.8\}$	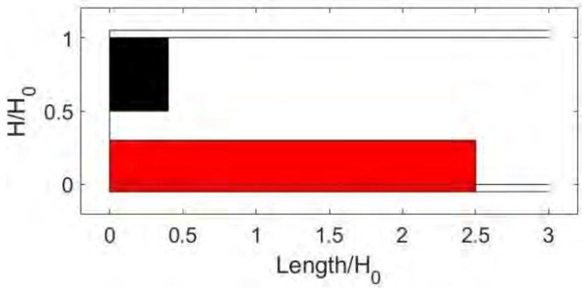
Case C: $0 < CH_1 \le 0.5H_0$, $0 < CL_1 \le 0.6H_0$ $0 < CL_2 \le 1.8H_0$, $\frac{t_{loss}}{t_{web}}$ *taking values of* {0.2,0.4,0.6,0.8} $1 < \frac{Cf}{Cl} \le 2$, $\frac{t_{loss}}{t_{flange}}$ *taking values of* {0.2,0.4,0.6,0.8}	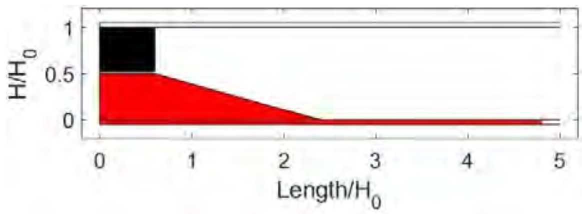

Case A is the first extreme corrosion scenario in the web and flange, with full height corrosion and length up to 35% of H0. The corroded area is often located before the diaphragm, which is illustrated with black in the figures of this report. Case B is the second extreme corrosion scenario in the web and flange. The corroded area extends longitudinally in the web above the flange. Case C is the third extreme corrosion scenario in the web and flange.

2.3.3.4.2. M1 Holes

Table 34: Final corrosion patterns for W1 and W2 with holes (beam ends with a diaphragm) - MassDOT

<table>
<tr><th>Description</th><th>W1 and W2 pattern</th></tr>
<tr><td>Helpful sketches
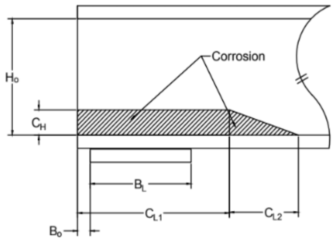
</td><td>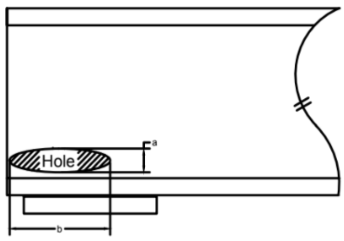
</td></tr>
<tr><td>M1 holes were equally distributed between web corrosion scenarios CASE A and CASE B, with maximum length $1.4H_0$ and height $0.21H_0$. M2 mainly appeared in the third scenario.</td><td>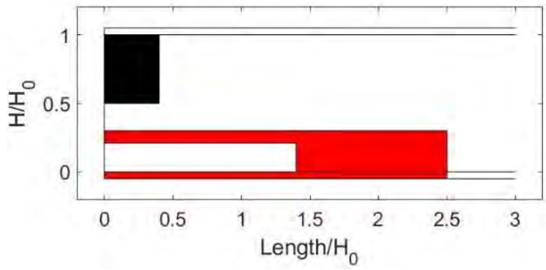
</td></tr>
</table>

2.3.3.4.3. M2 Holes

Table 35: Final corrosion patterns for W1 and W2 with holes (beam ends with a diaphragm) - MassDOT

<table>
<tr><th>Description</th><th>W1 and W2 pattern</th></tr>
<tr><td>Helpful sketches
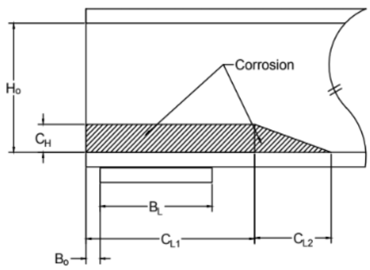
</td><td>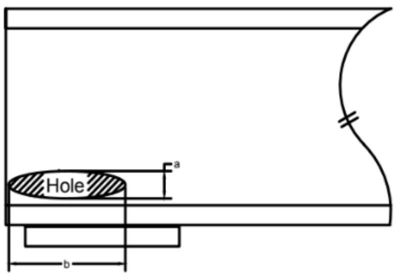
</td></tr>
<tr><td>M2 hole pattern projected on the extreme third web corrosion pattern. With black color is illustrated the diaphragm in a possible configuration, with a<=0.11, and b<=0.3.</td><td>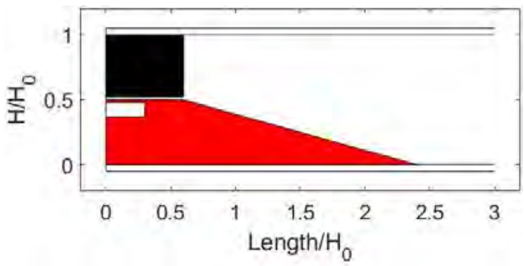
</td></tr>
</table>

2.3.3.4.4. W3 and W4

As discussed earlier in the report, W3 and W4 were merged for analysis. However, in this case, both patterns were examined separately, and three extreme scenarios were identified. It was noticed that extreme scenarios of W3 are the most critical. Following this, two main trends were found: a) full height corrosion, or b) corrosion up to 30% of H_0.

Table 36: Final corrosion patterns for W3 and W4 without holes (beam ends with a diaphragm) - MassDOT

Description	W3 and W4 pattern
Helpful sketch	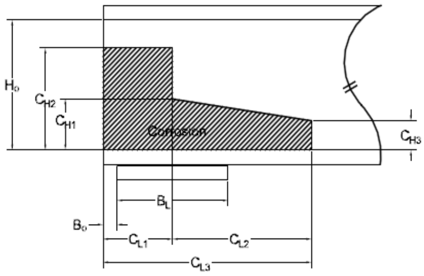
Case A: $0.25H_0 < CL_3 \leq 0.6H_0$, $0.1H_0 < CL_1 \leq 0.2H_0$ $0.06H_0 < CH_1 = CH_3 \leq 0.16H_0$, $\frac{t_{loss}}{t_{web}}$ *takes values of* $\{0.4, 0.6\}$ $\frac{Cf}{Cl} = 1.2$ and $\frac{t_{loss}}{t_{flange}}$ *takes values of* $\{0.3, 0.6\}$	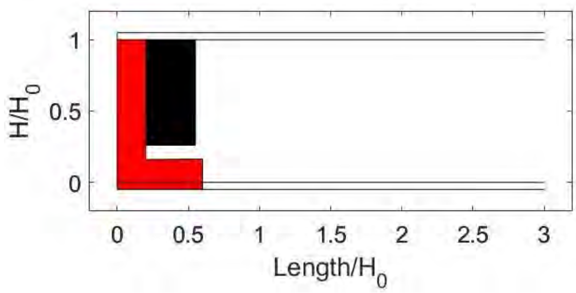
Case B: $0.6H_0 < CL_3 \leq 2.3H_0$, $0.2 < CL_1 \leq 0.6H_0$ $0.05 < CH_1 = CH_3 \leq 0.30H_0$, $\frac{t_{loss}}{t_{web}}$ *takes values of* $\{0.4, 0.6, 0.8\}$, $\frac{Cf}{Cl} = 1$ and, $\frac{t_{loss}}{t_{flange}}$ *takes the value of* $\{0.65\}$	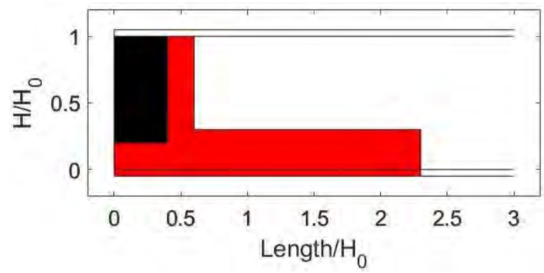
Case C: $0.5H_0 < CL_3 \leq 3H_0$, $0.1H_0 < CL_1 \leq 0.75H_0$ $0.05H_0 < CH_1 \leq 0.25H_0$, $0.05H_0 < CH_3 \leq 0.18H_0$, $\frac{t_{loss}}{t_{web}}$ *takes values of* $\{0.4, 0.6, 0.8\}$ $\frac{Cf}{Cl} = 1$ and $\frac{t_{loss}}{t_{flange}}$ *takes values of* $\{0.3, 0.6, 0.8\}$	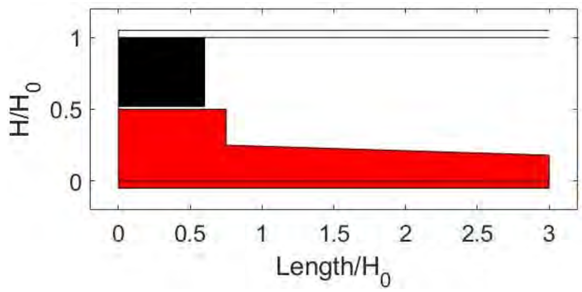

2.3.3.4.5. M1 Holes

Table 37: Final corrosion patterns for W3 and W4 with holes (beam ends with a diaphragm) - MassDOT

<table>
<tr><th>Description</th><th>W3 and W4 pattern</th></tr>
<tr><td>Helpful sketches
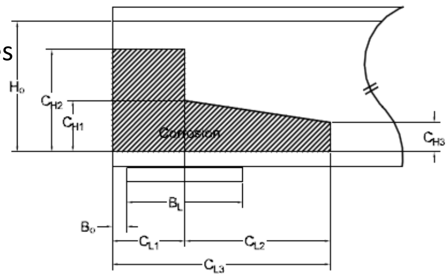
</td><td>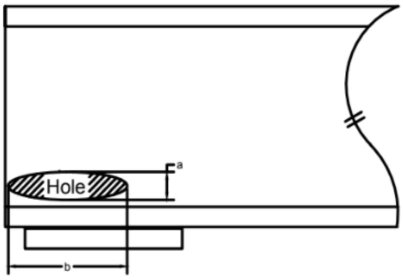
</td></tr>
<tr><td>Holes appeared mainly with a full height corroded web and they seem to be mainly thin and long across the web. Most of the cases have ratio of hole's length to height up to 6, and length up to 50% of H$_o$. Thus, for the extreme hole scenario, hole's height is considered as 0.083.

For W4, M1 hole appears as pit hole (0.0044 x 0.0044).</td><td>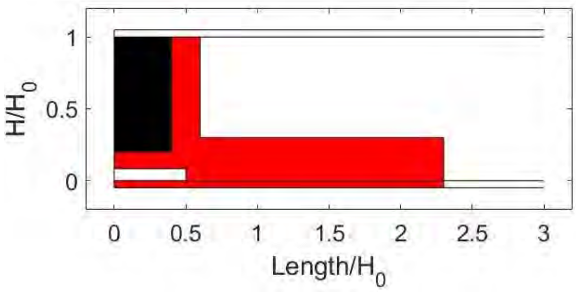
</td></tr>
</table>

2.3.3.4.6. M2 Holes

Table 38: Final corrosion patterns for W3 and W4 with holes (beam ends with a diaphragm) - MassDOT

<table>
<tr><th>Description</th><th>W3 and W4 pattern</th></tr>
<tr><td>Helpful sketches
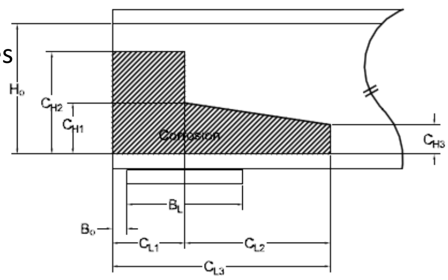
</td><td>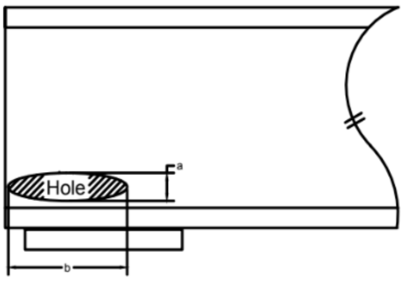
</td></tr>
<tr><td>M2 holes were examined together for both patterns W3 and W4 because there were found only 7 times. The extreme hole scenario with a$\leq$ $\mathbf{0.1}$ and b$\leq$ $\mathbf{0.25}$ is projected on the Case B extreme web corrosion scenario.</td><td>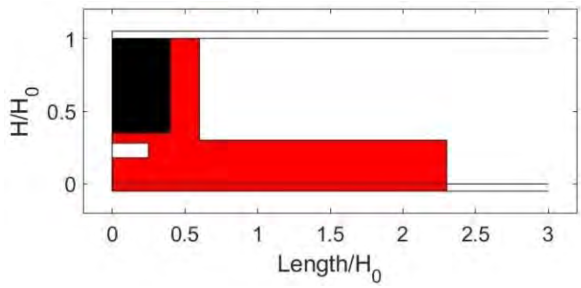
</td></tr>
</table>

2.3.3.4.7. W5

Table 39: Final corrosion patterns for W5 with holes (beam ends with a diaphragm) - MassDOT

Description	W5 pattern
Helpful sketch	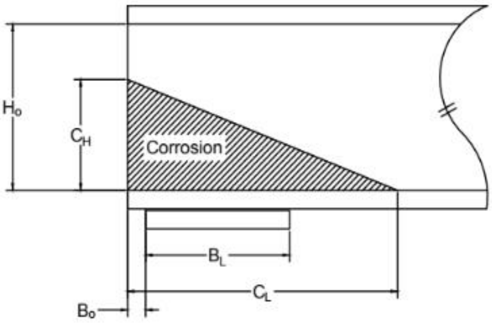
$0.3H_0 \leq CL_1 \leq 0.85H_0, 0.15H_0 < CH_1 \leq 0.30H_0$ $\frac{t_{loss}}{t_{web}}$ *takes the value* $\{0.35\}$ $\frac{t_{loss}}{t_{flange}}$ *takes the values* $\{0.3,0.6,0.8\}$ with $\frac{C_f}{C_l}$ *taking the values of* $\{1, 1.6\}$	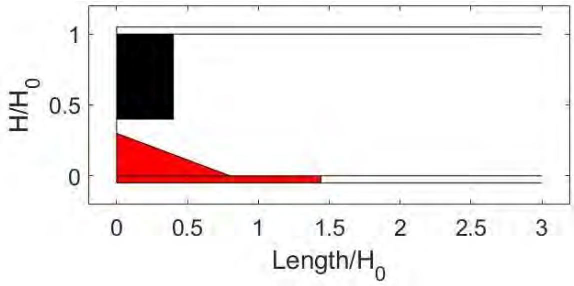

2.3.4. New Hampshire

As described earlier, the bridge inspection reports from the state of New Hampshire did not provide enough documentation to allow the research team to match corrosion patterns to current damage in the beams of the bridge structures. For this reason, it was not possible to account for the most common corrosion topologies. The results the research team was able to obtain from the documentation provided by NHDOT can be found in the Appendix of this report.

2.3.5. Rhode Island

2.3.5.1. General Metrics

Following the methodology explained above, the research team was able to compile information on 88 beam ends from the inspection reports provided by RIDOT. It is important to note that beam ends without corrosion are not considered in this count. To ease the understating of the behavior of corrosion and extract more meaningful results, patterns W1 and W2 were grouped, as well as patterns W3 and W4. With these groupings, the research team was able to easily distinguish the relevant web corrosion patterns and relevant hole patterns present in the bridge structures for the state of Rhode Island. Table 40 and Table 41 depict the results obtained by grouping the corrosion patterns of beams with and without diaphragm.

Table 40: Beam end categorization metrics for beam ends without a diaphragm

	Frequency	No Hole	M1	M2	M3	M4	M1 and M2	M1 and M3	M2 and M4
W1 and W2	26	24	2	0	0	0	0	0	0
W3 and W4	21	19	0	0	1	1	0	0	0
W5	4	4	0	0	0	0	0	0	0
W6	0	0	0	0	0	0	0	0	0
Total	51	47	2	0	1	1	0	0	0

Table 41: Beam end categorization metrics for beam ends with a diaphragm

	Frequency	No Hole	M1	M2	M3	M4	M1 and M2	M1 and M3	M2 and M4
W1 and W2	28	25	2	0	1	0	0	0	0
W3 and W4	9	8	0	0	0	1	0	0	0
W5	0	0	0	0	0	0	0	0	0
W6	0	0	0	0	0	0	0	0	0
Total	37	33	2	0	1	1	0	0	0

2.3.5.2. Final Corrosion patterns

From the data shown above, it becomes clear that most of the beam end deterioration does not include holes. In addition, it is also very clear that most of the beam ends belong to W1, W2, W3 and W4 patterns. It is worthwhile pointing out that although patterns W1 and W2 and W3 and W4 were grouped together, these patterns were separately analyzed. Besides that, the results of isolated patterns can be found in the appendix.

Based on Table 40 and Table 41, the research group was able to determine the most dominant cases, which are shaded in green in Table 42 and Table 43. On the other hand, cases shaded in red were disregarded, as they were very view.

Table 42: Dominant cases for beams without a diaphragm

	Number	No Hole	M1	M2	M3	M4	M1 and M2	M1 and M3	M2 and M4
W1 and W2	26	24	2	0	0	0	0	0	0
W3 and W4	21	19	0	0	1	1	0	0	0
W5	4	4	0	0	0	0	0	0	0
W6	0	0	0	0	0	0	0	0	0
Total	51	47	2	0	1	1	0	0	0

Table 43: Dominant cases for beams with a diaphragm

	Number	No Hole	M1	M2	M3	M4	M1 and M2	M1 and M3	M2 and M4
W1 and W2	28	25	2	0	1	0	0	0	0
W3 and W4	9	8	0	0	0	1	0	0	0
W5	0	0	0	0	0	0	0	0	0
W6	0	0	0	0	0	0	0	0	0
Total	37	33	2	0	1	1	0	0	0

2.3.5.3. Beams ends without a diaphragm

2.3.5.3.1. W1 and W2

Based on the 49 appearances of the W1 and W2 patterns without a diaphragm, our team was able to determine the most common cases regarding web and flange corrosion for each, and the most common interaction between the parameters of a pattern. Table 44, Table 45 and Table 46 depict the most common trends observed in the compiled data. The graphs which allowed one to observe these behaviors can be found in the Appendix of this report.

Table 44: Final corrosion patterns for W1 and W2 without holes (beam ends without a diaphragm) - RIDOT

Auxiliary Sketch

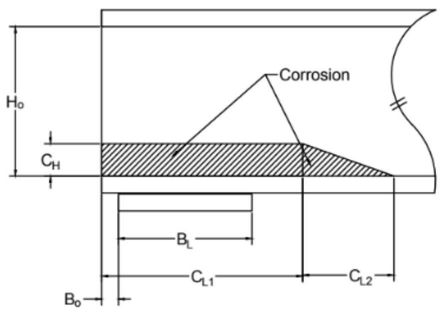

Description

Pattern W1

Case A

$$0 < CH_1 < 0.5H_0, 0 < CL_1 < 3H_0$$

$$0 < \frac{t_{loss}}{t_{web}} \leq 0.3$$

$$1 \leq \frac{C_f}{C_l} \leq 3, \text{with } 0.2 \leq \frac{t_{loss}}{t_{flange}} \leq 0.7$$

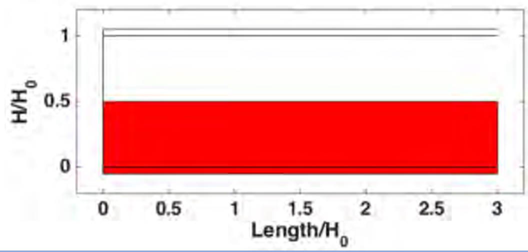

Case B

Extreme Scenario

$$0 < CH_1 < 0.5H_0, 0 < CL_1 < 9.2H_0$$

$$0 < \frac{t_{loss}}{t_{web}} \leq 0.3$$

$0 < \frac{C_f}{C_l} \leq 6.4$, with $\frac{t_{loss}}{t_{flange}}$ *taking values of* $\{0.2\}$	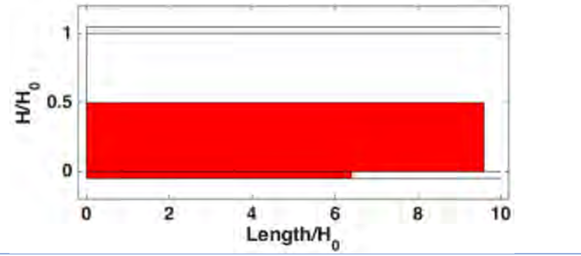

2.3.5.3.2. W3 and W4

Table 45: Final corrosion patterns for W3 and W4 without holes (beam ends without a diaphragm) - RIDOT

Auxiliary Sketch	
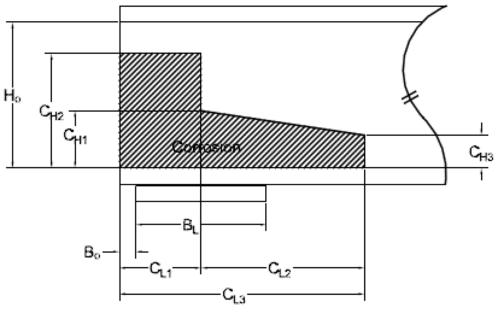	
Description	Pattern W3
Case A $0 < CH_1 < 0.6H_0$, CH_2 *takes the value of* $\{1H_0\}$, $0.5H_0 < CH_3 < 2.5H_0$, $0 < CL_1 < 0.5H_0$, $0.3H_0 < CL_2 < 2H_0$, $0.5H_0 < CL_3 < 2.5H_0$ $0 < \frac{t_{loss}}{t_{web}} \leq 0.5$ $0 < \frac{C_f}{H_0} \leq 2$, with $0 < \frac{t_{loss}}{t_{flange}} \leq 0.6$	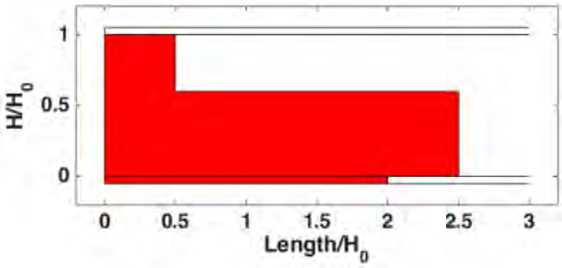

2.3.5.4. Beams ends with a diaphragm

2.3.5.4.1. W1 and W2

The goal of this section was to understand the interaction between the parameters of the corrosion patterns. To do this, the main trends in patterns W1 and W2 were observed. As discussed in the previous sections, patterns W1 and W2 were grouped. Our team was able to generate W1 from W2, i.e., W1 can be expressed from the W2 pattern if CL2 is zero.

Additionally, the existence of the diaphragm makes the understating of the problem harder, as one is not able to predict where the diaphragm will be placed. For this reason, in this section, only observed cases of corrosion were plotted.

Table 46 : Final corrosion patterns for W1 and W2 without holes (beam ends with a diaphragm) - RIDOT

Auxiliary Sketch	
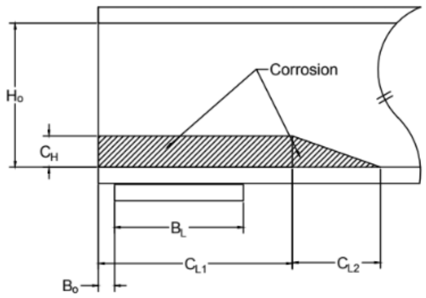	
Description	Pattern W1
Case A (Report 01807, CT, Span 1, G4, Pier 1) $0 < CH_1 < 0.2H_0, 0.3H_0 < CL_1 < 2.5H_0$ $0.1 \le \frac{t_{loss}}{t_{web}} \le 0.3$ $0.3 \le \frac{c_f}{c_l} \le 3$, with $0.1 \le \frac{t_{loss}}{t_{flange}} \le 0.3$	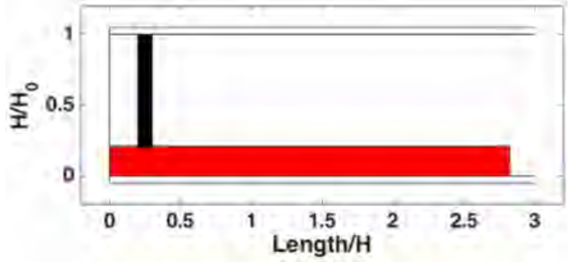
Case B **Extreme Scenario (042801, RI, P2, Gk,S3)** $0 < CH_1 < 1H_0, 0 < CL_1 < 0.6H_0$ $0.1 \le \frac{t_{loss}}{t_{web}} \le 0.7$	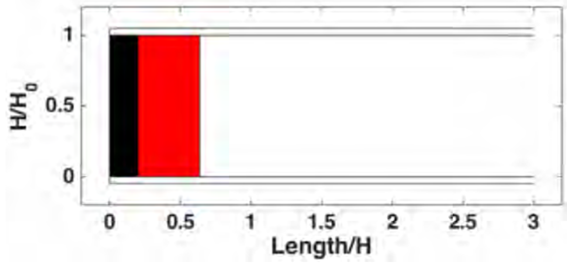

2.3.6. Vermont

As discussed earlier in the report, the bridge inspection reports did not provide enough documentation to allow the research team to match the corrosion patterns. For this reason, it was not possible to account for the most common corrosion topologies. The results the research team were able to obtain from the documentation provided by VTrans can be found in the Appendix of this report.

3. Conclusions

In this task of the project, our team analyzed 225 reports from six states in the New England region; Connecticut, Rhode Island, Maine, New Hampshire, Vermont, and Massachusetts. This allowed for the analysis of 1,723 total beam ends across all the states. The most important finding that we found through this analysis was the vast presence of the W1 corrosion pattern across the beam ends of the New England states. While this was the most important finding in this task, there were many trends our team noticed among reporting and beam end conditions upon analysis of the state inspection reports.

Several trends were found after compiling, summarizing, and post processing data obtained from the states of the New England region. These trends reflect several important components of this project and the goal of this work overall. Reflecting on the tasks of the project and this report, our team observed these trends to be categorized by two types, the way states report the inspection of a bridge structure and the corrosion patterns observed in those bridge structures via the inspection reports.

Inspection Report Comparisons Among New England States

When considering the reporting methods of each state, our team concluded that sub-dividing the New England region was helpful to the post-processing of data. As discussed in the report, the state's departments of transportation were placed into two groups:

- MaineDOT, NHDOT and VTrans in Group 1 and
- RIDOT, MassDOT and CTDOT in Group 2.

It is important to note that inspection reports where no data could be gathered were not included in the finalized conclusions, data, and graphs of this report.

The trends found in terms of inspection reports can be summarized as follows:

- The most common trend found in the methods of inspection were that the Northern New England States (Group 1) have inspection reports which rarely provide sketches where the Southern New England States (Group 2) often provide sketches and photographs. It is again important to note that the methods of Group 2 were developed over time and had performed inspection methods much like those of Group 1 until nearly recently.
- An additional trend that was identified was the span of years in which many of these bridge structures were built. There were trends identified at a state and regional level. It is important to note here that there was only one report in our finalized compilation from **Vermont** which indicated the year a single bridge was built (1991). The majority of bridges our team analyzed in the New England region were built between 1928 and 1978. We then separated this information by state. For **Connecticut**, many bridges were built between 1955 and 1970. Regarding **Massachusetts**, most of the bridges were built between 1947 and 1969. For the state of **Maine**, our team found that many bridges were built between 1928 and 1991. Regarding **Rhode Island**, we found that all of the bridges analyzed were built between 1935 and 1975. For the state of **New Hampshire**, most of the bridges analyzed were built between 1920 and 1994. This information is

imperative in order to identify the grade of steel and the beam dimensions used for the steel beams used in construction.

- Another common trend found in several reports from Group 1 is the way corrosion is reported. In many reports from the states in Group 1, corrosion information is provided in a generic form, which results from a visual inspection. No finite measurements and thickness losses were reported. Some conclusions our team was able to draw from these reporting trends were that while reporting and documenting corrosion varies from state to state, there tended to be general uniformity among the report structures. This allowed our team to compile the reports more efficiently.

Corrosion Phenomenon Comparisons Among New England States

At a general level, the results of post-processing data analysis for the inspection reports can be divided into two groups as discussed above. While the results in previous sections of this report focus on the presentation of the reports by each New England state, this information ultimately determines the corrosion pattern results. In the case of Group 1, MaineDOT, NHDOT and VTrans, the reports provided do not present sufficient documentation to create common corrosion patterns for their states. This documentation primarily refers to sketches or dimensional measurements, which is likely not provided due to inspections being visually conducted.

This allowed our research team to further isolate results of the states of the New England region who had sufficient documentation to allow for the creation of common corrosion patterns found by state. These states departments of transportation were in Group 2, which included RIDOT, MassDOT, and CTDOT. Upon isolating the states that provided enough information, each state had patterns generated specific to the data gathered from their reports. These patterns included the several types of corrosion shapes and damage discussed earlier in this report. Additionally, the patterns considered structures with and without diaphragms as part of the structural system. It can be observed that the presence of a diaphragm changes the corrosion patterns observed and is considered a separate pattern from structures without diaphragms.

There are several conclusions that can be drawn from the data analyzed by Massachusetts, Rhode Island, and Connecticut **when a diaphragm system is present**. Each state has its most prominent corrosion pattern found in the reports:

- For **Massachusetts**, the most common corrosion pattern was the W1 corrosion pattern closely followed by the W3 corrosion pattern. Regarding the state of **Rhode Island**, the most common corrosion pattern was W1. For the state of **Connecticut**, the most common corrosion pattern was W1 corrosion.
- It can be seen from the states which corrosion patterns could be generated for bridges with diaphragms present, that the W1 corrosion pattern is the most prevalent.
- Across all patterns and states with a diaphragm present, it was found that the thickness loss had great range from no thickness loss to complete thickness loss.
- The most prominent range for thickness loss was around 18% to 55% across all states and corrosion patterns for structures with diaphragms.

- In addition to the corrosion shapes, there were also holes observed in the beam end specimens with a diaphragm present from the different states. Among the data from **Connecticut, Massachusetts,** and **Rhode Island**, it was found that the M1 hole corrosion pattern was the most common.
- The following conclusions discuss the corrosion measurement parameters, shapes, and the trends found. It is worth noting again that this section only applies to **Connecticut, Massachusetts,** and **Rhode Island** where corrosion parameters and patterns could be identified and generated.
    - Our team discovered that among beams with a diaphragm system that the W1 pattern has parameters that followed a very interesting trend; the CH height parameter had many cases varying from minimal height corrosion to half height corrosion. Additionally, our team saw that in the **Connecticut** and **Massachusetts** specimens specifically, full height corrosion showed a strong presence. This is very different from the CH height parameter for beams without a diaphragm, which had many cases varying from minimal height corrosion to half height corrosion. Via the parameter graphics created for the CL parameters in **Massachusetts** and **Rhode Island,** it appeared that many of the beam ends had smaller ranges for corrosion length when compared to beam ends without a diaphragm system present. This is particularly interesting because the W1 corrosion pattern was the most prominent corrosion pattern identified in the analysis.
    - Another interesting trend our team found in the analysis was in the parameters of the W3 corrosion pattern. Our team found that the most intriguing of the parameters here were the CH2 height parameter and the CL3 length parameter. These parameters represent the largest height and length in the W3 corrosion pattern, respectively. In the case of beams with a diaphragm present, the CH2 parameter often equaled full height corrosion. Regarding the CL3 parameter for the W3 case with a diaphragm system, the length had large variation. Our team observed extreme cases in which CL3 was approximately 500% of the web height in Massachusetts. Among Connecticut and Rhode Island, there were cases that reached around 250% and 300% of web height, respectively.

There are several conclusions that can be drawn from the data analyzed by Massachusetts, Rhode Island, and Connecticut **when no diaphragm system is present**. Each state has its most prominent corrosion pattern found in the reports:

- For **Massachusetts**, the most common corrosion pattern was W1 corrosion. The state of **Rhode Island** had W1 as its most common corrosion pattern but also had several W3 corrosion patterns present throughout the bridge specimens. Regarding **Connecticut**, the most common corrosion pattern was W1 corrosion.
- It can be seen from the states which corrosion patterns could be generated for bridges without diaphragms present, that the W1 corrosion pattern is the most common.
- Across all patterns and states without a diaphragm present, it was found that the web thickness loss had great range from no thickness loss to complete thickness loss. The most prominent range for thickness loss was around 18% to 50% across all states and corrosion patterns.

- Similar to the structures with a diaphragm, there were also holes observed in the beam end specimens without a diaphragm present from the different states. From the data analyzed and compiled from **Massachusetts, Rhode Island,** and **Connecticut,** it was found that the M1 hole corrosion pattern was the most prevalent.
- The following conclusions discuss the corrosion measurement parameters, shapes, and the trends found. It is worth noting again that this section only applies to **Connecticut, Massachusetts,** and **Rhode Island** where corrosion parameters and patterns could be identified and generated.
    - Our team discovered that among beams without a diaphragm system that the W1 pattern, the most prominent pattern, has parameters that followed a very interesting trend; the CH height parameter was often less than half of the height of a given beam. This was true across **Rhode Island**, **Connecticut**, and **Massachusetts**. While this was true for the height, the length parameter CL varied from minimal length corrosion to a length corrosion of approximately 300% the height of the web. Among **Rhode Island**, **Connecticut**, and **Massachusetts**, the corrosion length maximum was greater than the full web height. This is particularly interesting because the W1 corrosion pattern was the most prominent corrosion pattern identified in the analysis.
    - An interesting trend our team found in the analysis was in the parameters of the W3 corrosion pattern. As discussed above, our team found that the most intriguing of the parameters here were the CH2 height parameter and the CL3 length parameter. These parameters represent the largest height and length in the W3 corrosion pattern, respectively. In the case of beams with a diaphragm present, the CH2 parameter often equaled full height corrosion. A critical note here is that this was also the case when a diaphragm is present, as described above. Similar to cases with a diaphragm, the CL3 parameter for the cases of W3 without a diaphragm system had large variation in the length. Our team observed extreme cases in which CL3 had extreme cases in **Connecticut** and **Massachusetts**. These were approximately 300% and 225% of web height, respectively. The interesting part of both the height and length measurements for the W3 corrosion patterns was the similarity regardless if a diaphragm is present.

The comparison of these corrosion patterns may suggest that many similarities arise among the parameters of given corrosion patterns throughout the states of New England.

Connection with next phases of the project

These findings are crucial to our work on this project for several reasons. Recognizing corrosion patterns and thickness losses across the beams of several states allowed our team to sort and generate data for the next part of this project. Once the damage done by corrosion to beam end specimens can be identified and understood, the goal then becomes finding the remaining beam capacity. Based on the common corrosion patterns and thickness loss measurements, the remaining capacity of the beams can be found.

The main conclusions that can be drawn from the analyses conducted and discussed throughout this report is that corrosion patterns can be generated, as there are clear trends identified of the phenomenon These trends are helpful in identifying types of damage and will ultimately contribute to finding the remaining capacity of a beam and the overall bridge structure.

Compiling and analyzing bridge inspection reports to identify corrosion patterns and trends from state to state does not directly give our team the remaining capacity of the bridge. While this is true, it provides great insight and information to ensure we can fulfill the task of calculating and experimenting to find the capacity of the corroded beam ends and provide new and more accurate procedures which will be used by the New England DOTs for assessing the remaining capacity of corroded beam ends. Infrastructure continuously needs to be repaired and maintained, especially in its current condition throughout the United States. This work is critical to assist in ensuring our nation's, and our world's structures are serviceable and safe for the public for whom we serve.

Within this work, there were limitations in the main corrosion patterns our team was able to identify for each state. If a bridge inspection was conducted and corrosion is reported qualitatively, measurement parameters become difficult to establish. This limitation ultimately means that corrosion patterns cannot be generated. Another limitation of the work is the amount of data that can be received and used for the project. This could be lack of information presented in the inspection reports, minimal inspection reports to process, and the overall validity of the beams via the scope of the project.

The next task in this project will be to isolate bridge beams even further to determine ideal candidates for laboratory tests. The corrosion patterns and thickness loss identified in this report will be helpful in identifying these potential beam candidates and their remaining capacity after corrosion occurs.

4. Appendix I – Detailed data and processing graphs for beam ends without a diaphragm

4.1. Connecticut

4.1.1. Introduction

As discussed in previous sections, the data was divided by state as the number of beams ends was significantly different from one state to the other. Thus, to not introduce bias in the results, all states were individually analyzed. Beyond this, the beam ends were divided into two sub-groups: ends with diaphragm and the ends without diaphragms. In this section, all information and graphs presented focus on beams ends without diaphragms from the state of Connecticut.

Figure 27 depicts the frequency of patterns obtained for beam ends without diaphragm from the reports provided by CTDOT.

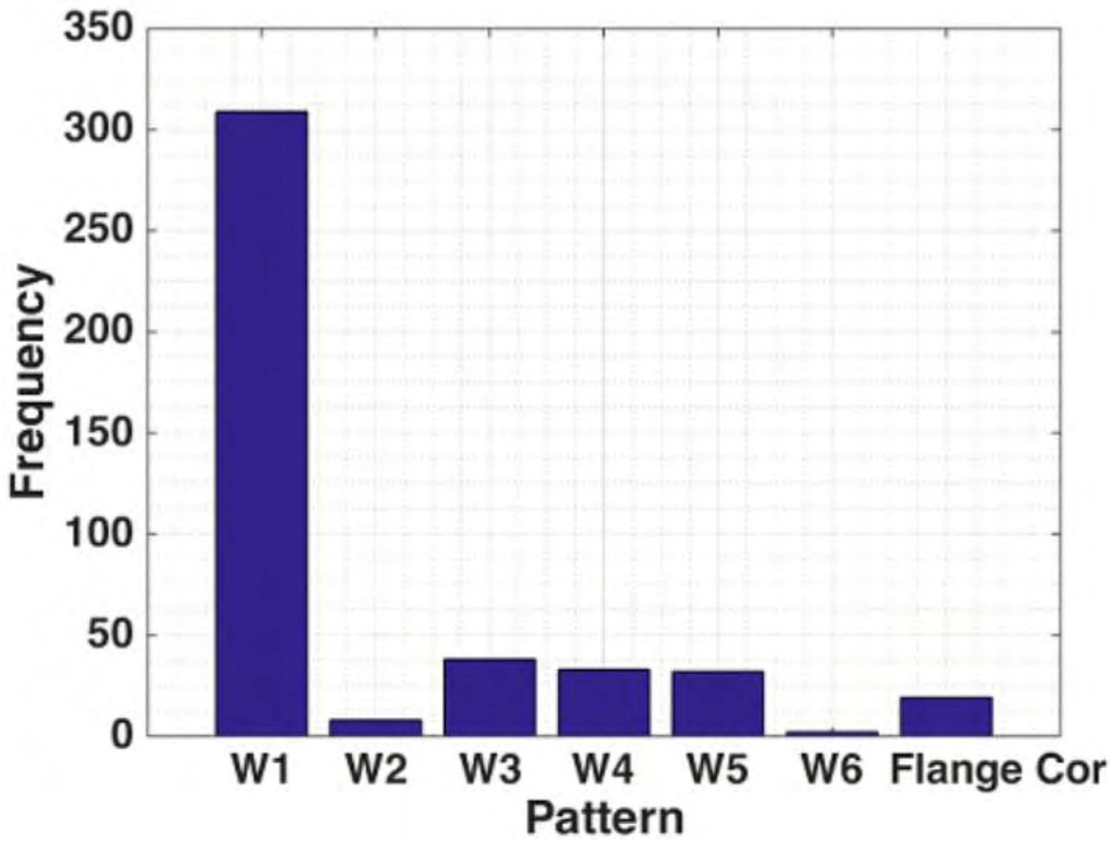

Figure 27: Web corrosion patterns distribution for beams ends without a diaphragm – CTDOT

It is worthwhile pointing out that the characteristic dimensions of the patterns - i.e., CH1, CH2, CH3, CL1, CL2, CL3 - were normalized with the web height, H0, where $H_0 = H - 2\ t_f$.

4.1.2. Pattern W1

4.1.2.1. Web corrosion

The distribution of CH1 for this pattern is depicted in Figure 28. From Figure 28 two dominant trends can be seen: (i) full height corrosion, or (ii) corrosion up to 40% of the web, which can be written as:

$$0 < CH_1 \leq 0.4H \; and \; 0.9H \leq CH_1 \leq 1H$$

The parameters for the corrosion patterns can be found with corresponding diagrams in Section 1.5 *Corrosion Patterns* of this report.

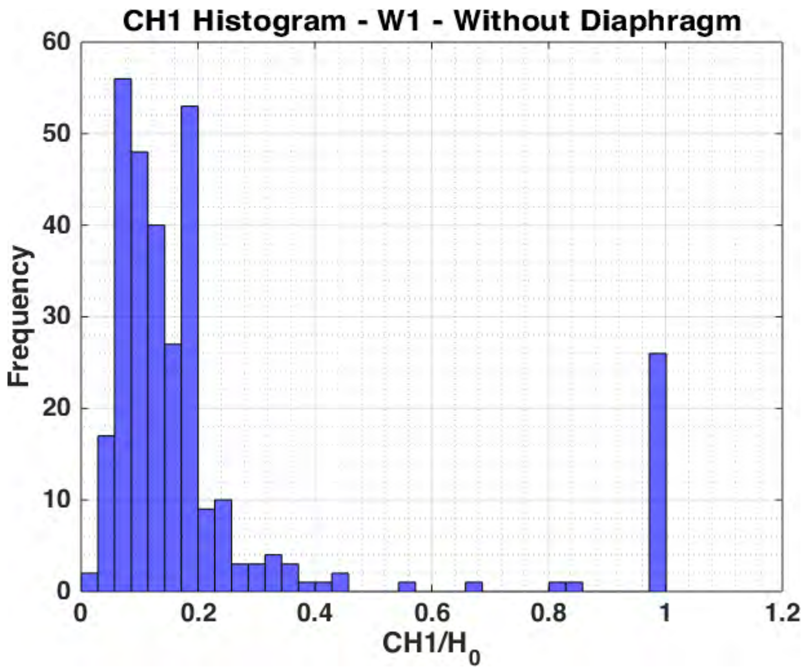

Figure 28: CH1 distribution of W1 pattern for beams without a diaphragm - CTDOT

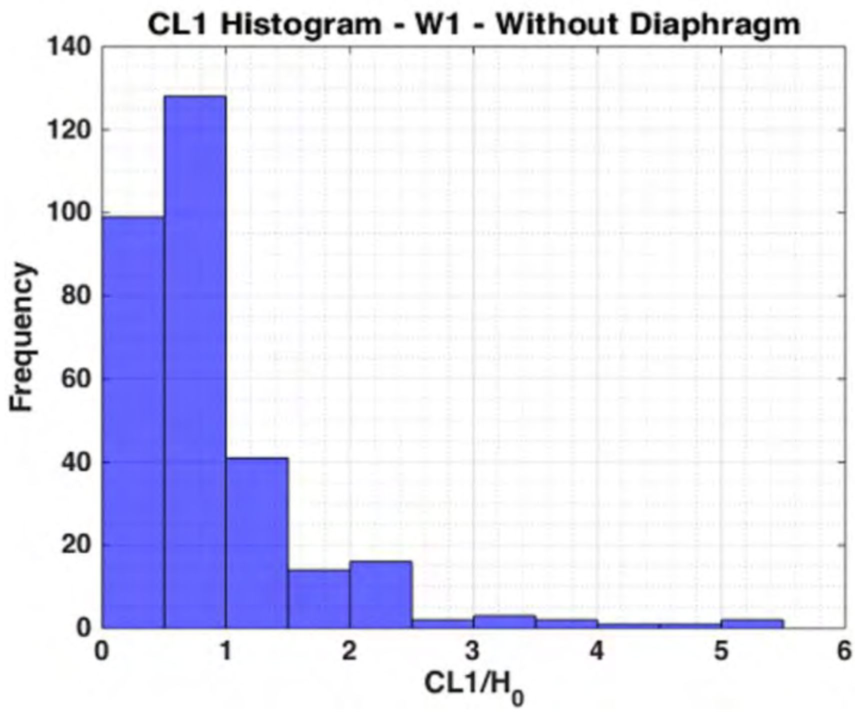

Figure 29: CL1 distribution of W1 pattern for beams without a diaphragm – CTDOT

Upon investigation of Figure 29, no major trend could be found. While no dominant trend could be seen, it is reasonable to state that the corrosion present for W1 is dominated by values smaller than 2.5H0.

Aiming to compare the length and height of corrosion, Figure 30 depicts the ratio between the length and height of corrosion. It is possible to observe that the length is usually several times greater than the height.

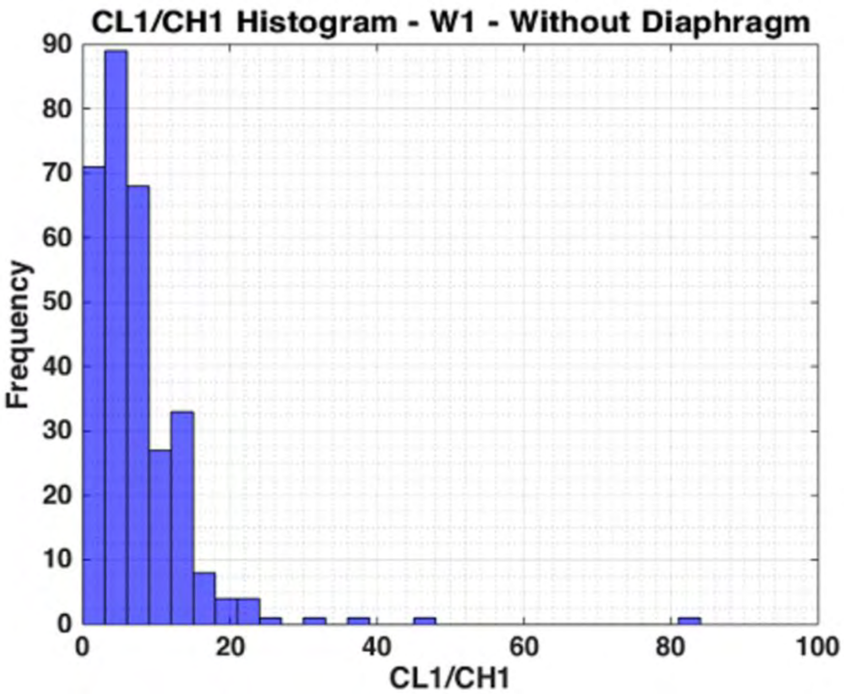

Figure 30: Ratio of corrosion length (CL1) to corrosion height (CH1) of W1 pattern for beams without a diaphragm - CTDOT

As many lengths are less than 2.5H, our team was able to check the ratio for beams ends where CL1 <2.5H. The resulting histogram is depicted in Figure 31.

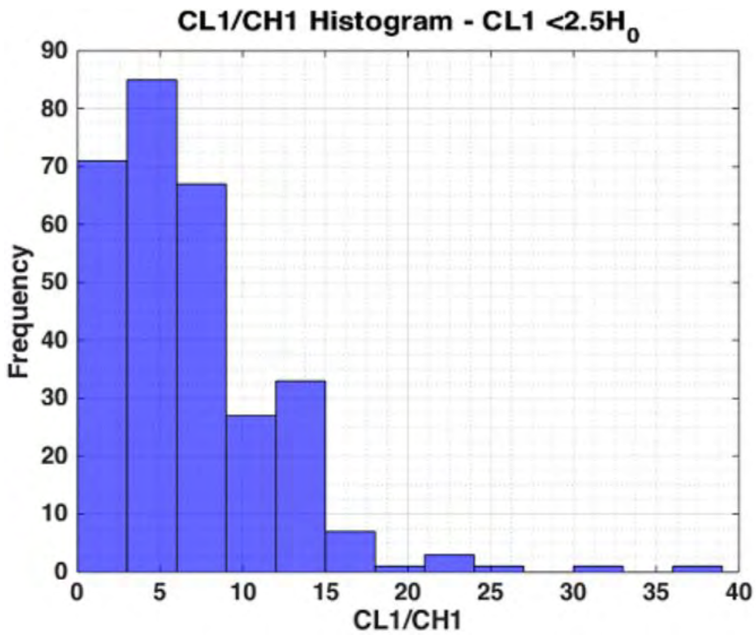

Figure 31: Ratio of corrosion length (CL1) to corrosion height (CH1) for CL1 < 2.5H0 - CTDOT

Beyond this, to deepen the understanding regarding the interaction between CH1 and CL1, our team could isolate trends depicted in the CH1 distribution. As a result, our team could plot the length of corrosion for CH1<0.3H0. Figure 32 depicts the final distribution of CL1 for this case.

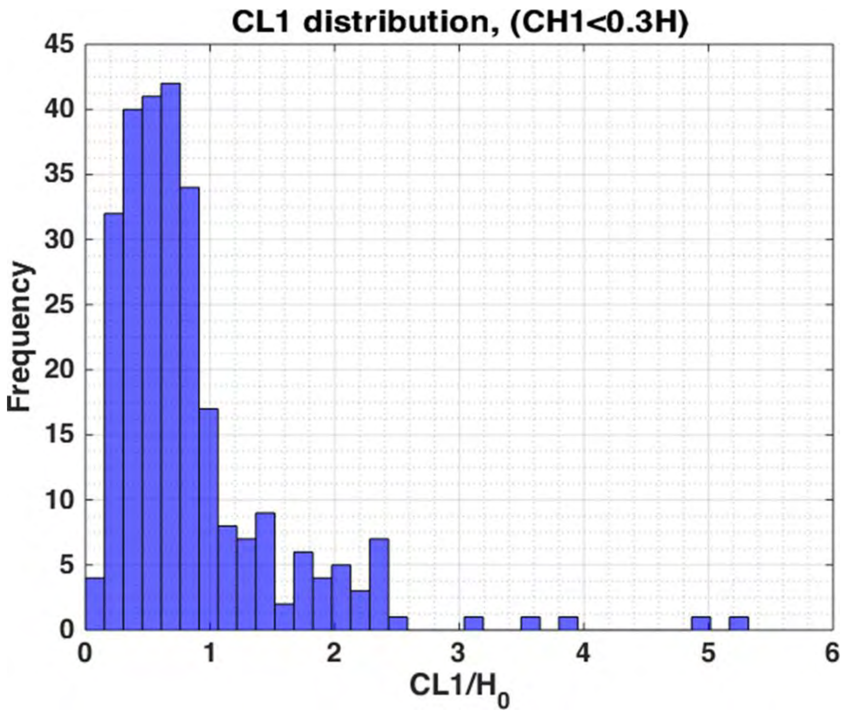

Figure 32: CL1 distribution for CH1 <0.3H - CTDOT

A similar study to the CH1<0.3H0 case, our team conducted a study on the case where CH1>0.9H. Figure 33 below depicts the final distribution for this case.

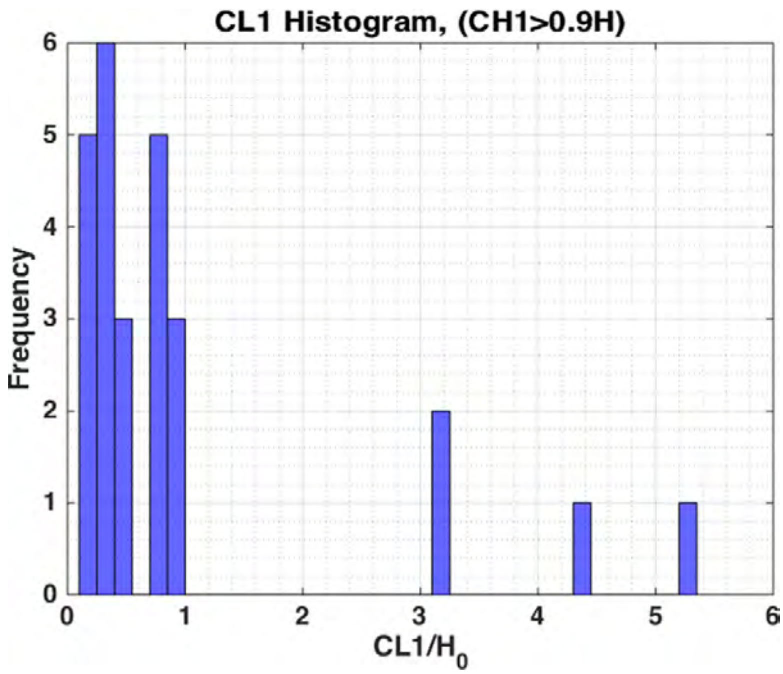

Figure 33: CL1 distribution for CH1 >0.9H - CTDOT

When comparing Figure 32 to Figure 33, it is apparent that when the corrosion height is large, the corrosion length is often smaller. On the other hand, for small heights of corrosion, the corrosion length tends to be greater than the corrosion height.

Figure 34 depicts the distribution of web thickness loss for pattern W1. It is noticeable that much of the thickness loss for the W1 case is no greater than 50%.

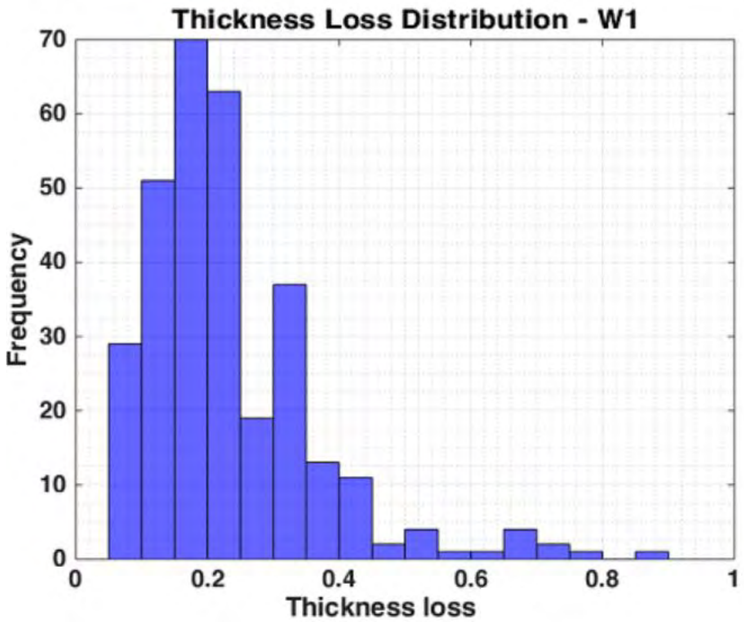

Figure 34: Web thickness loss distribution for pattern W1 - CTDOT

Similar to the analysis conducted for corrosion length, our team was able to study the thickness loss for the two main trends detected previously. The resulting distributions are depicted in the Figure 35 and Figure 36.

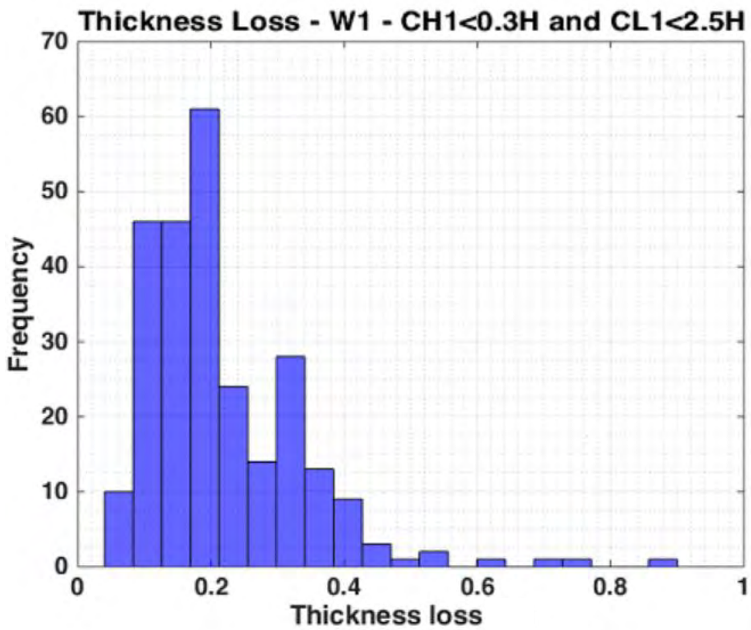

Figure 35: Web thickness loss distribution for CH1<0.3H and CL1<2.5H - CTDOT

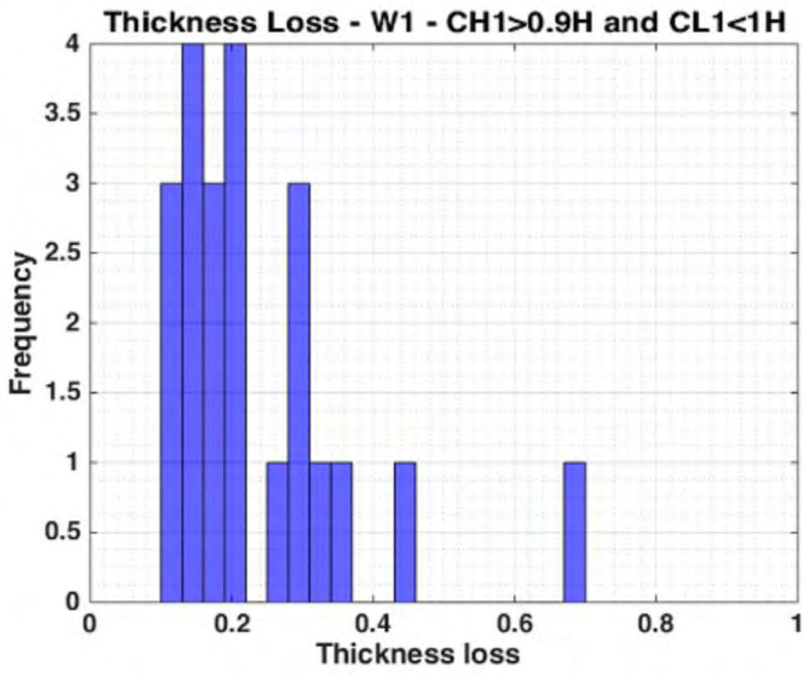

Figure 36: Web thickness loss distribution for Ch1<0.9H and CL1<1H - CTDOT

4.1.2.2. Flange corrosion

Figure 37 depicts the length of corrosion in the flanges. It is worthwhile in recognizing that there is significantly less information regarding flange corrosion.

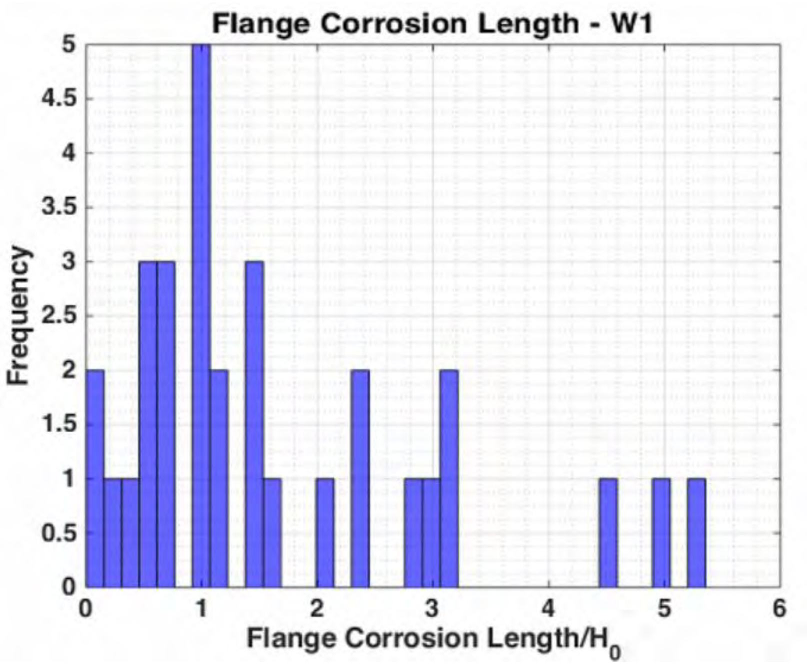

Figure 37: Distribution of corrosion length for pattern W1 - CTDOT

To compare the length of corrosion in the flanges with the length of corrosion in the web, Figure 38 was created. Here, the graph depicts the ratio of Cf/Cl, where Cf is the length of corrosion in the flanges and Cl is the web length corrosion.

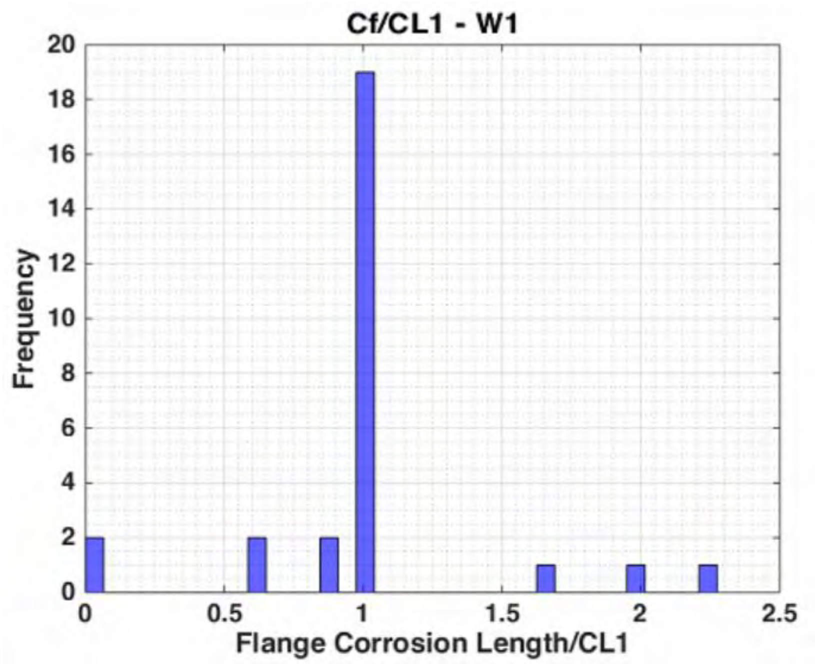

Figure 38: Ratio between flange corrosion length for pattern W1 - CTDOT

From Figure 38, it was valid to assume that the length of corrosion is the same for both web and flange. Therefore, for trends previously identified, our team assumed that the length of corrosion in the flange was equal to the corrosion in the web.

Regarding the thickness loss of the flanges, the research team was able to plot the distribution depicted in Figure 39.

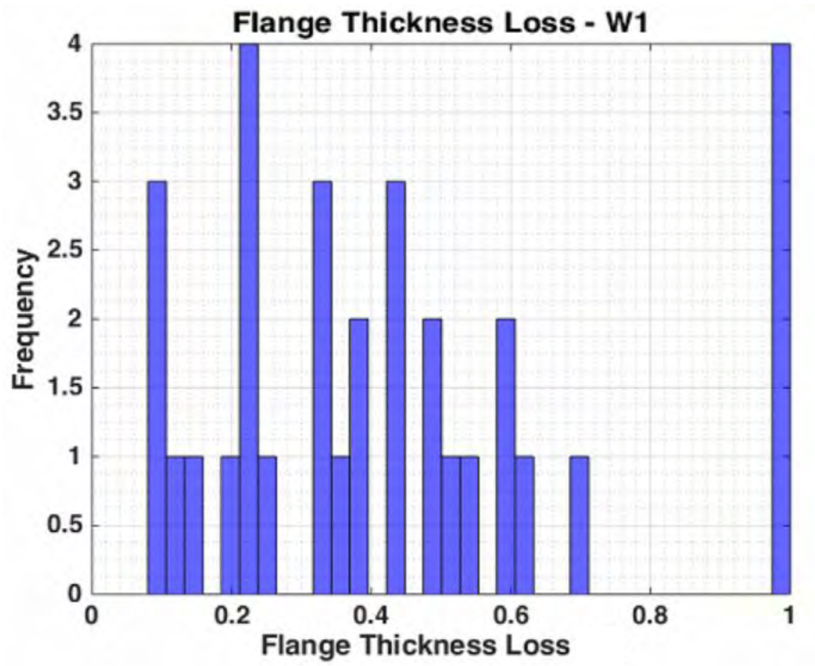

Figure 39: Flange thickness Loss for pattern W1 - CTDOT

Similarly, our team was able to isolate the thickness loss for either trends found previously, as depicted in Figure 40 and Figure 41.

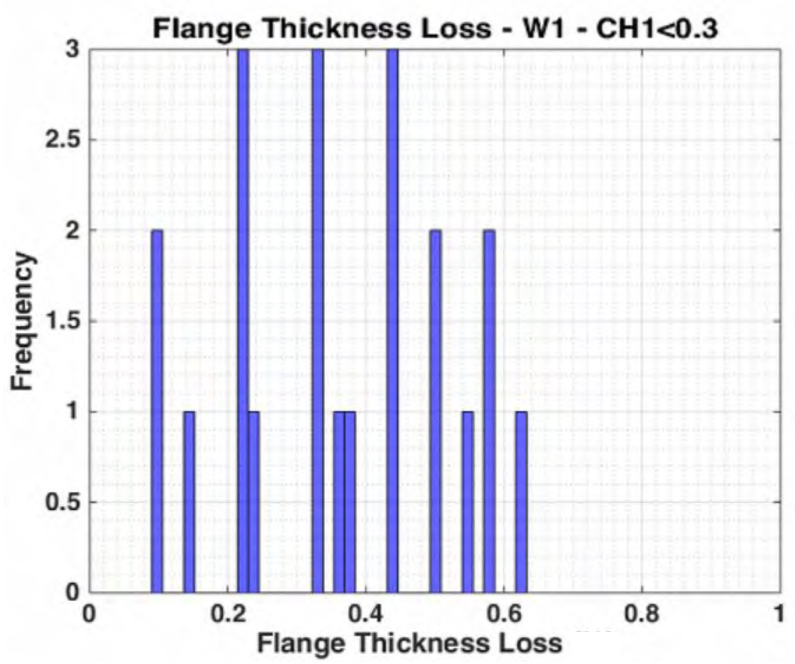

Figure 40: Flange thickness loss distribution for CH1<0.3 - CTDOT

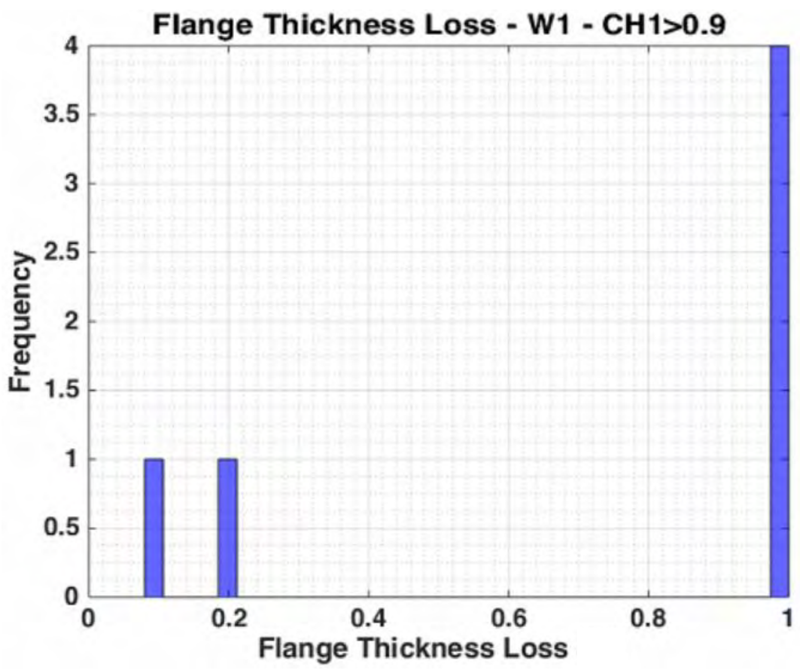

Figure 41: Flange thickness loss distribution for CH1>0.9 - CTDOT

For beam ends which CH1 is less than 0.3H, the thickness loss on the flanges tended to be small. This was different for cases which CH1 is greater than 0.9H, which resulted in a thickness loss of almost 100%. This allowed our team to assume the beams described by W1 patterns present the two patterns described in Table 47.

Table 47: Summary of extreme scenarios of W1 pattern - CTDOT

#	Pattern	CH1	CL1	tloss/tweb	Cf	tloss/tflange
1	W1	(0,0.4]	(0,2.5]	(0, 0.5]	(0,2.5]	[0.1,0.6]
2	W1	1	(0,1]	(0,0.4]	(0,1]	[0.9, 1]

Based on Table 47, our team was able to plot the extreme corrosion scenarios for pattern W1.

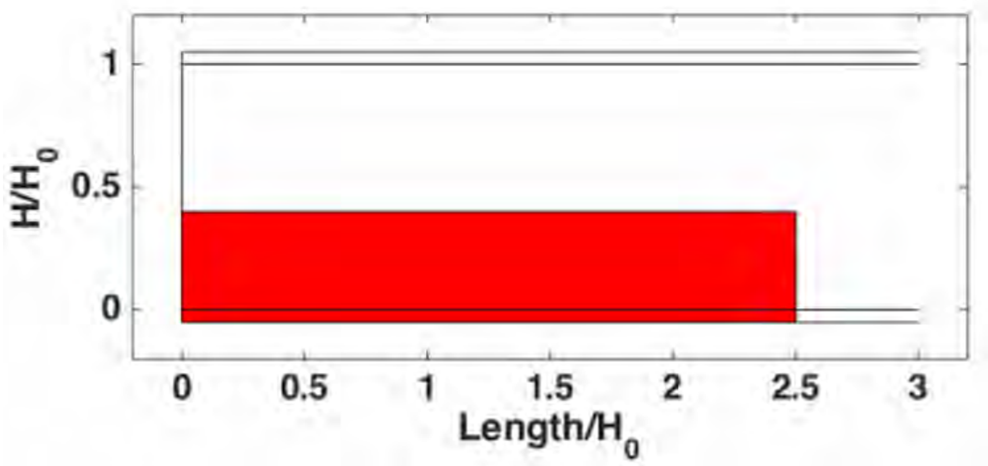

Figure 42: Extreme scenario for pattern W1 - CTDOT

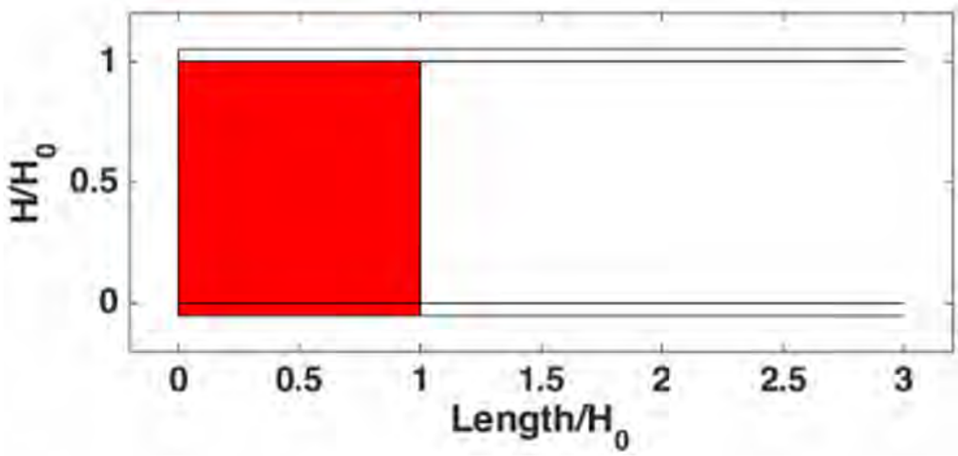

Figure 43: Extreme scenario for pattern W1 - CTDOT

4.1.2.3. Holes

The frequency of hole appearance is portrayed in Table 48.

Table 48: Holes and patterns for beams without a diaphragm - CTDOT

	Number	No Hole	M1	M 2	M 3	M 4	M1 and M2	M1 and M3	M2 and M4
W1	309	290	3	1	2	2	0	1	0
W2	6	5	0	0	0	1	0	0	0
W3	38	35	1	0	1	0	0	1	0
W4	33	30	2	0	1	0	0	0	0
W5	34	34	0	0	0	0	0	0	0
W6	2	2	0	0	0	0	0	0	0

It is imperative to acknowledge that corrosion holes are frequently reported just in the notes of these reports. This means that, although more holes have been reported in the provided reports, not all corrosion holes had dimensions or pictures. For this reason, they were not able to count on our database.

The web thickness loss distribution for beam ends with M1 holes is:

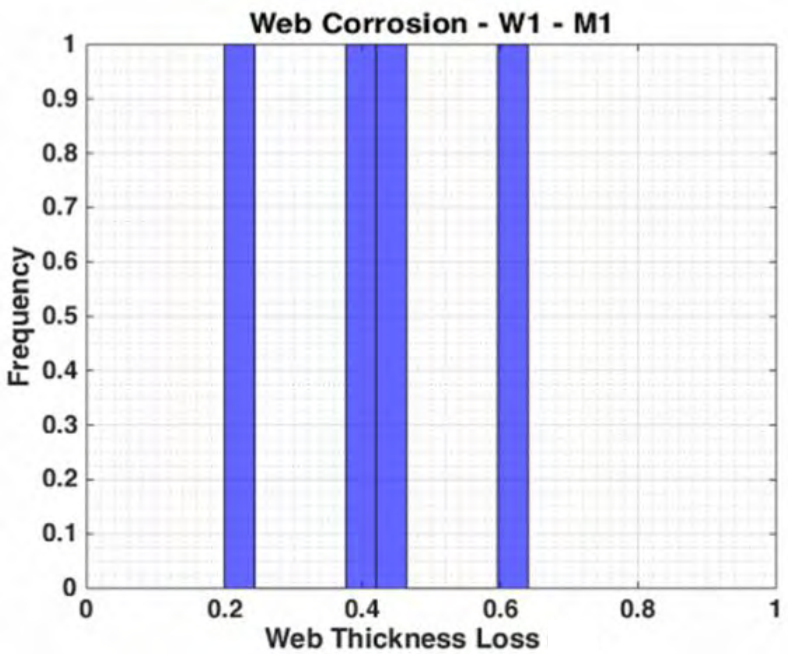

Figure 44: Web thickness loss for beam ends with M1 holes - CTDOT

The web thickness loss distribution for beam ends with M2 holes is:

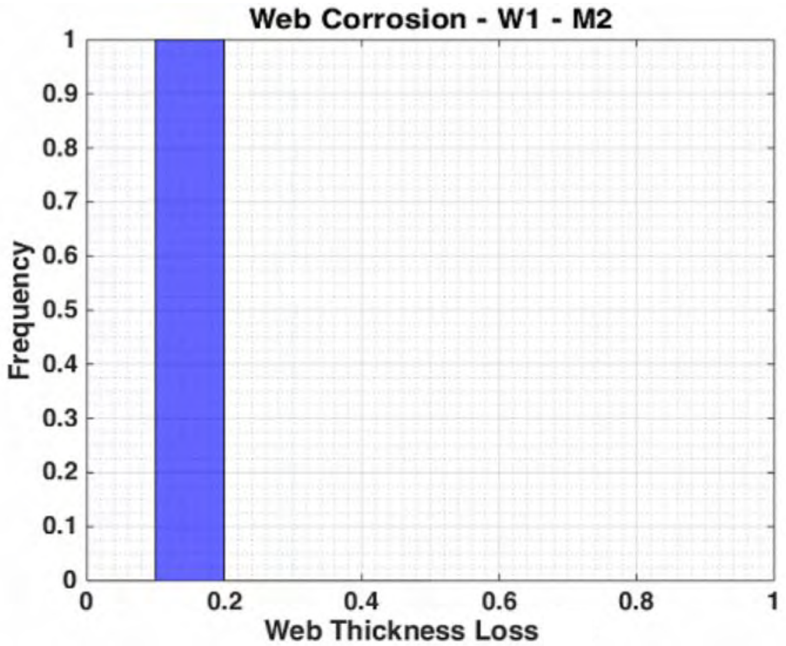

Figure 45: Web thickness loss for beam ends with M2 holes - CTDOT

The web thickness loss distribution for beam ends with M3 holes is:

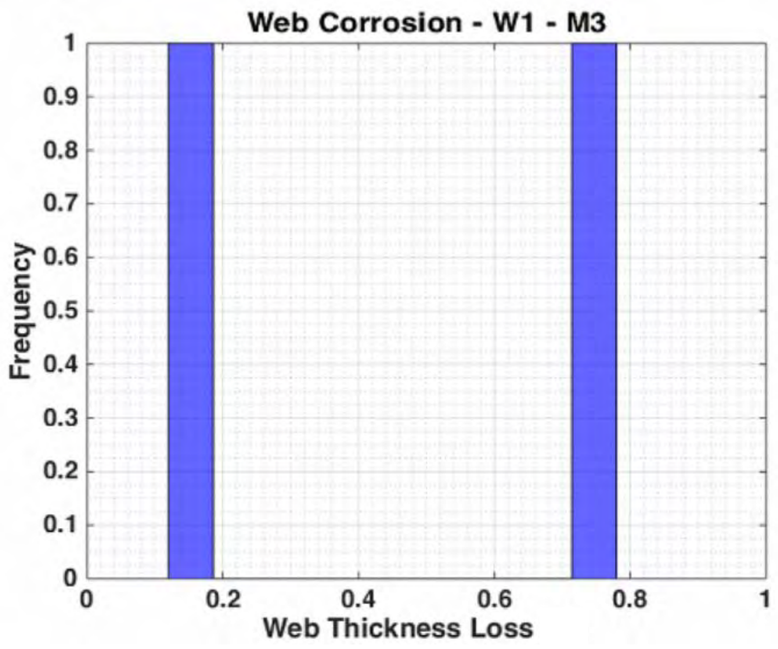

Figure 46: Web thickness loss for beam ends with M3 holes - CTDOT

The web thickness loss distribution for beam ends with M4 holes is:

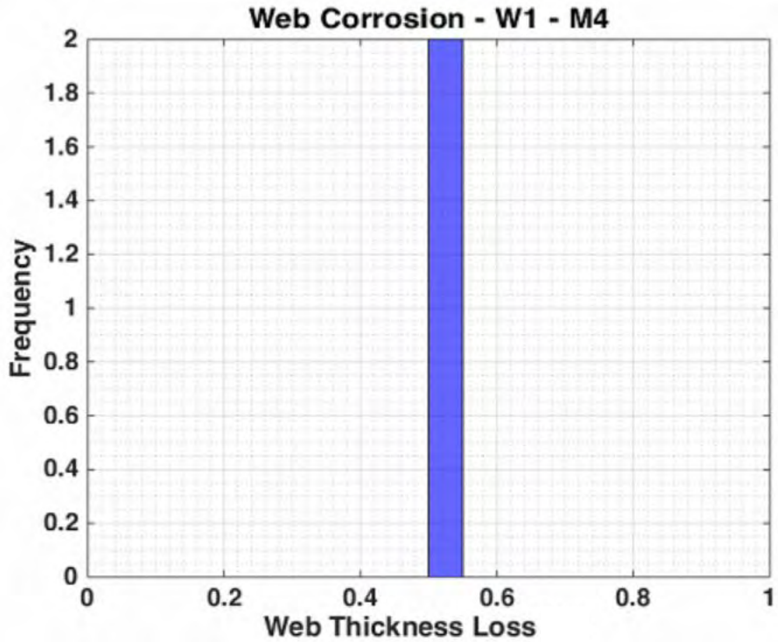

Figure 47: Web thickness loss for beam ends with M4 holes - CTDOT

From Figure 44, Figure 45, Figure 46, and Figure 47 is not possible to determine the thickness in which the holes will appear. While this is a clear observation, the figures hint that corrosion holes can appear even for cases in which the thickness loss is not extreme. As a result of this, and due to the small amount of data regarding corrosion holes, it is not possible to define any trend or try to make any prediction of what causes the holes to appear.

4.1.3. Pattern W2

4.1.3.1. Web corrosion

The W2 corrosion pattern was observed only six times throughout the reports from the state of Connecticut. In a similar way to how W1 was recorded, the measurements for the W2 pattern provided in the reports were normalized by H0. Figure 48, Figure 49 and Figure 50 depict the distribution of the parameters of pattern W2. The parameters for the corrosion patterns can be found with corresponding diagrams in Section 1.5 *Corrosion Patterns* of this report.

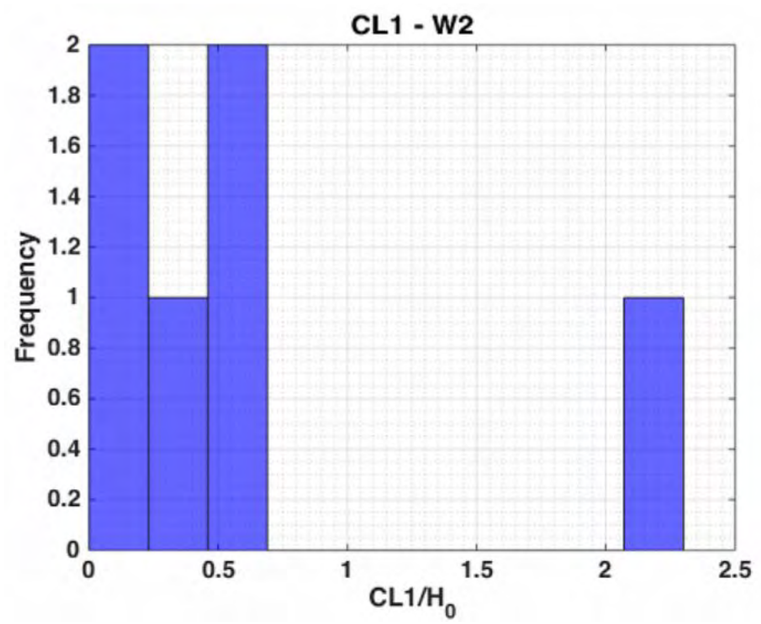

Figure 48: CL1 distribution for W2 pattern - CTDOT

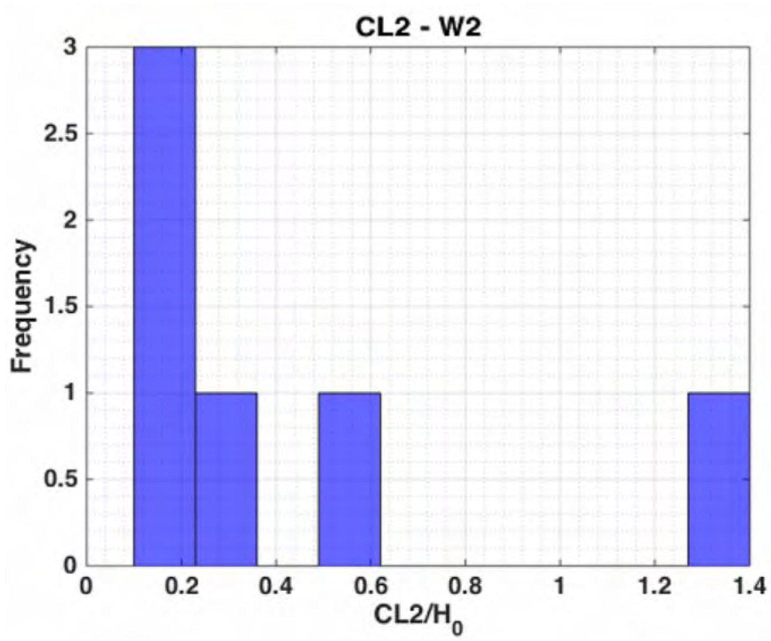

Figure 49: CL2 distribution for W2 pattern - CTDOT

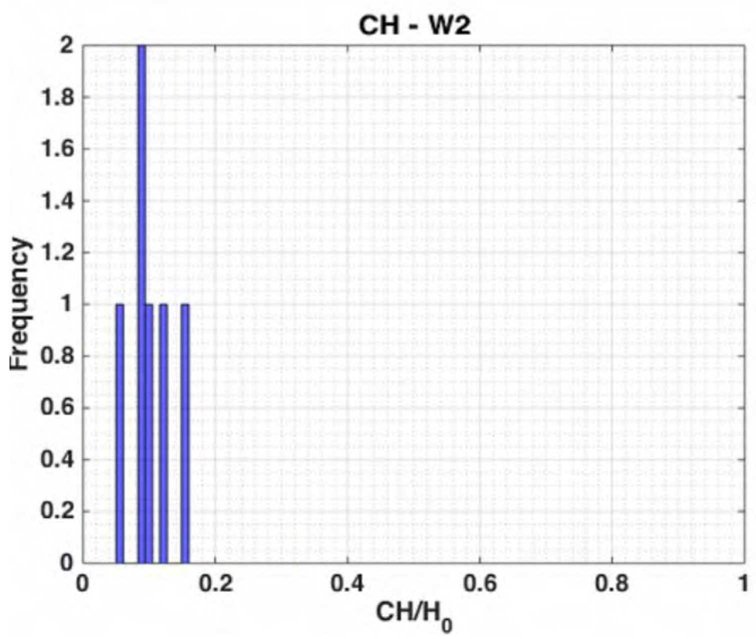

Figure 50: CH distribution for W2 pattern - CTDOT

The distribution of web thickness loss depicted in Figure 51.

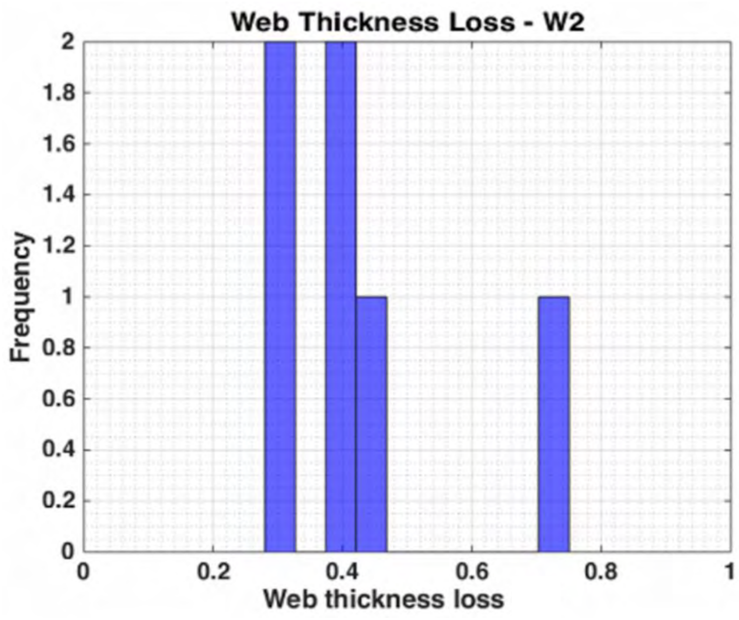

Figure 51: Web thickness loss for W2 pattern - CTDOT

From Figure 48, there is a trend present regarding CL1, as CL1<0.6H0 for most of the beam ends reported. This allowed our team to analyze the behavior of the other parameters given that CL1<0.6H0.

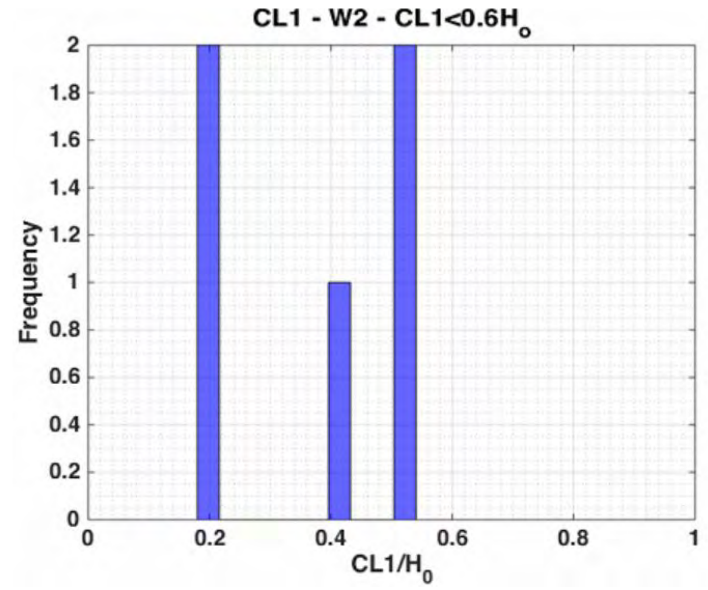

Figure 52: CL1 distribution for W2 pattern and CL1<0.6H - CTDOT

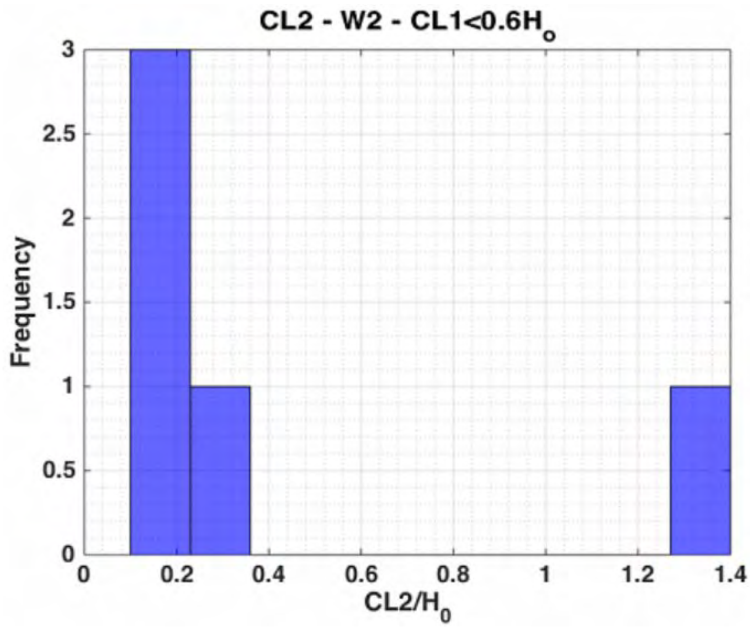

Figure 53: CL2 distribution for W2 pattern and CL1<0.6H - CTDOT

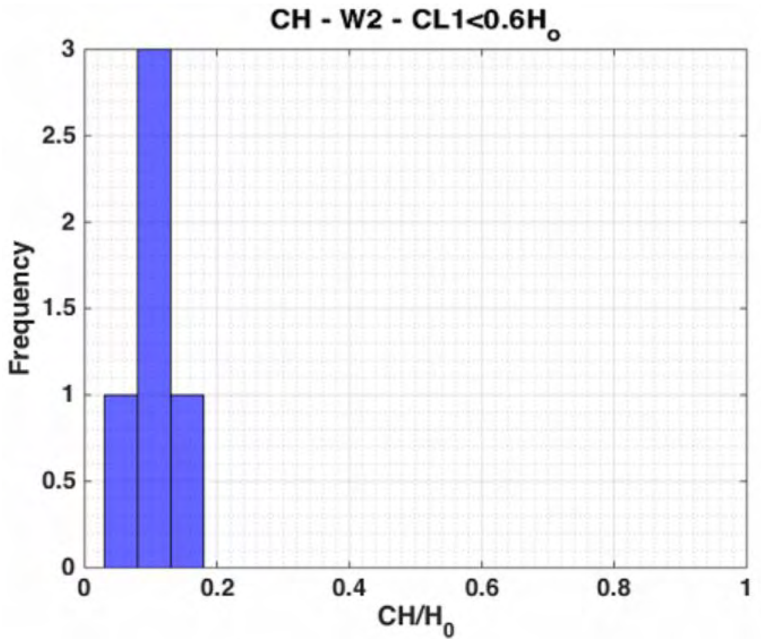

Figure 54: CH distribution for W2 pattern and CL1<0.6H - CTDOT

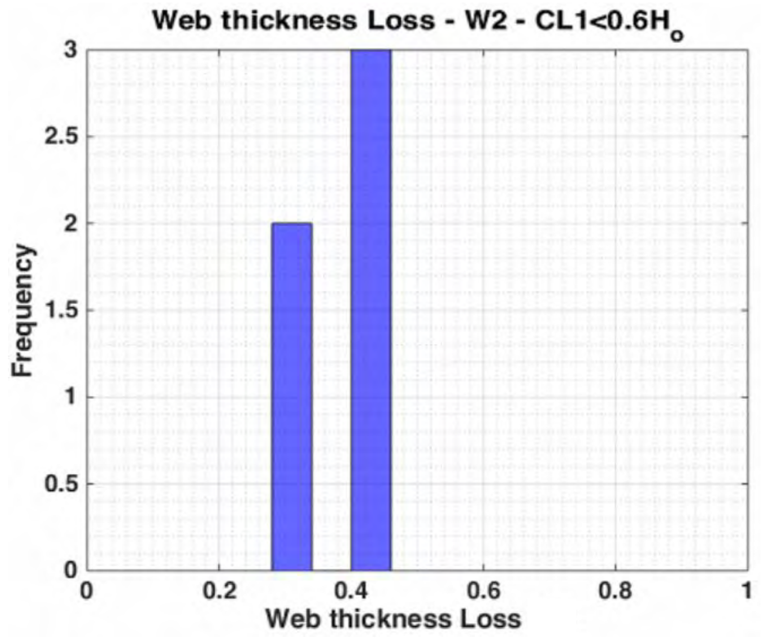

Figure 55: Web thickness loss for W2 pattern and CL1<0.6H - CTDOT

Therefore, it is valid to assume that $0 < CL_1 \leq 0.6H_0$, $0.1H_0 \leq CL_2 \leq 0.4H_0$, $0 < CH \leq 0.2H_0$] and $0.3 \leq \frac{t_{loss}}{t_{web}} \leq 0.45$. The extreme scenario for W2 is depicted in Figure 56.

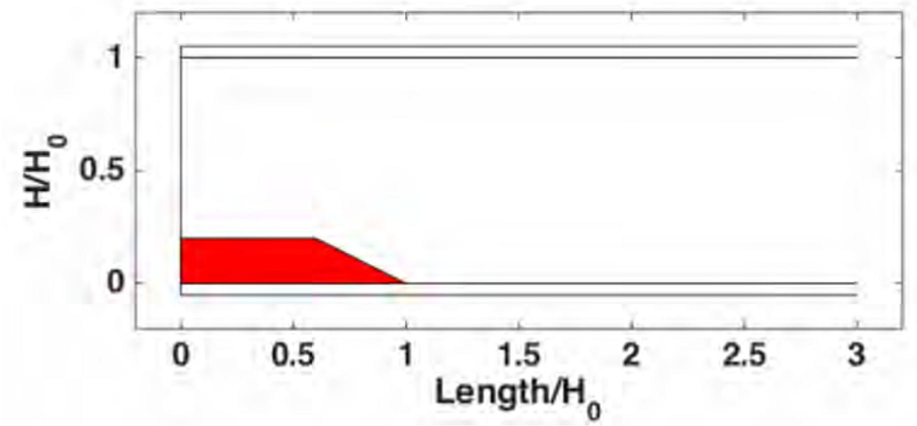

Figure 56: Extreme corrosion scenario for pattern W2 - CTDOT

4.1.3.2. Flange corrosion

It was not possible to perform flange corrosion analyzes for pattern W2 as no information about corrosion in the flanges was provided for the beam ends identified with a W2 corrosion pattern.

4.1.3.3. Holes

Only a single hole was reported for this pattern. The topology of the recorded hole is an M4 corrosion hole pattern. The dimensions for the given hole are: $a = 0.18, b = 1.42$, and $c = 1.36$.

4.1.4. Pattern W3

4.1.4.1. Web corrosion

The analysis began by studying the distribution of CH2, depicted in Figure 57. The parameters for the corrosion patterns can be found with corresponding diagrams in Section 1.5 *Corrosion Patterns* of this report.

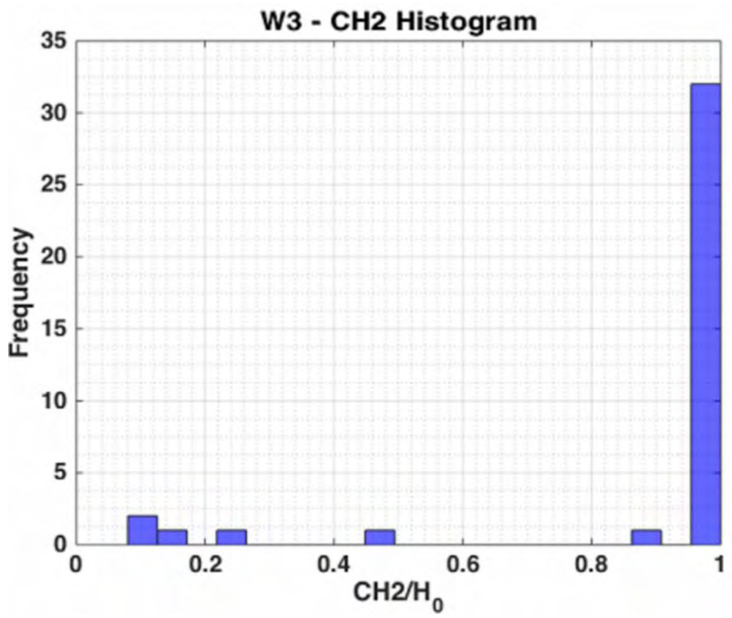

Figure 57: CH2 distribution for W3 pattern - CTDOT

A single trend for when CH2 >0.9H0 is clearly observed in Figure 57. Given that CH2>0.9H0, our team could plot the distribution of the other parameters of the corrosion pattern given that CH2>0.9H0. This is shown in the following figures.

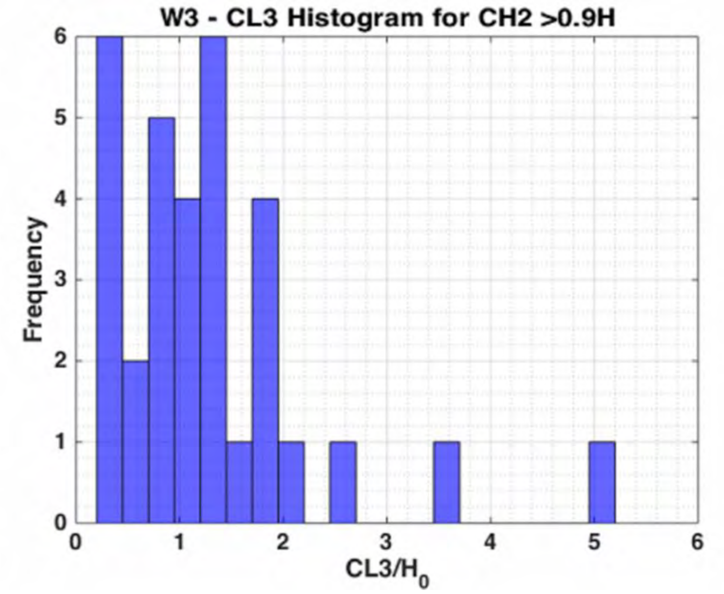

Figure 58: CL3 distribution for W3 pattern - CTDOT

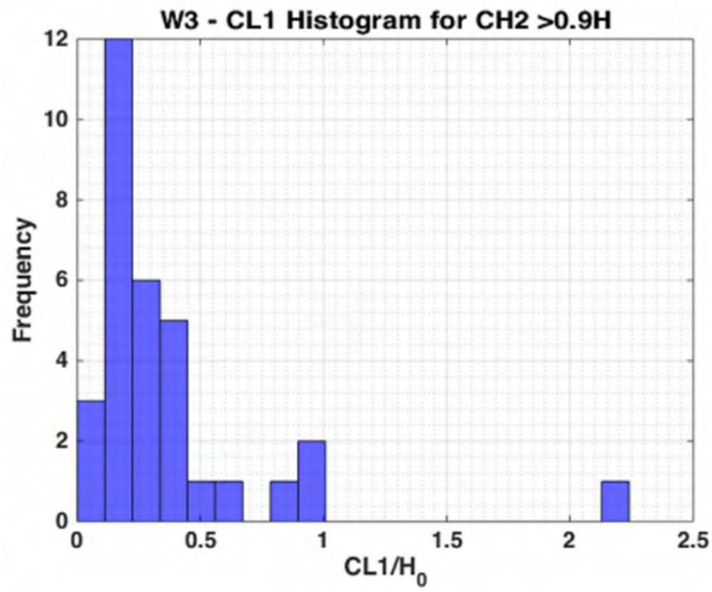

Figure 59: CL1 distribution for W3 pattern and CH2>0.9H - CTDOT

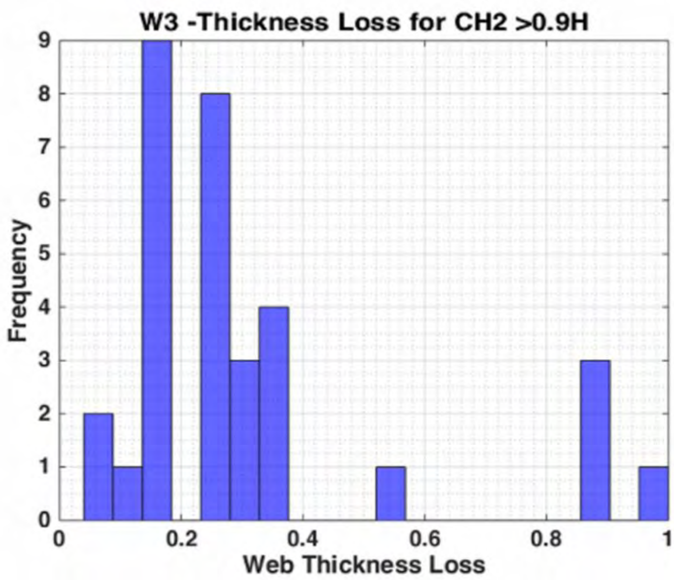

Figure 60: Web thickness loss distribution for W3 pattern and CH2>0.9H - CTDOT

From the last figures, our team was able to conclude that:

$$0 < CH_1 \leq 0.4H_0$$
$$0.9H_0 \leq CH_2 \leq 1H_0$$
$$0 < CH_3 \leq 0.4H_0$$
$$0 < CL_1 \leq 1H_0$$
$$0 < CL_2 \leq 1.5H_0$$
$$0 < CL_3 \leq 2.5H_0$$
$$0 < \frac{t_{loss}}{t_{web}} \leq 0.4$$

This resulted in the extreme scenario for pattern W3:

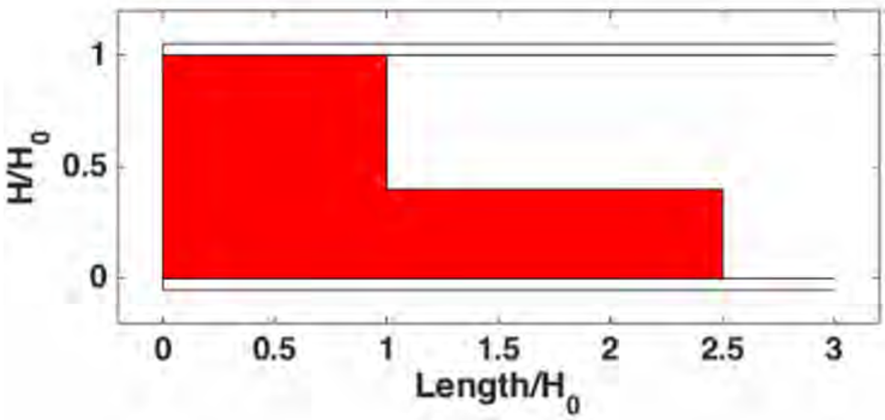

Figure 61: Extreme corrosion scenario for W3 pattern – CTDOT

4.1.4.2. Flange corrosion

The ratio between the length of corrosion in the flanges and the total corroded length (CL3) is depicted in Figure 62. Figure 63 depicts the raw corrosion length in the flange.

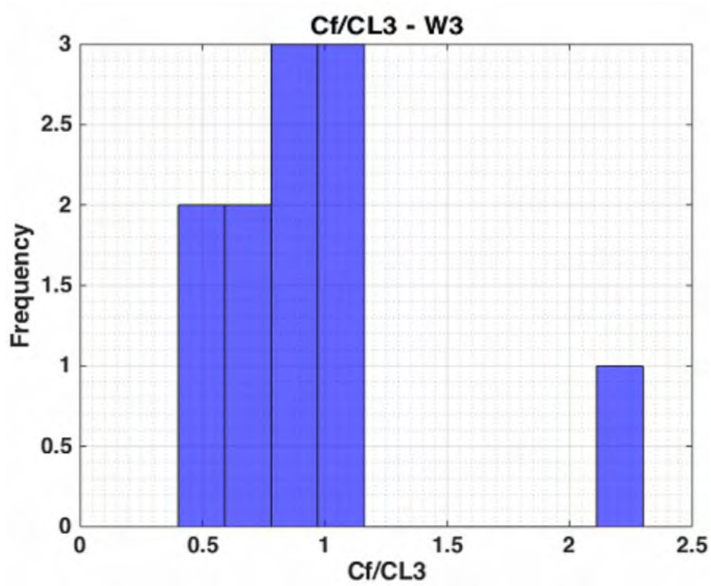

Figure 62: Ratio between corrosion length in the flanges and CL3 for W3 pattern - CTDOT

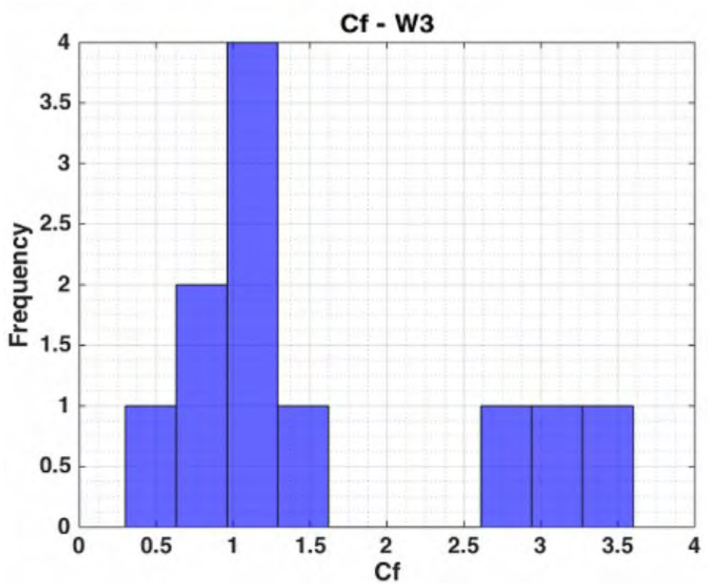

Figure 63: Raw corrosion length in the flanges for W3 pattern - CTDOT

Figure 64 depicts the distribution of the thickness loss in the flanges. Similar to the previous sections, our team could assess the distribution of thickness loss for CH2>0.9. This case is depicted on Figure 65.

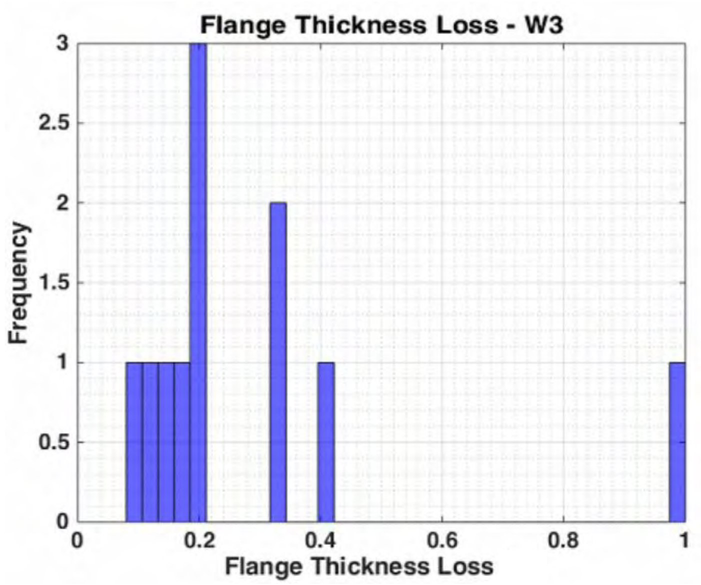

Figure 64: Flange thickness loss for W3 pattern - CTDOT

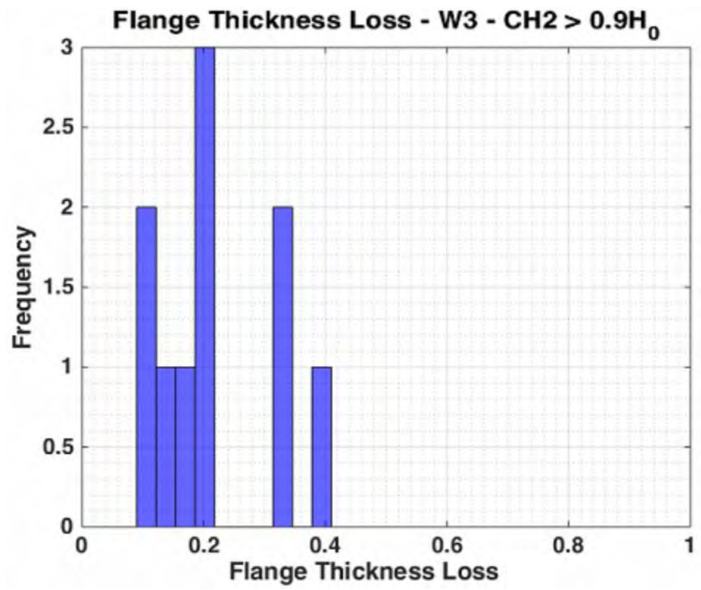

Figure 65: Flange thickness loss for W3 pattern and CH2>0.9H - CTDOT

As a result, for the case of CH2>0.9H0, our team assumed that $0.1 < \frac{t_{loss}}{t_{flange}} < 0.4$.

4.1.4.3. Holes

Only four corrosion holes were observed in the reports provided by CTDOT. Additionally, two of the holes were observed in the same beam end. Due to the limited amount of information, the research team was not able to draw conclusions or trends from the information provided.

4.1.5. Pattern W4

4.1.5.1. Web Corrosion

Like the other studies conducted, this study started by analyzing CH2, depicted in Figure 66. The parameters for the corrosion patterns can be found with corresponding diagrams in Section 1.5 *Corrosion Patterns* of this report.

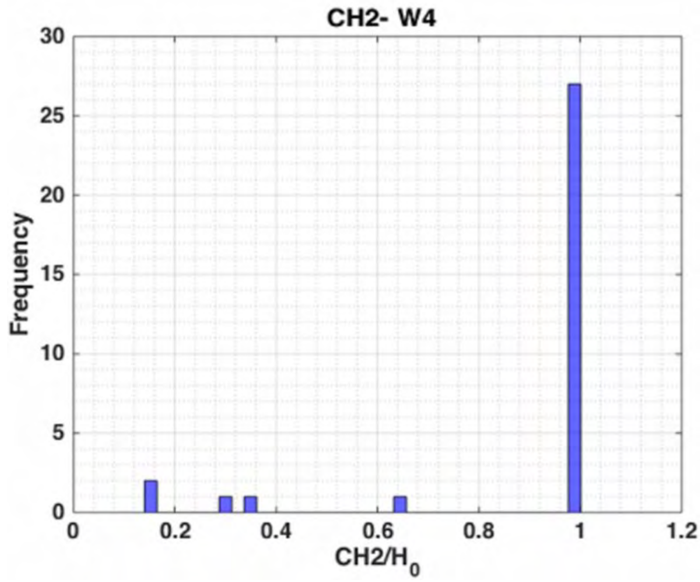

Figure 66: CH2 distribution for W4 pattern - CTDOT

Figure 66 clearly depicts that CH2 is equal to 1 for most beam ends reported. Using this information, our team was able to further analyze the other parameters for CH2>0.9H0. The following figures depict the behavior of the other parameters for CH2>0.9H0.

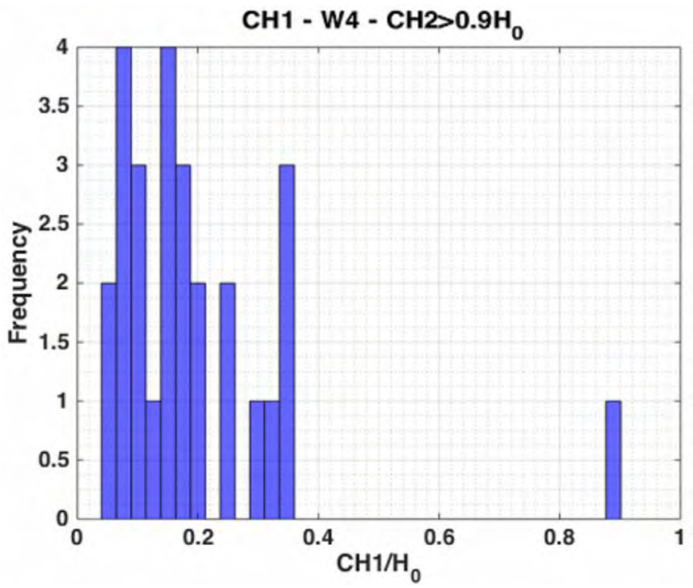

Figure 67: CH1 distribution for W4 pattern and CH2>0.9H - CTDOT

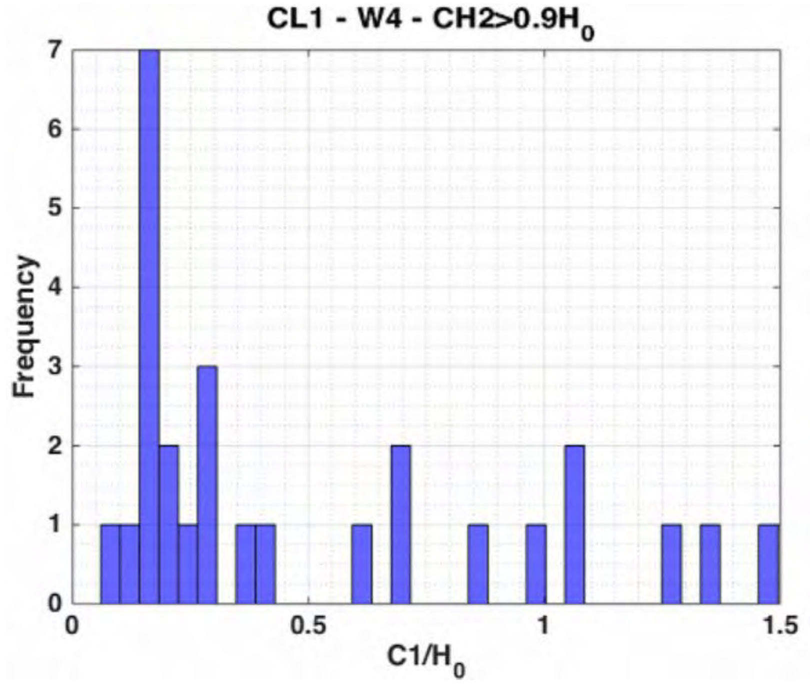

Figure 68: CL1 distribution for W4 pattern and CH2>0.9H - CTDOT

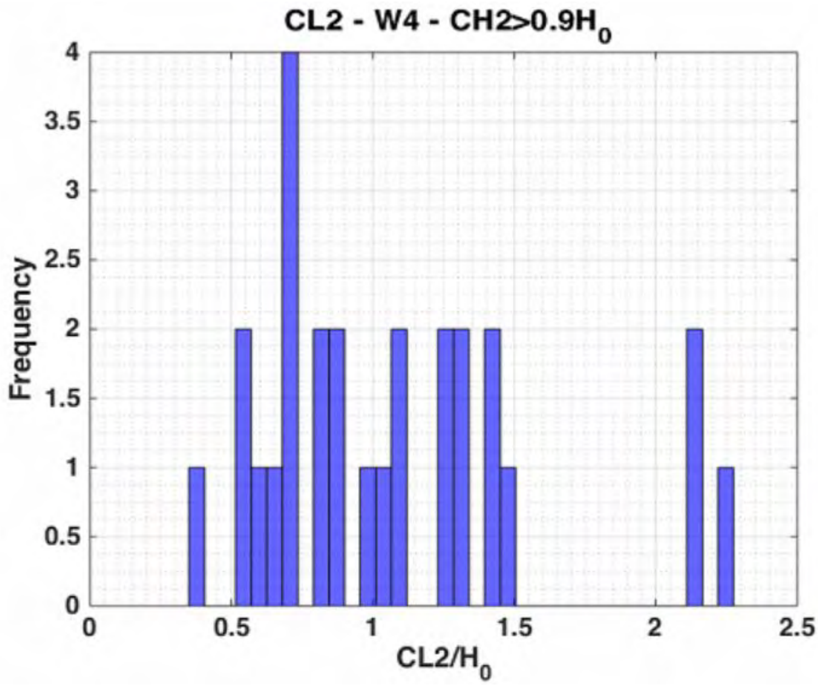

Figure 69: CL2 distribution for W4 pattern and CH2>0.9H - CTDOT

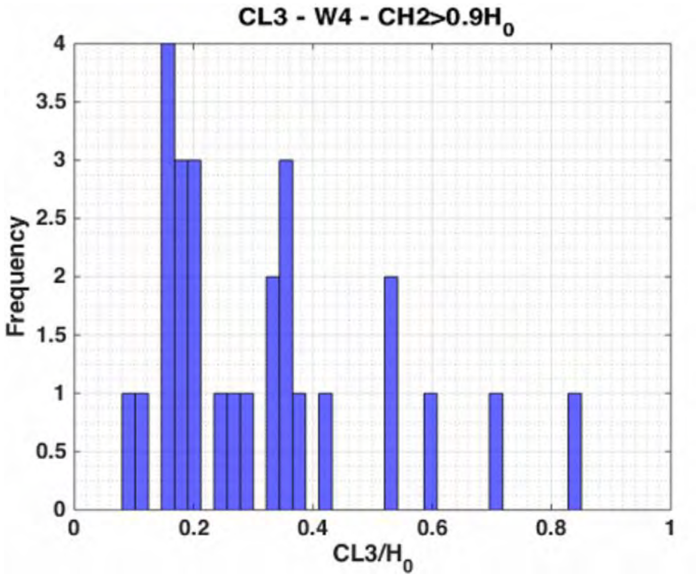

Figure 70: CL3 distribution for W4 pattern and CH2>0.9H - CTDOT

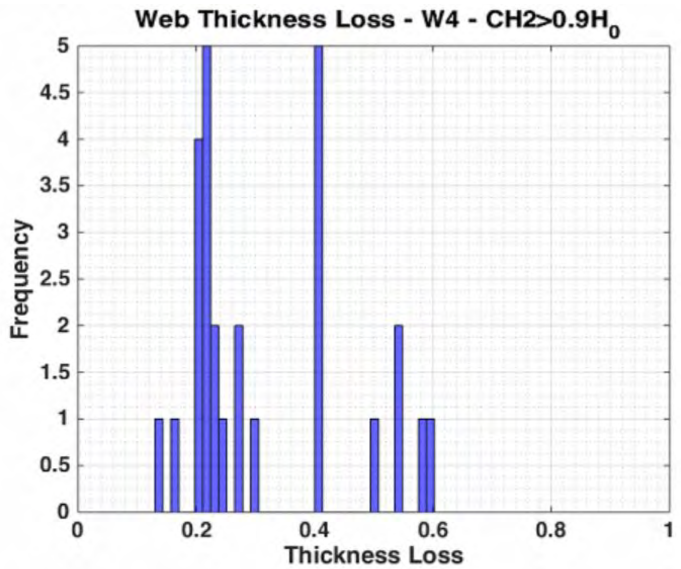

Figure 71:Web thickness loss distribution for W4 pattern and CH2>0.9H - CTDOT

From these figures, our team was able to conclude that:

$$0 < CH_1 \leq 0.4H_0$$
$$0.9H_0 \leq CH_2 \leq 1H_0$$
$$0 < CL_1 \leq 1H_0$$
$$0.5H_0 < CL_2 \leq 1.5H_0$$
$$0.1H_0 < CL_3 \leq 0.5H_0$$
$$0.1 \leq \frac{t_{loss}}{t_{web}} \leq 0.6$$

Thus, the extreme scenario for pattern W4 is:

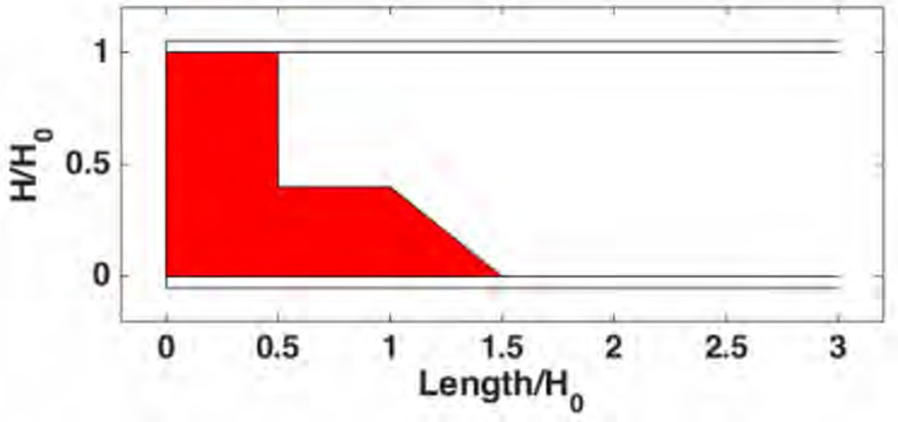

Figure 72: Extreme corrosion scenario for W4 pattern - CTDOT

4.1.5.2. Flange Corrosion

The information regarding flange corrosion combined with the W4 corrosion pattern was rarely observed in the reports analyzed from CTDOT. For this reason, the research team was not able to draw any conclusion nor trends from the available data. The histogram of the two observed flange corrosion scenarios can be found in Figure 73.

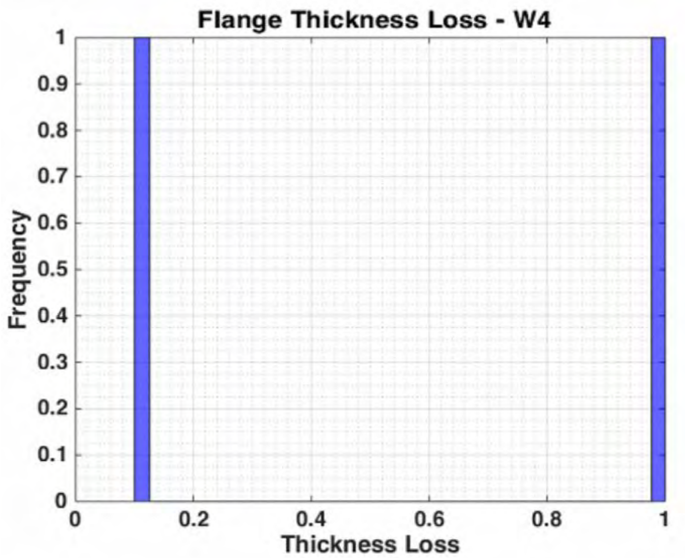

Figure 73: Flange thickness loss for W4 pattern - CTDOT

4.1.5.3. Holes

For the corrosion combination of W4 with holes, only three holes were observed with the W4 pattern. It is important to note that the data here is not enough in order to draw conclusions via the histograms in Figure 74, Figure 75, Figure 76, and Figure 77. These depict the dimensions of the holes observed.

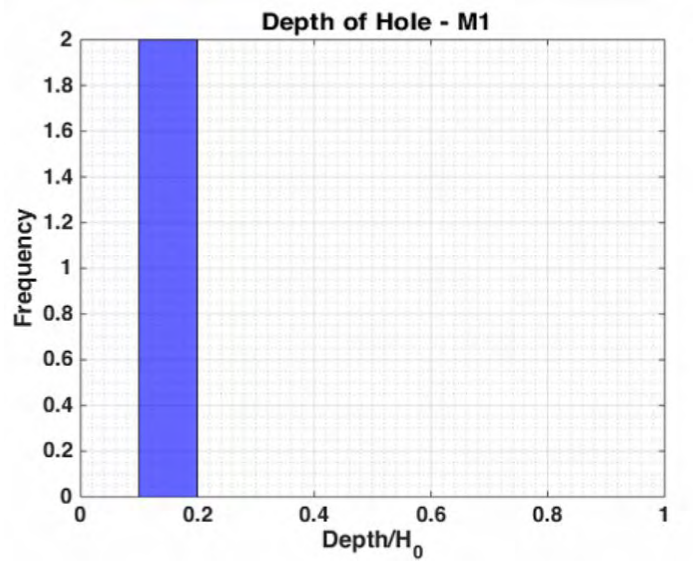

Figure 74: Depth of hole M1 combined with W4 pattern - CTDOT

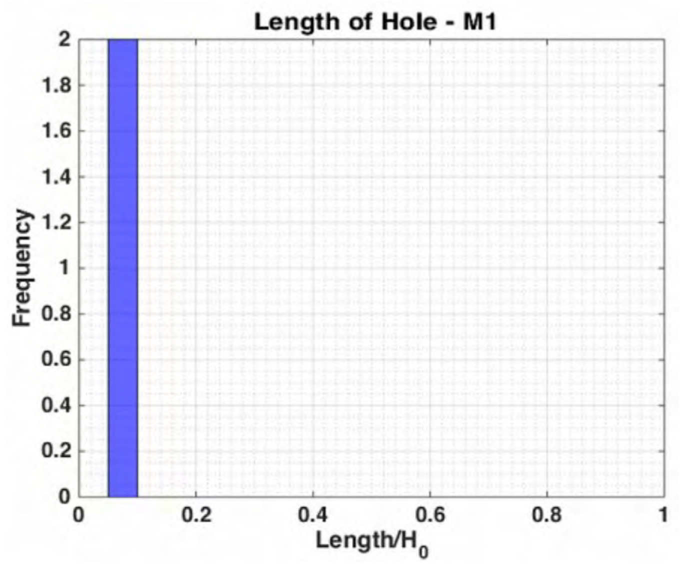

Figure 75: Length of hole M1 combined with W4 pattern - CTDOT

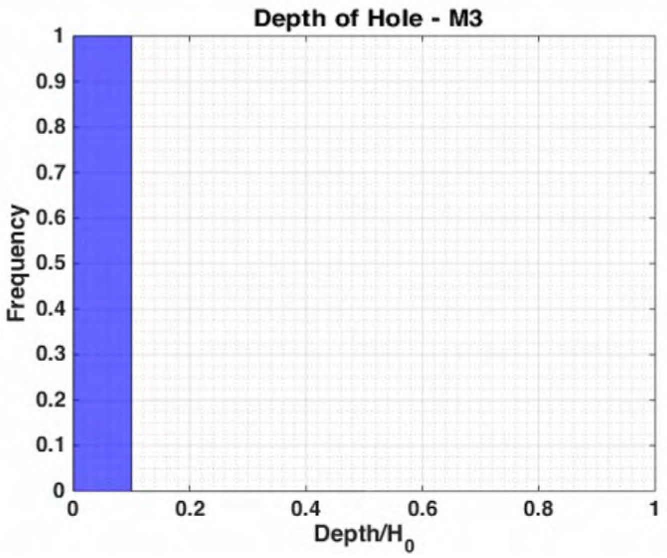

Figure 76: Depth of hole M3 combined with W4 pattern - CTDOT

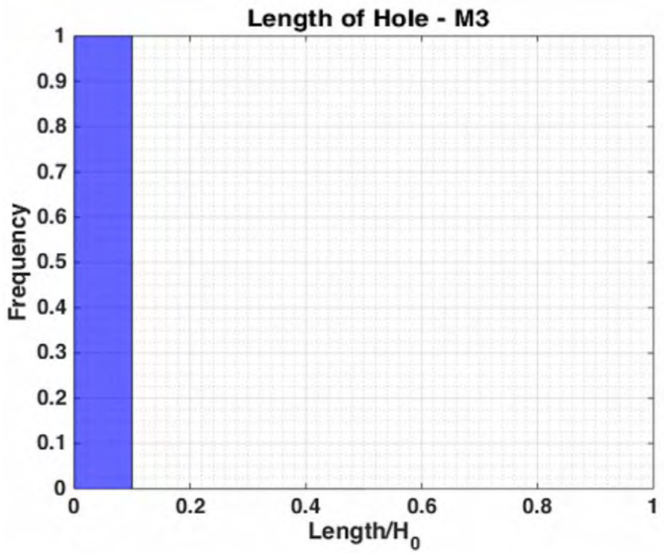

Figure 77: Length of hole M3 combined with W4 pattern - CTDOT

4.1.6. Pattern W5

4.1.6.1. Web corrosion

The study began by analyzing the height of corrosion. Figure 78 depicts the distribution of CH1 for pattern W5. The parameters for the corrosion patterns can be found with corresponding diagrams in Section 1.5 *Corrosion Patterns* of this report.

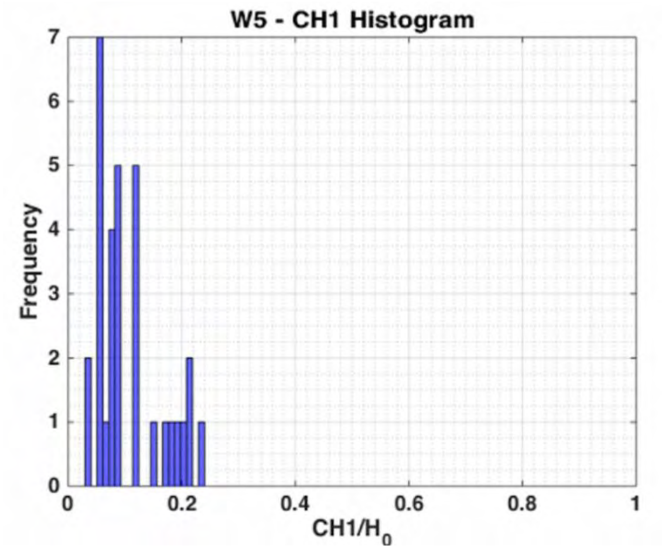

Figure 78: CH1 distribution of W5 pattern for beams without a diaphragm – CTDOT

Figure 78 clearly depicts that CH1 tends to be smaller than 0.2H0. This means that when analyzing the behavior of CL1 for when CH1<0.2Ho, we found:

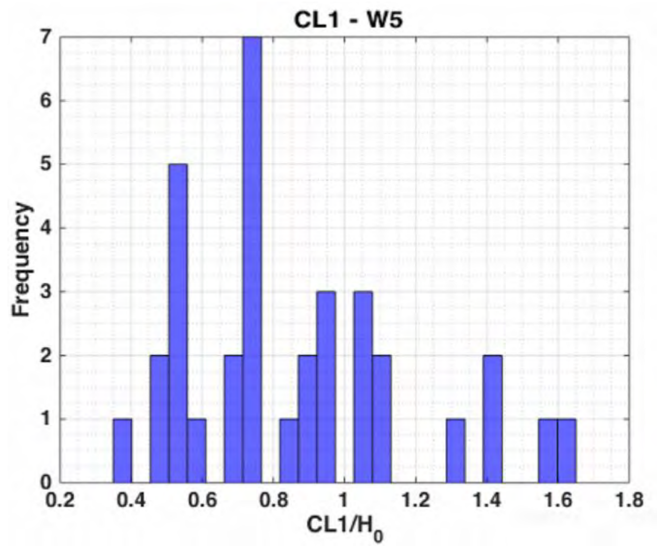

Figure 79: CL1 distribution of W5 pattern for beams without a diaphragm – CTDOT

Figure 80 depicts the web thickness loss for CH2>0.9H0:

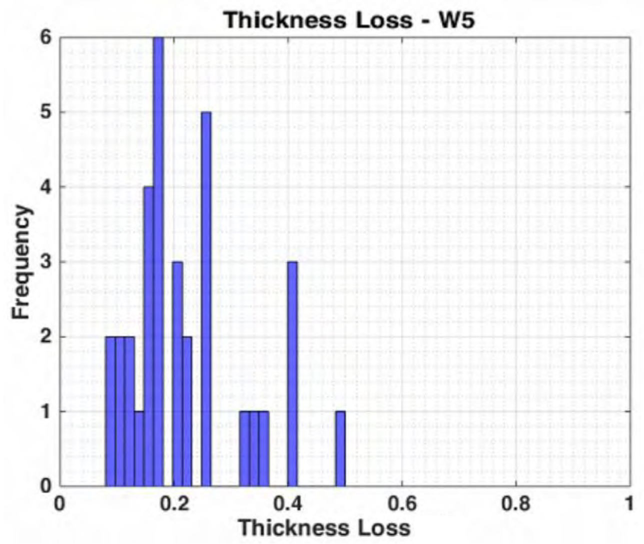

Figure 80: Web thickness loss distribution of W5 pattern for beams without a diaphragm – CTDOT

From the last figures, our team concluded that:

$$0 < CH_1 \leq 0.2H_0$$
$$0.4H_0 \leq CL_1 \leq 1.5H_0$$
$$0.1 \leq \frac{t_{loss}}{t_{web}} \leq 0.5$$

The extreme scenario for W5 pattern is:

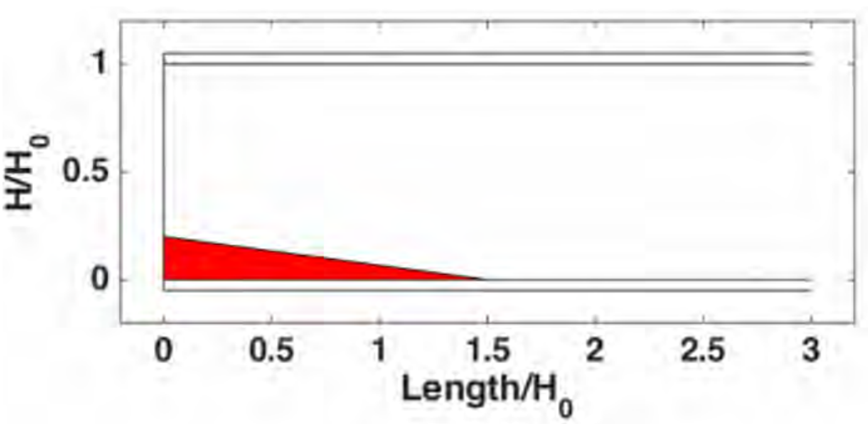

Figure 81: Extreme corrosion scenario for pattern W5 - CTDOT

4.1.6.2. Flange corrosion

Data regarding flange corrosion was very limited in the reports analyzed. Only two beam ends had a combination of the W5 corrosion pattern and flange corrosion. For this reason, the research team was not able to draw conclusion regarding flange corrosion.

4.1.6.3. Holes

No hole corrosion patterns combined with the W5 corrosion pattern were observed in the bridge inspection reports provided by CTDOT.

4.2.Maine

4.2.1. Introduction

As discussed in previous sections, the reports from Maine DOT do not provided specific information regarding corrosion. Due to the absence of measurements, photographic records and sketches, the research team was not able to identify the corrosion patterns from the inspection reports provided.

While this was the case, the reports often reported information regarding thickness loss in the flanges and webs. It is worthwhile pointing out, however, that the information presented in the reports usually does not refer to a specific beam of the bridge. For these cases, the research team opted to store the information as if it referred to a single beam of the bridge, instead of assuming it a common feature for all the beams of the bridge. This means that several of the bridge inspection reports compiled by the research team comprise the information of a single beam.

The results are presented state by state as the amount of beam ends varies considerably from one state to the other. From the reports provided by MaineDOT, the research team was able to compile 39 beam ends. It is important to note that none of the beam ends reported presented diaphragms.

4.2.2. Web Corrosion

Most of the reports presented information regarding web thickness loss. The information is provided without specifically referring to a beam. Figure 82 depicts the histogram of web thickness loss for the beams ends provided by MaineDOT.

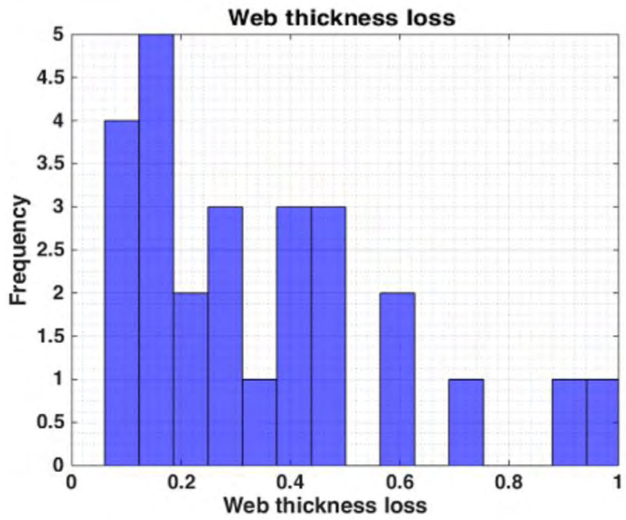

Figure 82: Web thickness loss histogram from the beam ends compiled - MaineDOT

The research team was not able to gather information regarding corrosion length or corrosion height from the reports provided by MaineDOT. These parameters would be beneficial to have as they assist the team in developing common corrosion patterns and shapes.

4.2.3. Flange Corrosion

Most of the reports that contained information regarding the web thickness loss also included information regarding flange thickness loss. More precisely, 29 out of the 39 beams ends compiled presented information regarding corrosion in the flanges. Figure 83 and Figure 84 depict the flange thickness loss for the bottom and top flanges, respectively.

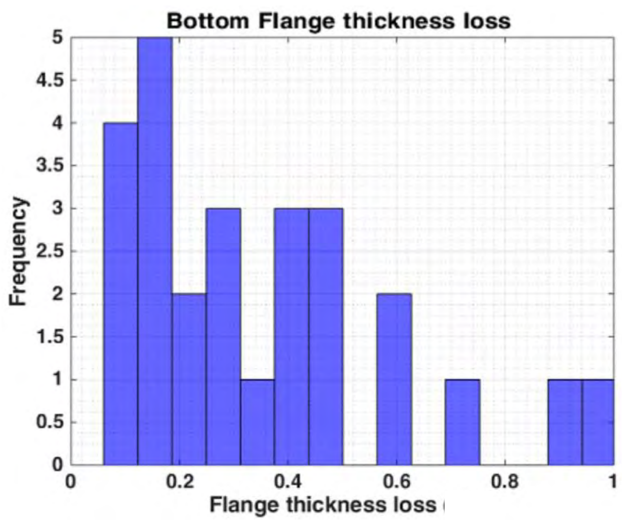

Figure 83: Bottom flange thickness loss histogram from the beam ends compiled - MaineDOT

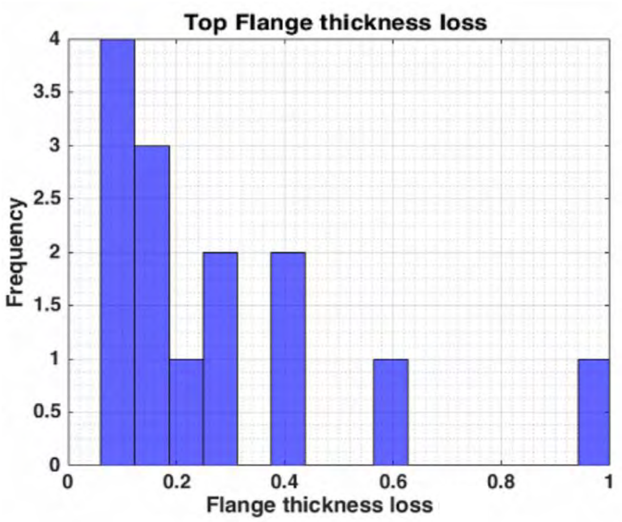

Figure 84: Top flange thickness loss histogram from the beam ends compiled - MaineDOT

The comparison between Figure 83 and Figure 84 clearly shows that the thickness loss of top flanges is smaller than the thickness loss of the bottom flanges. This is likely a result of how ice and water flow to the bottom flanges.

4.2.4. Holes

The holes documented in the inspection reports provided by MaineDOT always have measurements and dimensions. From the reports provided by MaineDOT, the research team was able to identify five holes among the beam ends. All the holes reported by the bridge inspection reports had pictures that clearly depicted the holes, allowing the research team to classify the beam end into a topology.

All five holes observed in the reports are M1. Additionally, Figure 85 and Figure 86 depict the dimensions of the holes observed in the bridge inspection reports from MaineDOT.

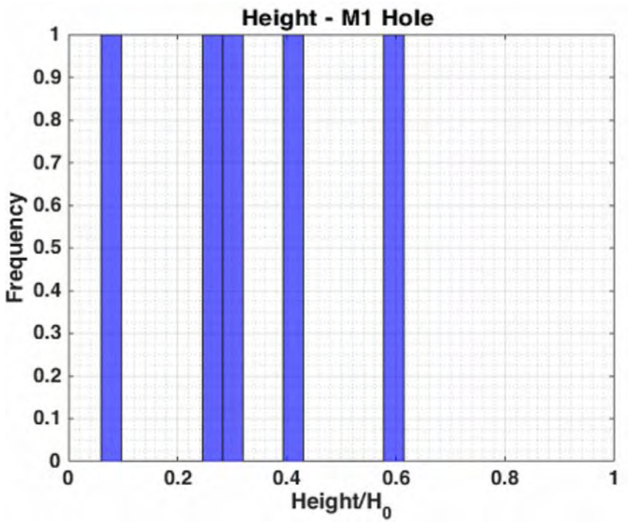

Figure 85: M1 web hole's height distribution of W1 web corrosion pattern for beams without a diaphragm - MaineDOT

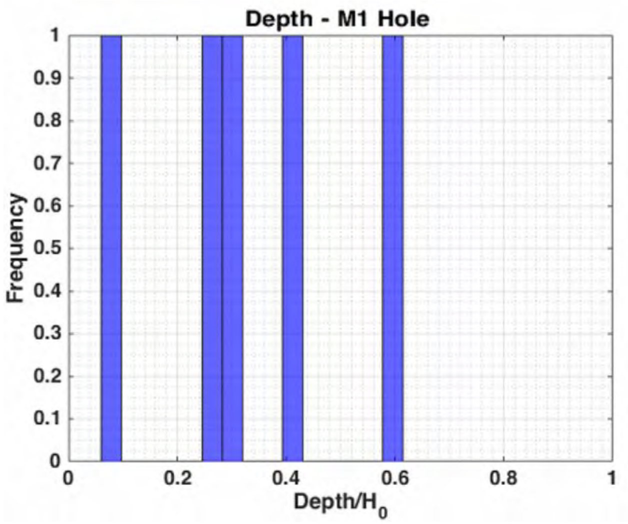

Figure 86: M1 web hole's depth distribution of W1 web corrosion pattern for beams without a diaphragm - MaineDOT

4.3. Massachusetts

4.3.1. Introduction

The data for Massachusetts was divided in two main categories, beams ends with a diaphragm and without a diaphragm. All the graphs in this part of the document represent the second case. Figure 87 contains the frequency of each of the defined corrosion patterns (the total amount of times each pattern appears in the reports).

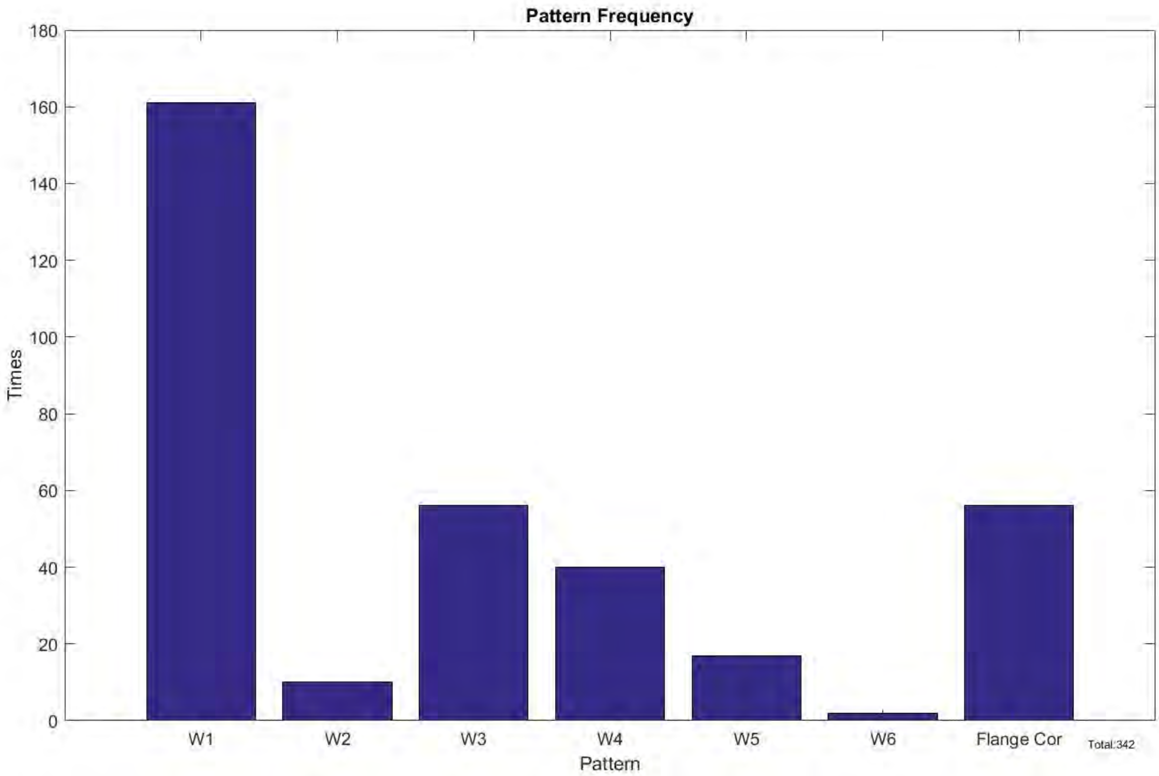

Figure 87: Web corrosion patterns distribution for beams without a diaphragm - MassDOT

For each web corrosion pattern, we have normalized the characteristic dimensions (CH_1, CH_2, CH_3, CL_1, CL_2, CL_3) with the height H_0, where $H_0 = H - 2t_f$.

4.3.2. Pattern W1

4.3.2.1. Web Corrosion

The distribution of CH_1 is shown in Figure 88. From this histogram, 2 main trends are noticed: either a) full height corrosion, or b) corrosion up to 30% of H_0. The parameters for the corrosion patterns can be found with corresponding diagrams in Section 1.5 *Corrosion Patterns* of this report.

$$0 < CH_1 \leq 0.3H \; and \; 0.9H \leq CH_1 \leq H$$

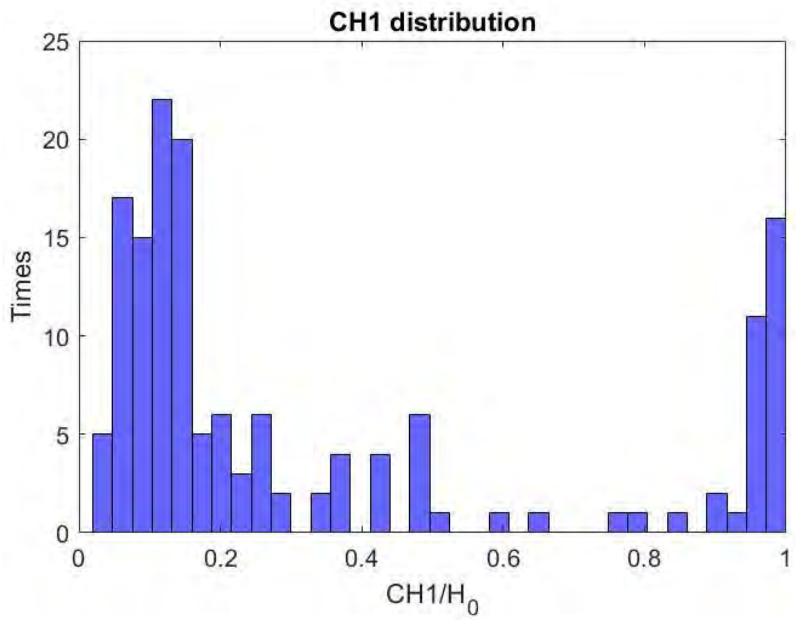

Figure 88: CH_1 distribution of W1 pattern for beams without a diaphragm - MassDOT

Similarly, the CL_1 distribution is shown in Figure 89. From this histogram, it is valid to say that most of the web corrosion length is up to 1.5 times the H_0.

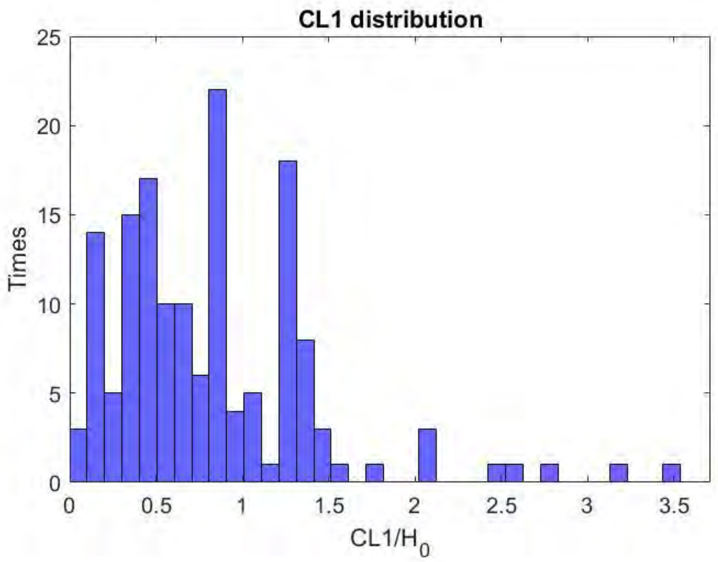

Figure 89: CL_1 distribution of W1 pattern for beams without a diaphragm - MassDOT

Figure 90 shows the ratio of CL_1/CH_1 which indicates that in general, the length of the corroded area is bigger than its height. Figure 91 focuses on the range 0-15 for the same distribution.

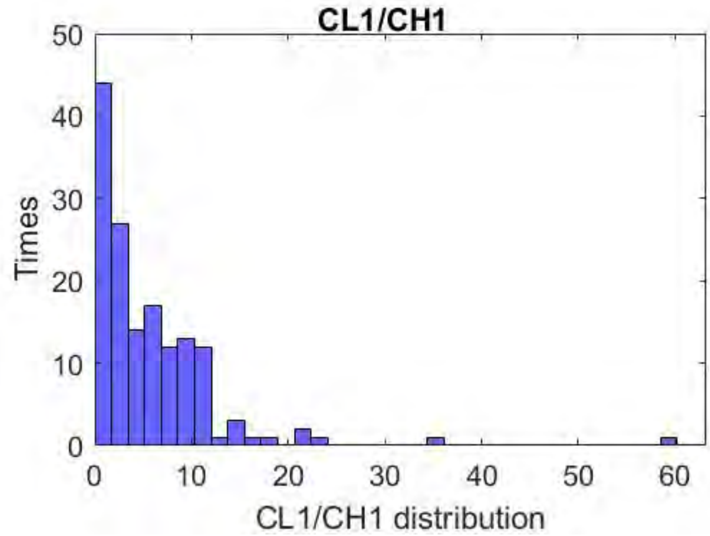

Figure 90: Ratio of corrosion length (CL_1) to corrosion height (CH_1) of W1 pattern for beams without a diaphragm - MassDOT

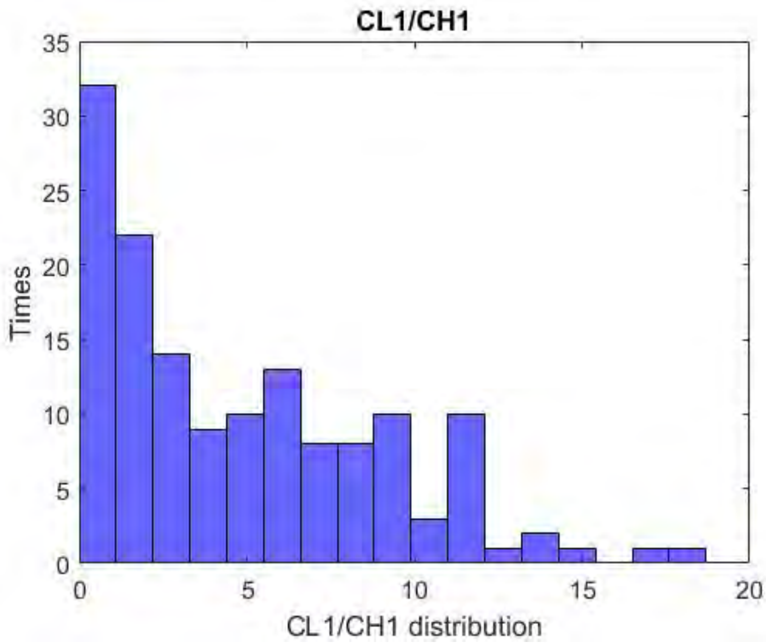

Figure 91: Ratio of corrosion length (CL_1) to corrosion height (CH_1) of W1 pattern for beams without a diaphragm (range 0-15) - MassDOT

As an additional step, the corrosion length and the web thickness loss distribution for each of the two cases of CH_1 were plotted, a) for $CH_1<0.3H_o$ (Figure 92) and b) for $CH_1>0.9H_o$ (Figure 93).

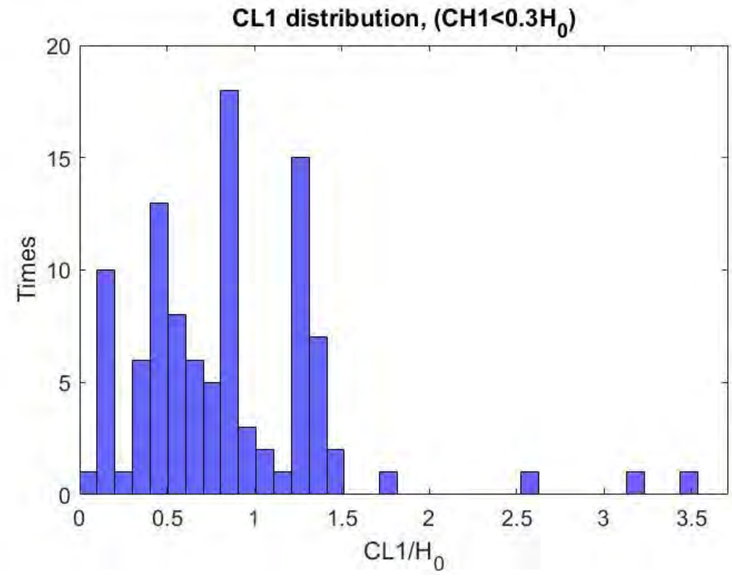

Figure 92: CL1 distribution of W1 web corrosion pattern, with corrosion height up to 30% of H0 for beams without a diaphragm - MassDOT

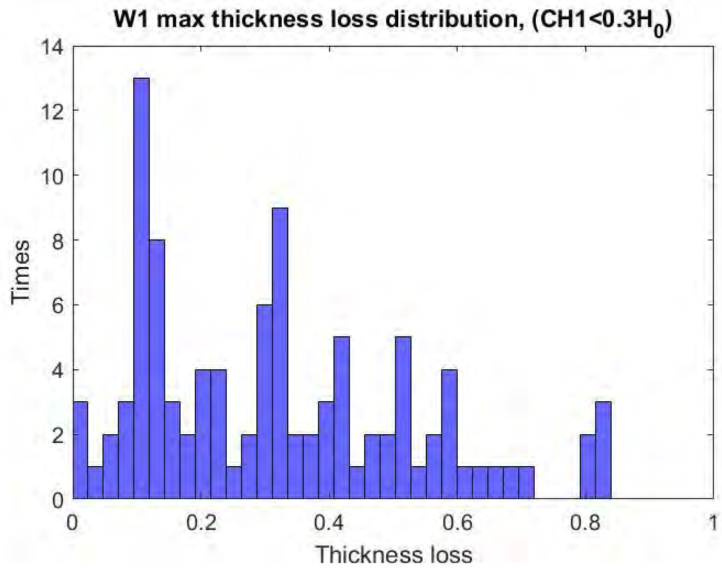

Figure 93: Max thickness loss distribution of W1 web corrosion pattern, with corrosion height up to 30% of H0 for beams without a diaphragm - MassDOT

Based on Figure 93, we can define as extreme case the following, which covers 103 out of the 161 beam ends that demonstrate a W1 corrosion pattern without diaphragms:

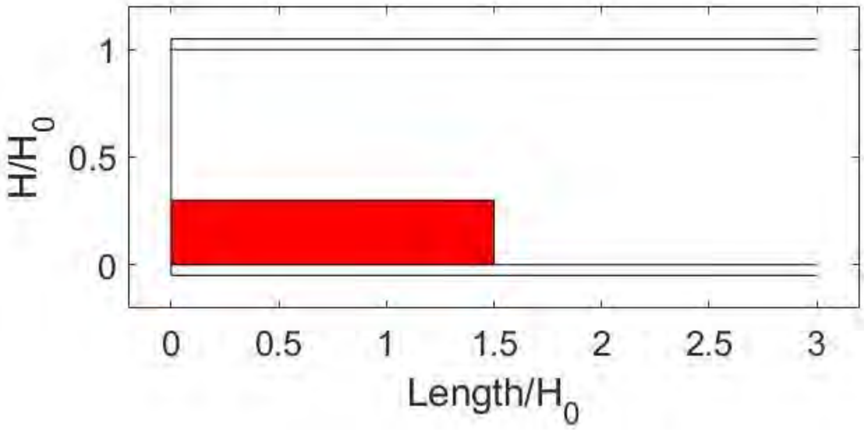

Figure 94: First extreme W1 web corrosion pattern, with corrosion height up to 30% of H0 for beams without a diaphragm - MassDOT

Based on Figure 94, the values for the web thickness loss are: $\frac{t_{loss}}{t_{web}}\ take\ values\ of\ \{0.2,0.4,0.6,0.8\}$

Figure 95 shows the distribution of CL_1 for the case when $CH_1>0.9H_o$.

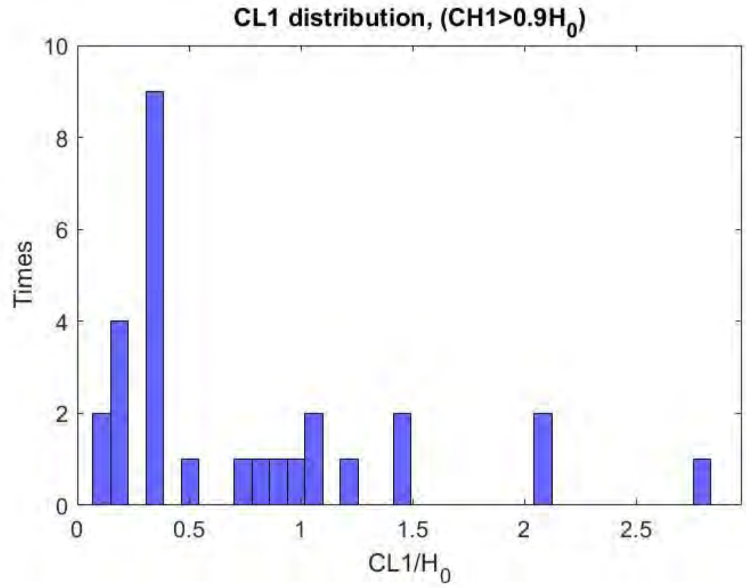

Figure 95: CL_1 distribution of W1 web corrosion pattern with corrosion greater than 90% of H_o for beams without a diaphragm - MassDOT

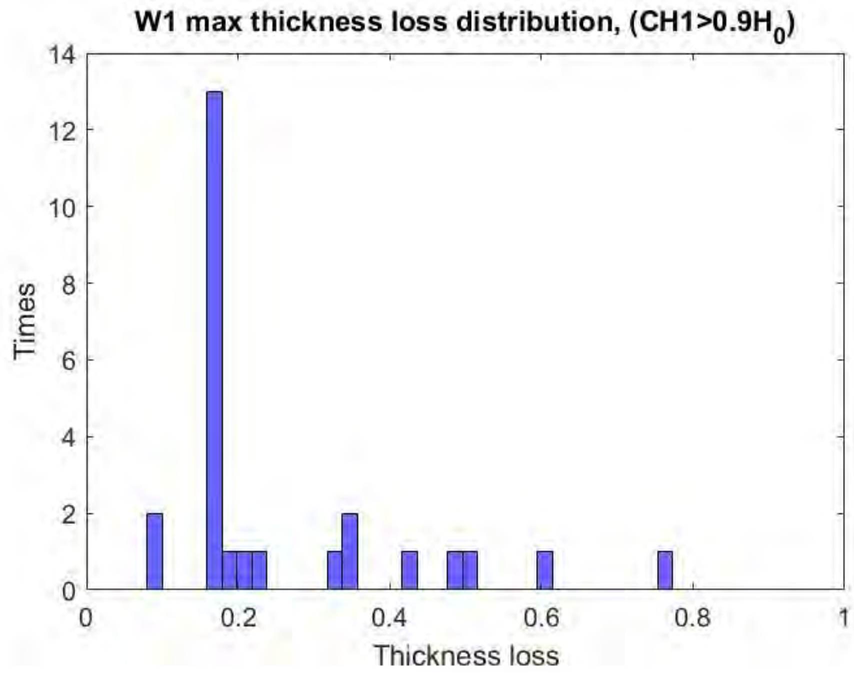

Figure 96: Max thickness loss distribution of W1 web corrosion pattern with corrosion height greater than 90% of H_o for beams without a diaphragm - MassDOT

Figure 96 shows the maximum thickness loss distribution for the same groups of beams. Therefore, for the full height corrosion (>$0.9H_o$), two different cases are identified as shown in Figure 97 and Figure 98.

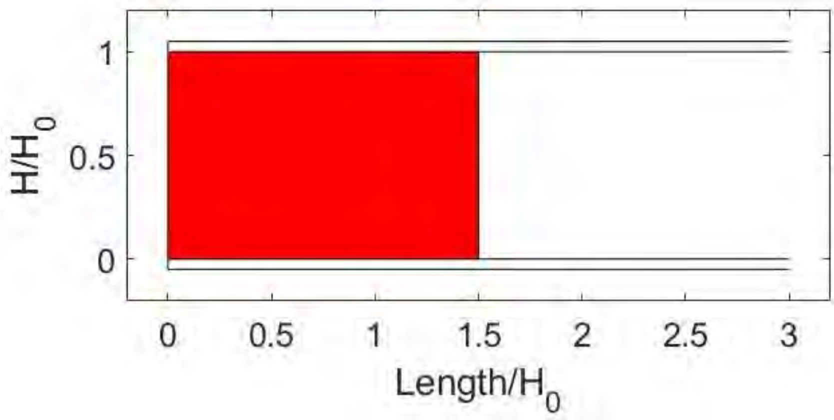

Figure 97: Second extreme W1 web corrosion pattern, with corrosion height greater than 90% of H_o for beams without a diaphragm - MassDOT

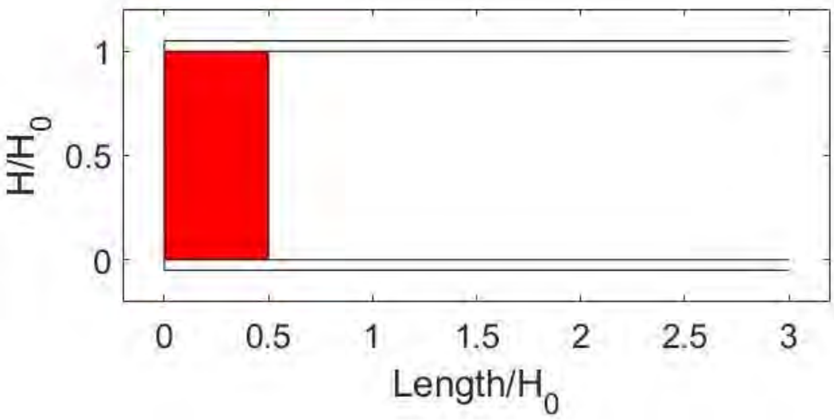

Figure 98: Third extreme W1 web corrosion pattern, with corrosion height greater than 90% of H_o for beams without a diaphragm - MassDOT

From Figure 96 we can conclude that the web thickness loss for this case is:

$\frac{t_{loss}}{t_{web}}$ $takes\ values\ of$ {0.2,0.8}

4.3.2.2. Flange Corrosion

For each of the three cases (Figure 94, Figure 97, Figure 98) the ratio of the length of the corroded flange over the length of the corroded web was plotted (figure Figure 99, Figure 100, Figure 101).

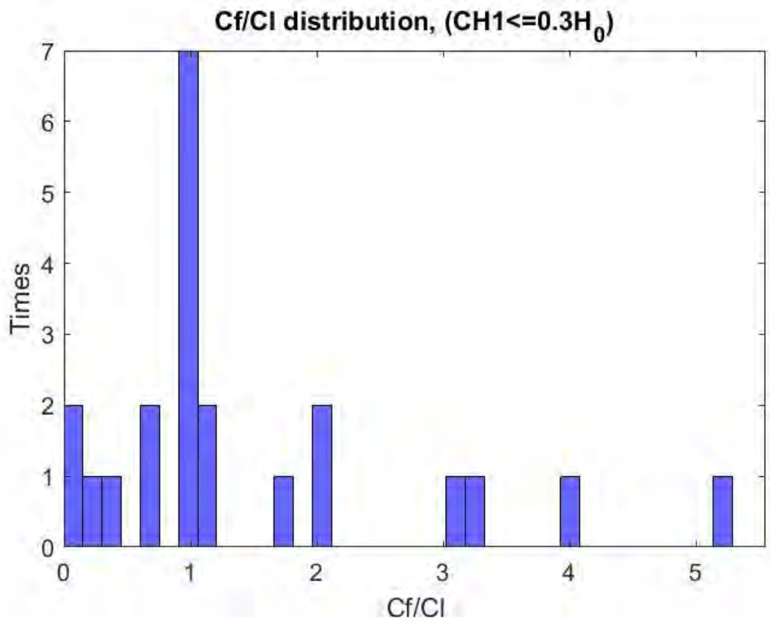

Figure 99: Ratio of flange to web corrosion length distribution of W1 web corrosion pattern with corrosion height up to 30% of H_o for beams without a diaphragm - MassDOT

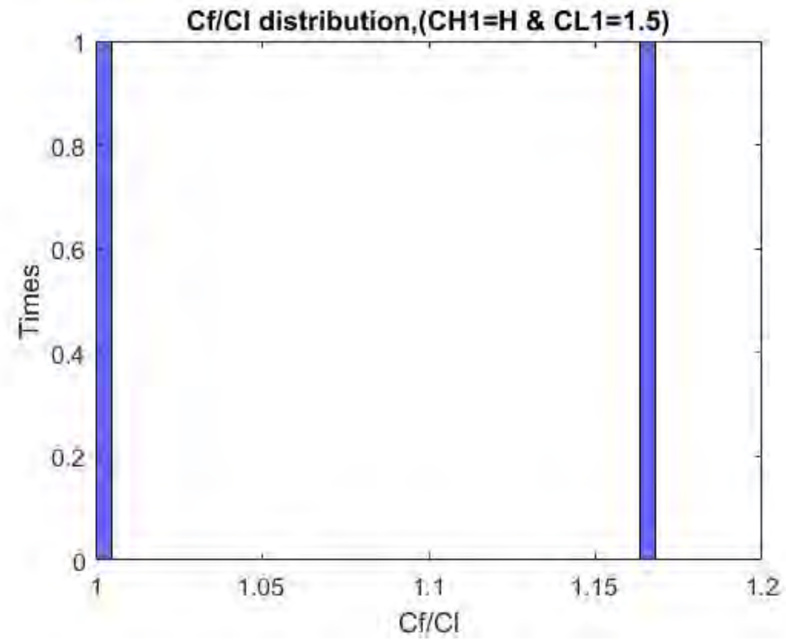

Figure 100: Ratio of flange to web corrosion length distribution of W1 web corrosion pattern for extreme scenario CASE B for beams without a diaphragm - MassDOT

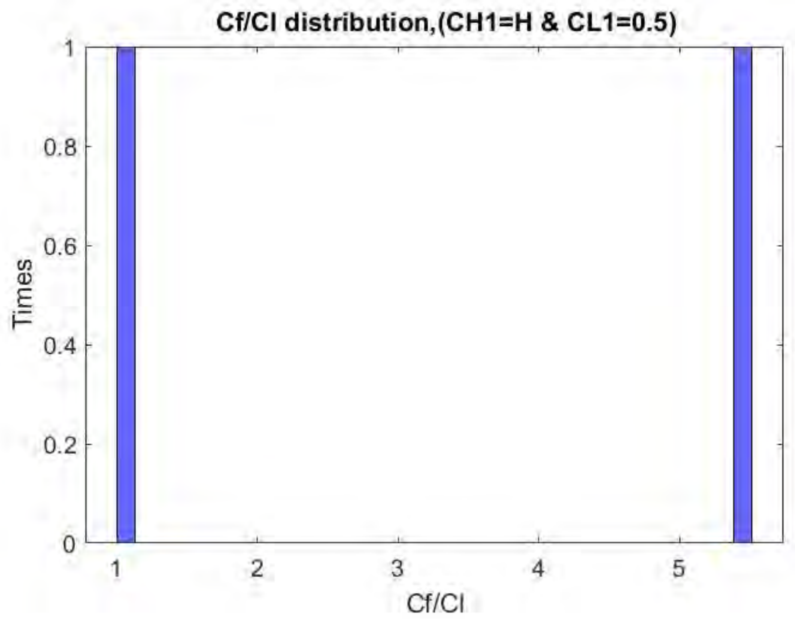

Figure 101: Ratio of flange to web corrosion length distribution of W1 web corrosion pattern for extreme scenario CASE C for beams without a diaphragm - MassDOT

The flange thickness loss is plotted in Figure 102:

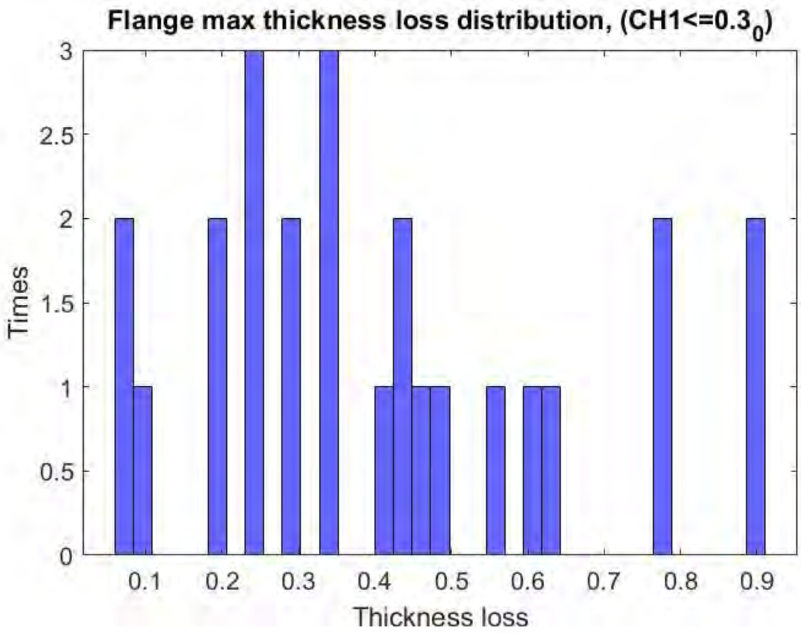

Figure 102: Max flange thickness loss distribution of W1 web corrosion pattern with corrosion height up to 30% of H0 for beams without a diaphragm - MassDOT

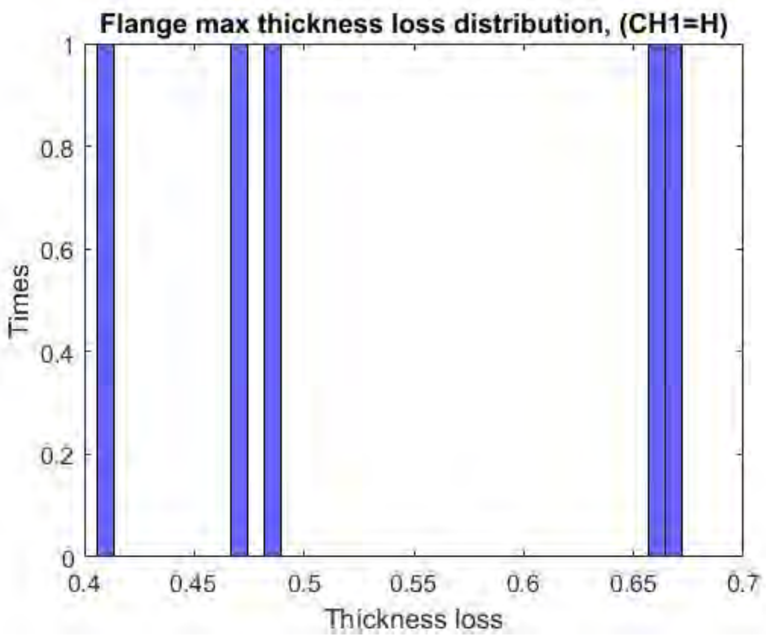

Figure 103: Max flange thickness loss distribution of W1 web corrosion pattern with full height corrosion for beams without a diaphragm - MassDOT

Thus, for Case A: $\frac{t_{loss}}{t_{flange}}$ $takes\ values\ of$ {0.2,0.4,0.6,0.8} (Figure 102) and for Cases B and C: $\frac{t_{loss}}{t_{flange}}$ $takes\ values\ of$ {0.45,0.65} (Figure 103).

For all cases $1 \leq \frac{C_f}{C_l} \leq 2$ (Figure 99, Figure 100, Figure 101).

4.3.2.3. Holes

The frequency of hole appearance is shown in Table 49.

Table 49: Hole appearances for beams without a diaphragm - MassDOT

	Number	No hole	M1	M2	M3	M4	M12	M13	M24
W1	161	146	9	1	3	0	0	2	0
W2	10	8	2	0	0	0	0	0	0
W3	56	44	7	0	3	1	0	1	0
W4	40	347	4	0	0	0	0	2	0
W5	17	13	3	1	0	0	0	0	0
W6	2	2	0	0	0	0	0	0	0

According to the table, the W1 pattern is combined 9 times with the M1 hole pattern (not all cases provide data). The web thickness loss at these cases is given as shown in Figure 104:

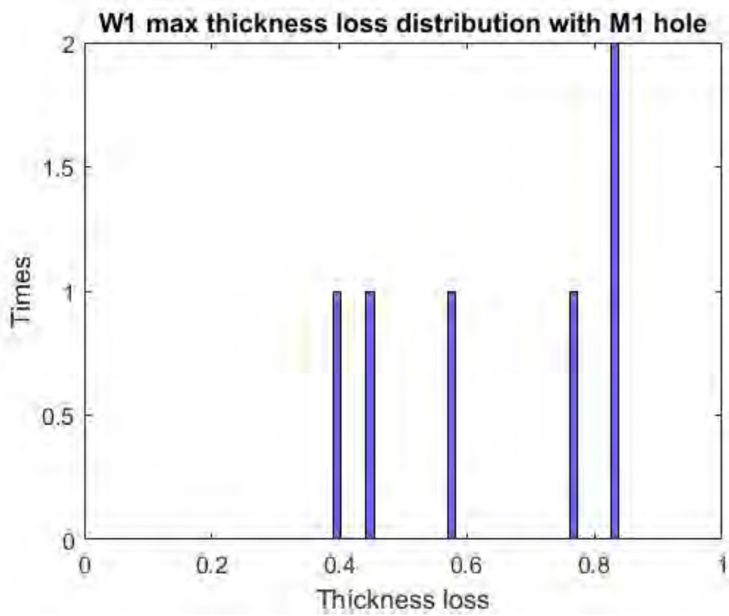

Figure 104: Max thickness loss distribution for W1 web corrosion patterns and M1 hole for beams without a diaphragm - MassDOT

Thus, we could say that the holes appear when the web thickness loss exceeds 40%. The distribution of the holes dimensions is shown below:

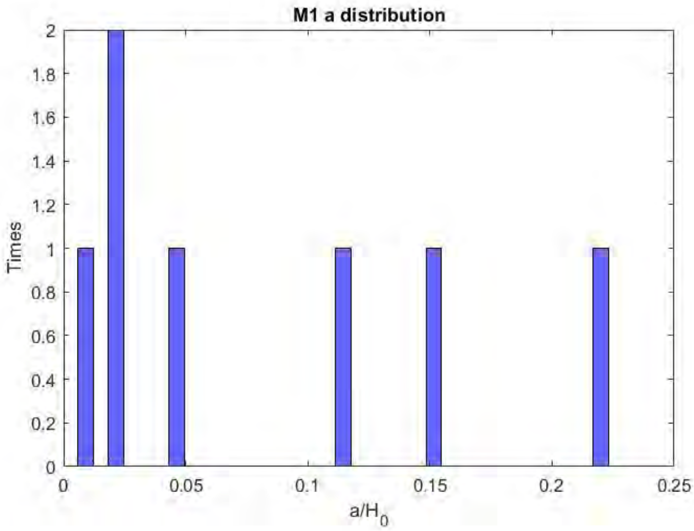

Figure 105: M1 web hole's pattern height distribution of W1 web corrosion pattern for beams without a diaphragm - MassDOT

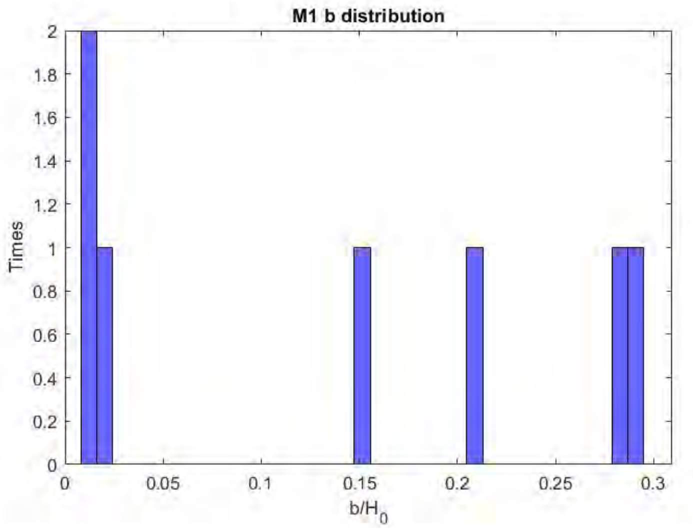

Figure 106: M1 web hole's pattern length distribution of W1 web corrosion pattern for beams without a diaphragm - MassDOT

Observing Figure 105 and Figure 106, our team decided that M1 appears in the form of pit holes (very small dimensions) or in a rectangular shape with the long side parallel to flange. Due to the small number of the available data for the holes, dimensions are not investigated for each case A, B, C separately.

The extreme scenario, projected on the W1 corrosion pattern Case C with a=0.22H and b=0.3H_0 is presented below:

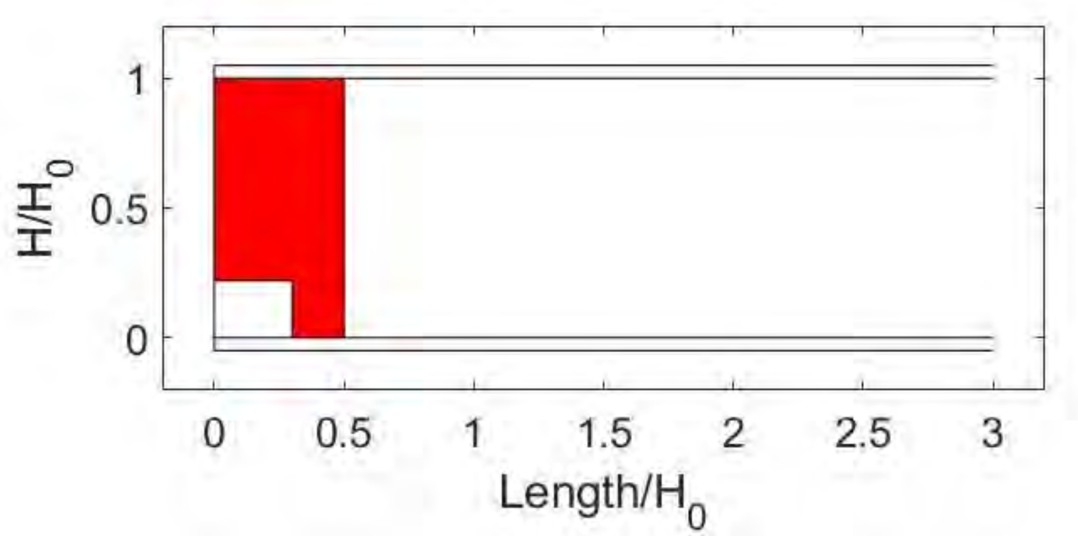

Figure 107: M1 extreme web hole pattern scenario of W1 web corrosion pattern, projected on W1 CASE A, for beams without a diaphragm - MassDOT

4.3.3. Pattern W2

4.3.3.1. Web corrosion

The W2 pattern was observed in total only 10 times. Similar to the W1 pattern, the distributions of all normalized dimensions and web thickness loss were plotted. The parameters for the corrosion patterns can be found with corresponding diagrams in Section 1.5 *Corrosion Patterns* of this report.

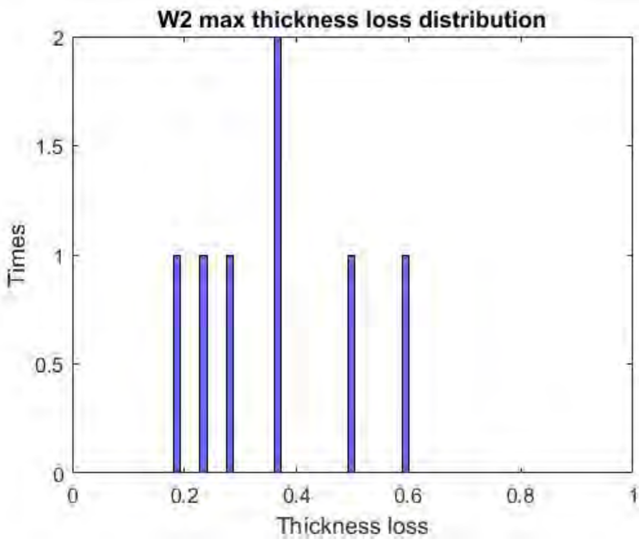

Figure 108: Web thickness loss distribution of W2 pattern for beams without a diaphragm - MassDOT

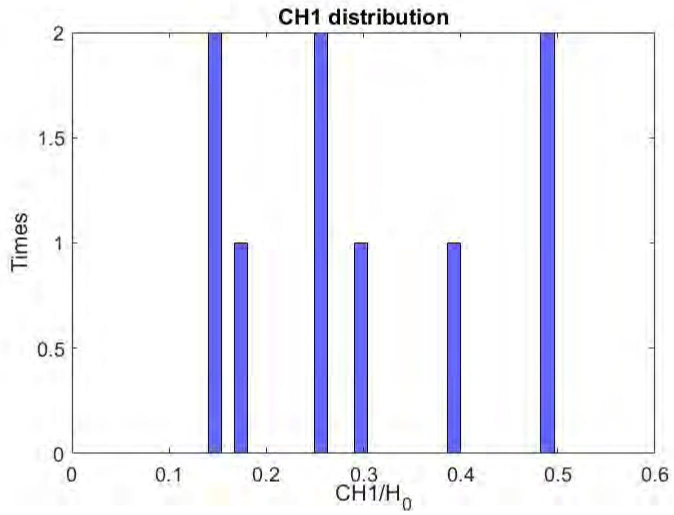

Figure 109: CH_1 distribution of W2 pattern for beams without a diaphragm - MassDOT

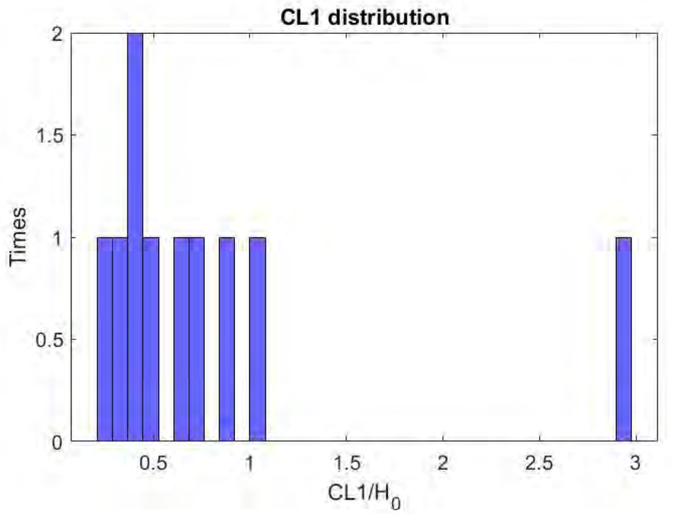

Figure 110: CL_1 distribution of W2 pattern for beams without a diaphragm - MassDOT

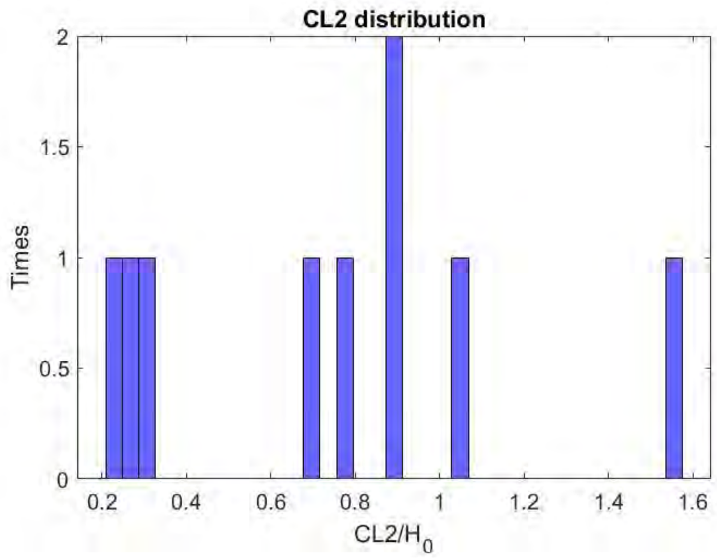

Figure 111: CL_2 distribution of W2 pattern for beams without a diaphragm - MassDOT

From Figure 109, for 6 out of 9 cases, the corrosion height is up to 0.3 H. For these cases, the web corrosion height, length and web thickness loss are presented below:

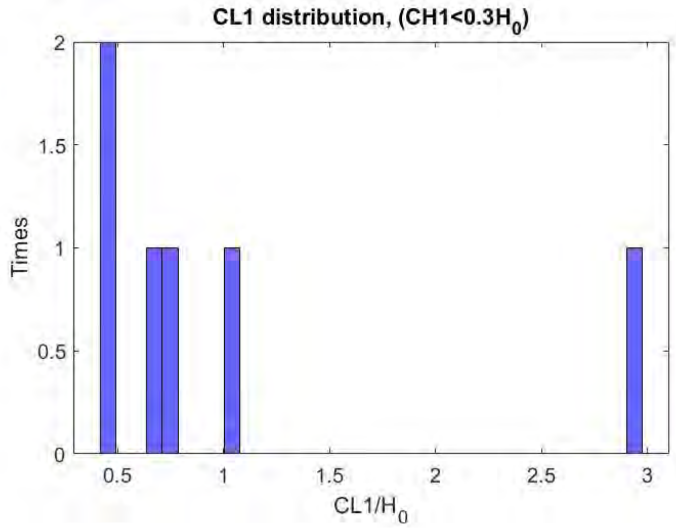

Figure 112: CL_1 distribution of W2 web corrosion pattern corroded up to 30% of H0 for beams without a diaphragm - MassDOT

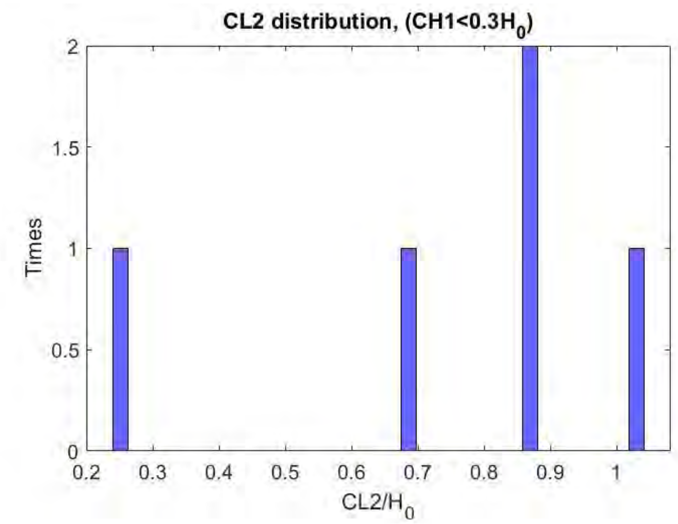

Figure 113: CL2 distribution of W2 web corrosion pattern corroded up to 30% of H0 for beams without a diaphragm - MassDOT

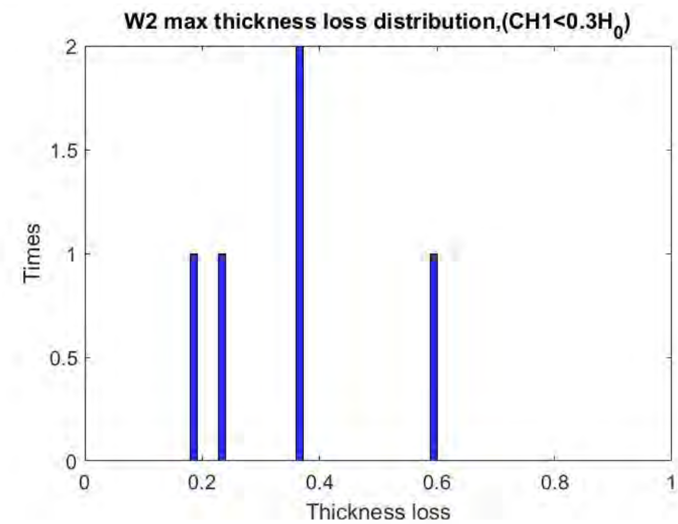

Figure 114: Max thickness loss distribution of W2 web corrosion pattern corroded up to 30% of H0 for beams without a diaphragm - MassDOT

From Figure 110 and Figure 111: $0.5 < CL_1 \leq 1.1H$, $0.25 < CL_2 \leq 1.2H$, where the extreme scenario is illustrated as:

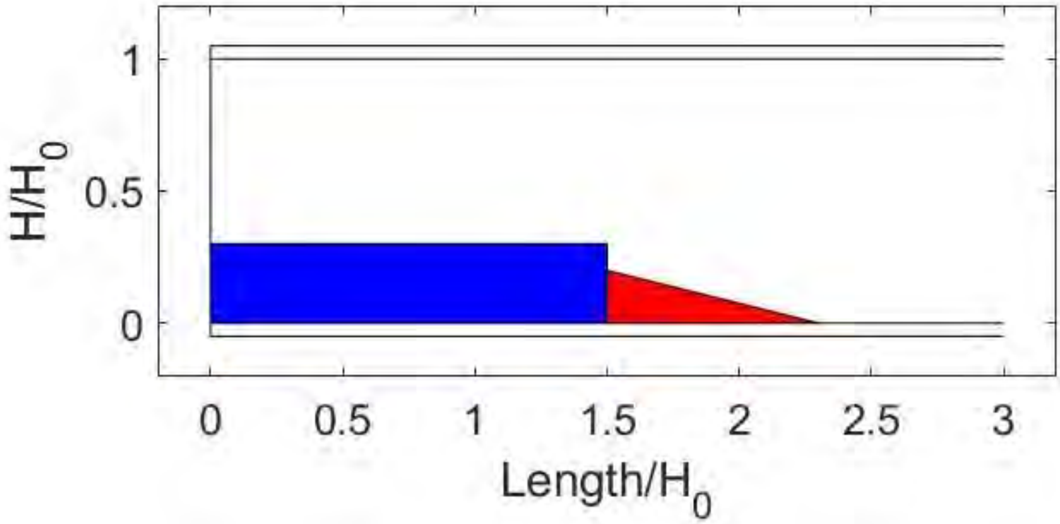

Figure 115: W1 Case A extreme web corrosion scenario projected over W2 extreme web corrosion scenario - MassDOT

The blue area indicates the Case A of W1 pattern, and with red the extreme W2 pattern scenario. Since the rest of W2 cases fit in the blue shadowed area, W1 case A can be merged with W2. According to Figure 108 the thickness loss for W2 is in the Case A-W1 range.

4.3.3.2. Flange corrosion

There was no analysis conducted on flange corrosion since the worst scenario is included in the W1 corrosion scenario.

4.3.3.3. Holes

In W2 pattern the M1 hole appears twice with dimensions a_1=b_1=0.05 and a_2=0.15 and b_2=0.5 which exceeds the W1 and M1 combination max hole length.

4.3.4. Pattern W3

4.3.4.1. Web Corrosion

The parameters for the corrosion patterns can be found with corresponding diagrams in Section 1.5 *Corrosion Patterns* of this report. The data analysis started with the CH2 distribution:

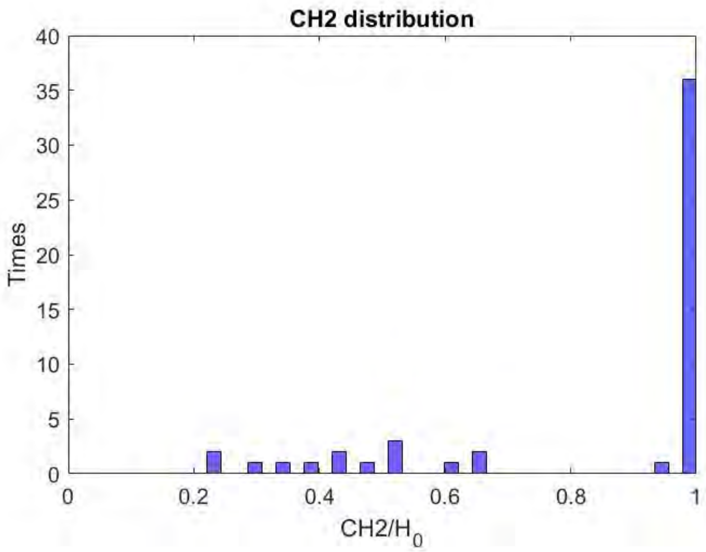

Figure 116: CH_2 distribution of W3 web corrosion pattern for beams without a diaphragm - MassDOT

From Figure 116, it is obvious that the dominant scenario is the full height corroded web case. For CH_2=H_0 the dimension and thickness distributions are presented.

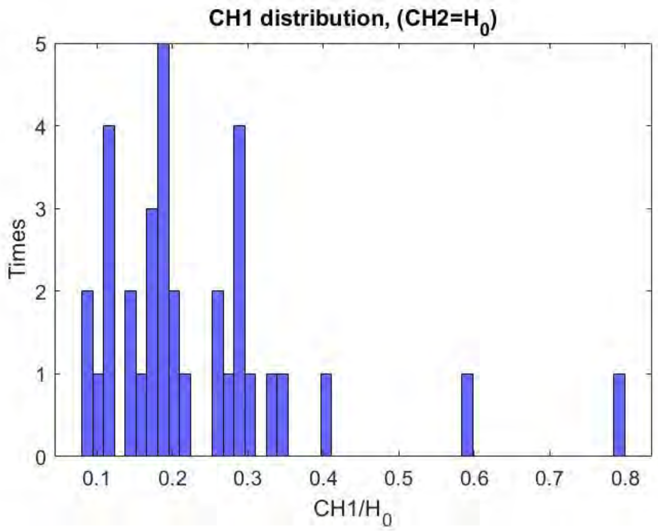

Figure 117: CH_1 distribution of W3 web corrosion pattern with full height corrosion for beams without a diaphragm - MassDOT

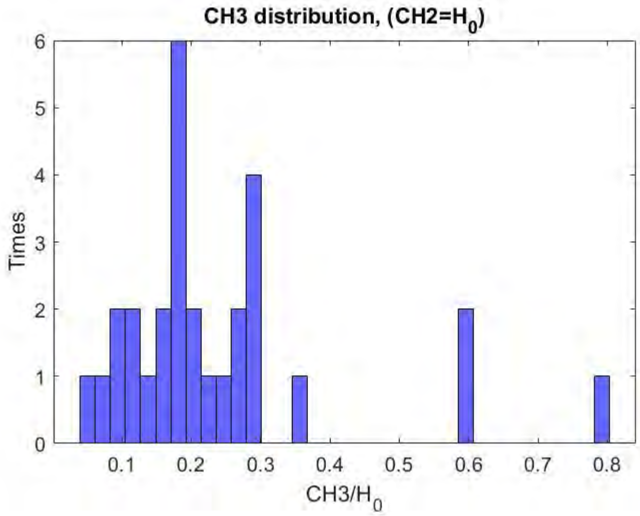

Figure 118: CH_3 distribution of W3 web corrosion pattern with full height corrosion for beams without a diaphragm - MassDOT

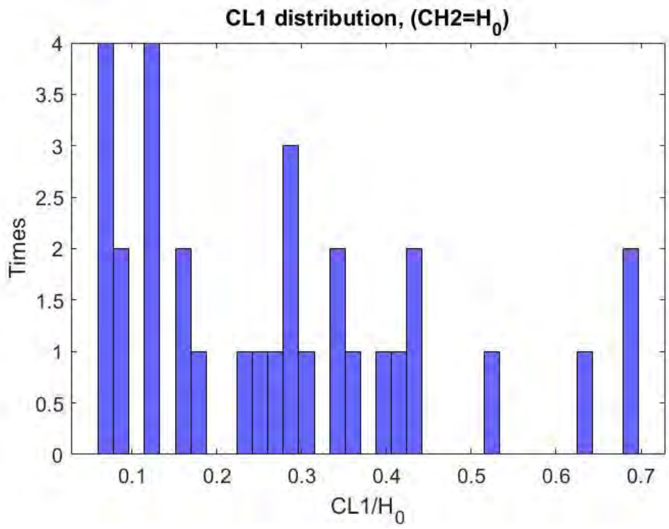

Figure 119: CL1 distribution of W3 web corrosion pattern with full height corrosion for beams without a diaphragm - MassDOT

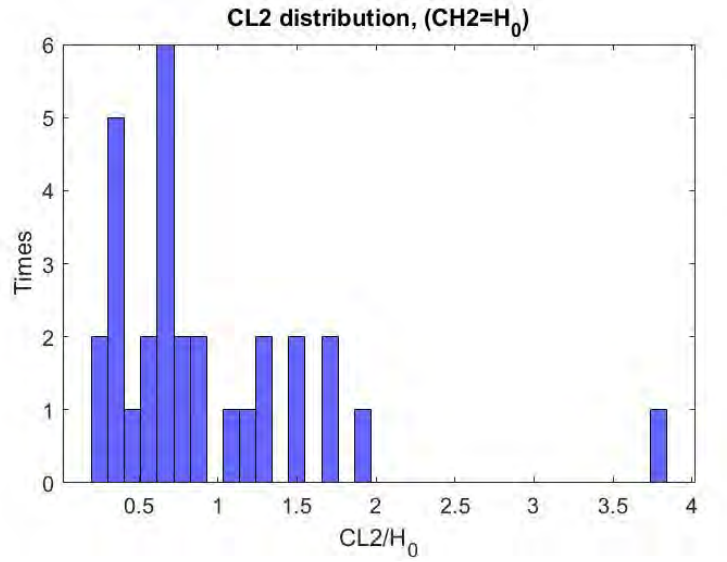

Figure 120: CL_2 distribution of W3 web corrosion pattern with full height corrosion for beams without a diaphragm - MassDOT

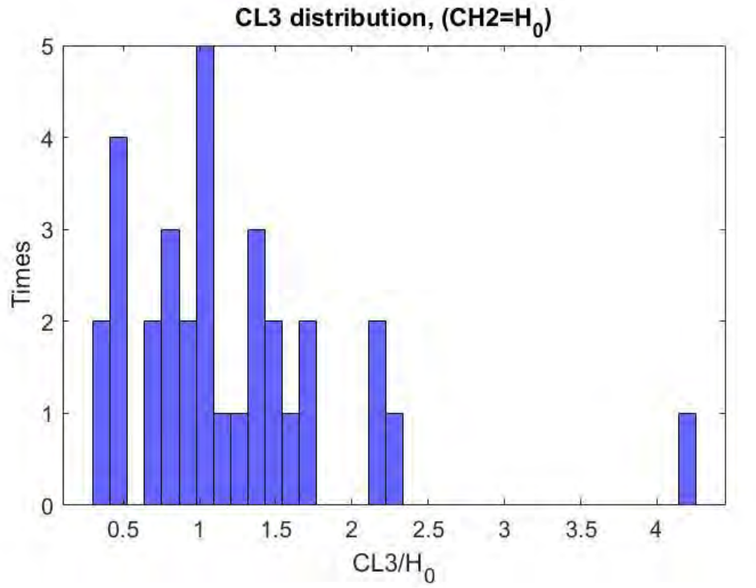

Figure 121: CL_3 distribution of W3 web corrosion pattern with full height corrosion for beams without a diaphragm - MassDOT

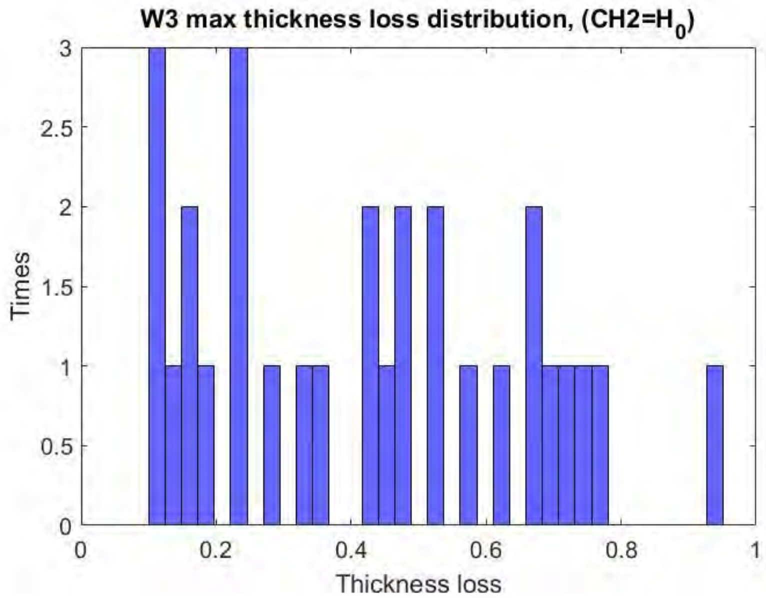

Figure 122: Max web thickness loss distribution of W3 web corrosion pattern with full height corrosion for beams without a diaphragm - MassDOT

From the last figures we can conclude that:

$$0 < CH_1 \leq 0.35$$

$$0 < CH_3 \leq 0.35$$

$$0.05 < CL_1 \leq 0.7$$

$$0.5 < CL_3 \leq 2.3$$

$$\frac{t_{loss}}{t_{web}} \, takes \, values \, of \, \{0.1,0.2,0.3,0.4,0.5,0.6,0.7,0.8\}$$

And therefore, the extreme scenario is:

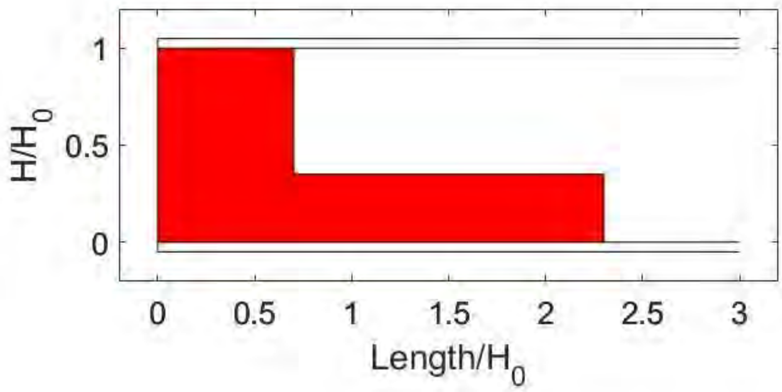

Figure 123: Extreme W3 web corrosion scenario for beams without a diaphragm - MassDOT

4.3.4.2. Flange Corrosion

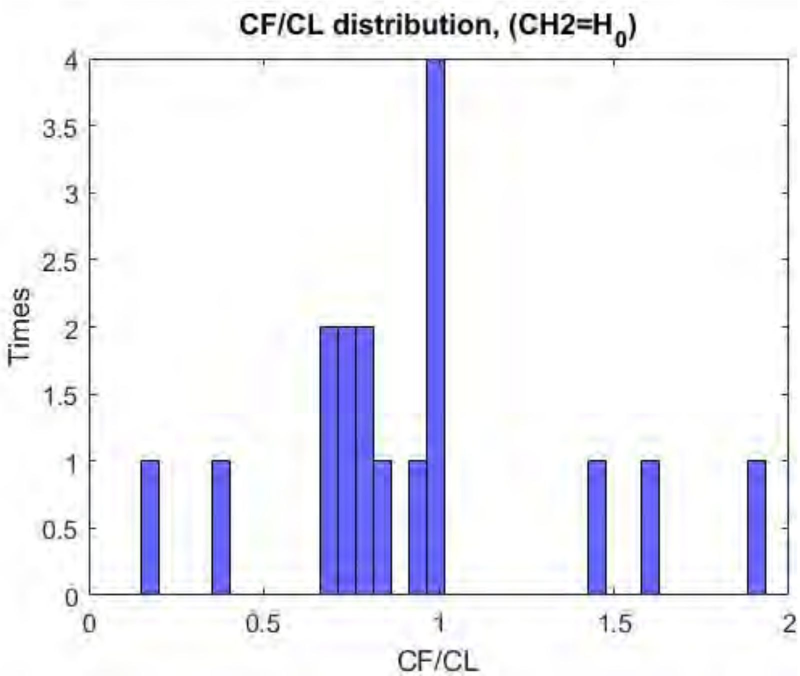

Figure 124: Ratio of flange to web corrosion length distribution of W3 web corrosion pattern with full height corrosion for beams without a diaphragm - MassDOT

Based on Figure 124, the parameter CF is considered equal to parameter CL.

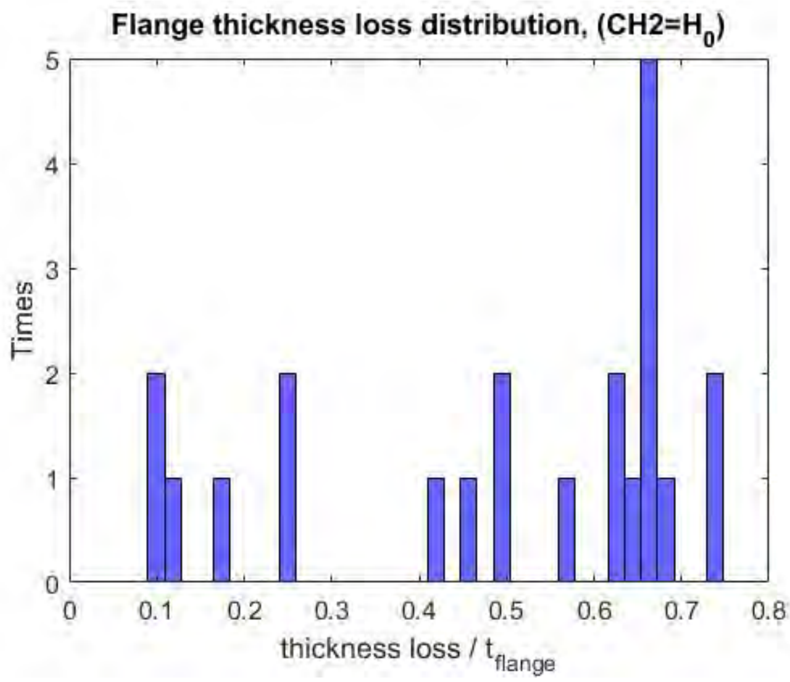

Figure 125: Max flange loss thickness distribution of W3 web corrosion pattern with full height corrosion for beams without a diaphragm - MassDOT

$$\frac{t_{loss}}{t_{flange}} takes\ values\ of \{0.4, 0.6, 0.8\}$$

4.3.4.3. Holes

Holes dimensions distribution:

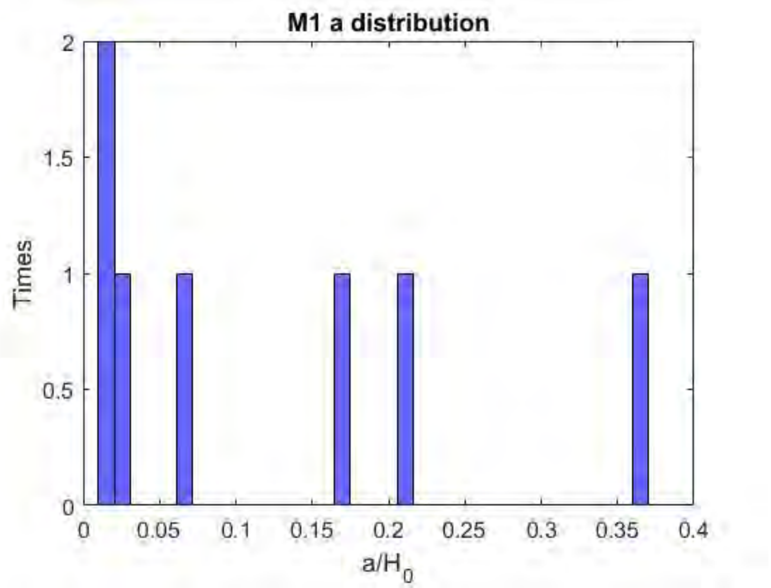

Figure 126: M1 web hole's pattern height distribution of W3 web corrosion pattern for beams without a diaphragm - MassDOT

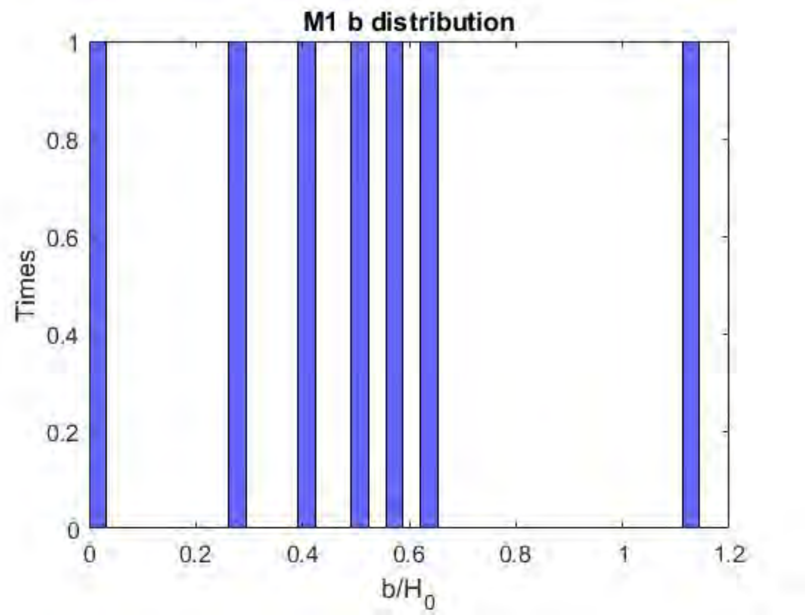

Figure 127: M1 web hole's pattern length distribution of W1 web corrosion pattern for beams without a diaphragm - MassDOT

The extreme corrosion hole scenario with parameters a=0.21 and b=0.63 are presented below. This extreme case is projected on the W3 pattern corroded area:

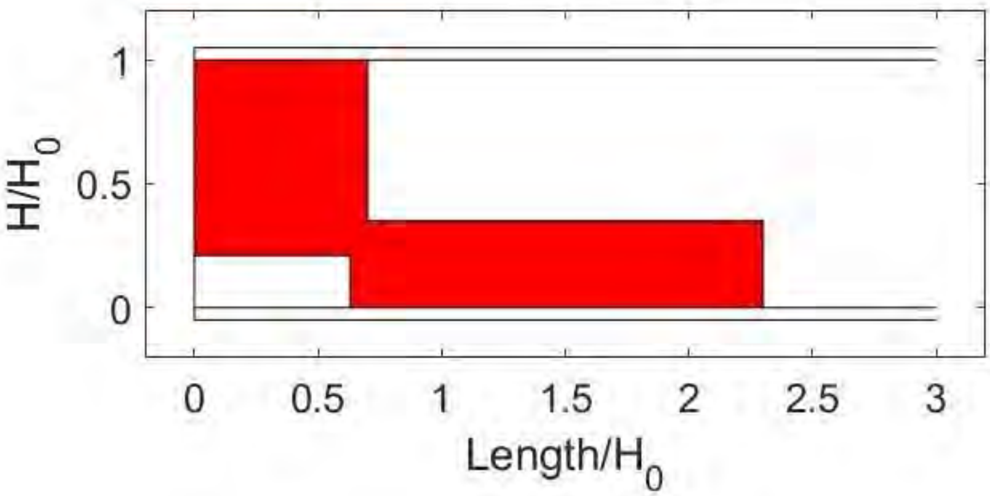

Figure 128: M1 extreme web hole pattern scenario of W1 web corrosion pattern, projected on W3 extreme corrosion scenario, for beams without a diaphragm - MassDOT

4.3.5. Pattern W4

4.3.5.1. Web Corrosion

The thickness loss, as well as the distribution of all normalized dimensions are plotted in the following figures. The parameters for the corrosion patterns can be found with corresponding diagrams in Section 1.5 *Corrosion Patterns* of this report.

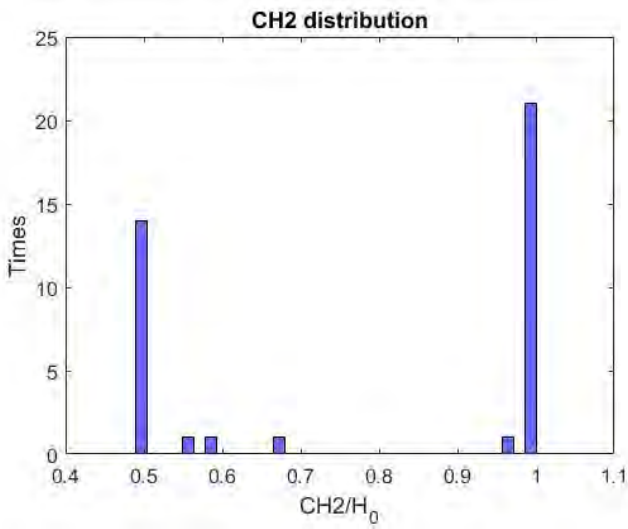

Figure 129: CH2 distribution of W4 web corrosion pattern for beams without a diaphragm - MassDOT

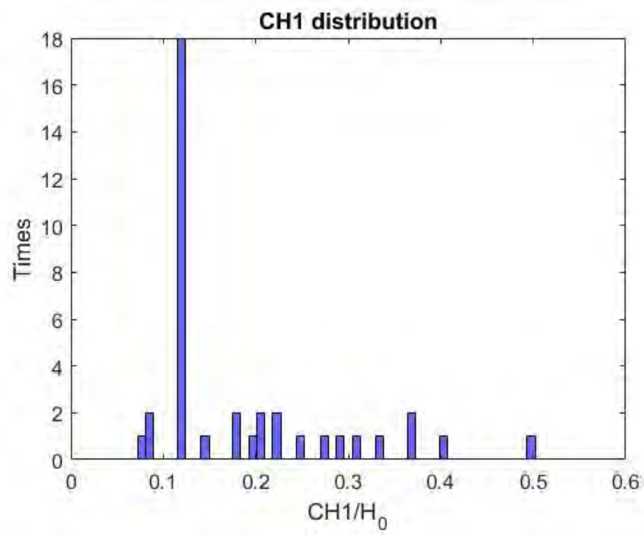

Figure 130: CH1 distribution of W4 web corrosion pattern for beams without a diaphragm - MassDOT

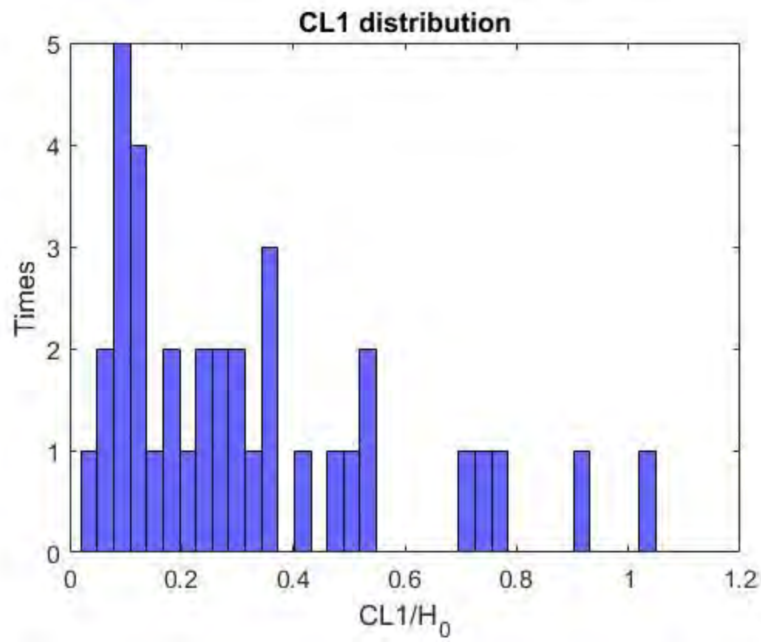

Figure 131: CL1 distribution of W4 web corrosion pattern for beams without a diaphragm - MassDOT

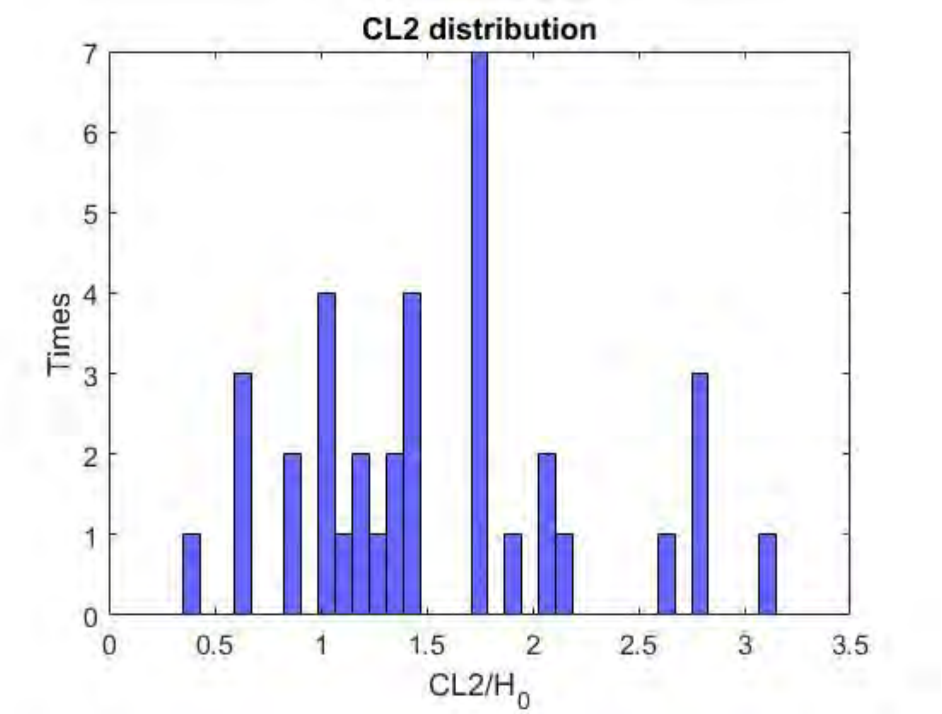

Figure 132: CL2 distribution of W4 web corrosion pattern for beams without a diaphragm - MassDOT

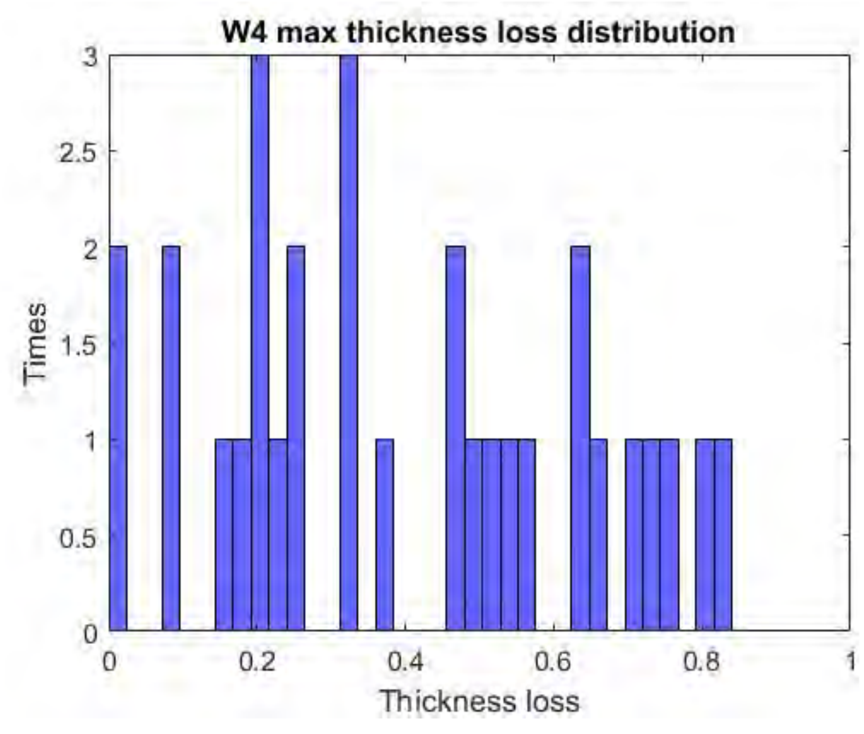

Figure 133: Max web thickness loss distribution of W4 web corrosion pattern for beams without a diaphragm - MassDOT

From the CH2 histogram (Figure 129), two main trends were noticed: either a) full height corrosion, or b) corrosion up to 50% of H_0. As an additional step, the corrosion dimensions (CH1, CL1, CL2, CL3) and the web thickness loss distribution for each of the two cases of CH1 were plotted, a) for CH1=0.5H_o and b) for CH1=H_o.

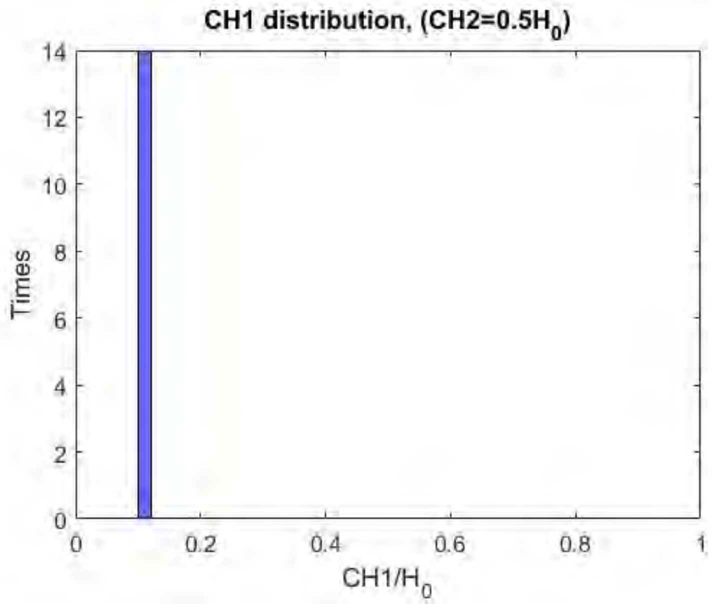

Figure 134 : CH1 distribution of W4 web corrosion pattern, with corrosion height up to 50% of H_0 for beams without a diaphragm - MassDOT

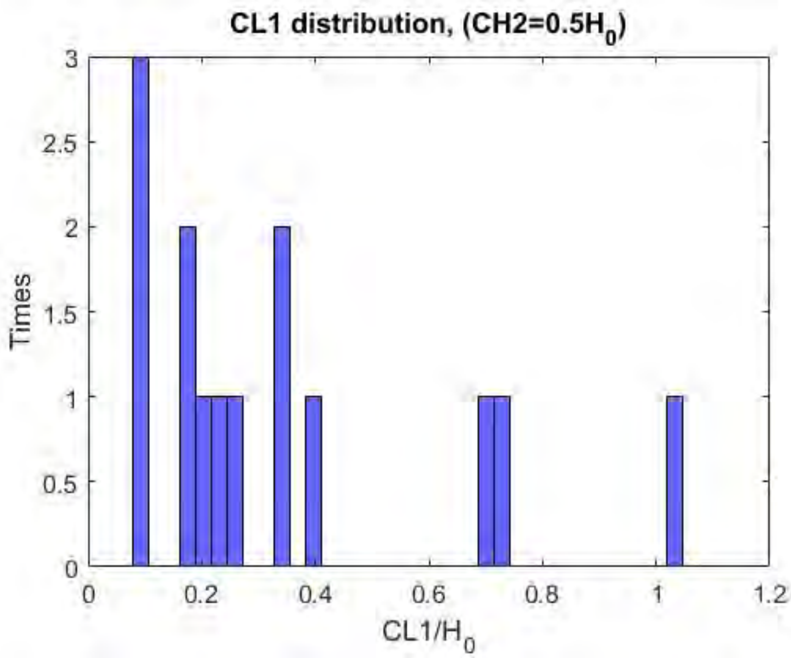

Figure 135: CL1 distribution of W4 web corrosion pattern, with corrosion height up to 50% of H_0 for beams without a diaphragm - MassDOT

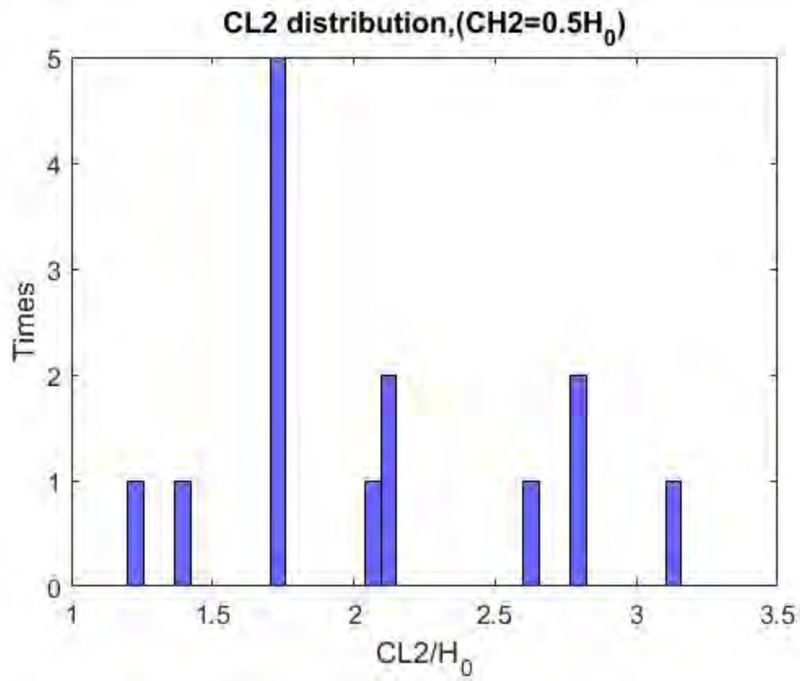

Figure 136: CL2 distribution of W4 web corrosion pattern, with corrosion height up to 50% of H_0 for beams without a diaphragm - MassDOT

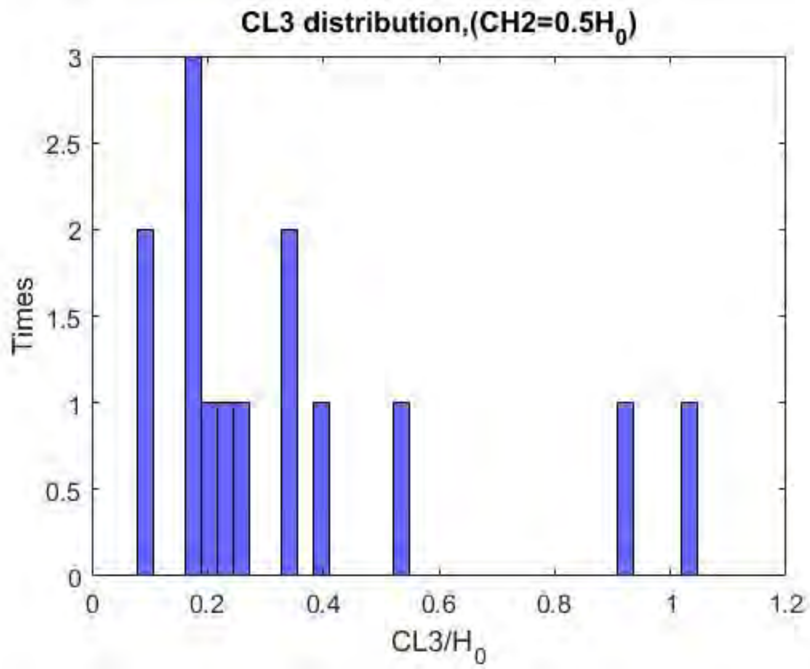

Figure 137: CL3 distribution of W4 web corrosion pattern, with corrosion height up to 50% of H_0 for beams without a diaphragm - MassDOT

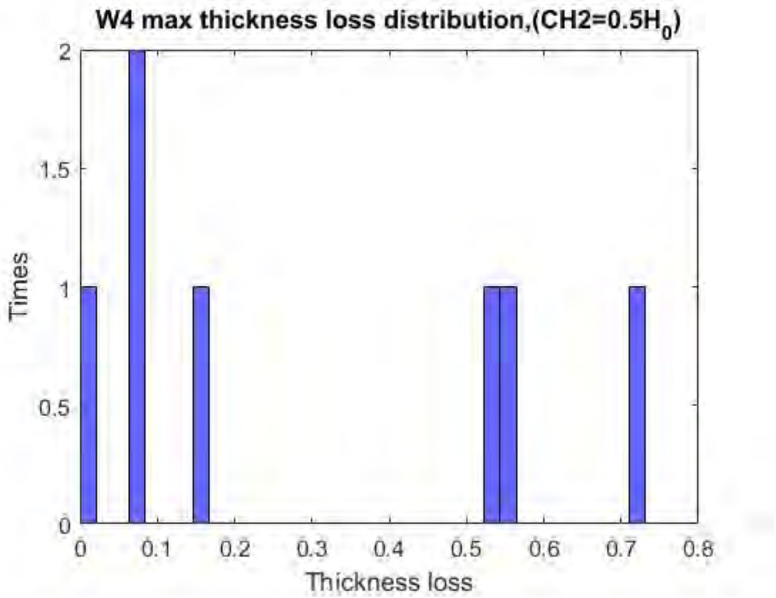

Figure 138: Max web thickness loss distribution of W4 web corrosion pattern, with corrosion height up to 50% of H_0 for beams without a diaphragm - MassDOT

Based on Figure 134, Figure 135, Figure 136, Figure 137, Figure 138:

$$CH_1 = 0.12H_0$$

$$1.2H_0 \le CL_2 \le 3.2H_0$$

$$0.2H_0 \le CL_1 \cong CL_3 \le 0.4H_0$$

$$\frac{t_{loss}}{t_{web}}\ takes\ values\ of\ \{0.05, 0.15, 0.55, 0.75\}$$

The extreme scenario is:

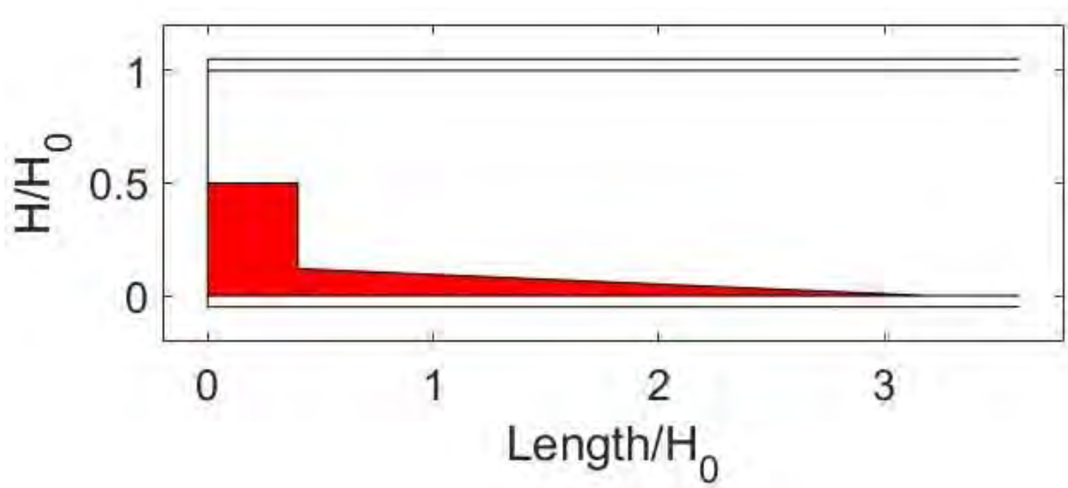

Figure 139: First extreme W4 web corrosion scenario for beams without a diaphragm - MassDOT

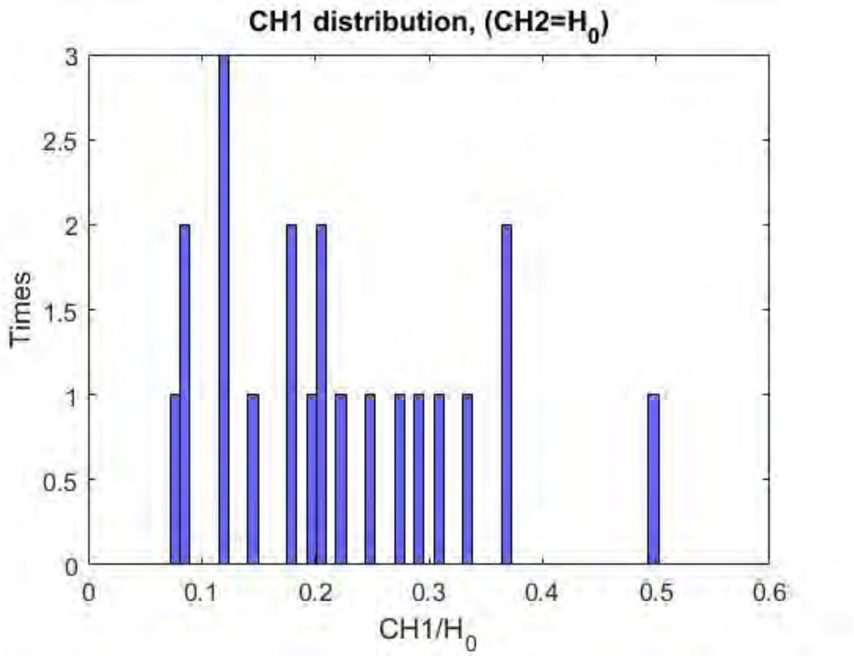

Figure 140: CH1 distribution of W4 web corrosion pattern, with full height corrosion for beams without a diaphragm - MassDOT

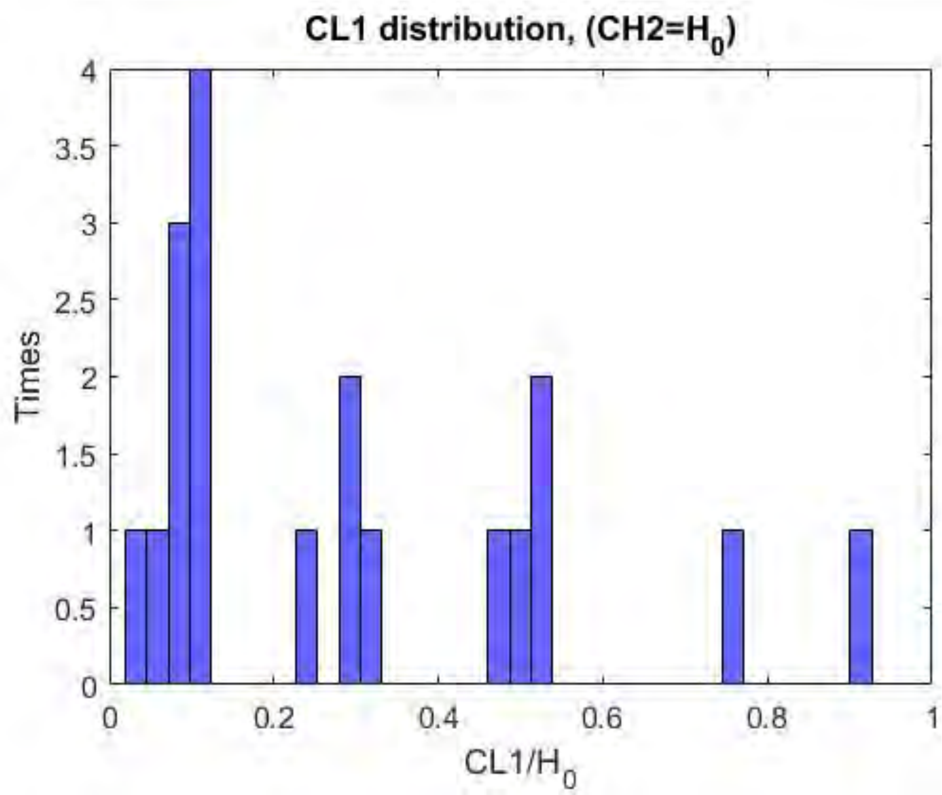

Figure 141: CL1 distribution of W4 web corrosion pattern, with full height corrosion for beams without a diaphragm - MassDOT

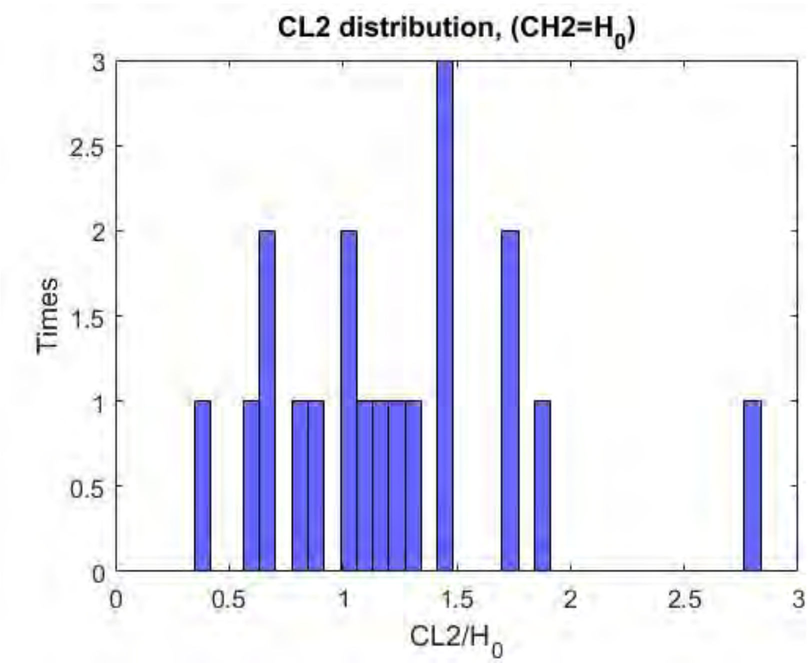

Figure 142: CL2 distribution of W4 web corrosion pattern, with full height corrosion for beams without a diaphragm - MassDOT

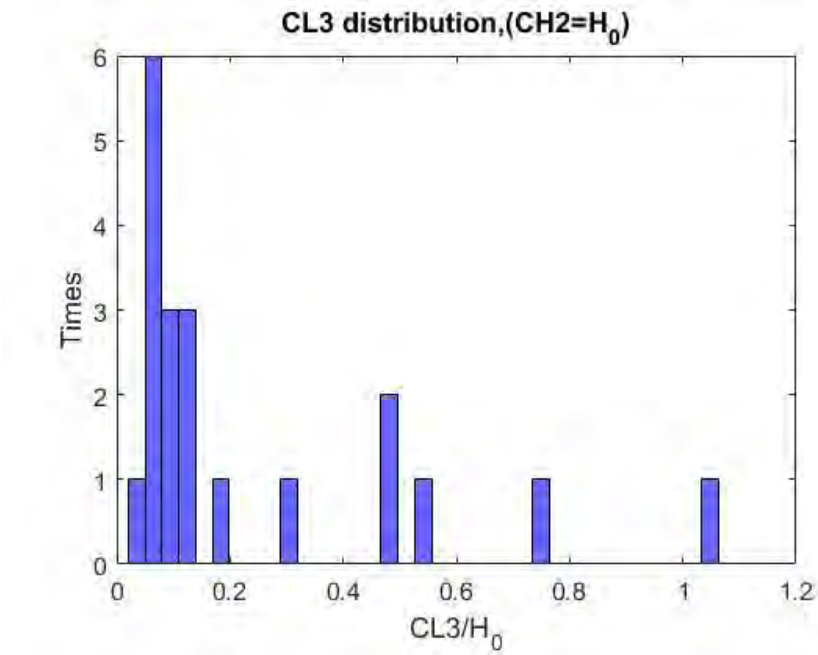

Figure 143: CL3 distribution of W4 web corrosion pattern, with full height corrosion for beams without a diaphragm - MassDOT

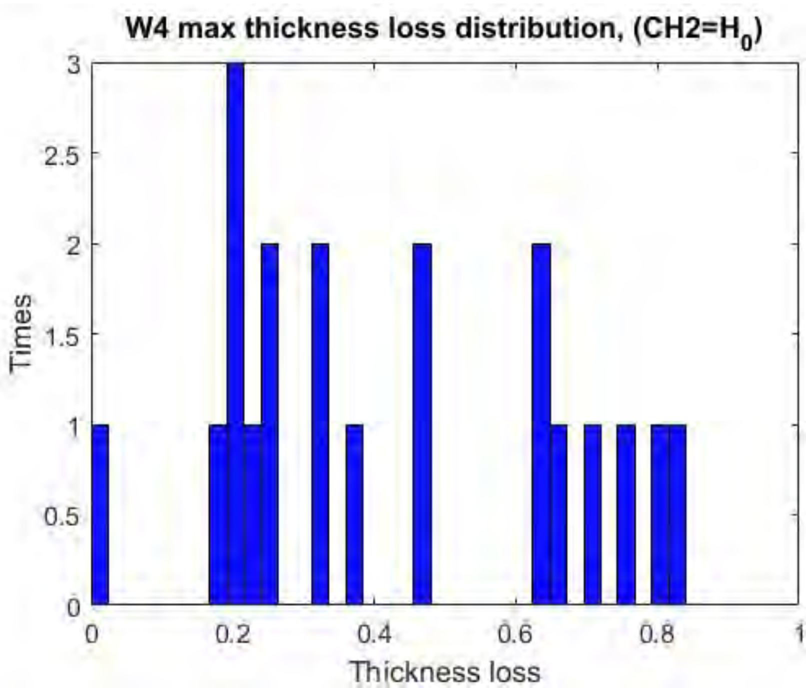

Figure 144: Max web thickness loss distribution of W4 web corrosion pattern, with full height corrosion for beams without a diaphragm - MassDOT

For the full height corrosion:

$$0.1H_0 \leq CH_1 \leq 0.5H_0$$

$$0 < CL_1 \leq \ 0.9H_0$$

$$0.5H_0 \leq CL_2 \leq 1.8H_0$$

$$0 < CL_3 \leq 0.2H_0$$

with thickness loss:

$$\frac{t_{loss}}{t_{web}}\ takes\ values\ of\ \{0.2,0..4,0.6,0.8\}$$

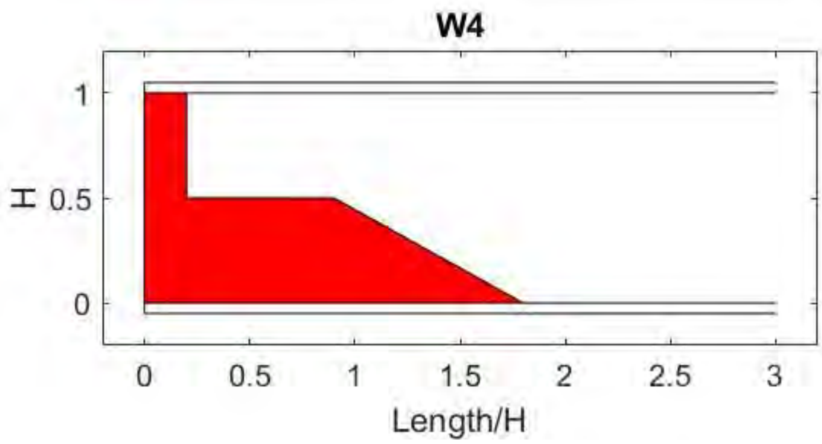

Figure 145: Second extreme W4 web corrosion scenario for beams without a diaphragm - MassDOT

The two W4 extreme scenarios are now projected over the extreme W3 scenario (blue colour):

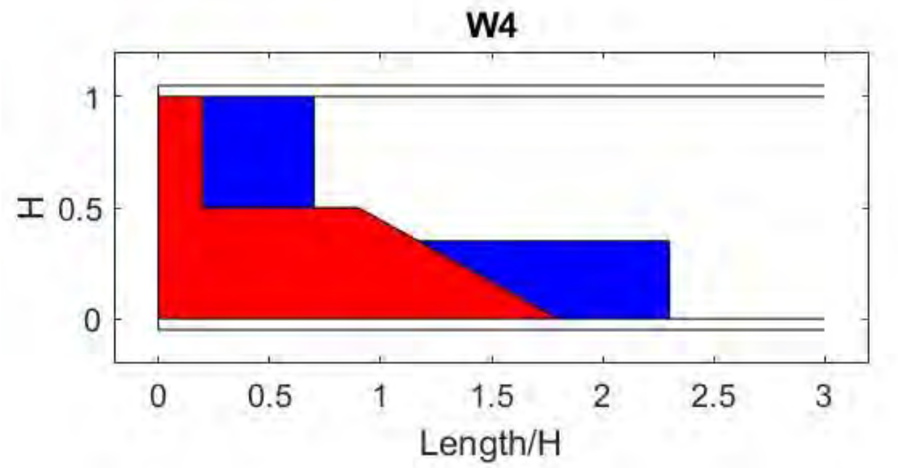

Figure 146: First extreme W4 scenario (red) projected over extreme W3 web corrosion scenario (blue) - MassDOT

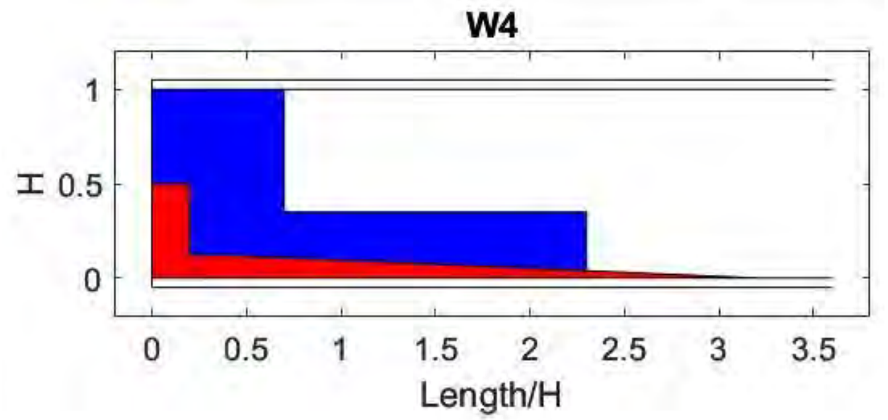

Figure 147: Second extreme W4 scenario (red) projected over extreme W3 web corrosion scenario (blue) - MassDOT

Considering the way W3 and W4 have been defined, W3 can be expressed by W4 if we set W4CL1=W4CL3 and W4CH3≠0. Figure 146 and Figure 147 demonstrate that W3 includes the extreme W4 scenarios, thus W3 and W4 could be merged to one pattern.

4.3.5.2. Flange Corrosion

There is no analysis of flange corrosion and the generation of a separate flange corrosion pattern since the worst scenario was included in the W3 corrosion scenario.

4.3.5.3. Holes

Table 50: Hole appearances for beams- MassDOT

	Number	No hole	M1	M2	M3	M4	M12	M13	M24
W1	161	146	9	1	3	0	0	2	0
W2	10	8	2	0	0	0	0	0	0
W3	56	44	7	0	3	1	0	1	0
W4	40	347	4	0	0	0	0	2	0
W5	17	13	3	1	0	0	0	0	0
W6	2	2	0	0	0	0	0	0	0

According to the table, the W4 pattern is combined four times with the M1 hole pattern. The available data are not enough to extract conclusions about the web thickness loss at these cases. The corrosion holes dimension distribution can be seen in the figures below:

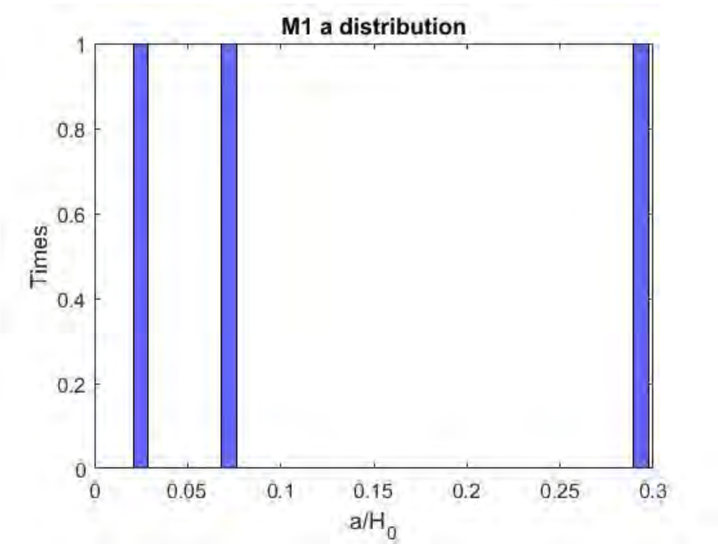

Figure 148: M1 web hole's pattern height distribution of W4 web corrosion pattern for beams without a diaphragm - MassDOT

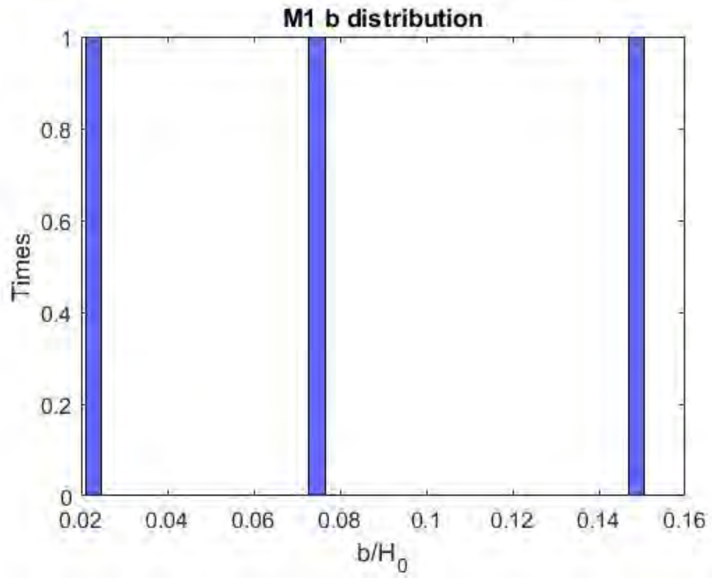

Figure 149: M1 web hole's pattern length distribution of W3 web corrosion pattern for beams without a diaphragm - MassDOT

The extreme hole corrosion cases belong in the range of the W3 pattern with M1 pattern holes (Figure 128).

4.3.6. Pattern W5

4.3.6.1. Web corrosion

Across the inspection reports, the W5 corrosion pattern was observed in total only 17 times. The parameters for the corrosion patterns can be found with corresponding diagrams in Section 1.5 *Corrosion Patterns* of this report. The normalized dimensions and the web thickness loss for the W5 pattern are presented below:

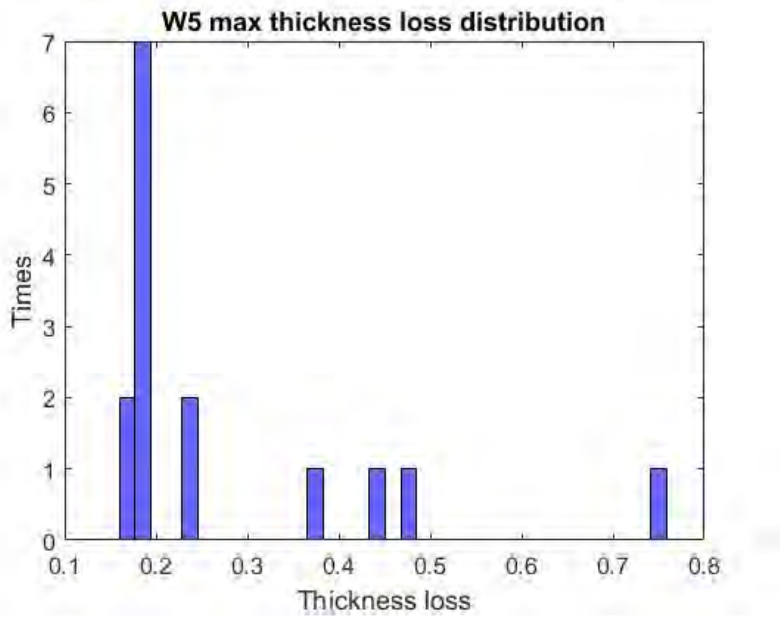

Figure 150. Max web thickness loss distribution of W5 web corrosion pattern for beams without a diaphragm - MassDOT

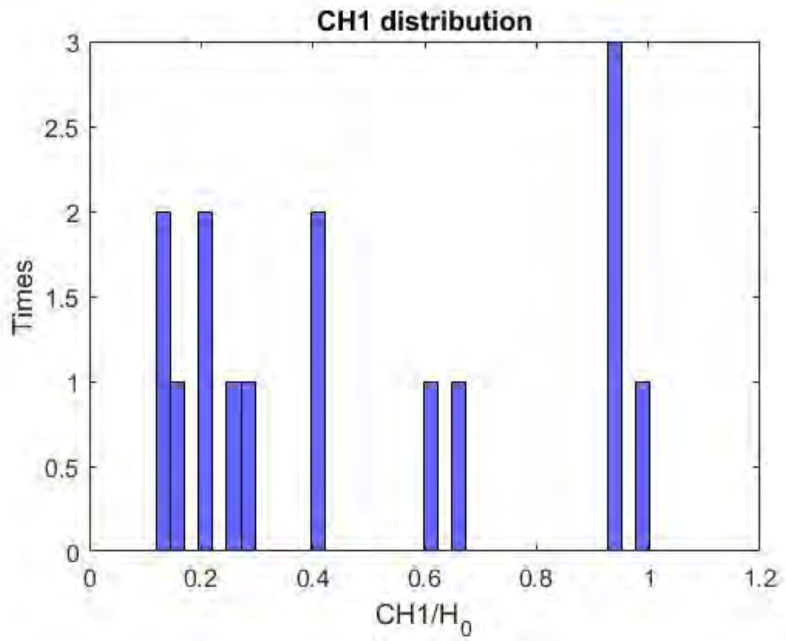

Figure 151: CH2 distribution of W5 web corrosion pattern for beams without a diaphragm - MassDOT

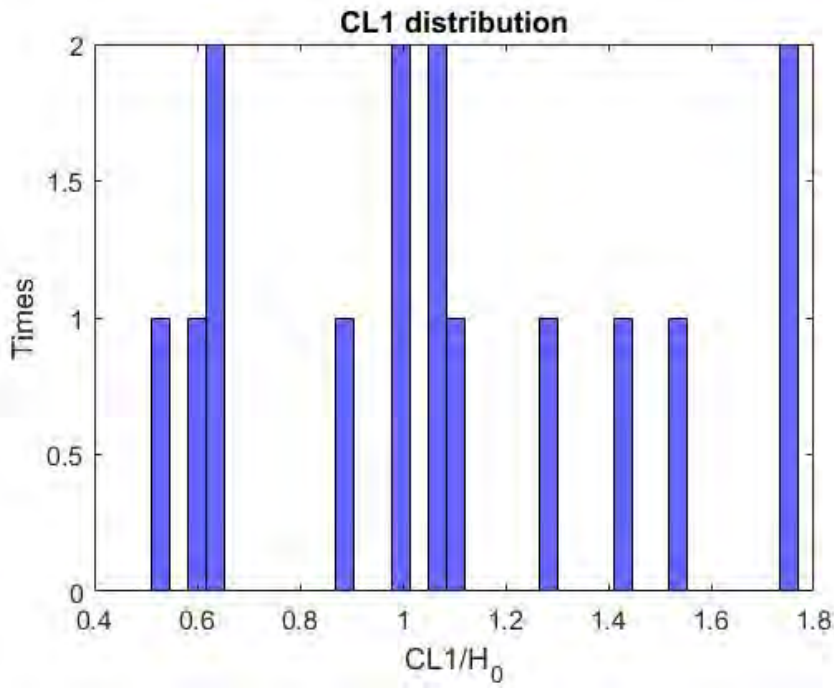

Figure 152: Max web thickness loss distribution of W5 web corrosion pattern for beams without a diaphragm - MassDOT

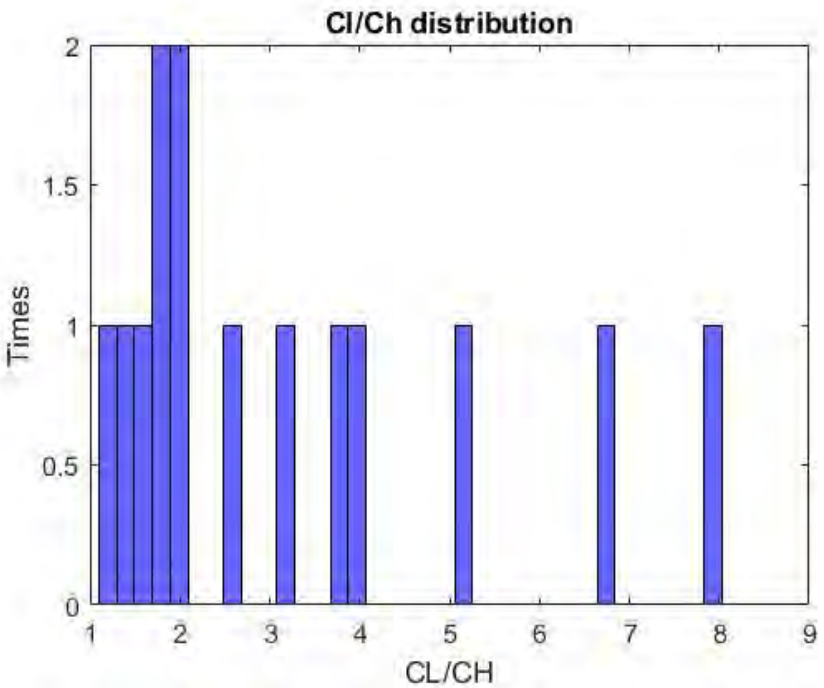

Figure 153:Ratio of corrosion length to height of W1 web corrosion pattern for beams without a diaphragm - MassDOT

From Figure 151, our team described the following: $0.15H_0 \leq CH_1 \leq H_0$

From Figure 152, our team described: $0.5H_0 \leq CH_1 \leq 1.8H_0$, with thickness loss: $\frac{t_{loss}}{t_{web}}\ that\ takes\ values\ of \{0.2, 0.5\}$

The extreme case:

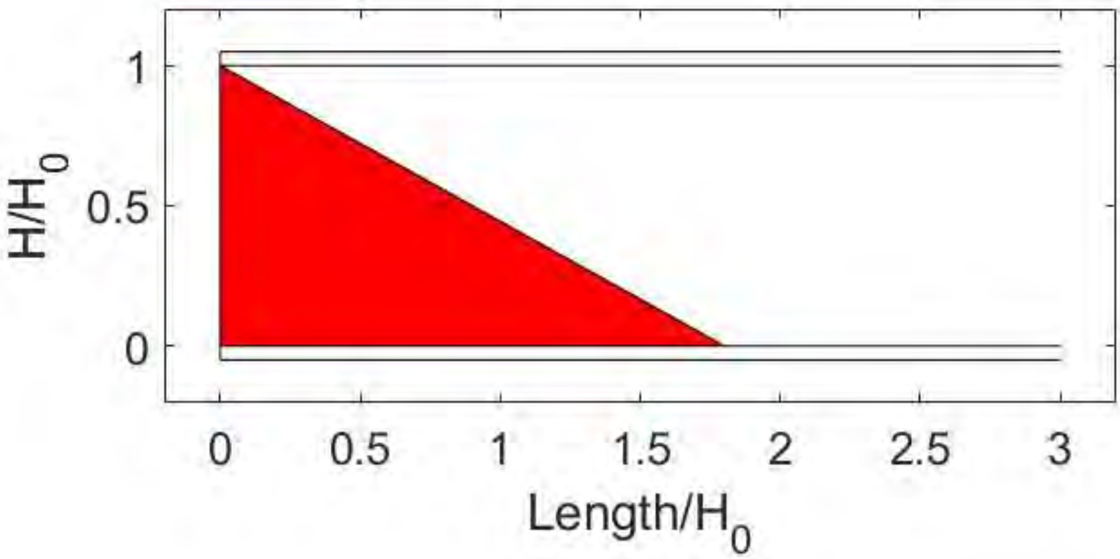

Figure 154: Extreme W4 web corrosion scenario for beams without a diaphragm - MassDOT

According to Figure 153 the tested cases should have a ratio $1 \leq \frac{CL}{CH} \leq 4$.

4.3.6.2. Flange corrosion

Our team plotted the ratio of the length of the corroded flange over the length of the corroded web in the following figure.

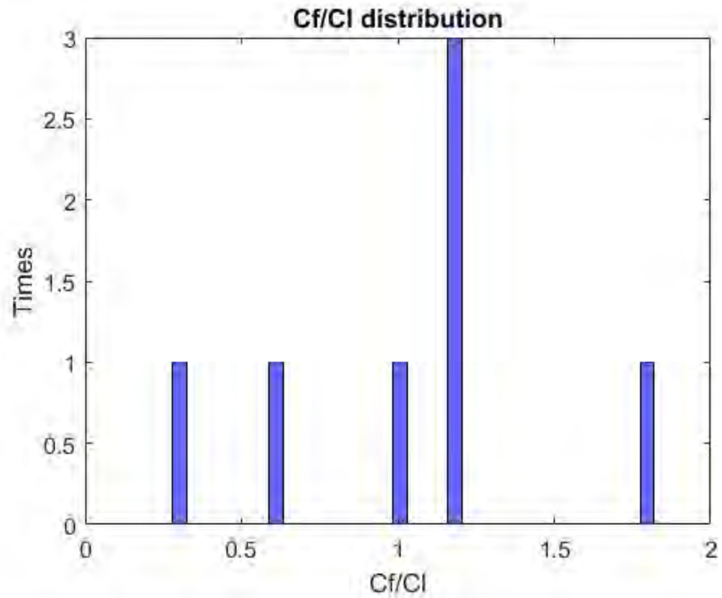

Figure 155: Ratio of flange to web corrosion length distribution of W5 web corrosion pattern for beams without a diaphragm - MassDOT

Thus, our team stated the following: $1 \leq \frac{Cf}{Cl} \leq 1.8$

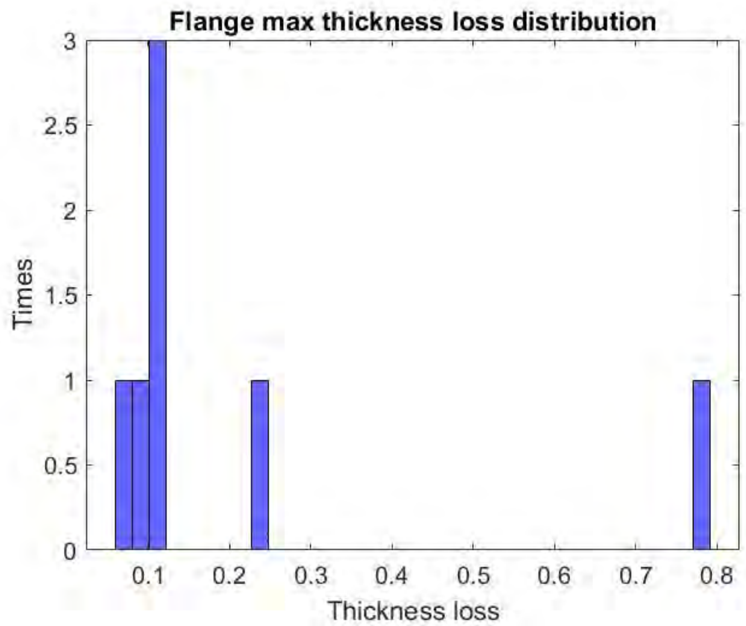

Figure 156: Max flange thickness loss distribution of W5 web corrosion pattern for beams without a diaphragm - MassDOT

4.3.6.3. Holes

There are very few cases found in the inspection reports with corrosion holes. To have an accurate data set, more data is necessary. As a result, and for validity, these cases were disregarded.

4.4. New Hampshire

4.4.1. Introduction

Similar to the inspection reports from MaineDOT, the reports provided by NHDOT do not provide the dimensions of the corroded areas of the beams. Additionally, the corrosion information provided for web and flange thickness loss are clearly linked to the beams.

Altogether, the research team was able to compile 13 out of the 15 reports provided by NHDOT. From the compiled reports, the research team was able to gather corrosion information of exactly 41 beam ends. Most of the information consists of the thickness loss of flanges and webs. It is worthwhile mentioning that none of the beam ends had diaphragms.

4.4.2. Web corrosion

The inspection reports do not always provide information regarding web thickness loss. More precisely, only 20% of the reports provided such information. Figure 157 depicts the histogram of the web thickness loss reported in the bridge inspection reports from NHDOT.

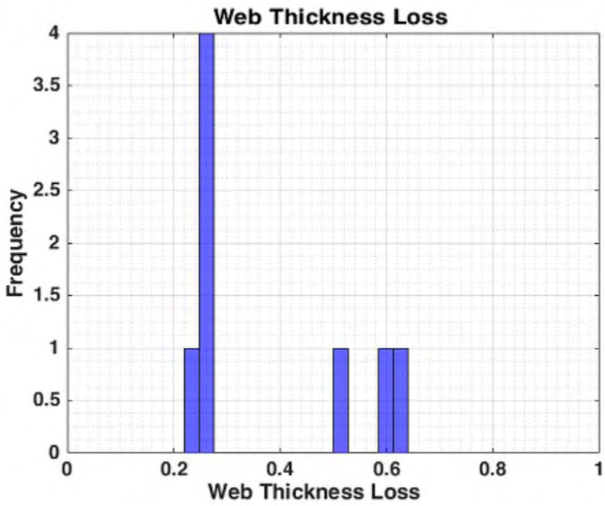

Figure 157: Web thickness loss histogram from the beam ends compiled - NHDOT

As discussed above, the research team was not able to gather information regarding corrosion length or corrosion height from the reports provided by NHDOT. This meant that our team could not create corrosion patterns for the bridge beams we analyzed via NHDOT's inspection reports.

4.4.3. Flange Corrosion

Many inspection reports provided by NHDOT had information regarding flange corrosion. Specifically, 36 out of the 40 compiled beam ends had information of flange corrosion either on the top flange or on the bottom flange. Figure 158 and Figure 159 depict the histogram of corrosion obtained for the bottom and top flanges, respectively.

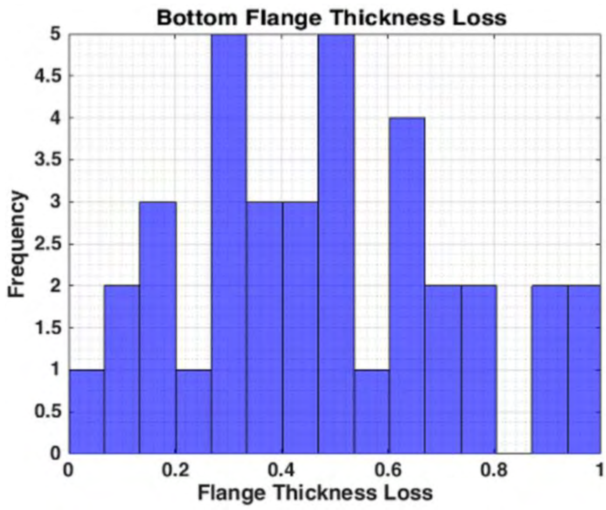

Figure 158: Bottom thickness loss histogram from the beam ends compiled - NHDOT

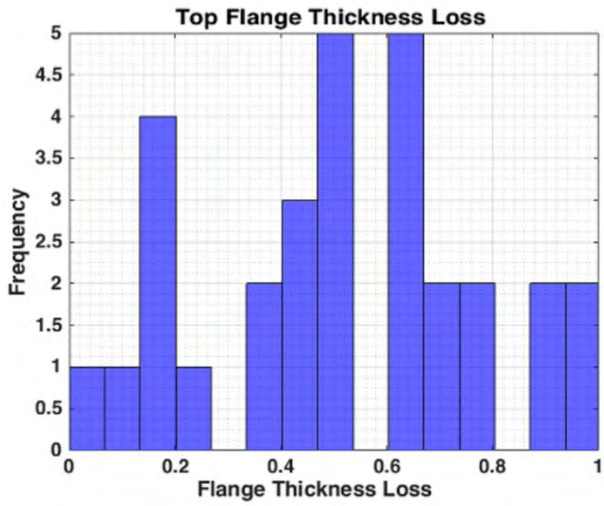

Figure 159 : Top thickness loss histogram from the beam ends compiled - NHDOT

4.4.4. Holes

Only two holes were observed in the inspection reports provided by NHDOT. Additionally, both holes were reported with photographs. The dimensions of the holes are described by the plots in Figure 160 and Figure 161.

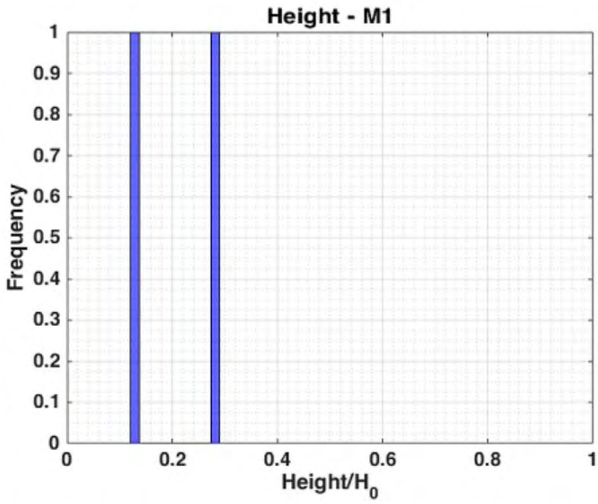

Figure 160: M1 web hole's height distribution of W1 web corrosion pattern for beams without a diaphragm - NHDOT

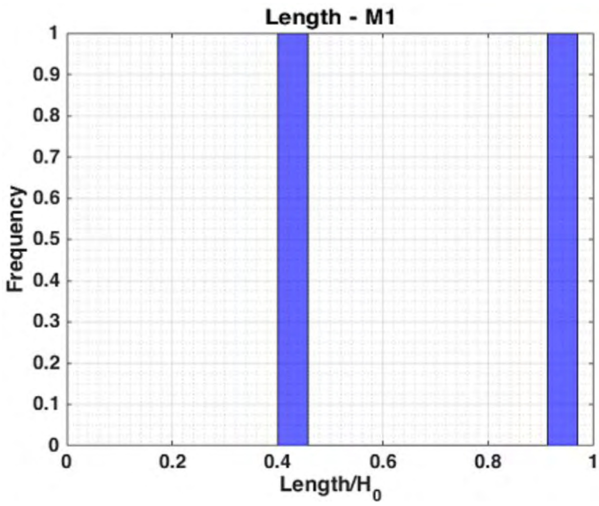

Figure 161: M1 web hole's length distribution of W1 web corrosion pattern for beams without a diaphragm - NHDOT

4.5. Rhode Island

4.5.1. Introduction

As discussed in the previous sections, the results are presented for each state individually as the amount of beam ends vary significantly from one state to the other. In addition to dividing data by state, the beam ends were also divided into two subgroups. The beam ends without a diaphragm system and the beam ends with a diaphragm system.

From the reports provided by RIDOT, the research team was able to gather corrosion information of 89 beam ends without a diaphragm. Figure 162 depicts the frequency of corrosion patterns for beam ends without a diaphragm.

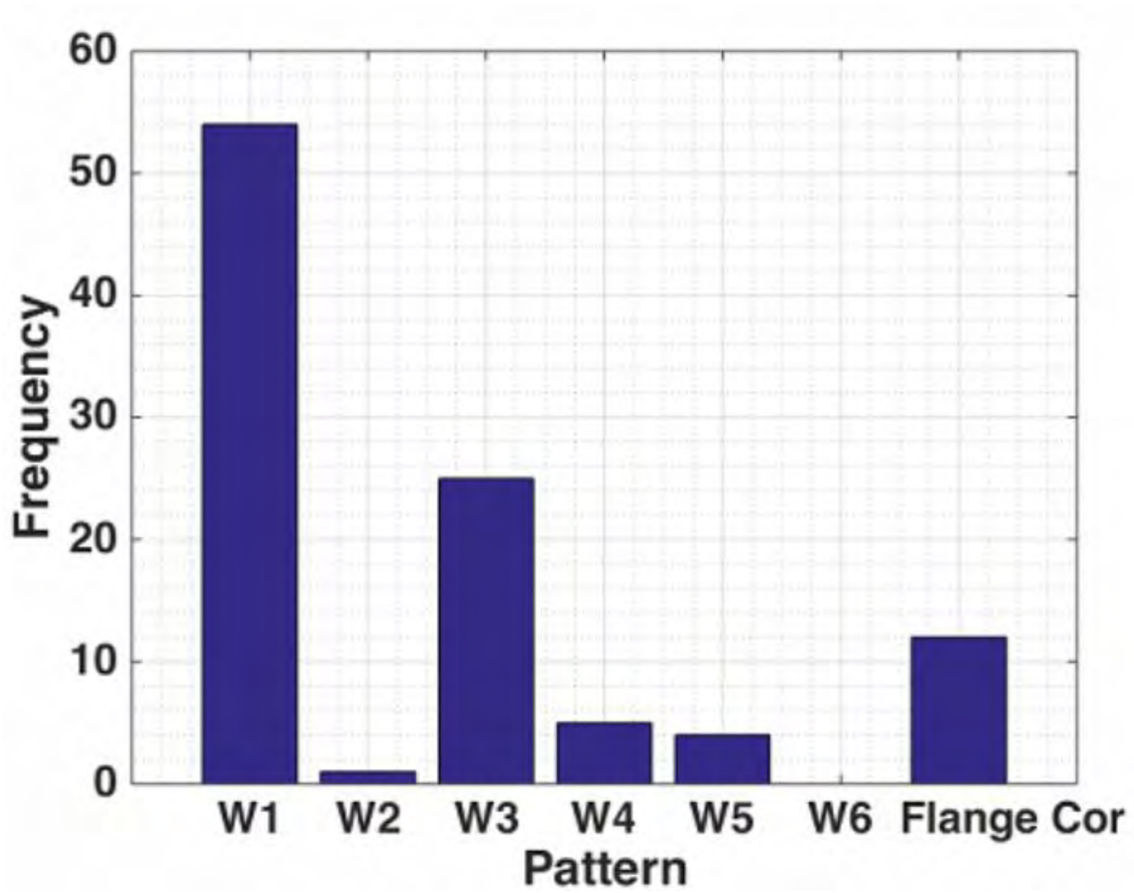

Figure 162 : Web corrosion patterns distribution for beams ends without diaphragm – RIDOT

4.5.2. Pattern W1

4.5.2.1. Web corrosion

The parameters for the corrosion patterns can be found with corresponding diagrams in Section 1.5 *Corrosion Patterns* of this report. The study starts by analyzing the height of corrosion for pattern W1, depicted in Figure 163.

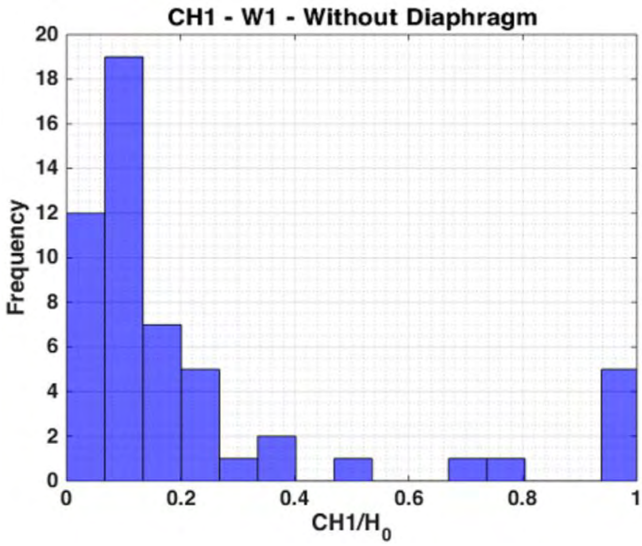

Figure 163: CH1 distribution of W1 pattern for beams without diaphragm - RIDOT

From Figure 163 is possible to observe that most of the beam ends have CH1 <0.5. Our team was able to isolate the beams which present CH1<0.5. By doing this, we expected to understand the interaction between the parameters of the corrosion pattern W1. Additionally, our team expected to detect a pattern from which there is opportunity to determine an extreme scenario.

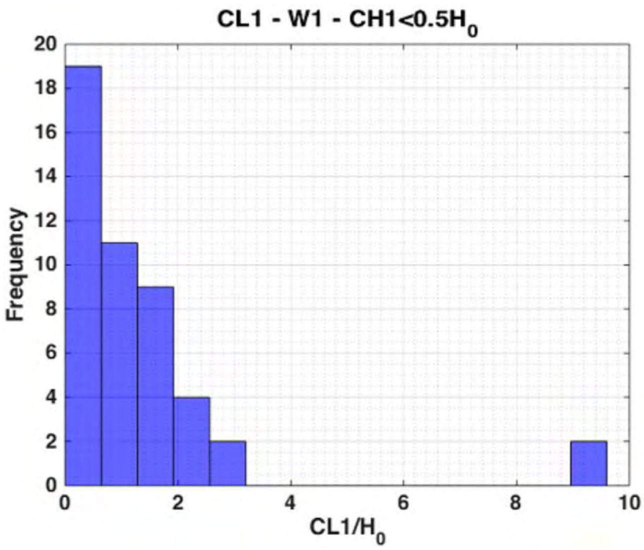

Figure 164: CL1 distribution of W1 pattern for beams without a diaphragm and CH1<0.5H0 – RIDOT

Figure 164 clearly depicts a trend, which is CL1<3. Therefore, our team assumed that:

$$0 < CH_1 \leq 0.5H_0$$

$$0 < CL_1 \leq 3H_0$$

Figure 165 depicts the web thickness loss for the case CH1<0.5H0 and CL1<3.

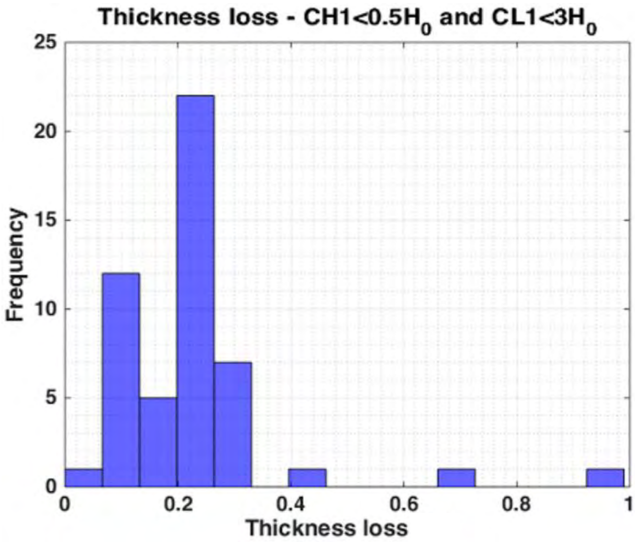

Figure 165: Web thickness loss of W1 pattern for beams without a diaphragm, CH1<0.5H0 and CL1< 3H0 – RIDOT

Figure 165 depicts that the thickness loss clusters between 0% until 30%. That, is:

$$0 < \frac{t_{web}}{t_{loss}} \leq 0.3$$

By gathering the intervals determined from Figure 163, Figure 164 and Figure 165, our team was able to determine the extreme case of corrosion for pattern W1. A schematic illustration of this extreme case of corrosion is depicted in Figure 166.

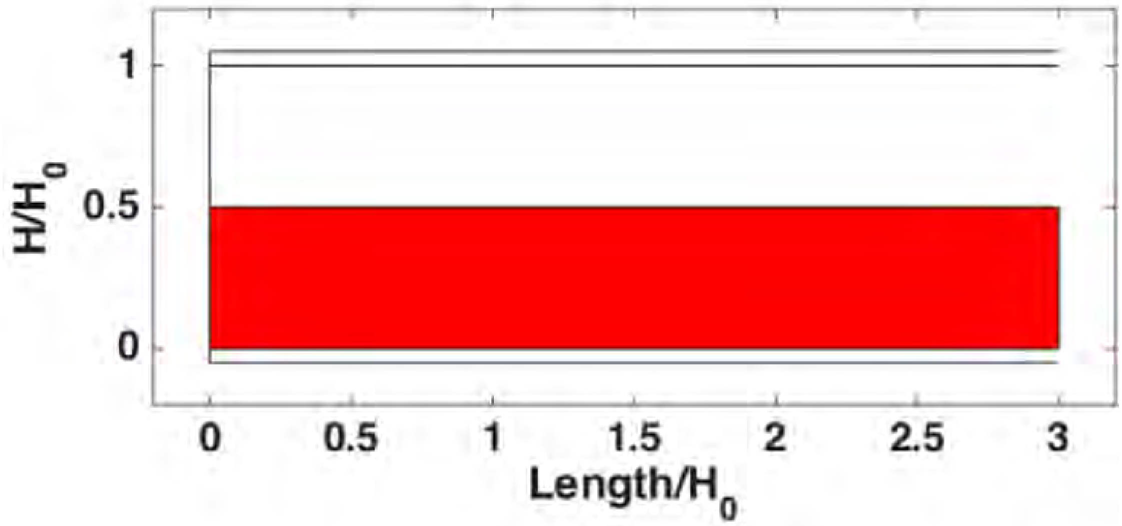

Figure 166: Extreme scenario for pattern W1 – RIDOT

4.5.2.2. Flange corrosion

The research team was able to record flange corrosion information for only 12 beam ends from the reports provided by RIDOT. Half of the recorded measurements are combined with pattern W1.

Due to the limited quantities of beams with flange corrosion, the team was not able to detect any trend regarding flange corrosion from the recorded data. Figure 167, Figure 168 and Figure 169 depict the statistics the research team was able to extract from the available data.

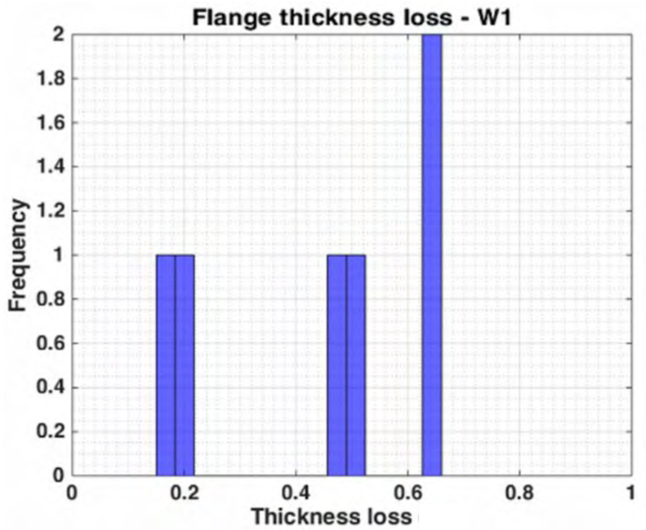

Figure 167: Flange thickness Loss for pattern W1 – RIDOT

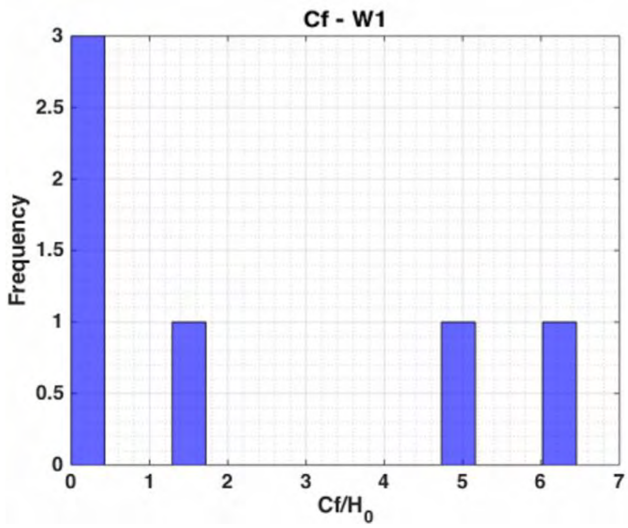

Figure 168: Flange corrosion length for pattern W1 – RIDOT

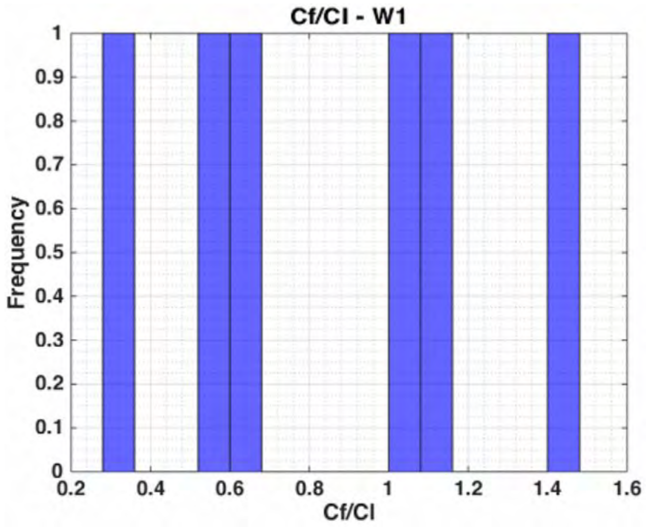

Figure 169: Ratio between flange corrosion length and web corrosion length for pattern W1 – RIDOT

4.5.2.3. Holes

Table 51**:** Holes and patterns for beams without a diaphragm – RIDOT portrays the frequency of corrosion patterns and holes that the research team was able to record from the bridge inspection reports provided by RIDOT.

Table 51: Holes and patterns for beams without a diaphragm – RIDOT

	Number	**No Hole**	**M 1**	**M 2**	**M 3**	**M 4**	**M1 and M2**	**M1 and M3**	**M2 and M4**
W1	54	49	4	0	1	0	0	0	0
W2	1	1	0	0	0	0	0	0	0
W3	25	21	0	0	1	2	0	0	0
W4	5	5	0	0	0	0	0	0	0
W5	4	4	0	0	0	0	0	0	0
W6	0	0	0	0	0	0	0	0	0

Therefore, only 5 holes were reported and were combined with the W1 corrosion pattern. Unfortunately, no trend was detected by the research team. Figure 170, Figure 171, Figure 172 and Figure 173 depicts the dimensions of the recorded corrosion holes.

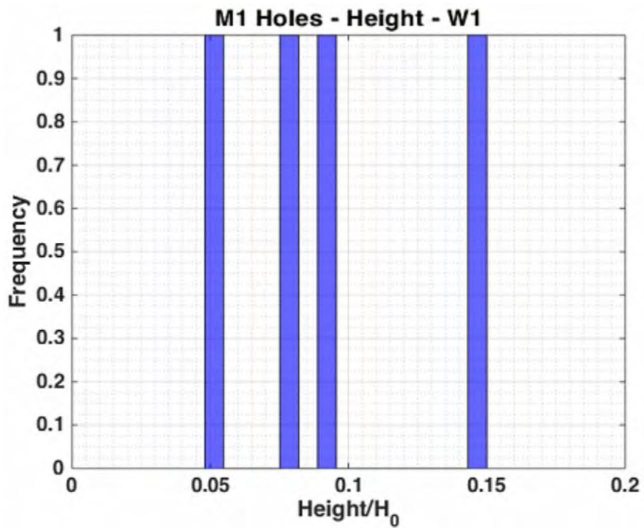

Figure 170: Height of M1 holes combined with W1 pattern – RIDOT

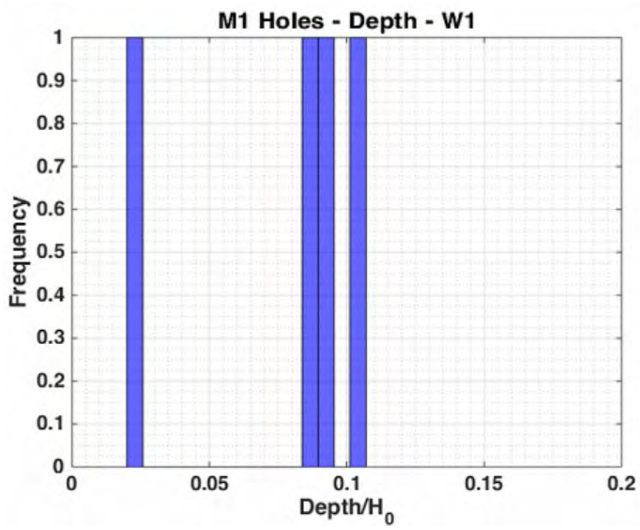

Figure 171: Depth of M1 holes combined with W1 pattern – RIDOT

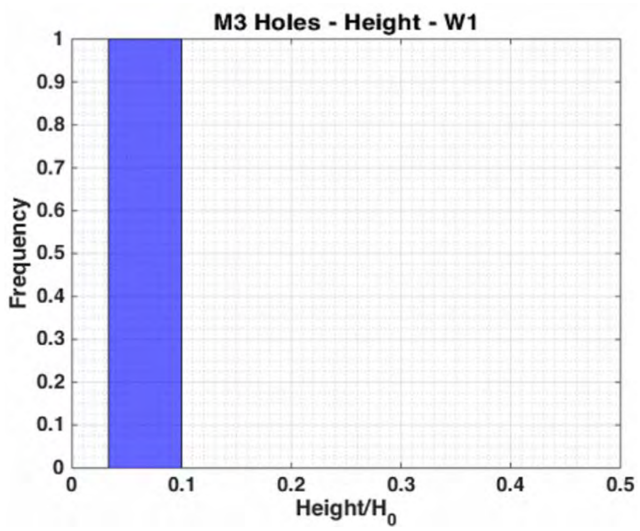

Figure 172: Height of M3 hole combined with W1 pattern – RIDOT

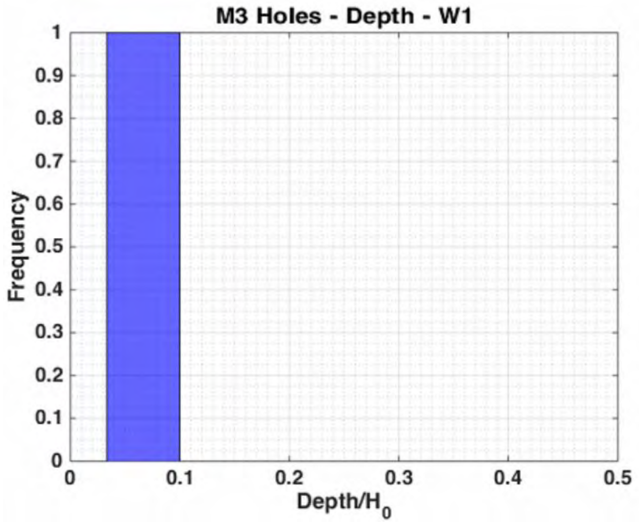

Figure 173: Depth of M3 holes combines with W1 pattern – RIDOT

4.5.3. Pattern W2

4.5.3.1. Web Corrosion

Just a single case of the W2 corrosion pattern was recorded. Therefore, it was not possible to study trends from the available data. The parameters for the corrosion patterns can be found with corresponding diagrams in Section 1.5 *Corrosion Patterns* of this report.

The dimensions of the recorded W2 case are:

$$\frac{CH_1}{H_0} = 11\%$$

$$\frac{CL_1}{H_0} = 26.2\%$$

$$\frac{CL_2}{H_0} = 16.6\%$$

$$\frac{t_{loss}}{t_{web}} = 24.4\%$$

Figure 174 depicts a schematic sketch of the recorded W2 case.

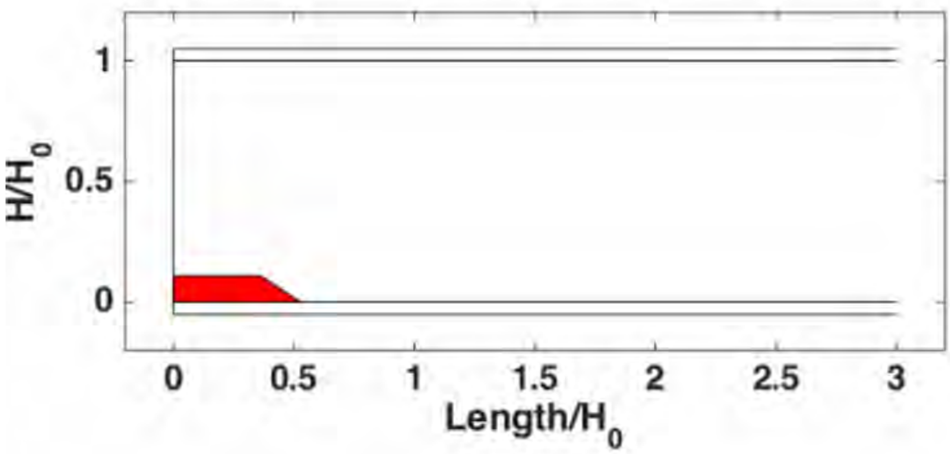

Figure 174: Schematic representation of W2 pattern – RIDOT

4.5.3.2. Flange Corrosion

There was no flange corrosion analyzed or recorded for this case.

4.5.3.3. Holes

There were no holes analyzed, recorded, or combined with this case.

4.5.4. Pattern W3

4.5.4.1. Web Corrosion

Similar to the other cases, the study of W3 corrosion pattern begins by the analysis of the total corrosion height, characterized by parameters CH2 of pattern W3. The parameters for the corrosion patterns can be found with corresponding diagrams in Section 1.5 *Corrosion Patterns* of this report. Figure 175 depicts the resulting distribution of CH2 for beams ends without diaphragm.

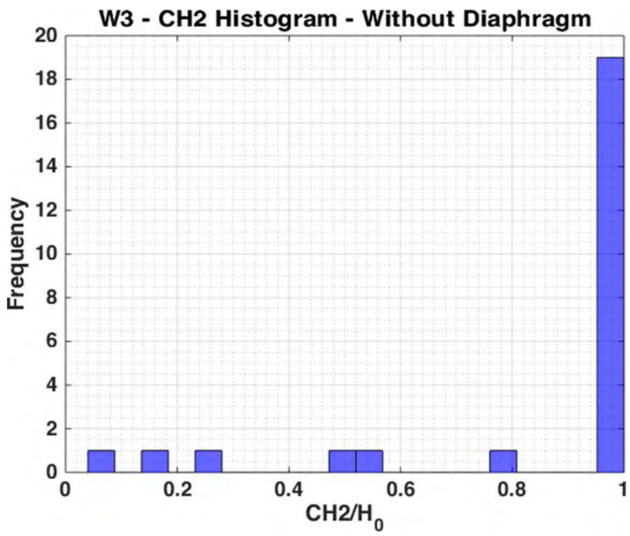

Figure 175: CH2 distribution for W3 pattern - RIDOT

Figure 175 depicts the clear trend that CH2>0.9H0. Therefore, one is able to obtain the distribution of the other parameters given that Ch2>0.9H0. Figures Figure 176, Figure 177,

Figure 178, Figure 179 and Figure 180 depict the behavior of the other parameters given that CH2>0.9H0.

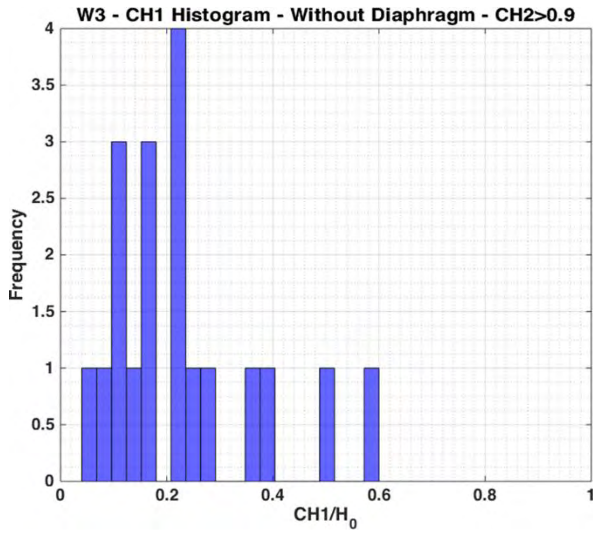

Figure 176: CH1 distribution for W3 pattern and CH2>0.9H0 - RIDOT

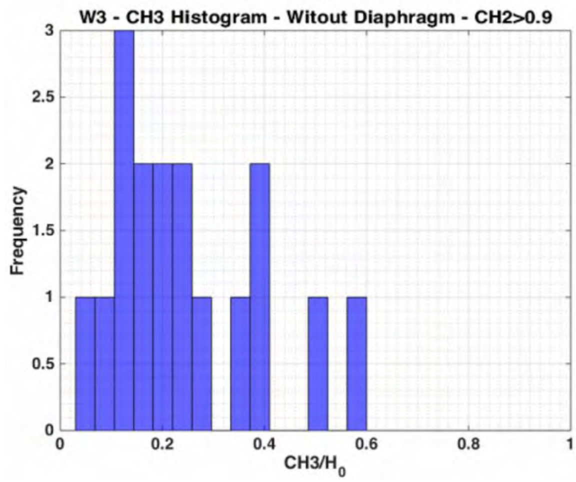

Figure 177: CH3 distribution for W3 pattern and CH2>0.9H0 - RIDOT

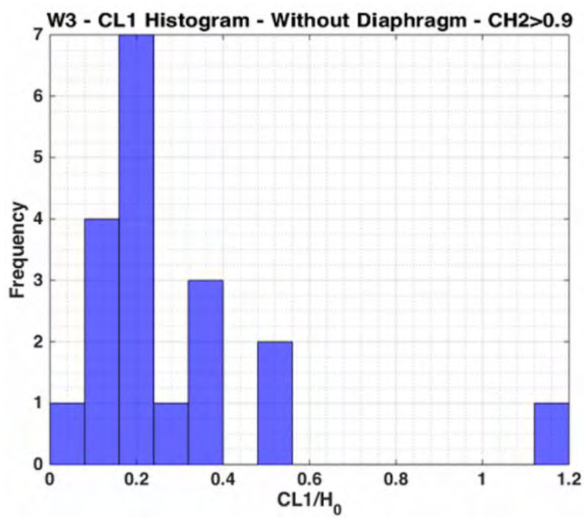

Figure 178: CL1 distribution for W3 pattern and CH2>0.9H0 - RIDOT

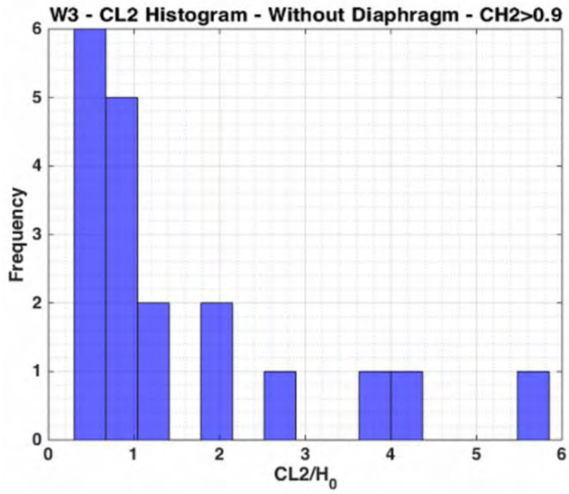

Figure 179: CL2 distribution for W3 pattern and CH2>0.9H0 - RIDOT

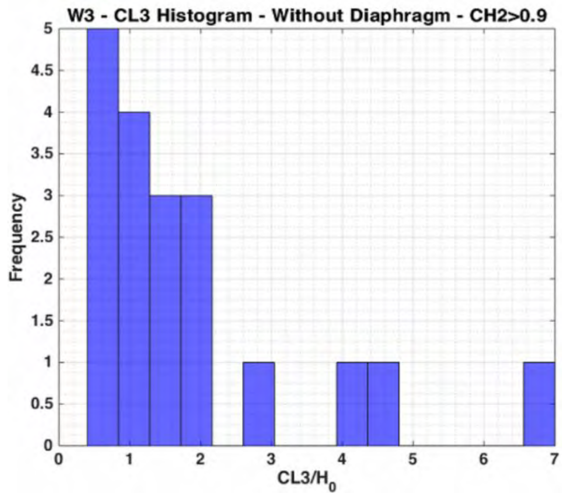

Figure 180: CL3 distribution for W3 pattern and CH2>0.9H0 - RIDOT

Figure 181 depicts the web thickness loss for the W3 corrosion pattern.

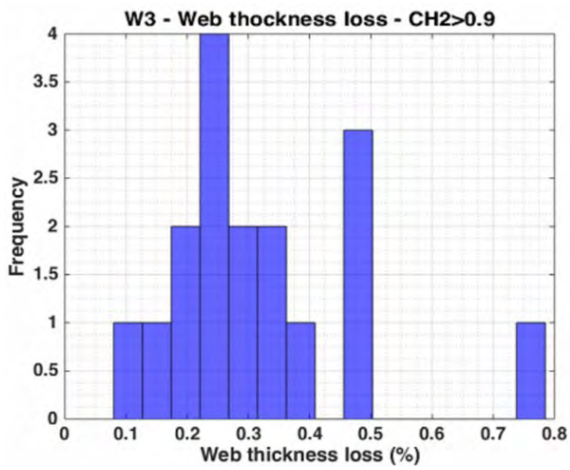

Figure 181: Web thickness loss distribution for W3 pattern and CH2>0.9H0 - RIDOT

From the previous figures, our team was able to determine the intervals for the W3 corrosion patterns, which can be written as:

$$0 \leq CH_1 \leq 0.4H_0$$

$$0.9H_0 \leq CH_2 \leq 1H_0$$

$$0 \leq CH_3 \leq 0.4H_0$$

$$0 \leq CL_1 \leq 0.5H_0$$

$$0 \leq CL_2 \leq 2.5H_0$$

$$0.5H_0 \leq CL_3 \leq \ 3H_0$$

$$0.1 \leq \frac{t_{loss}}{t_{web}} \leq 0.5$$

Figure 182 depicts a schematic representation of the extreme corrosion case for W3 corrosion pattern.

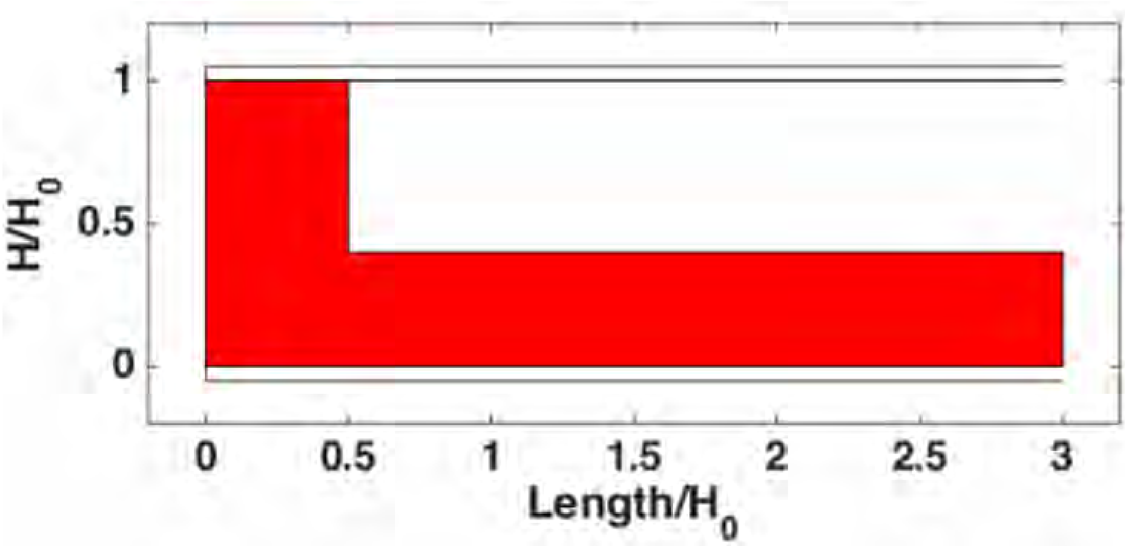

Figure 182: Extreme corrosion case for W3 pattern - RIDOT

4.5.4.2. Flange Corrosion

From the bridge inspection reports, the research team was able to record 4 cases of flange corrosion combined with the pattern W3. No trend was detected by the research team regarding the flange thickness loss. Figures Figure 183, Figure 184 and Figure 185 depict the statistics that the research team was able to obtain from the bridge inspection reports.

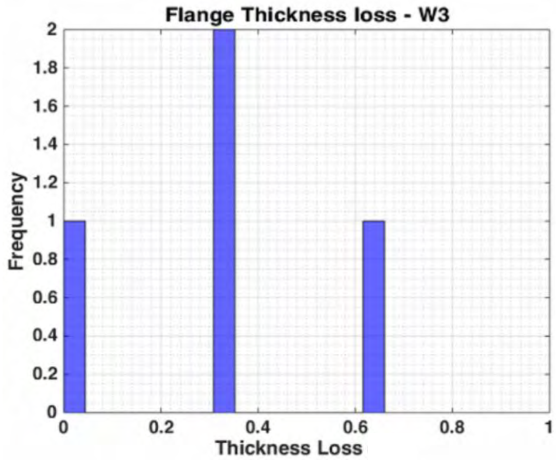

Figure 183: Flange thickness loss distribution for W3 pattern – RIDOT

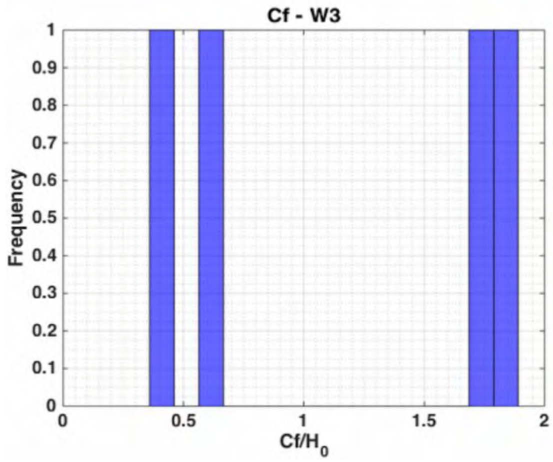

Figure 184: Flange corrosion length for W3 pattern – RIDOT

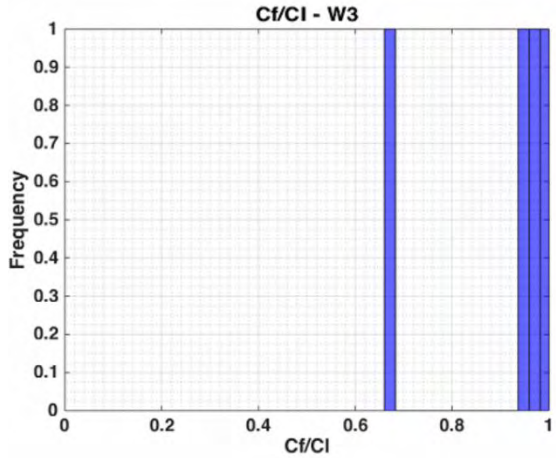

Figure 185: ratio between flange corrosion length and web corrosion length for W3 pattern – RIDOT

It is worth noting that, although no trend was depicted, it is possible to observe that the behavior of the corrosion of the flanges is similar to the corrosion of the web. That is, the length of corroded flange is close to the total length of web corrosion.

4.5.4.3. Holes

From the bridge inspection reports provided by RIDOT, the research team was able to record only 3 holes combined with the W3 corrosion pattern, as portrayed in Figures 186, 187, 188, and 189. As not all three holes belong to the same topology, the research team was not able to identify trends in the data.

Figure 186, Figure 187, Figure 188 and Figure 189 depict the dimensions of the recorded holes.

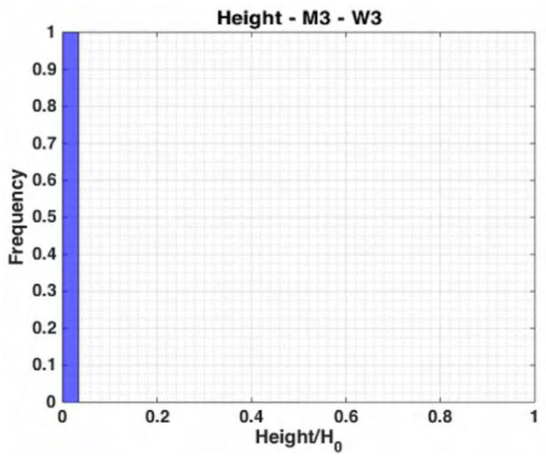

Figure 186: Height of M3 hole combined with W3 pattern – RIDOT

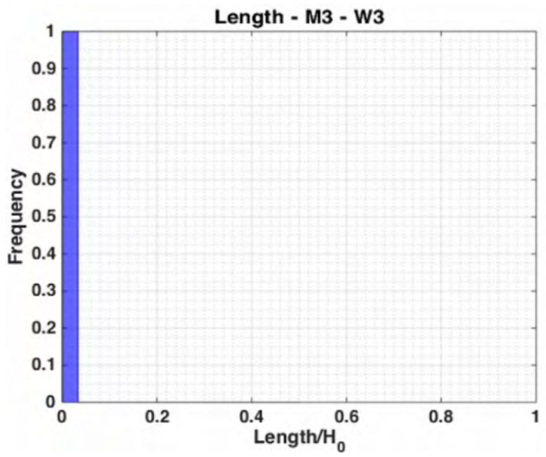

Figure 187: Length of M3 hole combined with W3 pattern – RIDOT

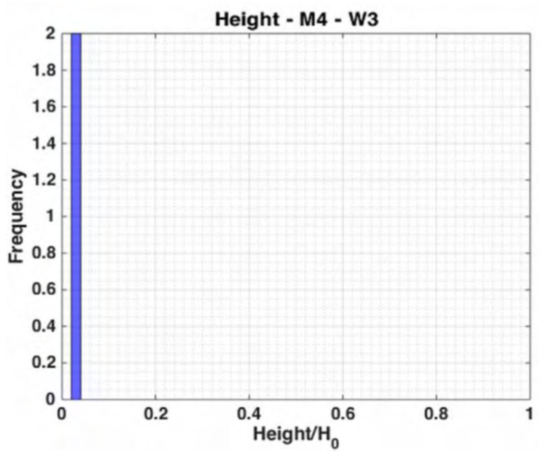

Figure 188: Height of M4 holes combined with W3 pattern – RIDOT

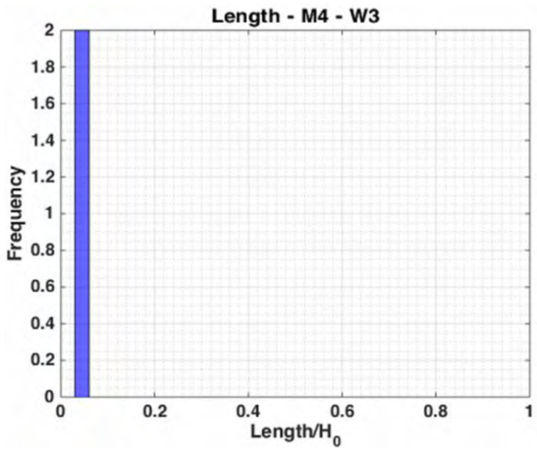

Figure 189: Length of M3 hole combined with W3 pattern – RIDOT

4.5.5. Pattern W4

4.5.5.1. Web Corrosion

Figure 190 depicts the distribution of CH2 of pattern W4. Figure 190 clearly depicts the trend of CH2>0.9H0. The research team was not able to detect trends as the other parameters of W4 pattern are scattered, which limited our research team in detecting trends. The parameters for the corrosion patterns can be found with corresponding diagrams in Section 1.5 *Corrosion Patterns* of this report. Figure 191, Figure 192, Figure 193 and Figure 194 depict the distribution of the other parameters recorded from the bridge inspection reports.

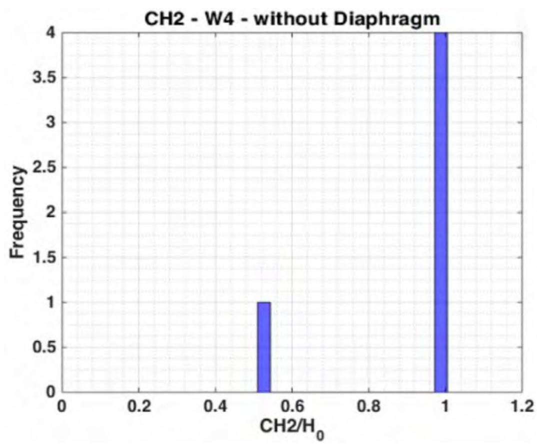

Figure 190: CH2 distribution for W4 pattern – RIDOT

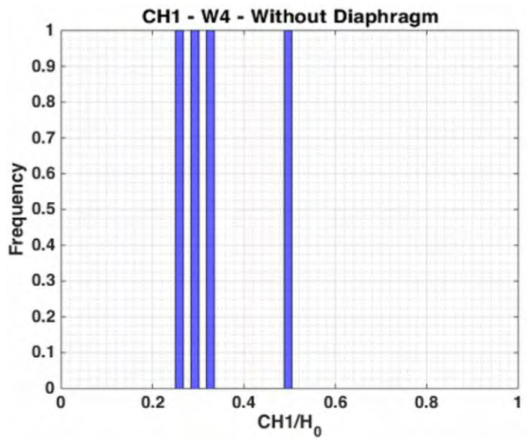

Figure 191: CH1 distribution for W4 pattern – RIDOT

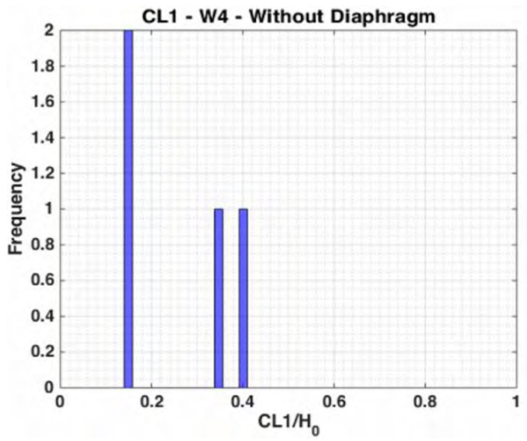

Figure 192: CL1 distribution for W4 pattern – RIDOT

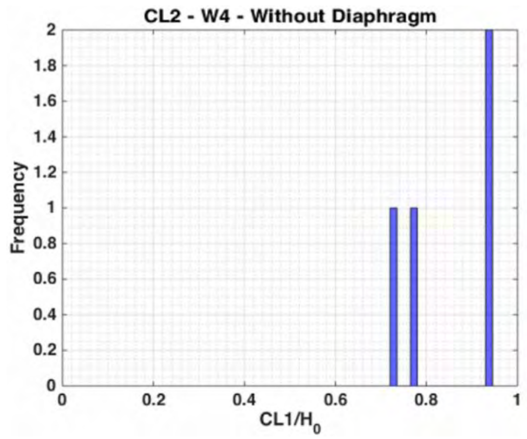

Figure 193: CL2 distribution for W4 pattern – RIDOT

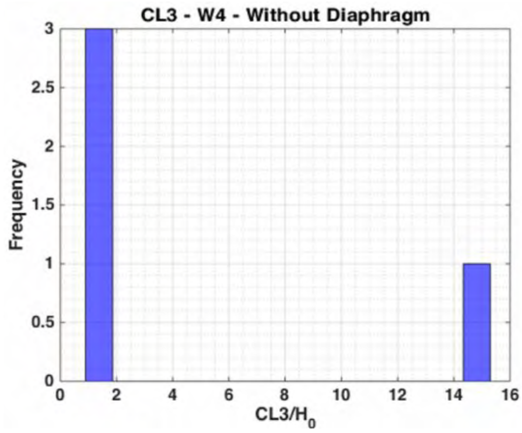

Figure 194: CL3 distribution for W4 pattern – RIDOT

Figure 195 depicts the web thickness loss of the W4 corrosion pattern.

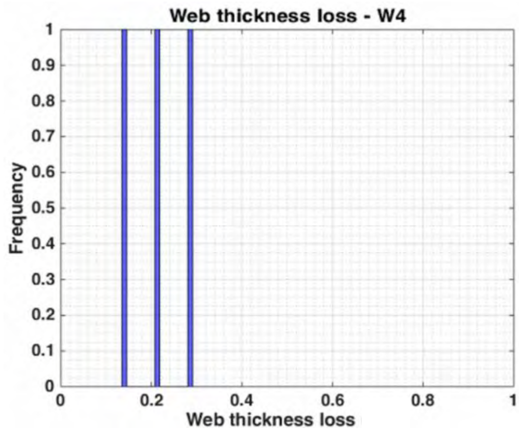

Figure 195: Web thickness loss distribution for W4 pattern – RIDOT

4.5.5.2. Flange Corrosion

From the bridge inspection reports, the research team was able to record just two measurements of flange corrosion combined with the W4 corrosion pattern. As two recorded pattern instances are not enough to define trends, Figure 196, Figure 197, and Figure 198 depict the measurements provided by the inspection reports.

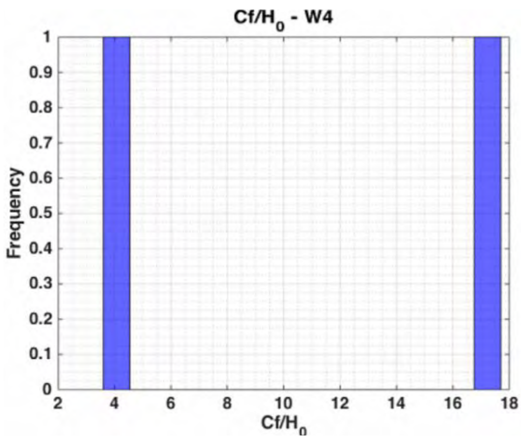

Figure 196: Flange corrosion length distribution for W4 pattern – RIDOT

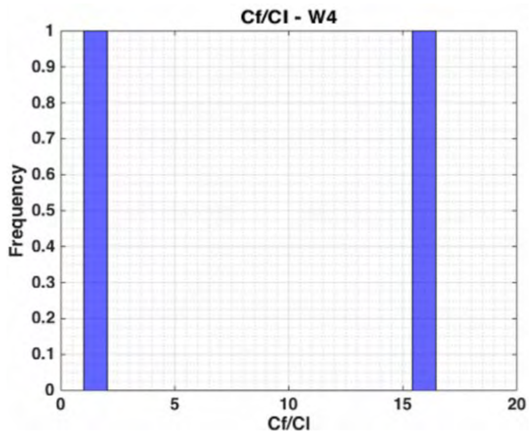

Figure 197: Ratio between flange corrosion length and corrosion length for W4 pattern – RIDOT

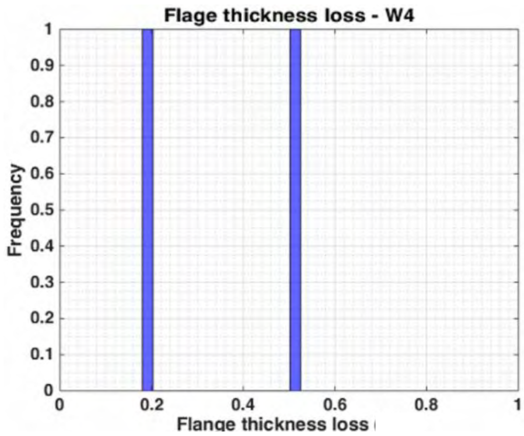

Figure 198: Flange thickness loss distribution for W4 pattern – RIDOT

4.5.5.3. Holes

No holes were reported in this section which combined with the W4 corrosion pattern.

4.5.6. Pattern W5

4.5.6.1. Web corrosion

The research team was able to record data from 4 cases of the W5 corrosion pattern. The parameters for the corrosion patterns can be found with corresponding diagrams in Section 1.5 *Corrosion Patterns* of this report. As the amount of data recorded was not enough to detect any trends, Figure 199 and Figure 200 depict only the histogram of the parameters.

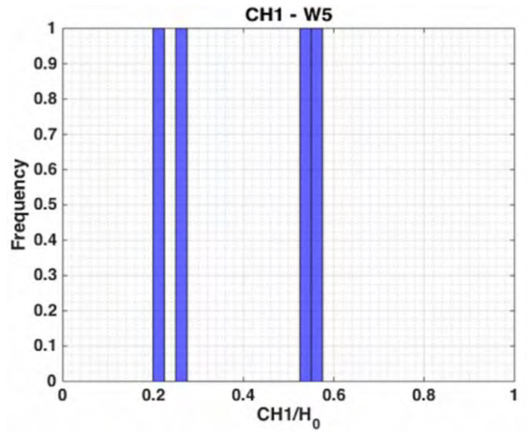

Figure 199: CH1 distribution for W5 pattern – RIDOT

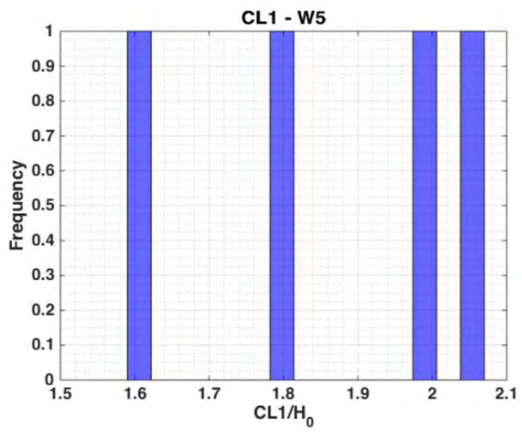

Figure 200: CL1 distribution for W5 pattern – RIDOT

Figure 201 depicts the web thickness loss for the W5 corrosion pattern.

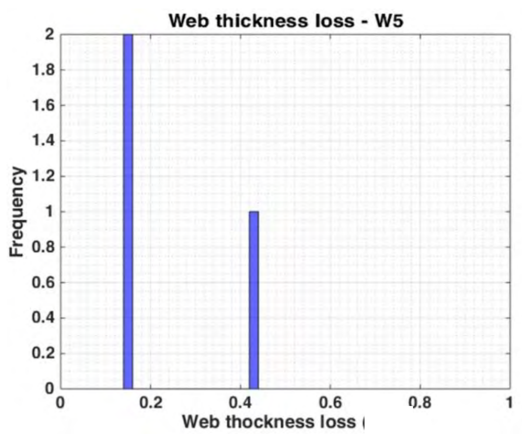

Figure 201: Web thickness loss for W5 pattern – RIDOT

4.5.6.2. Flange corrosion

No flange corrosion information was reported combined with the W5 corrosion pattern.

4.5.6.3. Holes

No holes were reported combined with the W5 corrosion pattern.

4.6. Vermont

4.6.1. Introduction

The research team was able to find corrosion information in only 15 out of approximately 70 reports provided by VTrans. From the compiled reports, we were able to gather information for 36 beams ends. Similar to the reports from MaineDOT and NHDOT, the reports from VTrans do not present the measurements of the corroded area. Therefore, only information regarding web and flange thickness loss were collected. Additionally, this means that corrosion patterns were not created due to the lack of parameters. It is also imperative to note that the reports did not clearly link the corrosion information to a specific beam. Aiming to treat the reports from all states equally, the information was compiled as if it referred to a single beam.

4.6.2. Web corrosion

As stated above, the absence of sketches and labels on the pictures hampered the research team to classify the corrosion topology. For this reason, the only information regarding web corrosion that the research team was able to obtain from the VTrans bridge inspection reports was the web thickness loss. Figure 202 depicts the histogram of web thickness loss obtained from the data provided by VTrans reports.

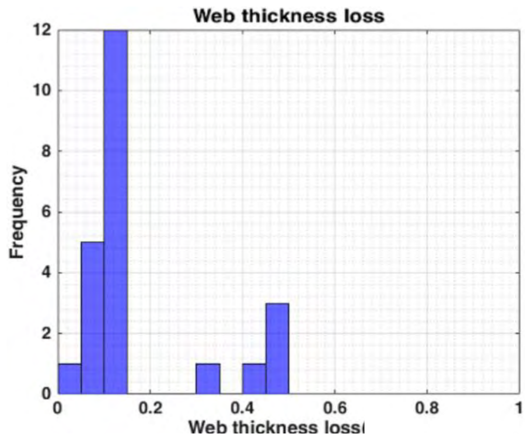

Figure 202: Web thickness loss histogram from the beam ends compiled - VTrans

4.6.3. Flange corrosion

Similar to the reports from MaineDOT and NHDOT, the reports from VTrans often present information regarding the thickness loss in the flanges. Figures Figure 203 and Figure 204 depict the thickness loss for bottom and top flanges, respectively.

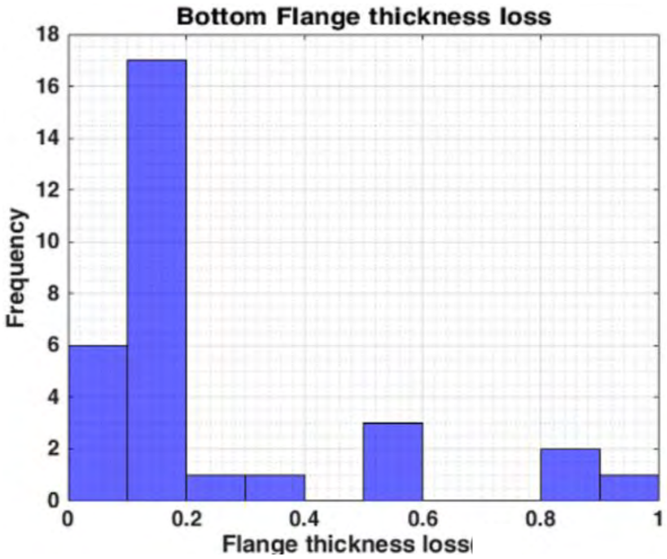

Figure 203: Bottom flange thickness loss histogram from the beam ends compiled - VTrans

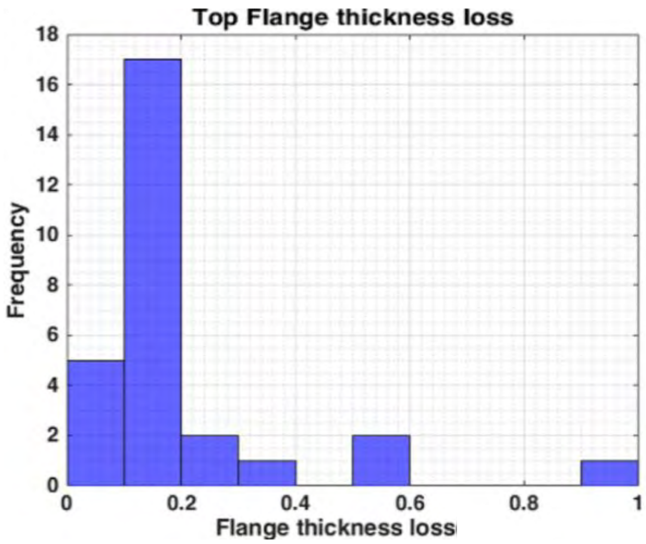

Figure 204: Top flange thickness loss histogram from the beam ends compiled - VTrans

4.6.4. Holes

Although a relatively small amount of beam ends was compiled, a significant number of holes were observed in the data. 11 holes were observed in the documents provided by VTrans. Table 52 denotes the topologies of the observed holes.

Table 52: Holes for beams ends from VTrans

Topology	**# of reported holes**
M1	5
M2	0
M3	2
M4	2
M1+M3	1
M1+M2	0
M2+M4	0

The dimensions of the holes are depicted in Figure 205, Figure 206, Figure 207, Figure 208, Figure 209, Figure 210, and Figure 211.

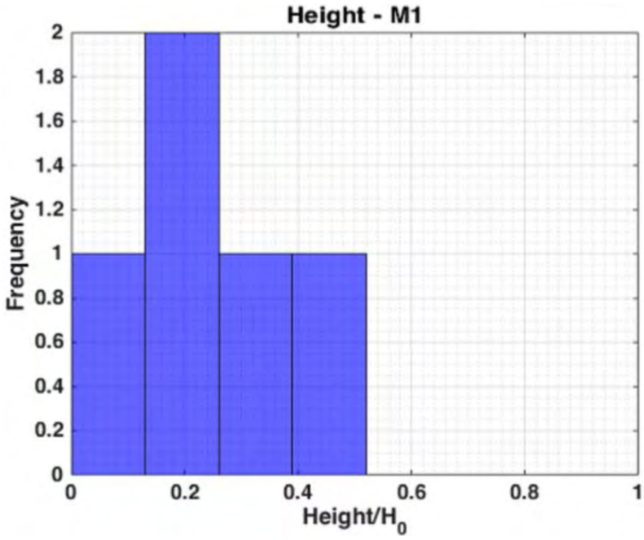

Figure 205: M1 web hole's height distribution beams without a diaphragm - VTrans

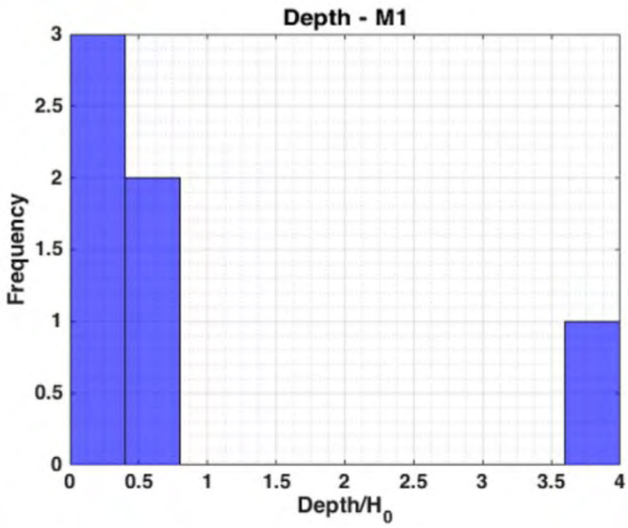

Figure 206: M1 web hole's depth distribution beams without a diaphragm - VTrans

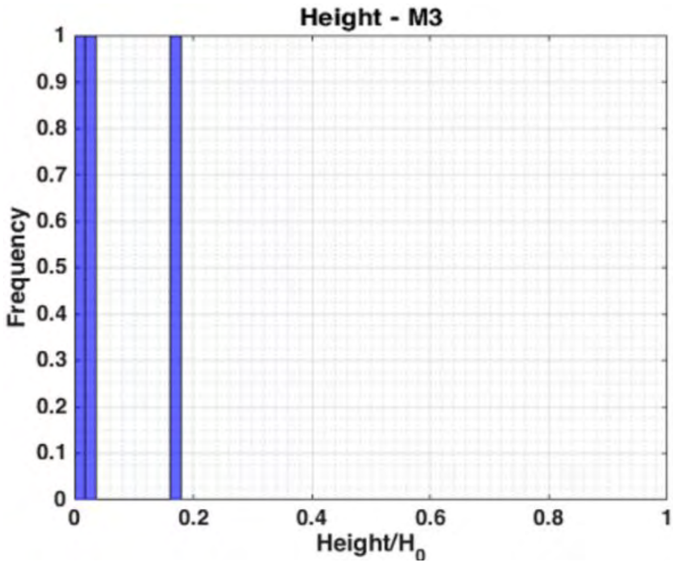

Figure 207: M3 web hole's height distribution beams without a diaphragm - VTrans

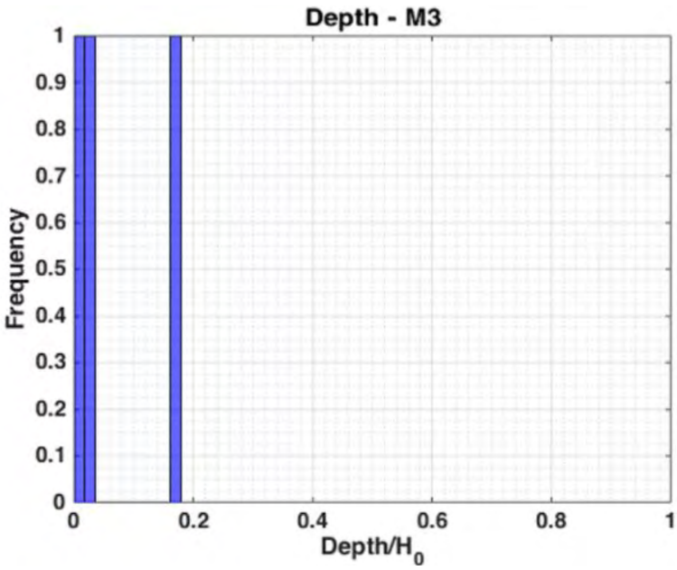

Figure 208 : M3 web hole's depth distribution beams without a diaphragm - VTrans

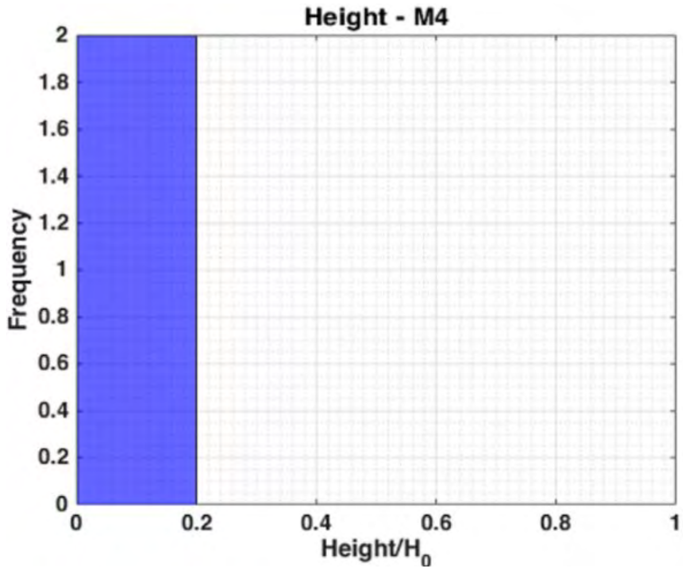

Figure 209: M4 web hole’s height distribution beams without a diaphragm - VTrans

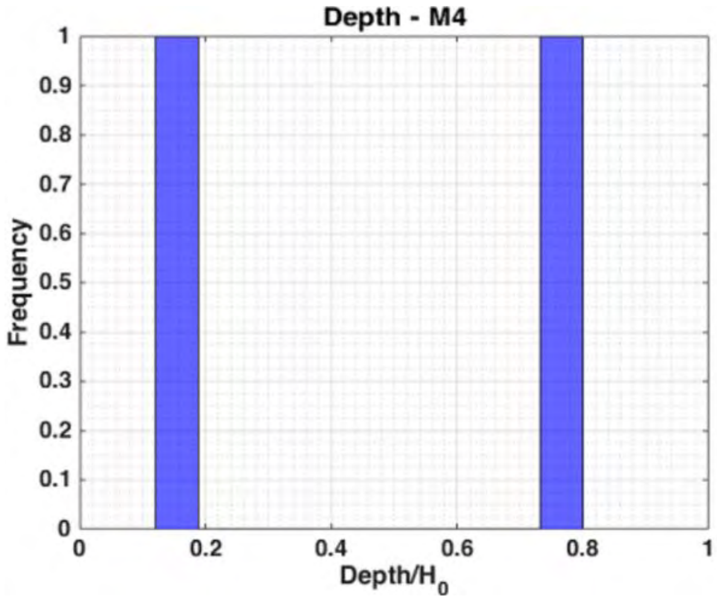

Figure 210: M4 web hole’s depth distribution beams without a diaphragm - VTrans

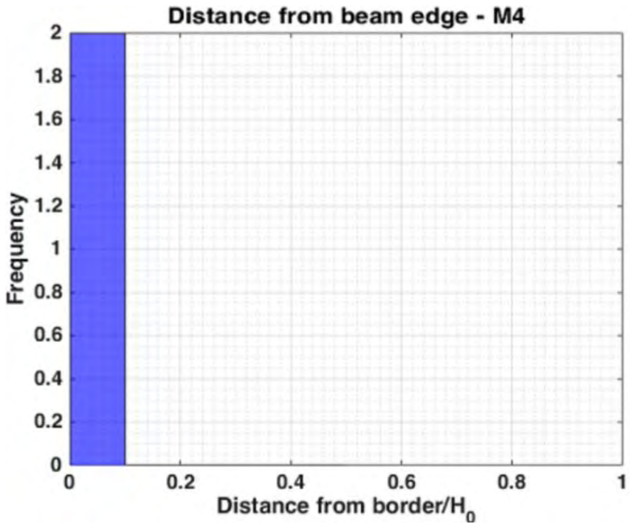

Figure 211 : M4 web hole's distance from beam edge distribution beams without a diaphragm - VTrans

5. Appendix II – Detailed data and processing graphs for beam ends with a diaphragm

5.1. Connecticut

5.1.1. Introduction

As commented in the previous sections, the data was divided by state as the number of beams ends were significantly different from one state to the other. Thus, to not introduce bias in the results, all states were individually analyzed. Following this initial grouping of the data, beam ends were divided into two sub-groups: the ones with diaphragm and the ones without. In this section all information and graphs presented regard the beams ends with a diaphragm system from Connecticut.

Figure 212 depicts the frequency of patterns obtained for beam ends with a diaphragm from the reports provided by CTDOT.

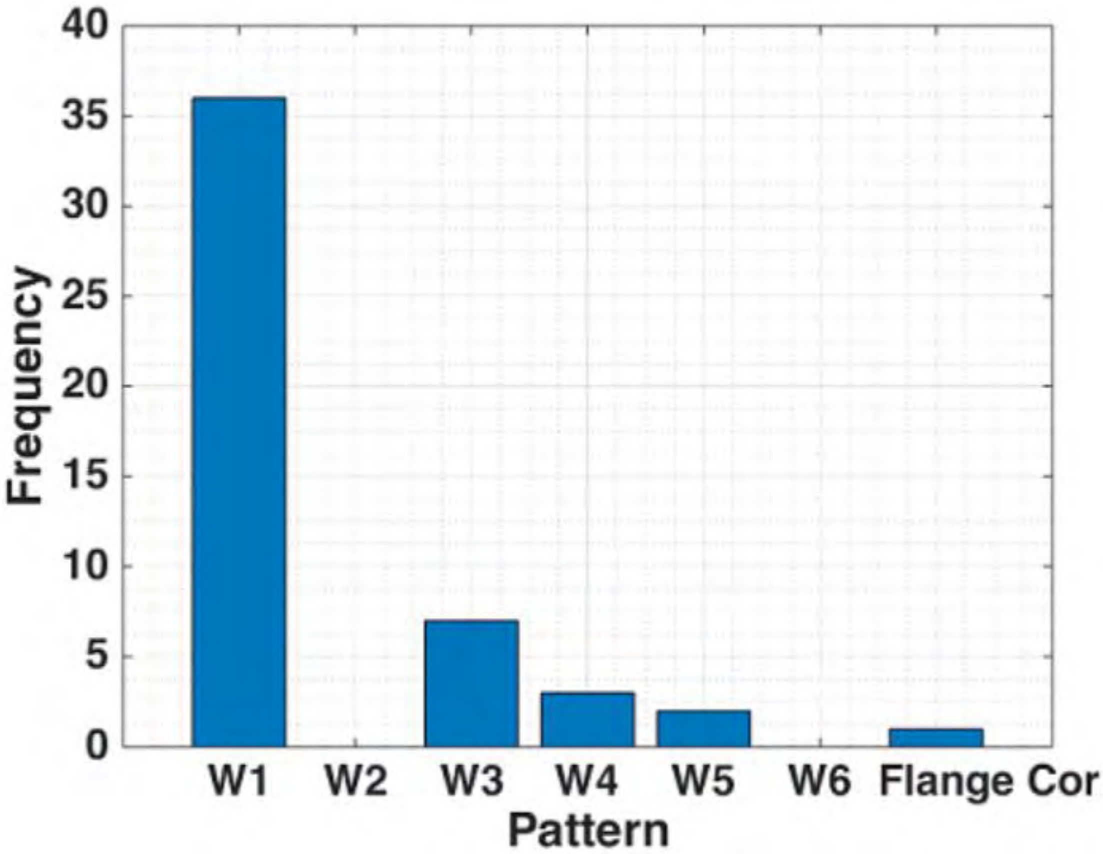

Figure 212: Web corrosion patterns distribution for beams ends with a diaphragm – CTDOT

Similar to all other cases, the dimensions CH1, CH2, CH3, CL1, CL2, CL3 are always normalized by H0, where $H_0 = H - 2t_f$.

5.1.2. Pattern W1

5.1.2.1. Web corrosion

The study began with the analysis of the distribution of the corrosion height, depicted in Figure 213. The parameters for the corrosion patterns can be found with corresponding diagrams in Section 1.5 *Corrosion Patterns* of this report.

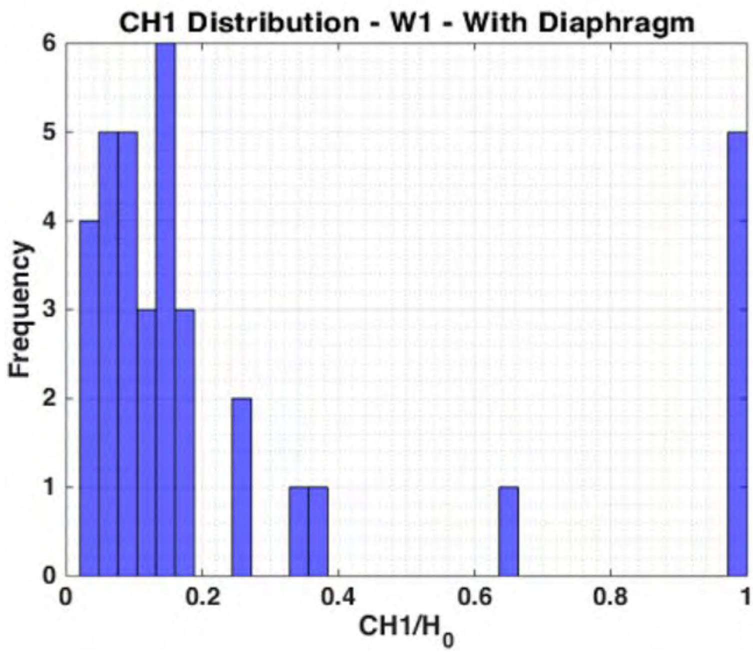

Figure 213: Distribution of corrosion height for W1 pattern – CTDOT

Our team discovered that, similar to the beams without a diaphragm, two trends are noticeable: (i) CH1<0.2H0, (ii) CH1 >0.9H0.

Figure 214 depicts the length of corrosion for CH1<0.2H0, whereas Figure 215 depicts the length corrosion distribution for CH1>0.9H0.

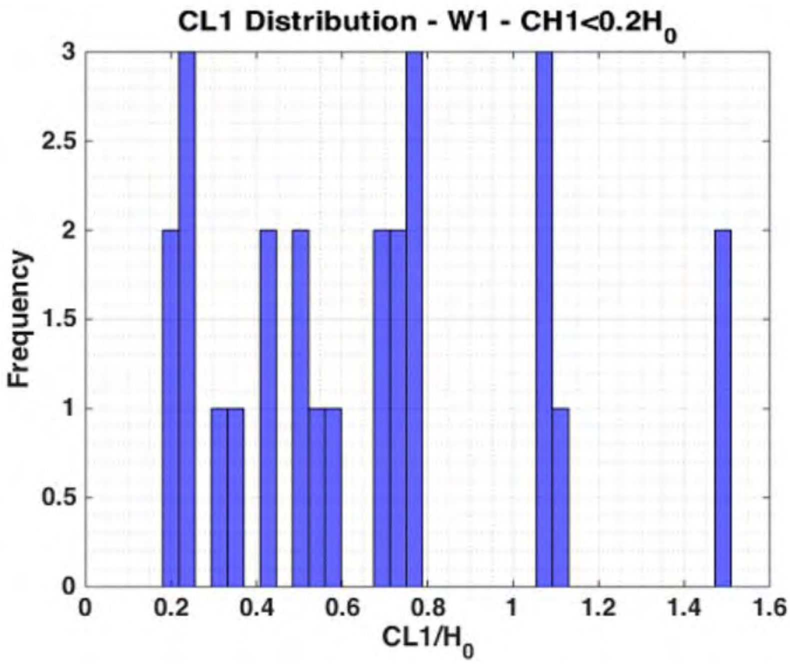

Figure 214: Corrosion length distribution for W1 pattern and CH1 <0.2H0 – CTDOT

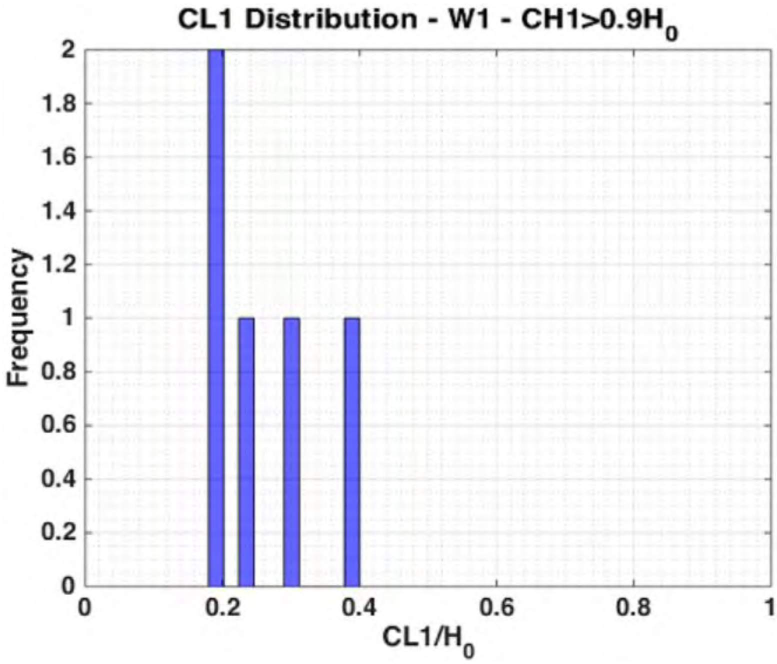

Figure 215 : Corrosion length distribution for W1 pattern and CH1 >0.9H0 – CTDOT

Figure 216 and Figure 217 depict the web thickness loss for CH1<0.2H0 and CH1>0.9H0, respectively.

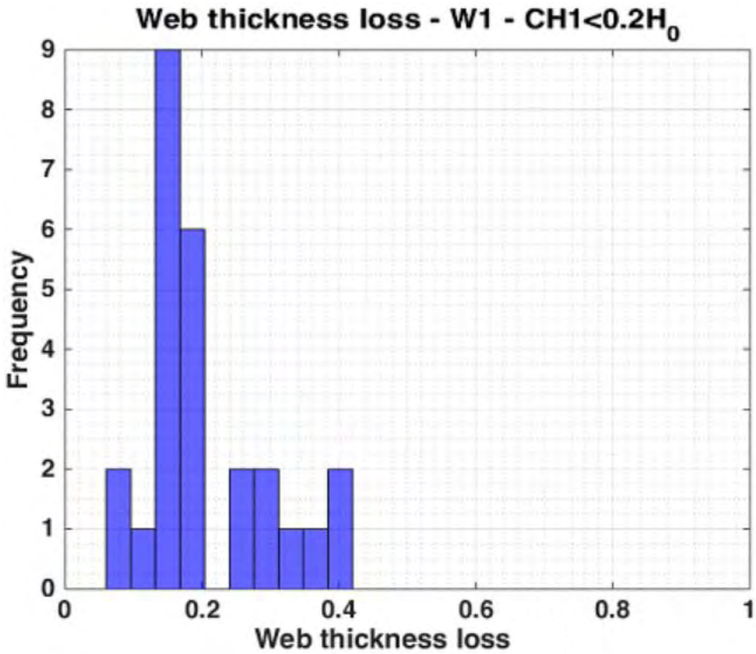

Figure 216 : Web thickness loss for W1 pattern and CH1<0.2H0 – CTDOT

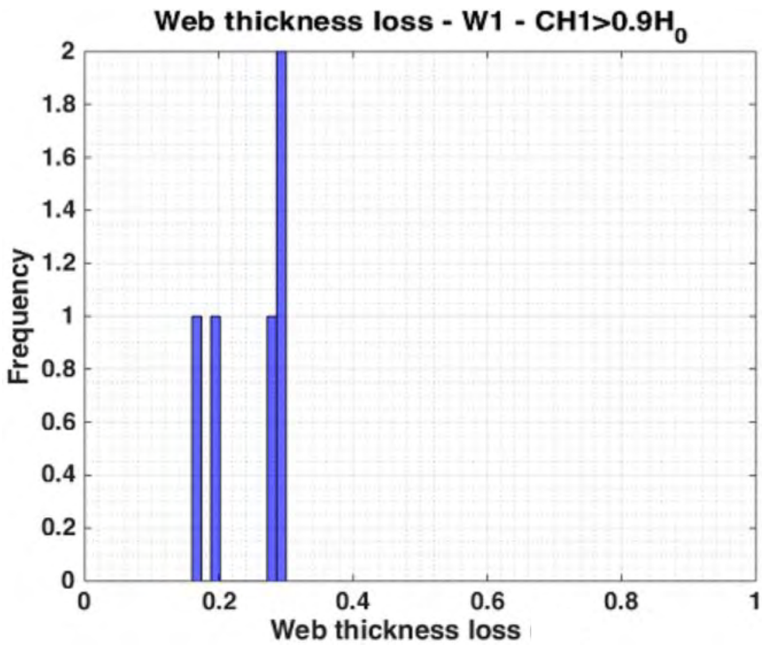

Figure 217 : Web thickness loss for W1 pattern and CH1>0.9H0 – CTDOT

Therefore, from the last figures, our team was able to define the following two corrosion cases:

$$Case\ A \begin{cases} 0 < CH1 \leq 0.2H_0 \\ 0.2H_0 \leq CL1 \leq 1.1H_0 \\ 0.1 \leq \dfrac{t_{loss}}{t_{web}} \leq 0.4 \end{cases}$$

$$Case\ B \begin{cases} 0.9H_0 \leq CH1 \leq 1H_0 \\ 0.2H_0 \leq CL1 \leq 0.4H_0 \\ 0.1 \leq \dfrac{t_{loss}}{t_{web}} \leq 0.3 \end{cases}$$

Figure 218 and Figure 219 depict Case A and B.

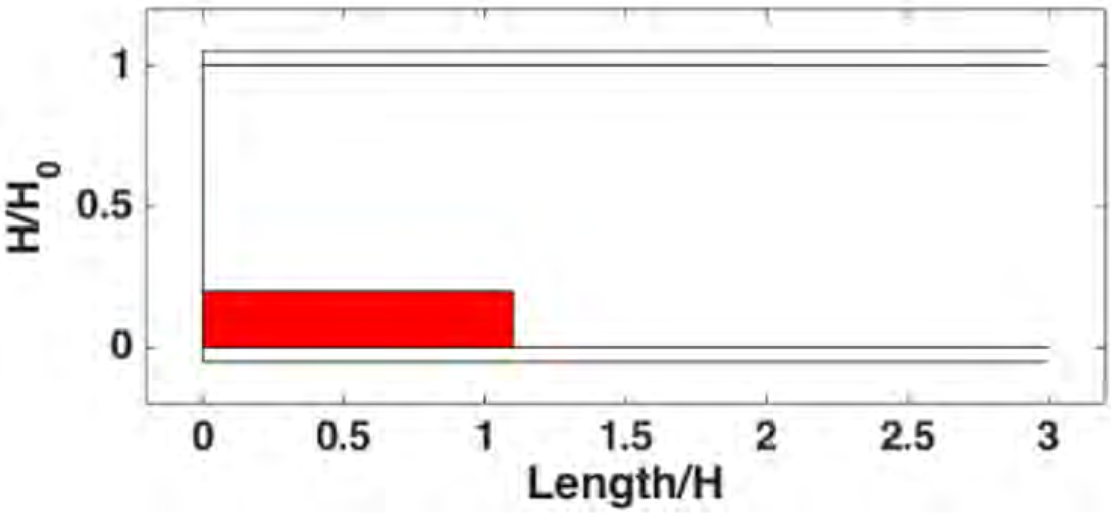

Figure 218: Extreme corrosion scenario (case A) for beams with a diaphragm, W1 pattern – CTDOT

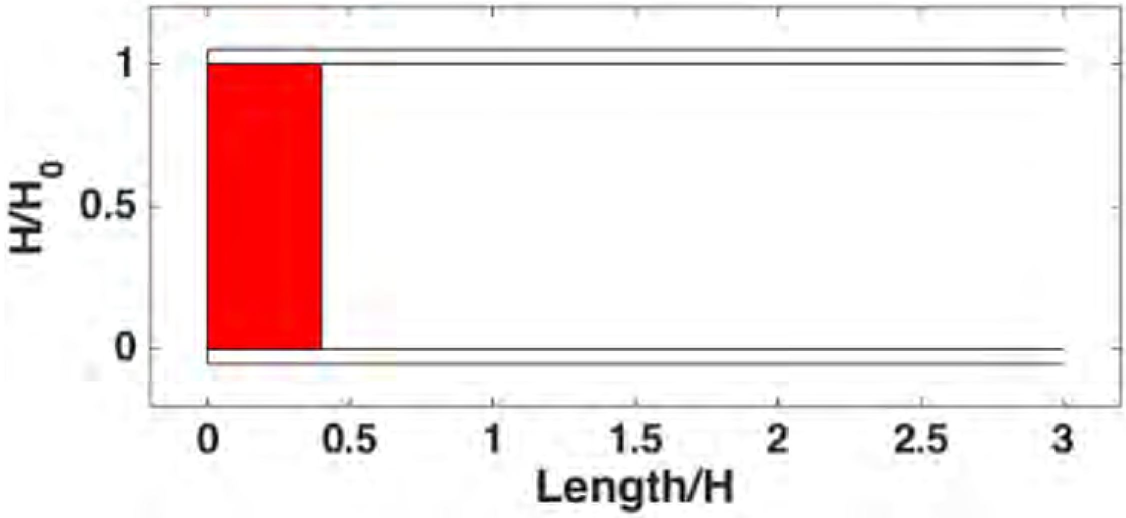

Figure 219: Extreme corrosion scenario (case B) for beams with a diaphragm, W1 pattern – CTDOT

Figure 220 and Figure 221 depict the overlapping of extreme corrosion cases for beams with and without a diaphragm system.

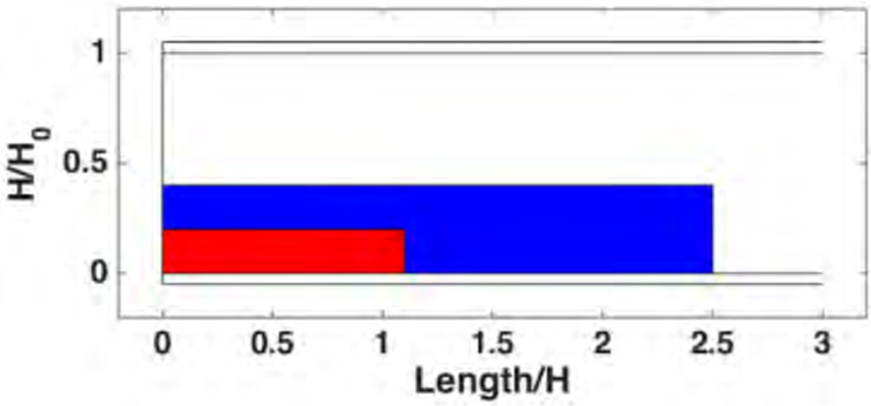

Figure 220: Comparison between extreme corrosion scenarios. Blue represents the extreme scenario for beams without diaphragm, whereas the region in red depicts extreme corrosion scenario for beams with a diaphragm – CTDOT

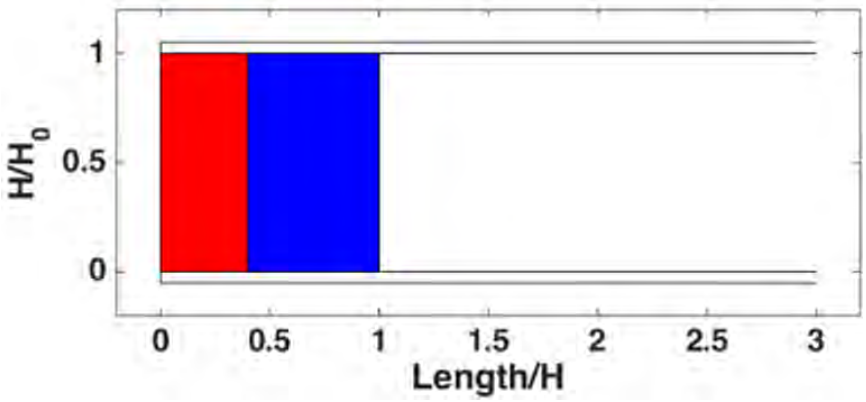

Figure 221: Comparison between extreme corrosion scenarios. Blue represents the extreme scenario for beams without diaphragm, whereas the region in red depicts extreme corrosion scenario for beams with a diaphragm – CTDOT

5.1.2.2. Flange corrosion

The research team was not able to collect information regarding flange corrosion for beam ends with a diaphragm system. For this reason, we were not able to study the flange corrosion of beams ends with a diaphragm from Connecticut.

5.1.2.3. Holes

Error! Reference source not found. presents the frequency of holes and patterns found for b eams ends with diaphragm.

Table 53: Holes and patterns for beams ends with diaphragm from CTDOT

	Number	No Hole	M 1	M 2	M 3	M 4	M1 and M2	M1 and M3	M2 and M4
W1	36	34	1	1	0	0	0	0	0
W2	0	0	0	0	0	0	0	0	0
W3	7	7	0	0	0	0	0	0	0
W4	3	2	1	0	0	0	0	0	0
W5	2	2	0	0	0	0	0	0	0
W6	0	0	0	0	0	0	0	0	0

According to Table 53, only two holes were observed combined with the W1 corrosion pattern. The small amount of data available meant that the research could not draw conclusions. The dimensions of the holes are:

Table 54: Dimensions of holes of pattern W3 for beam ends with a diaphragm – CTDOT

Hole topology	Length	Deep
M1	17.7%	17.7%
M2	24%	24%

5.1.3. Pattern W3

5.1.3.1. Web corrosion

Although just seven cases of the W3 corrosion pattern combined with diaphragms were recorded, all cases presented corrosion height equal to the height of the web, as depicted in Figure 222. The parameters for the corrosion patterns can be found with corresponding diagrams in Section 1.5 *Corrosion Patterns* of this report.

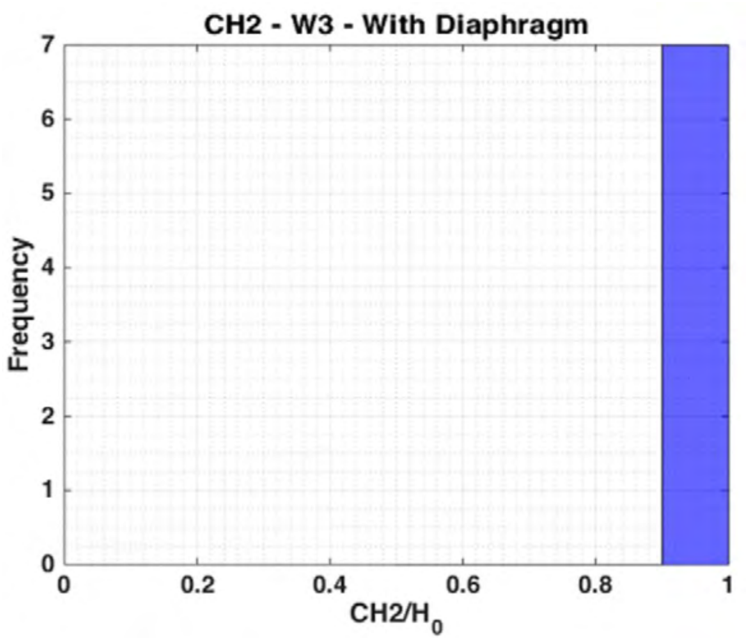

Figure 222: CH2 distribution for W3 pattern for beams with a diaphragm – CTDOT

The other parameters of the W3 corrosion pattern are plotted in Figure 223, Figure 224, Figure 225, Figure 226 and Figure 227.

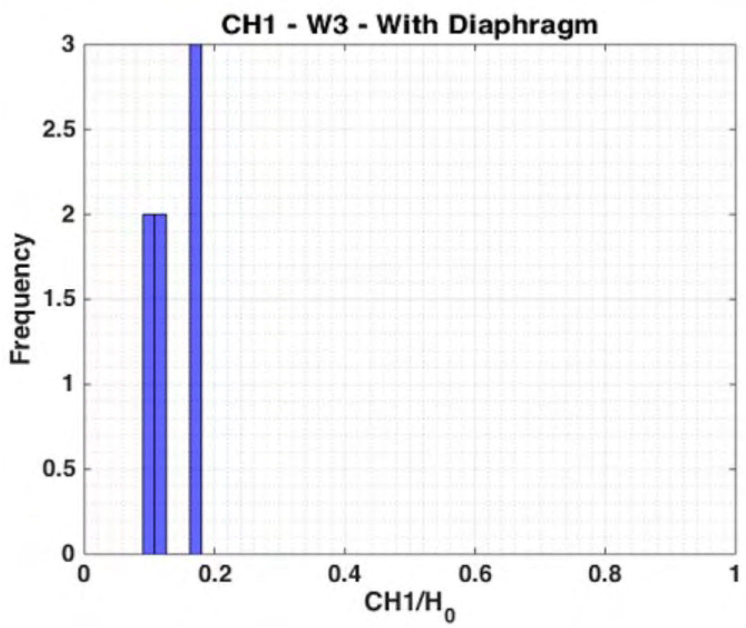

Figure 223: CH1 distribution for W3 pattern for beams with a diaphragm – CTDOT

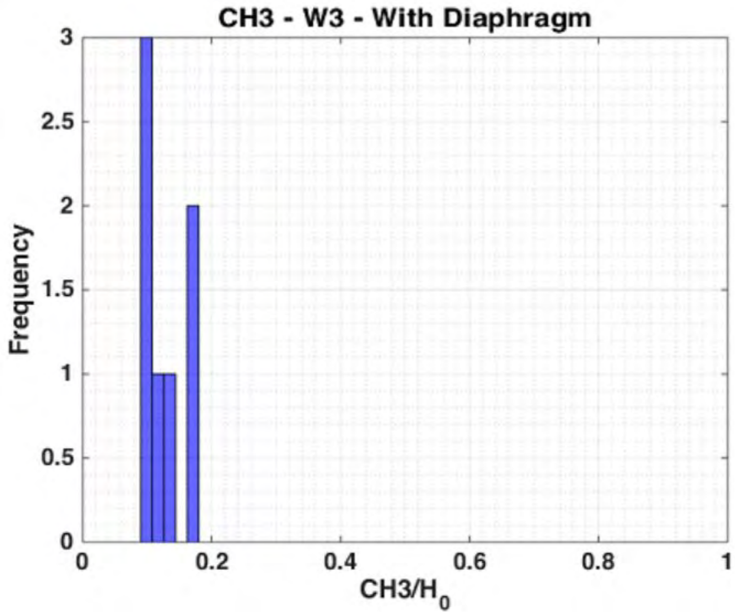

Figure 224: CH2 distribution for W3 pattern for beams with a diaphragm – CTDOT

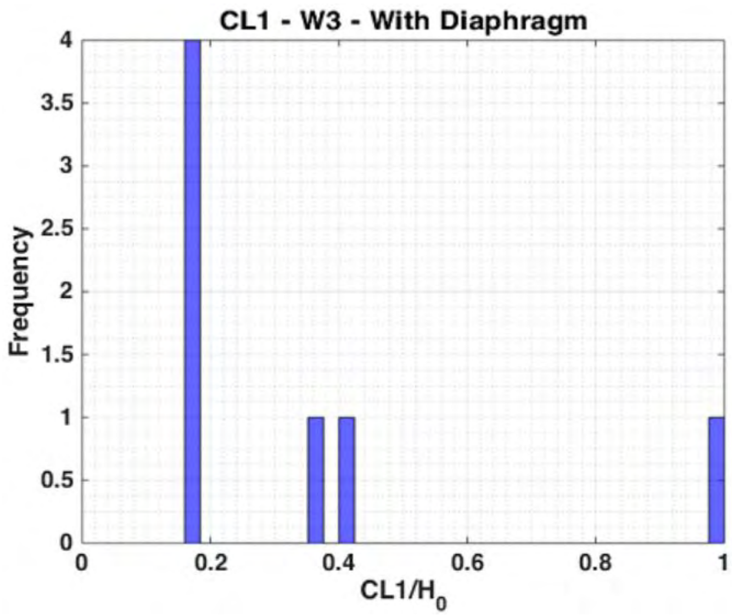

Figure 225: CL1 distribution for W3 pattern for beams with a diaphragm – CTDOT

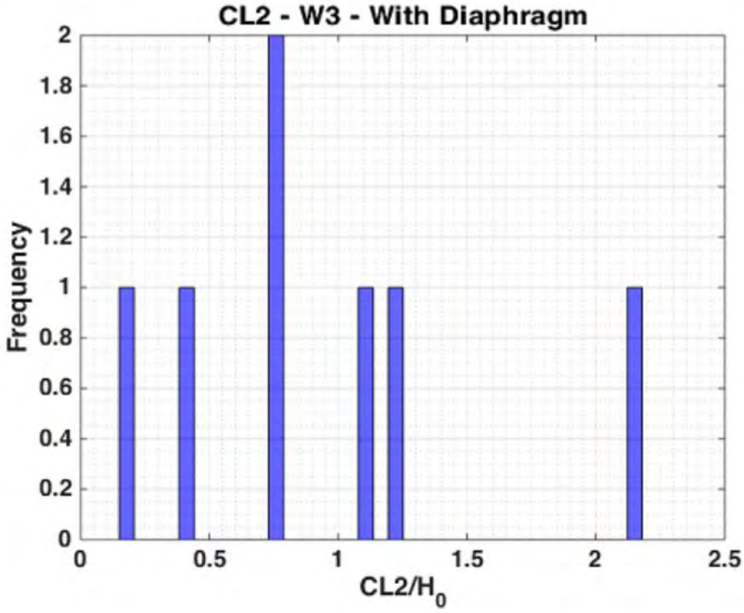

Figure 226: CL2 distribution for W3 pattern for beams with a diaphragm – CTDOT

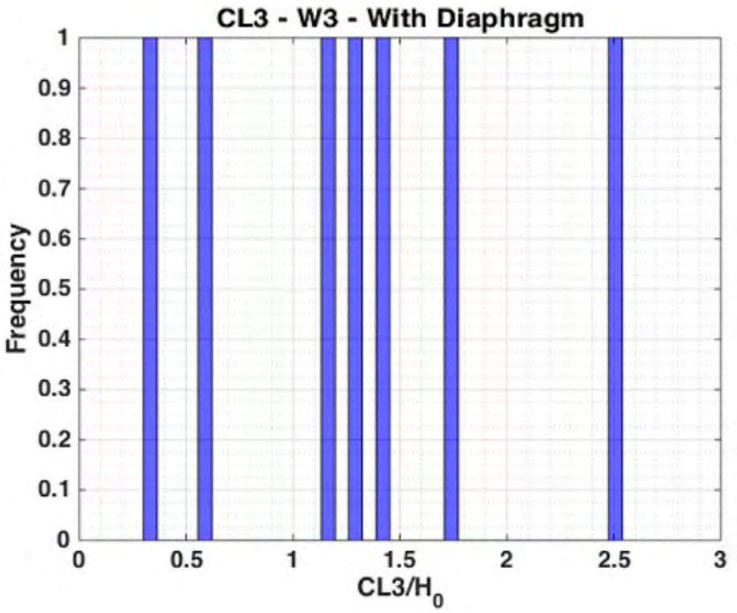

Figure 227: CL3 distribution for W3 pattern for beams with a diaphragm – CTDOT

Figure 228 depicts the web thickness loss distribution for pattern W3.

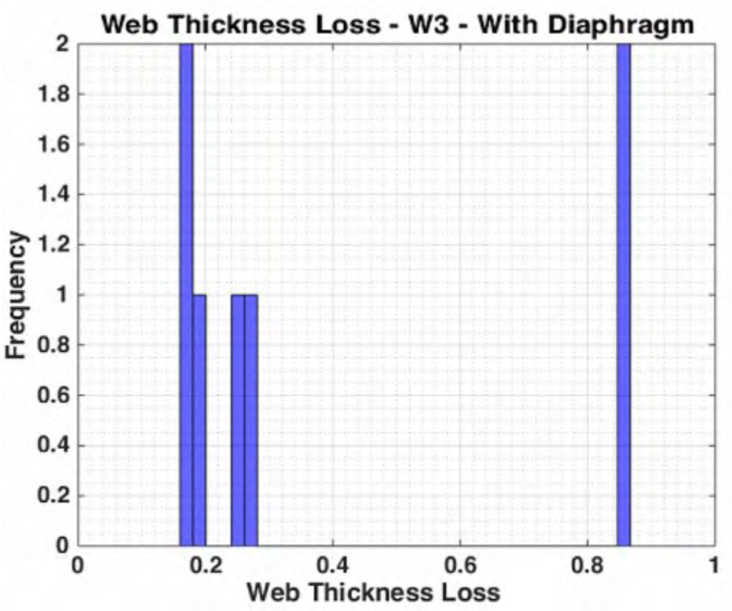

Figure 228: Web thickness loss distribution for W3 pattern for beams with a diaphragm – CTDOT

Therefore, from the last figures, our team was able to determine the intervals of the W3 corrosion pattern for beams ends with diaphragms.

$$0.1H_0 \leq CH_1 \leq 0.2H_0$$

$$CH_2 \; takes \; the \; value \; of \; \{1\}$$

$$0.1H_0 \leq CH_3 \leq \; 0.2H_0$$

$$0.2H_0 \leq CL_1 \leq 0.4H_0$$

$$0.4H_0 \leq CL_2 \leq 2.2H_0$$

$$0.4H_0 \leq CL_3 \leq 2.5H_0$$

$$\frac{t_{loss}}{t_{web}} \; takes \; the \; values \; of \; \{0.2, 0.25, 0.85\}$$

Figure 229 depicts the extreme case of the W3 corrosion pattern for beam ends with a diaphragm system.

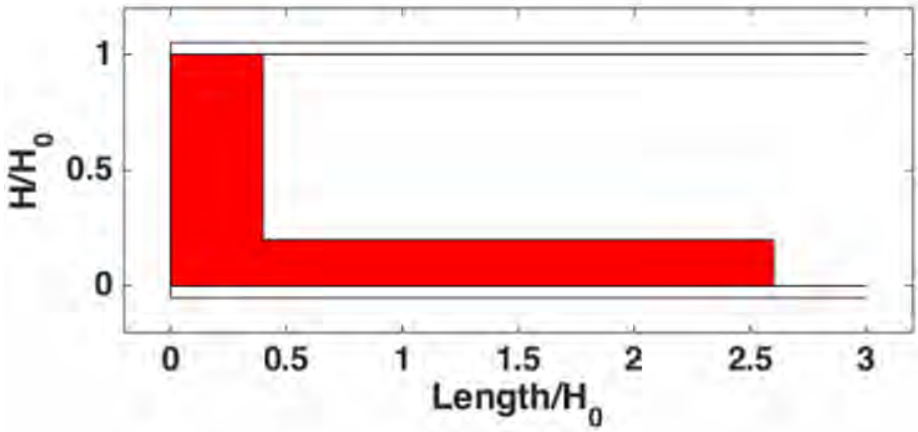

Figure 229: Extreme corrosion scenario of W3 pattern for beam ends with a diaphragm – CTDOT

Figure 230 displays the comparison between the corrosion for beam ends with and without a diaphragm system.

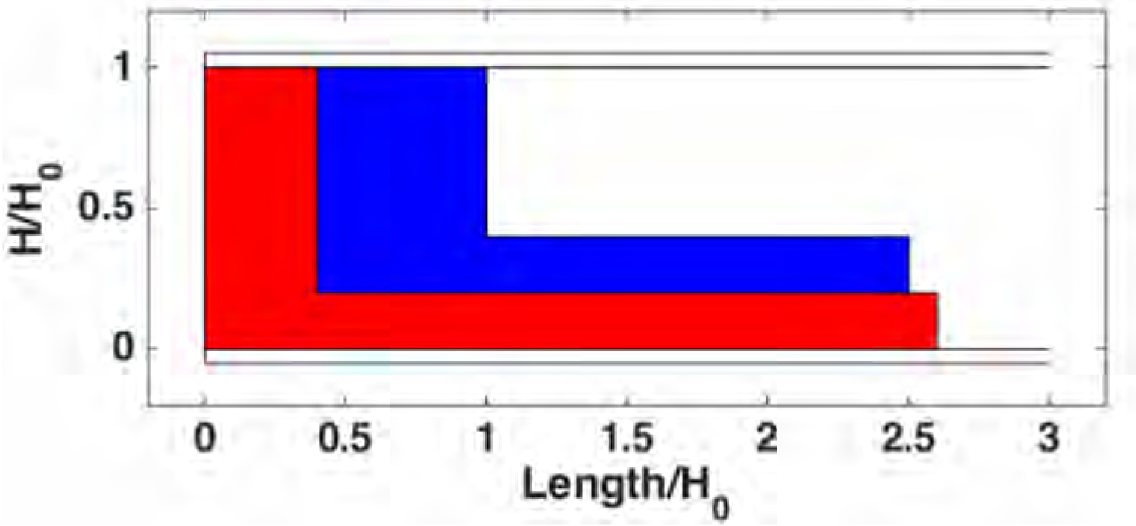

Figure 230: Comparison between extreme corrosion scenarios. Blue represents the extreme scenario for beams without diaphragm, whereas the region in red depicts extreme corrosion scenario for beams with a diaphragm – CTDOT

5.1.3.2. Flange corrosion

No information regarding flange corrosion combined with the W3 corrosion patterns for beam ends with a diaphragm were found in the reports provided by CTDOT.

5.1.3.3. Holes

As displayed in Table 53 , no holes were found combined with the W3 corrosion patterns in beam ends with a diaphragm.

5.2.Massachusetts

5.2.1. Introduction

The data was divided into two main categories, beams ends with a diaphragm system and beam ends without a diaphragm system. All the graphs in this part of the document represent the first case. The histogram below contains the frequency of each of the defined corrosion patterns (the total amount of times each pattern appears in the reports).

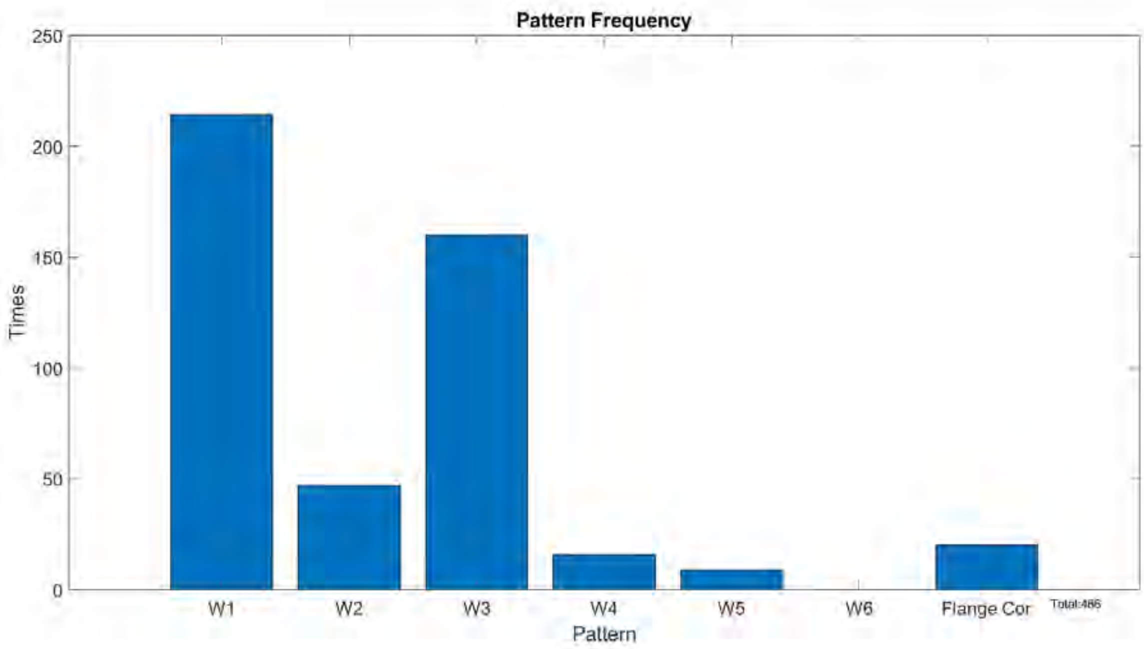

Figure 231. Web corrosion patterns distribution for beams with a diaphragm - MassDOT

For each web corrosion pattern, we have normalized the characteristic dimensions (CH1, CH2, CH3, CL1, Cl2, CL3) with the height H_0, where $H_0 = H - 2t_f$.

5.2.2. Pattern W1

5.2.2.1. Web Corrosion

The parameters for the corrosion patterns can be found with corresponding diagrams in Section 1.5 *Corrosion Patterns* of this report.

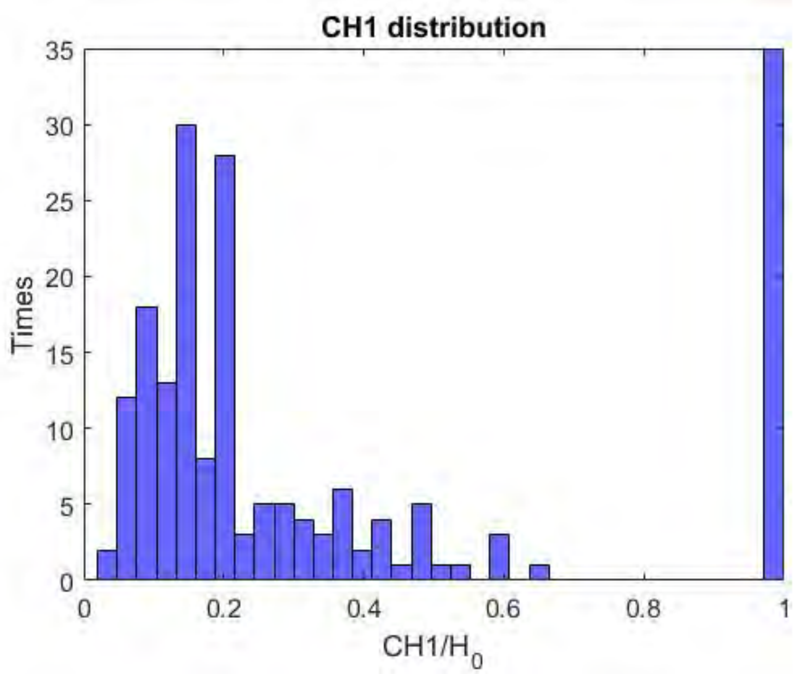

Figure 232. CH1 distribution of W1 web pattern for beams with a diaphragm (total 189). - MassDOT

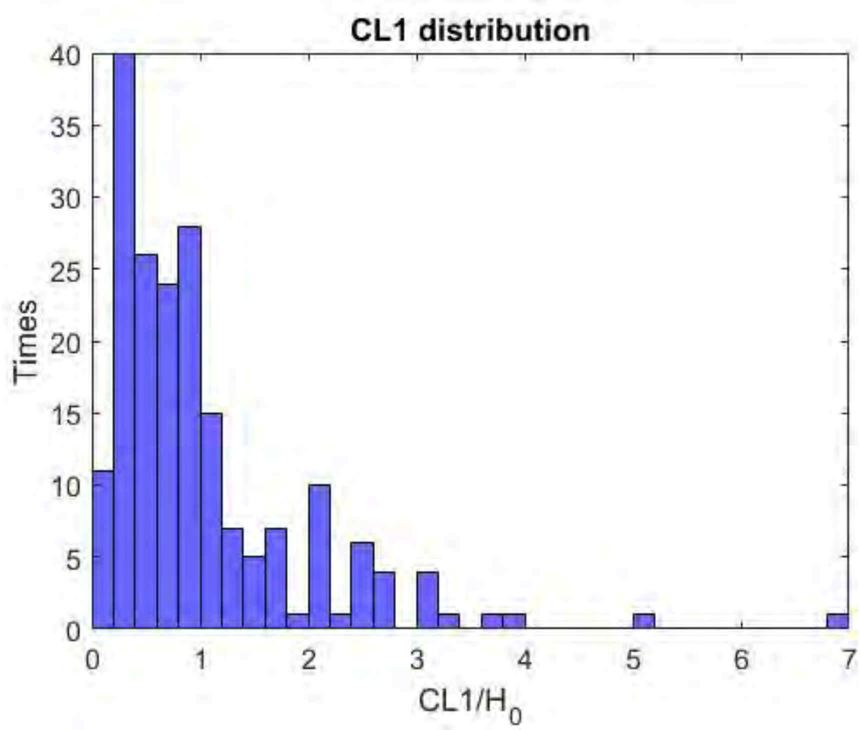

Figure 233: CL1 distribution of W1 web corrosion pattern for beams with a diaphragm - MassDOT

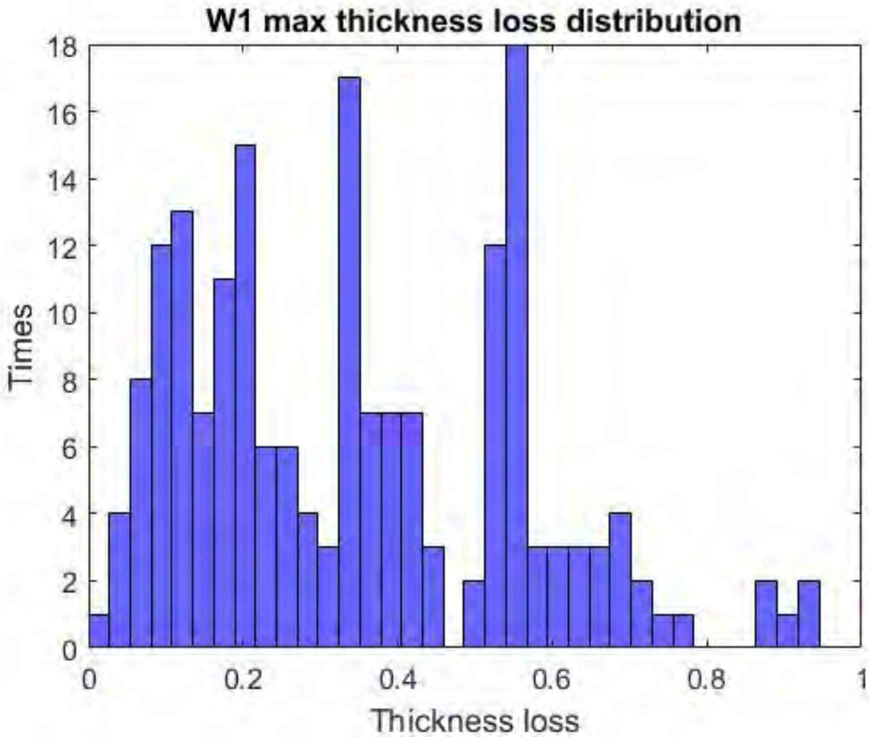

Figure 234: Max thickness loss distribution of W1 web corrosion pattern for beams with a diaphragm - MassDOT

From the CH1 histogram, two main trends are noticed, which cover almost the 85% of cases (158 out of 189): either a) full height corrosion, or b) corrosion up to 30% of H_0.

$$CH_1 = H_0 \ or \ 0 < CH_1 \leq 0.3H_0$$

For full height:

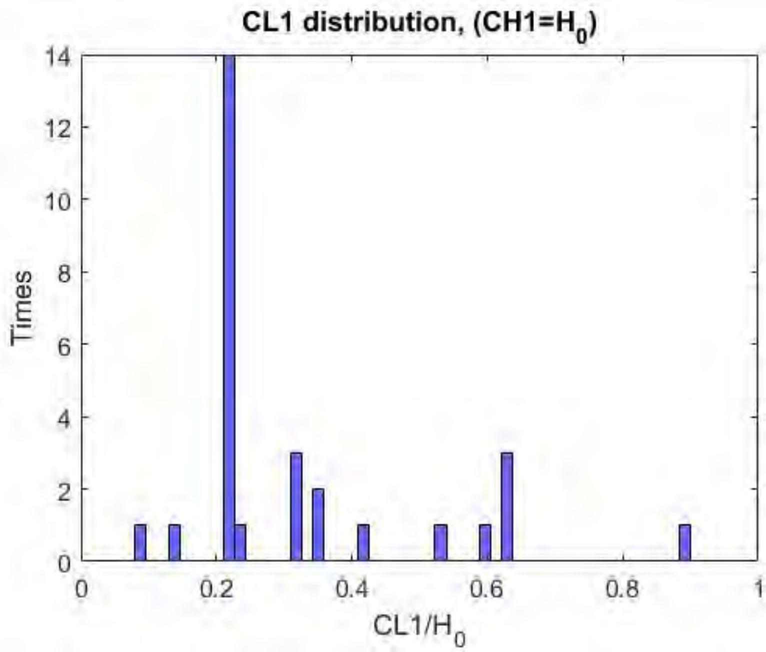

Figure 235: CL1 distribution of full height W1 web corrosion pattern for beams with a diaphragm - MassDOT

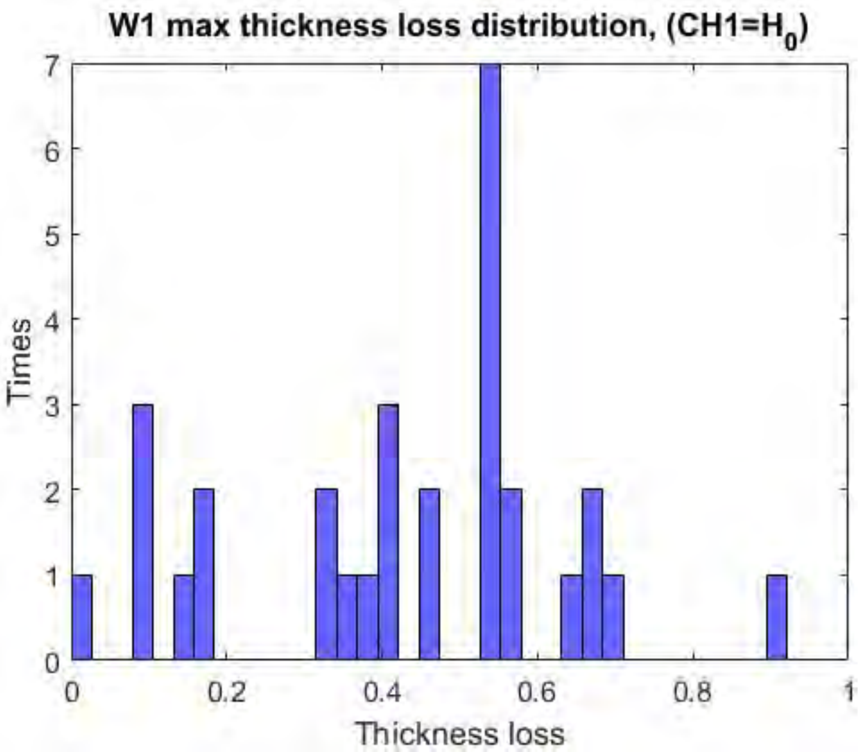

Figure 236: Max thickness loss distribution of full height W1 web corrosion pattern for beams with a diaphragm - MassDOT

By observing the figure for full height corrosion and CL<=0.35H, we saw:

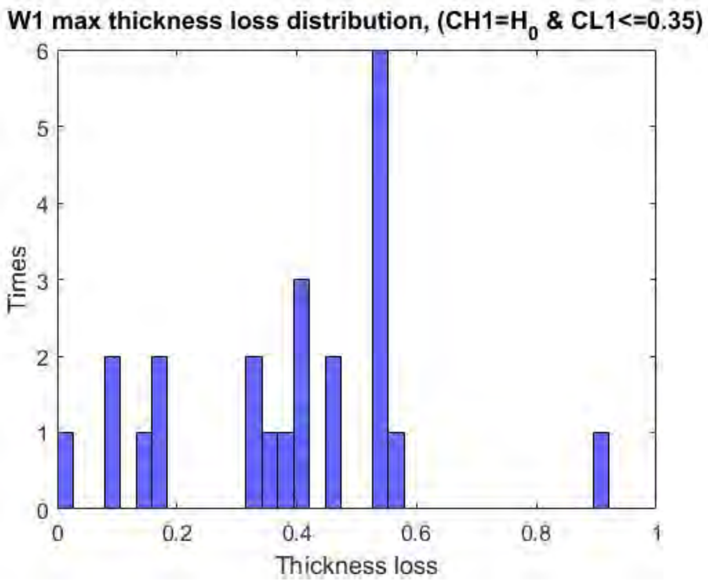

(8)

Figure 237: Max web thickness loss distribution of W1 web corrosion pattern, with corrosion height up to 35% of H_0, for beams with a diaphragm - MassDOT

For the full height corrosion case, one case is identified: **CASE A**

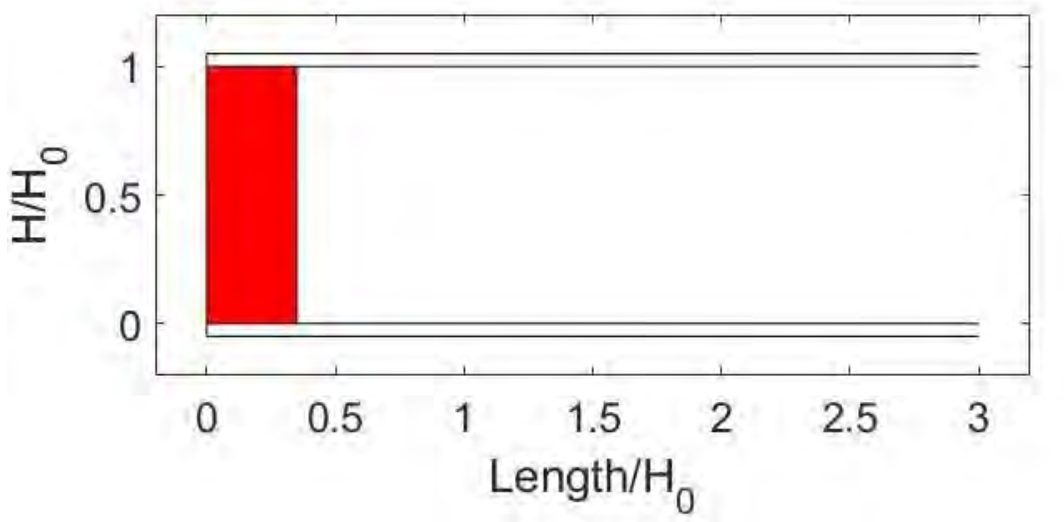

Figure 238: First extreme W1 web corrosion pattern, with full height corrosion for beams with a diaphragm - MassDOT

With web thickness loss $\frac{t_{loss}}{t_{web}}$ $takes\ values\ of$ {0.2,0.4,0.6} (Figure 86)

5.2.2.2. Flange Corrosion for Case A

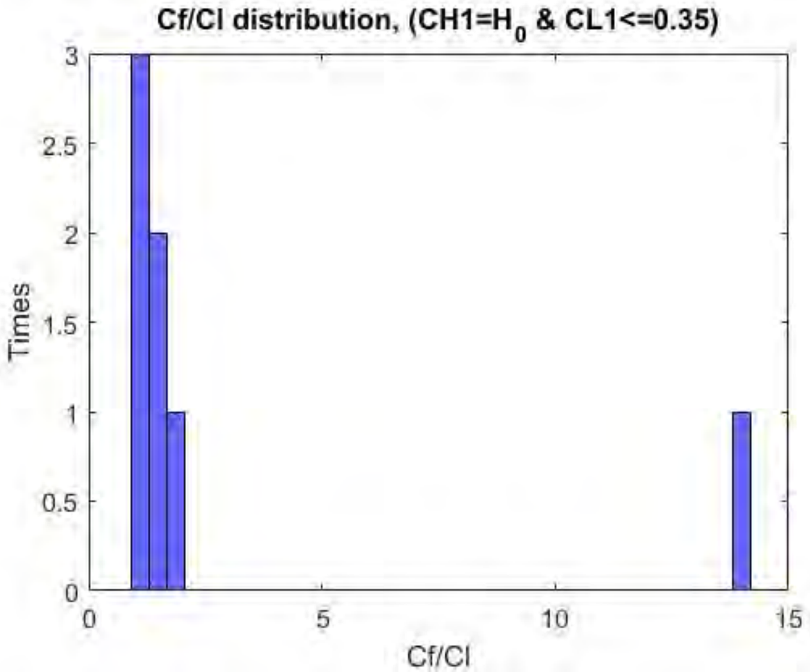

Figure 239: Ratio of flange to web corrosion length distribution of W1 web corrosion pattern, with full height corrosion and up to 35% of H_0 length, for beams with a diaphragm - MassDOT

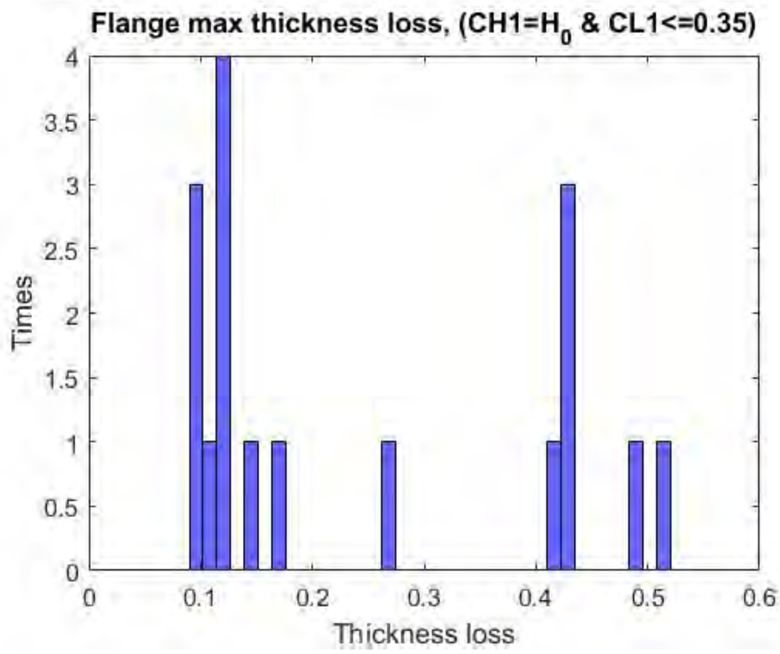

Figure 240: Max flange thickness loss distribution of W1 web corrosion pattern, with full height corrosion and up to 35% of H_0 length, for beams with a diaphragm - MassDOT

Thus, for case A: $\frac{t_{loss}}{t_{flange}}$ $takes\ values\ of$ {0.15,0.45} (Figure 240). The ratio of the length of the corroded flange over the length of the corroded web $1 \le \frac{Cf}{Cl} \le 1.7$

For $0 < CH_1 \le 0.3$

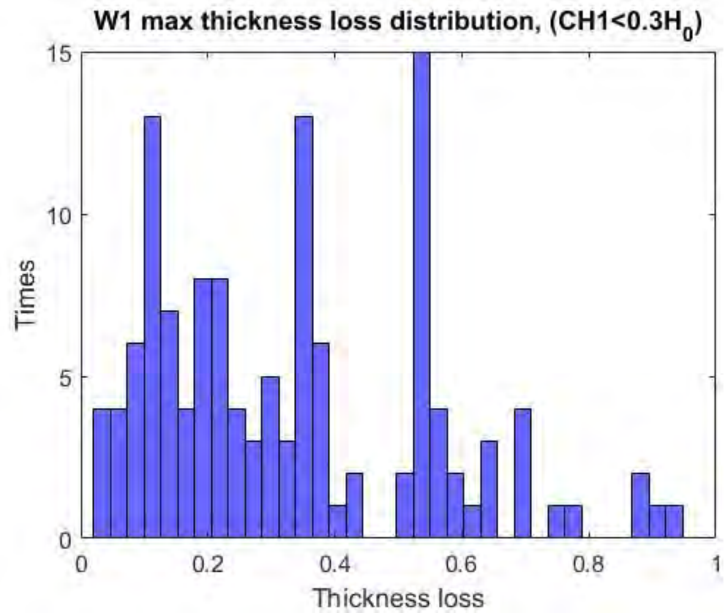

Figure 241: Max web thickness loss distribution of W1 web corrosion pattern with corrosion height up to 30% of H_0 for beams with a diaphragm - MassDOT

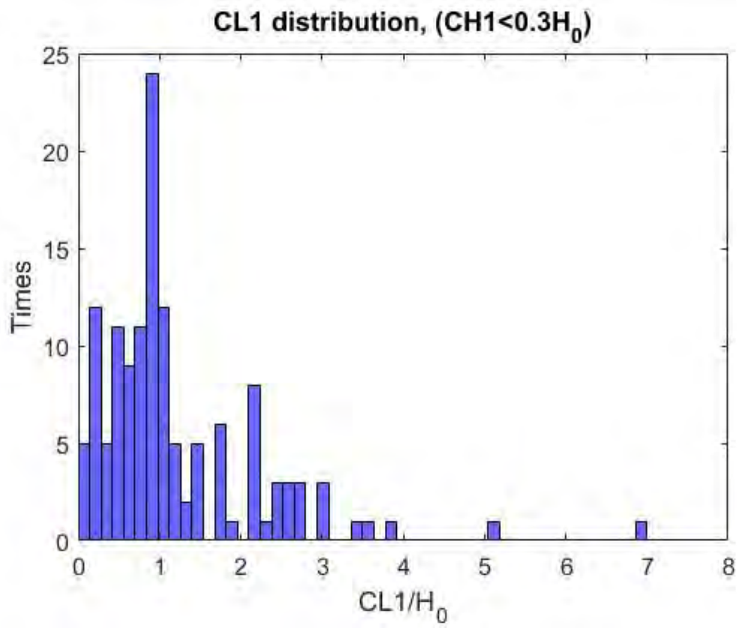

Figure 242: CL1 thickness loss distribution of W1 web corrosion pattern with corrosion height up to 30% of H_0 for beams with a diaphragm - MassDOT

From Figure 242,$0 < CL_1 \le 2.5$ with web thickness loss $\frac{t_{loss}}{t_{web}}$ $takes\ values\ of$ {0.2,0.4,0.6,0.8}.

CASE B

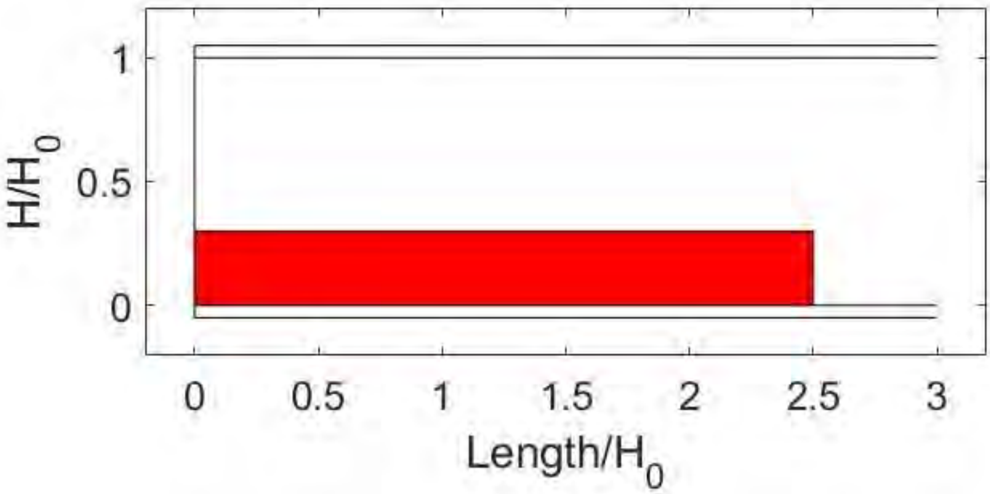

Figure 243: Second extreme W1 web corrosion pattern, with corrosion height up to 30% of H_0 for beams with a diaphragm - MassDOT

For Case B: $\frac{t_{loss}}{t_{flange}}$ $takes\ values\ of$ {0.2,0.4,0.6,0.8} (Figure 241). The ratio of the length of the corroded flange over the length of the corroded web $0 < \frac{Cf}{Cl} \leq 1$ (Figure 239).

5.2.2.3. Flange Corrosion for Case B

For CH1<0.3H$_0$

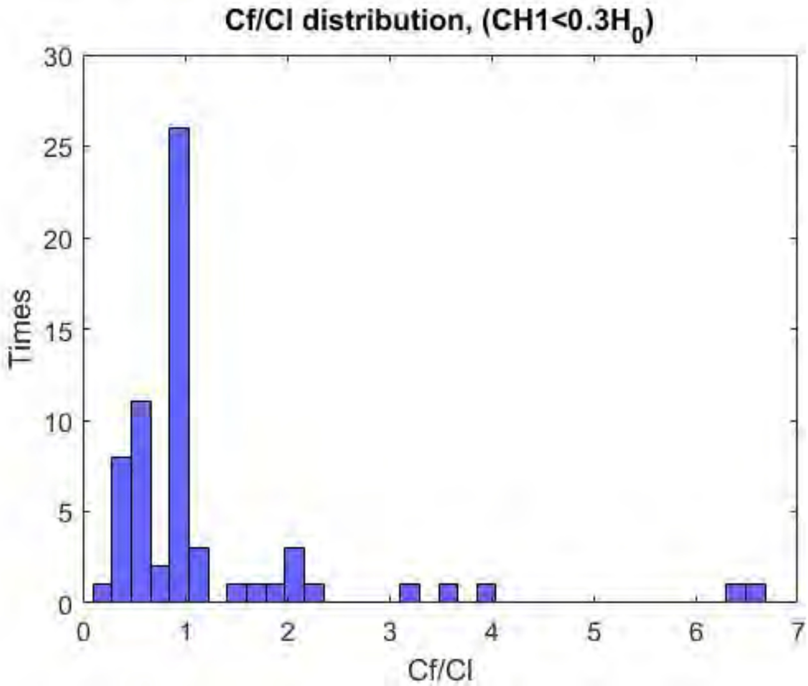

Figure 244: Ratio of flange to web corrosion length distribution of W1 web corrosion pattern with corrosion height up to 30% of H_0 for beams with a diaphragm - MassDOT

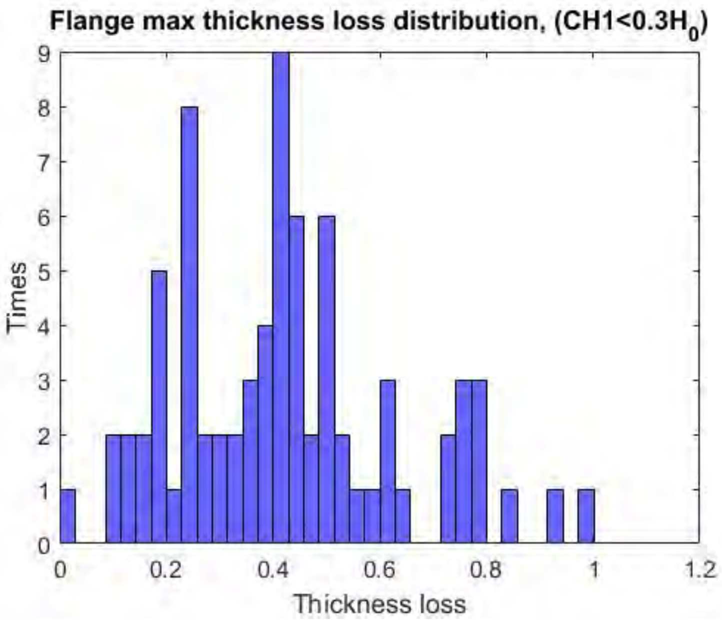

Figure 245: Max flange thickness loss distribution of W1 web corrosion pattern with corrosion height up to 30% of H_0 for beams with a diaphragm - MassDOT

5.2.2.4. Holes

The W1 corrosion pattern is combined 11 times with the M1 hole corrosion pattern. The web thickness loss, holes dimensions, and corrosion height at these cases are given as:

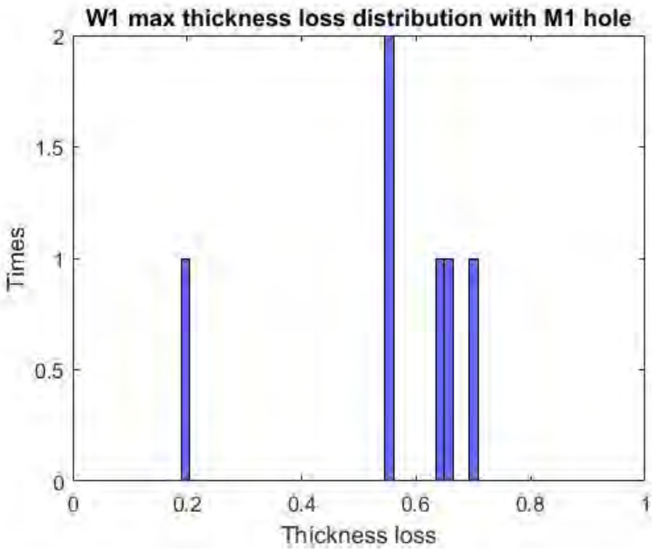

Figure 246. Max thickness loss distribution for W1 web corrosion patterns and M1 hole for beams with a diaphragm - MassDOT

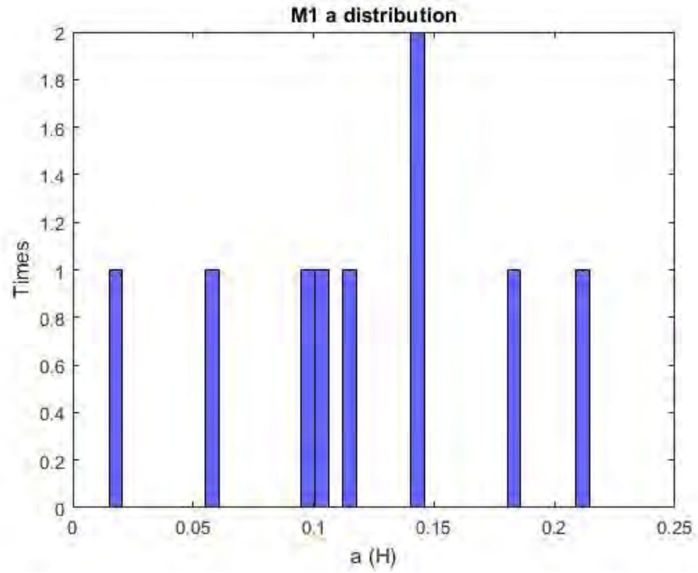

Figure 247: M1 web hole's pattern height distribution of W1 web corrosion pattern for beams with a diaphragm - MassDOT

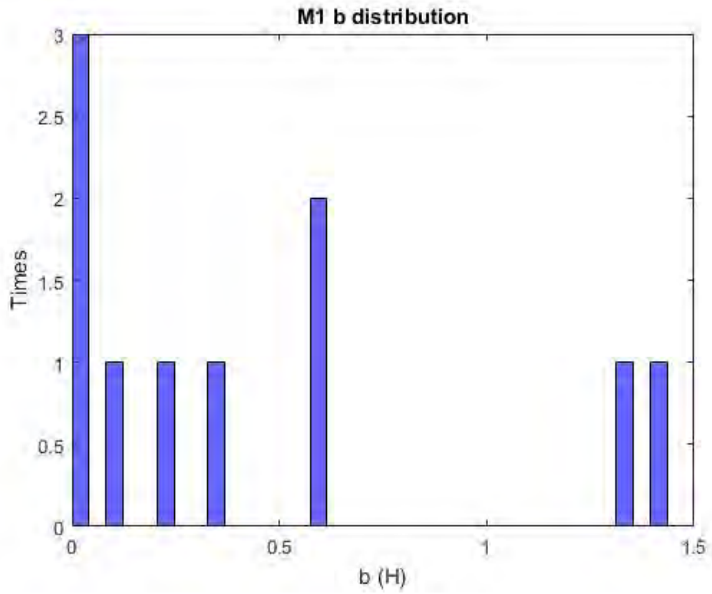

Figure 248: M1 web hole's pattern length distribution of W1 web corrosion pattern for beams with a diaphragm - MassDOT

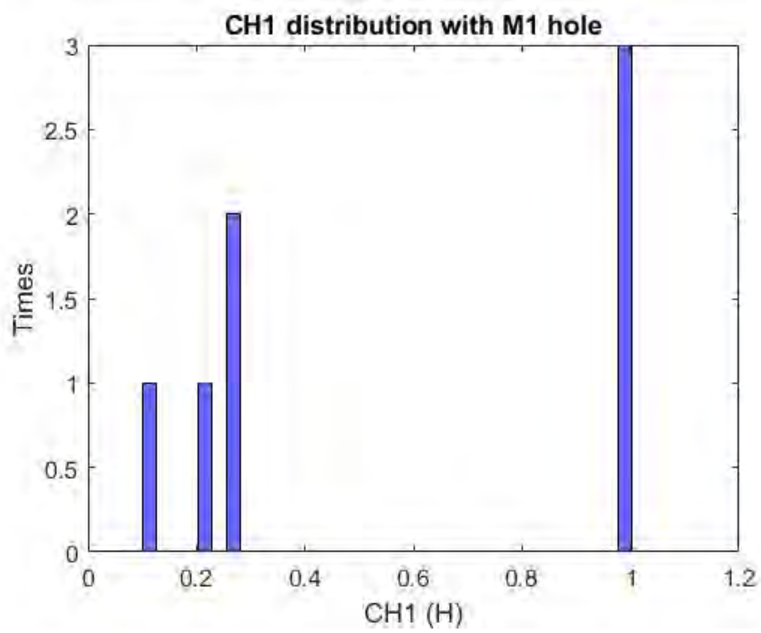

Figure 249: CH1 distribution for beams with M1 hole and W1 web corrosion pattern and a diaphragm - MassDOT

From Figure 249, we can conclude that holes are equally distributed between web corrosion scenarios CASE A and CASE B. It is worth mentioning that there are two cases of long holes that are parallel to flange holes (Figure 248). The two longest holes ($1.3H_0$ and $1.4\ H_0$) are also the corrosion holes with the highest height (0.18 and 0.21) respectively. As a result, an extreme hole case is considered the following (projected on Case B web corrosion scenario):

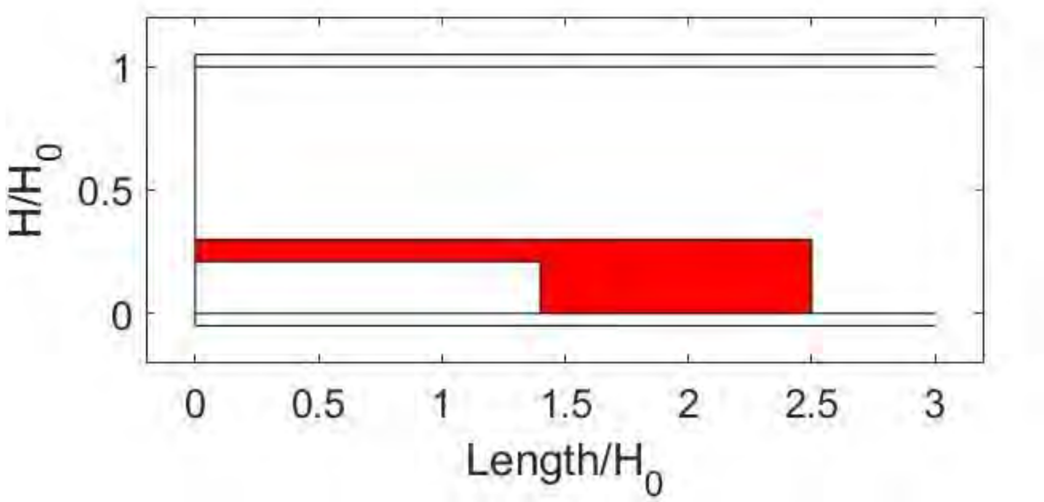

Figure 250: M1 extreme web hole pattern scenario of W1 web corrosion pattern, for beams with a diaphragm - MassDOT

There are also 4 cases of the M2 corrosion hole pattern. The web thickness loss, holes dimensions, and corrosion height at these cases are given as:

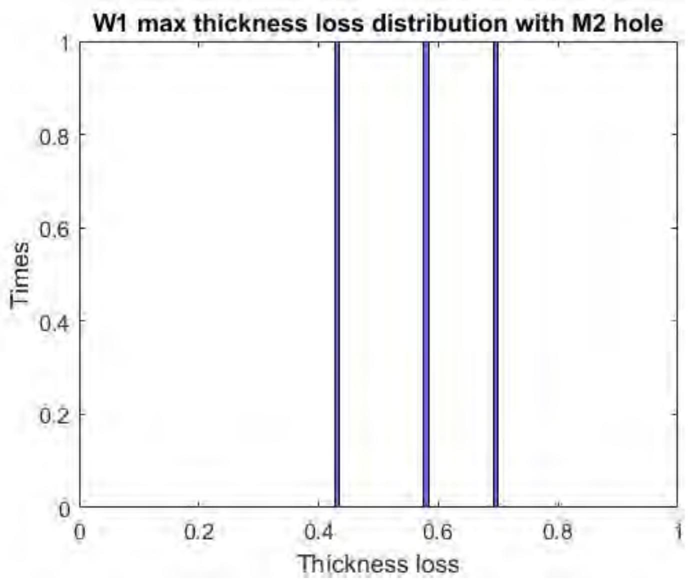

Figure 251. Max thickness loss distribution for W1 web corrosion patterns and M2 hole for beams with a diaphragm - MassDOT

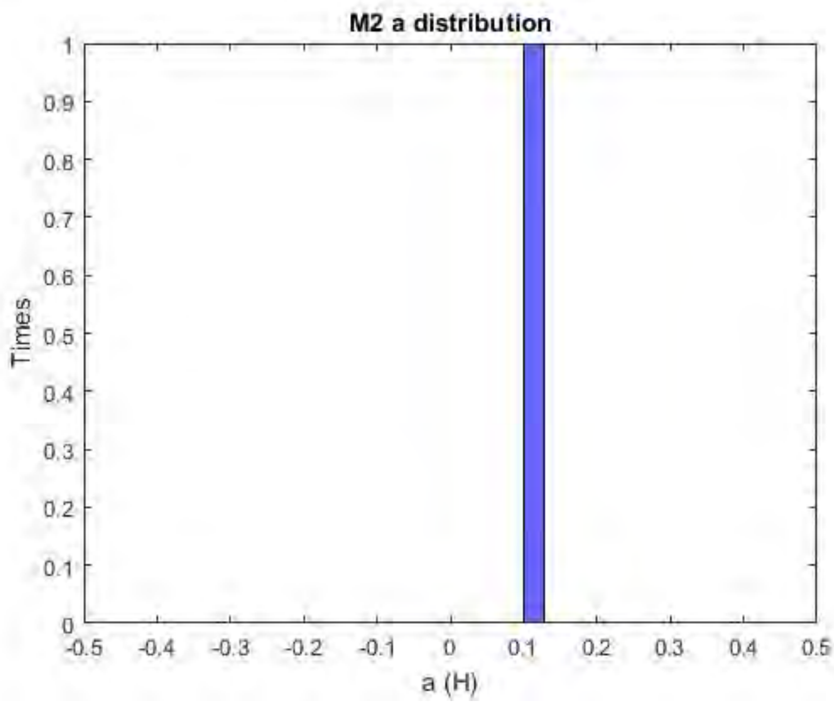

Figure 252: M2 web hole's pattern height distribution of W1 web corrosion pattern for beams with a diaphragm - MassDOT

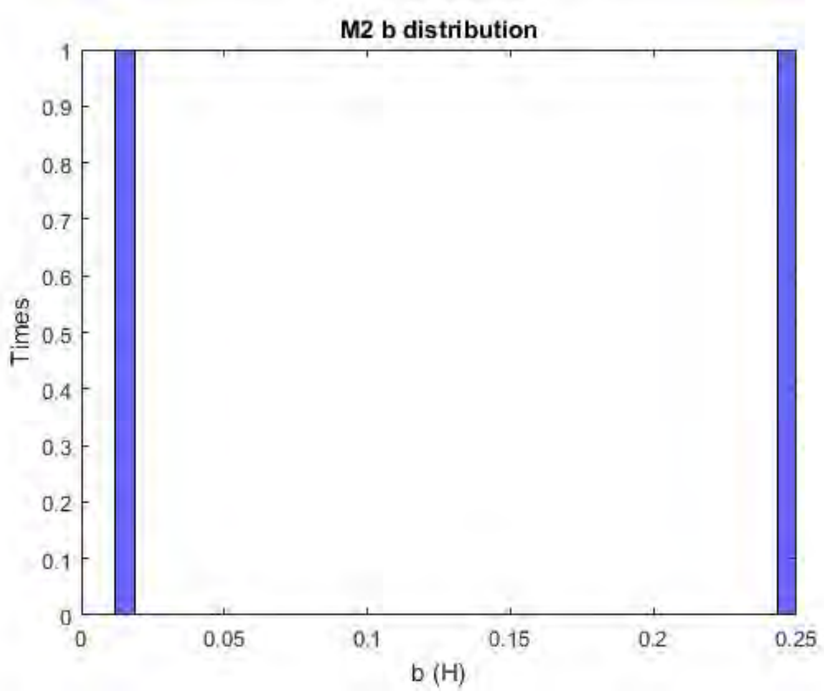

Figure 253: M2 web hole's pattern length distribution of W1 web corrosion pattern for beams with a diaphragm - MassDOT

The data gathered from the inspection reports is very small for the research team to extract valid conclusions.

5.2.3. Pattern W2

5.2.3.1. Web Corrosion

The W2 corrosion pattern was observed in total only 47 times. The parameters for the corrosion patterns can be found with corresponding diagrams in Section 1.5 *Corrosion Patterns* of this report.

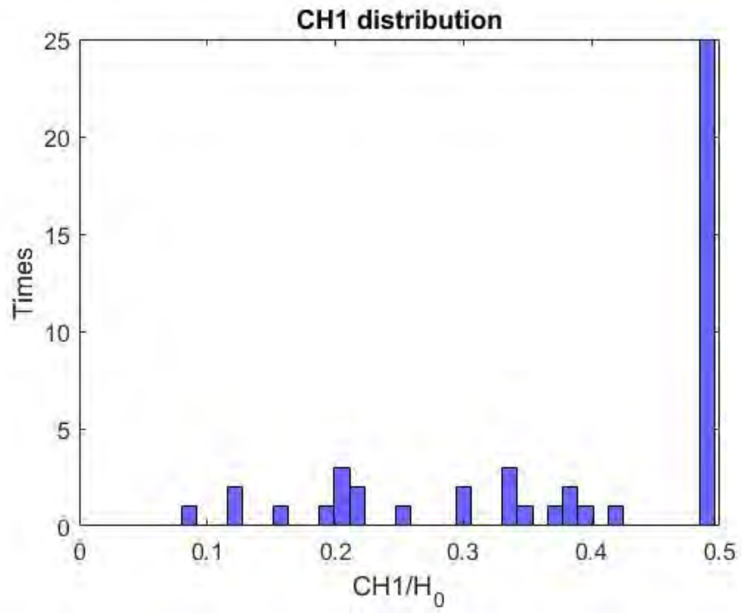

Figure 254. CH1 distribution of W2 pattern for beams with a diaphragm - MassDOT

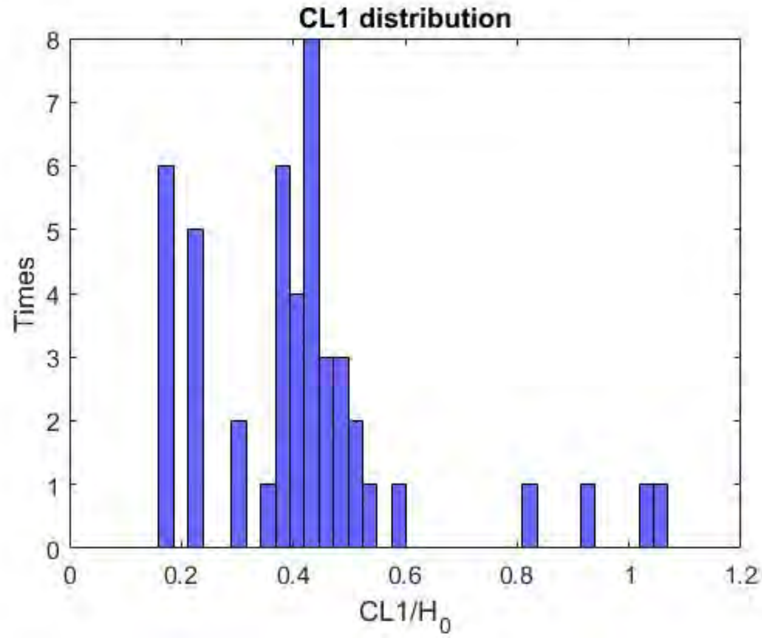

Figure 255: CL1 distribution of W2 pattern for beams with a diaphragm - MassDOT

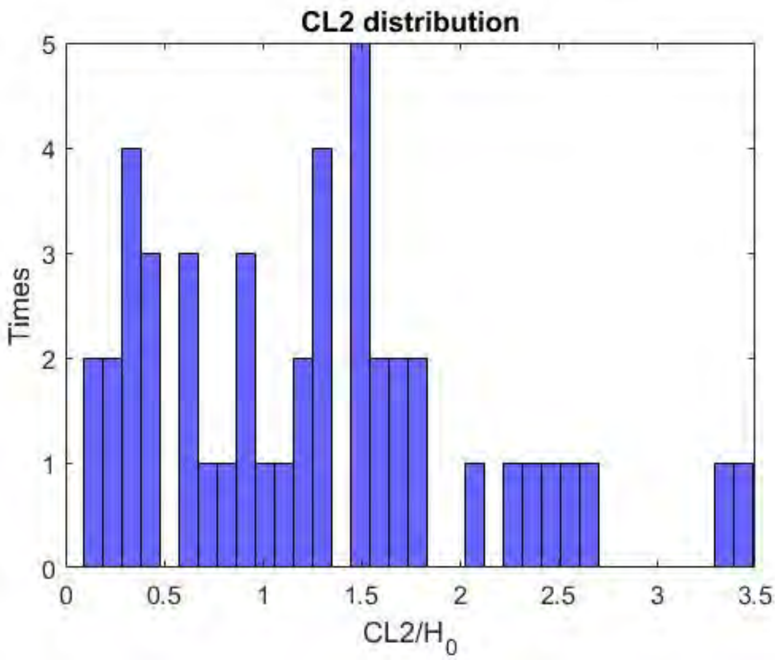

Figure 256: CL2 distribution of W2 pattern for beams with a diaphragm - MassDOT

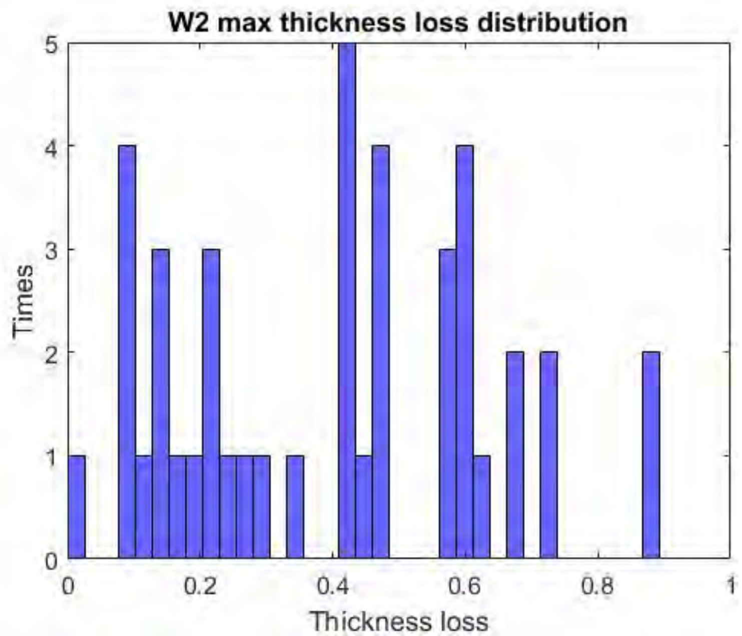

Figure 257: Web thickness loss distribution of W2 pattern for beams with a diaphragm - MassDOT

From the above figure, our team stated:

$$0 < CH_1 \leq 0.5H_0$$

$$0 < CL_1 \leq 0.6H_0$$

$$0 < CL_2 \leq 1.8H_0$$

$$\frac{t_{loss}}{t_{web}}\ takes\ values\ of\ \{0.2, 0.4, 0.6, 0.8\}$$

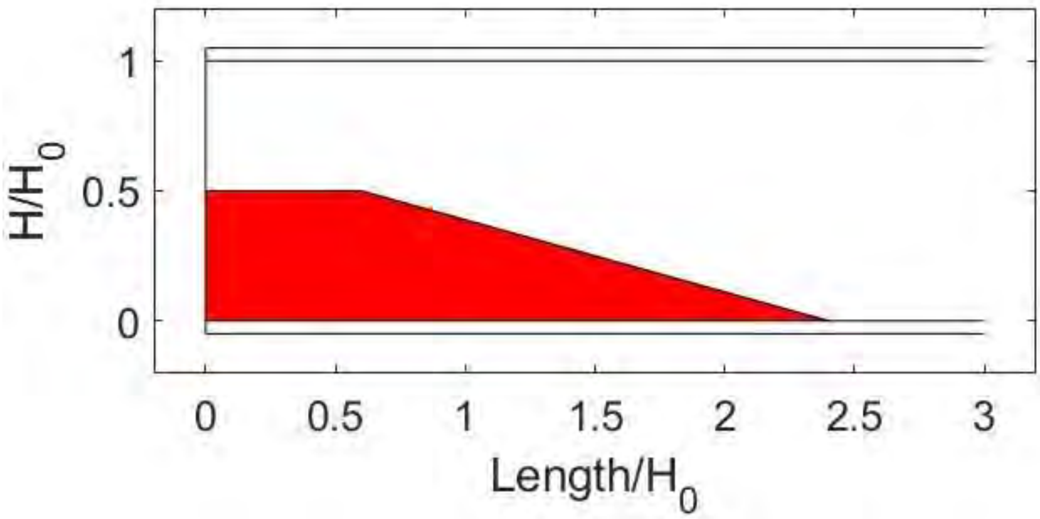

Figure 258: Extreme W2 web corrosion pattern for beams with a diaphragm - MassDOT

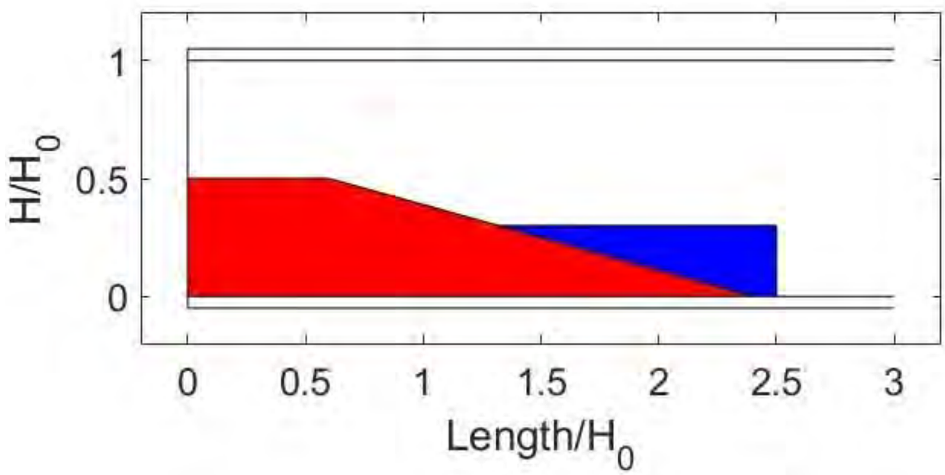

Figure 259: W2 extreme web corrosion scenario (with red color) projected over W1 CASE B extreme web corrosion scenario (with blue color) - MassDOT

The W1 corrosion pattern can be considered as a case of W2 with CL2 equal to zero here.

5.2.3.2. Flange Corrosion

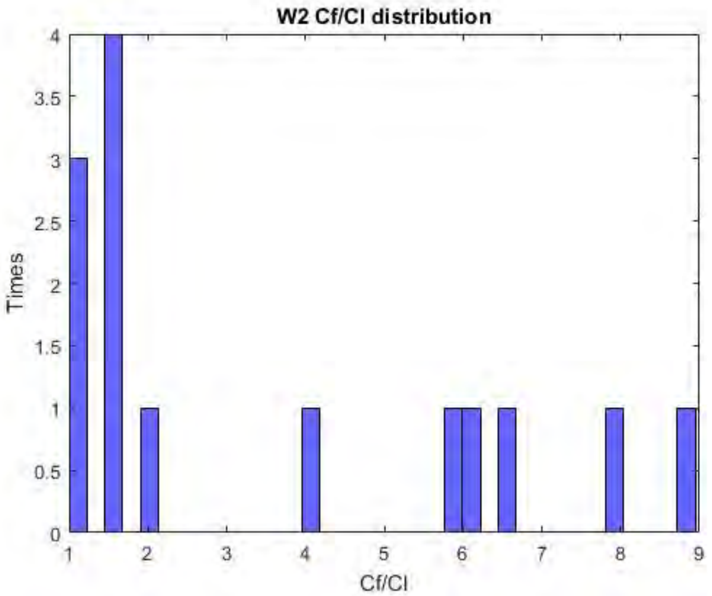

Figure 260: Ratio of flange to web corrosion length distribution of W2 web corrosion pattern corrosion for beams with a diaphragm - MassDOT

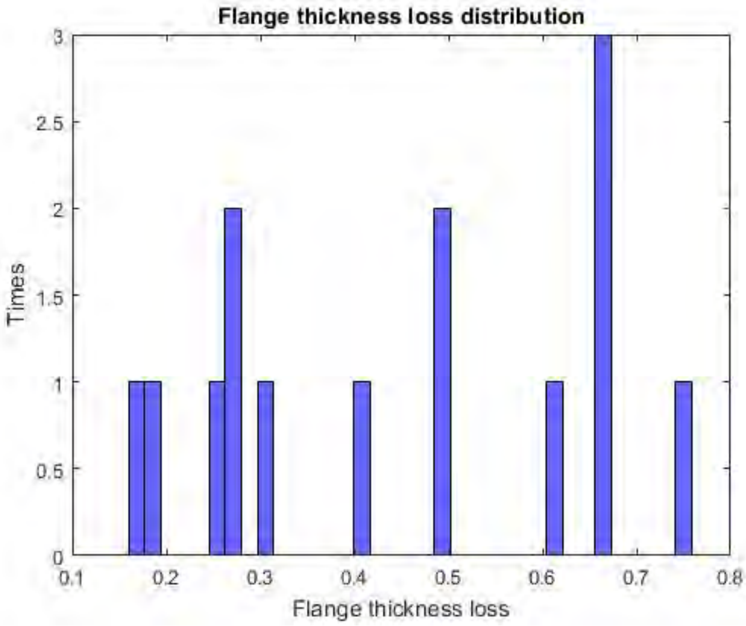

Figure 261: Max flange loss thickness distribution of W2 web corrosion pattern for beams without a diaphragm – MassDOT

5.2.3.3. Holes

Table 55: Holes for beams with a diaphragm – MassDOT

	Number	No hole	M1	M2	M3	M4	M12	M13	M24
W1	214	190	11	4	5	2	2	0	0
W2	47	41	1	4	0	0	1	0	0
W3	160	112	23	5	6	2	7	4	1
W4	16	13	1	2	0	0	0	0	0
W5	9	9	0	0	0	0	0	0	0
W6	0	0	0	0	0	0	0	0	0

According to the table above, the W2 corrosion pattern is combined once with the M1 hole corrosion pattern and 4 times with the M2 hole corrosion pattern. As it was already mentioned W2 and W1 will be combined and used as one pattern. Thus, for the M1 hole corrosion pattern our team checked if the dimensions of the unique hole belong in the range of the W1 pattern and M1 pattern combination. The unique hole with $a=0.089H_0$ and $b=0.31H_0$ satisfies the limits of Figure 100.

For M2 hole corrosion pattern, th+e sample for the W1 pattern was very small, so the team was not able to extract conclusions. This lead our team to process the M2 hole corrosion pattern for both W1 and W2 together:

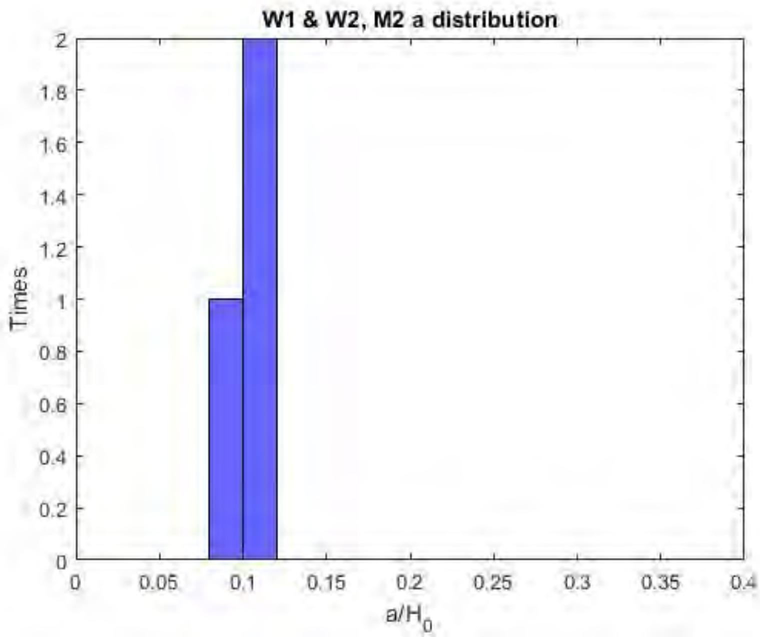

Figure 262: M2 web hole's pattern height distribution of W1 and W2 web corrosion patterns for beams with a diaphragm - MassDOT

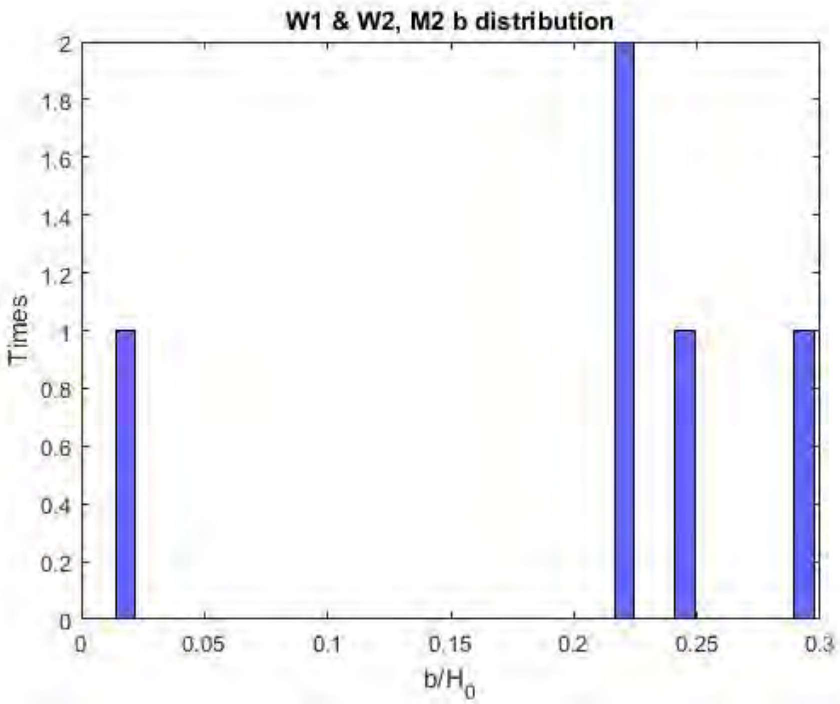

Figure 263: M2 web hole's pattern length distribution of W1 and W2 web corrosion patterns for beams with a diaphragm - MassDOT

Following this grouping, our team still found the sample to be very small (3 values for M2a, and 5 for M2b). We then assumed that M2 holes present thin and long 100% material loss areas underneath the diaphragm:

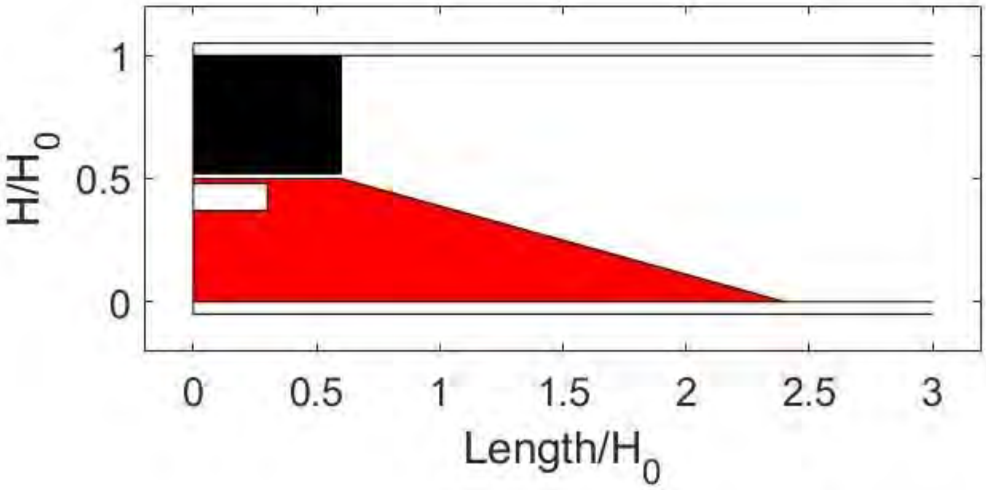

Figure 264: M2 hole pattern projected on the extreme W2 web corrosion pattern. With black color is illustrated the diaphragm that could be found with these patterns. The parameters are a<=0.11, and b<=0.3 - MassDOT

5.2.4. Pattern W3

5.2.4.1. Web Corrosion

The data analysis started with the CH2 distribution. The parameters for the corrosion patterns can be found with corresponding diagrams in Section 1.5 *Corrosion Patterns* of this report.

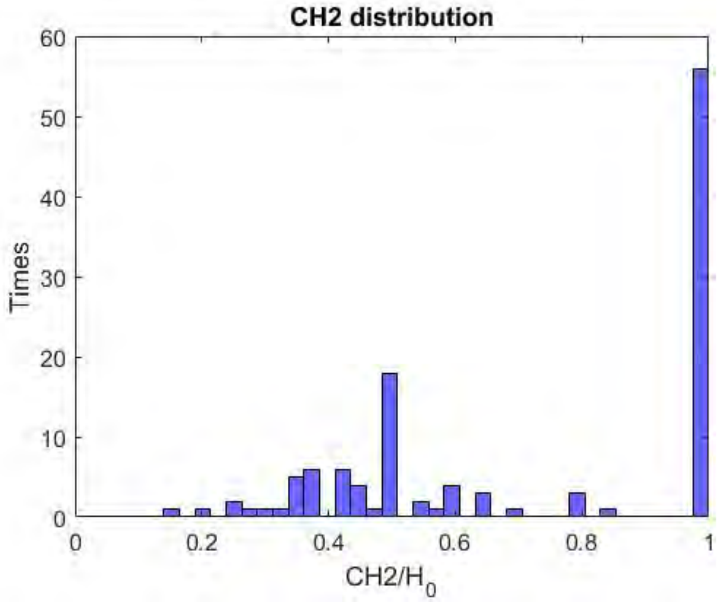

Figure 265. CH2 distribution of W3 web corrosion pattern for beams with a diaphragm - MassDOT

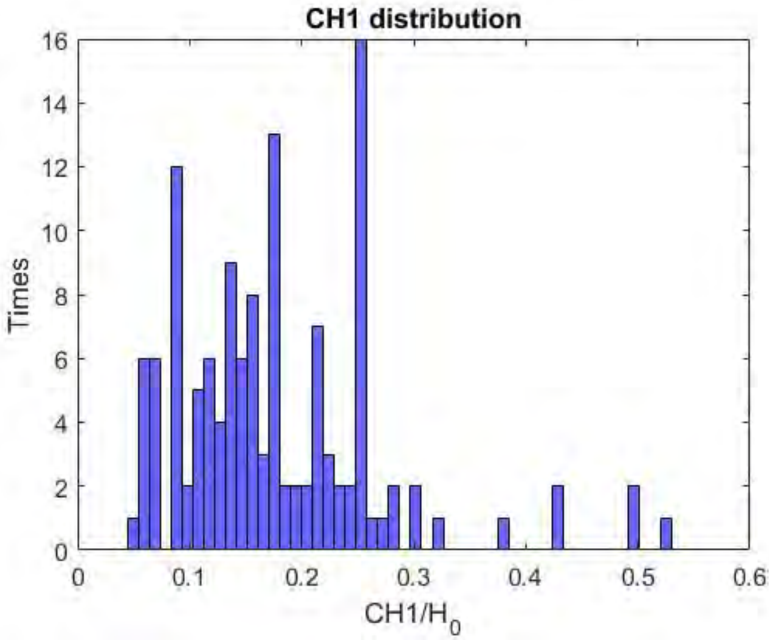

Figure 266: CH1 distribution of W3 web corrosion pattern for beams with a diaphragm - MassDOT

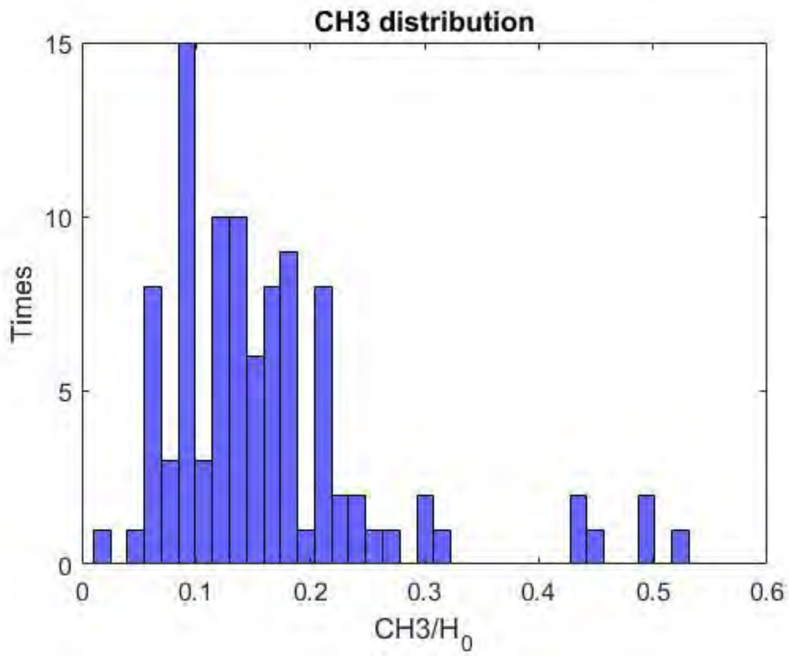

Figure 267: CH3 distribution of W3 web corrosion pattern for beams with a diaphragm - MassDOT

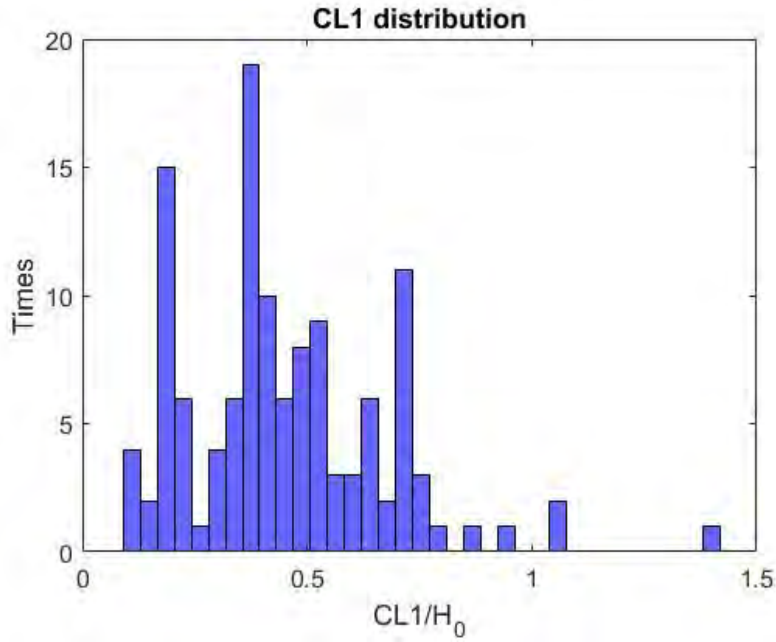

Figure 268: CL1 distribution of W3 web corrosion pattern for beams with a diaphragm - MassDOT

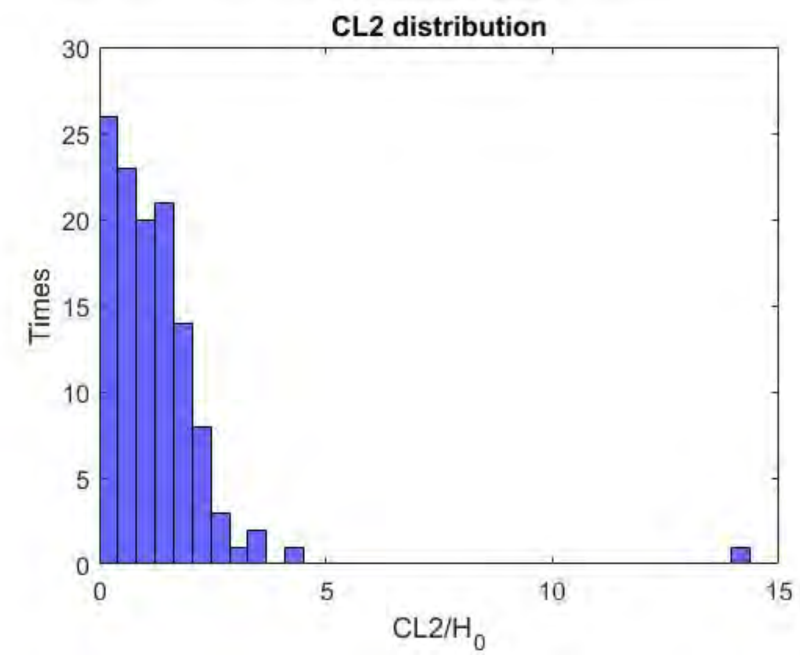

Figure 269: CL2 distribution of W3 web corrosion pattern for beams with a diaphragm - MassDOT

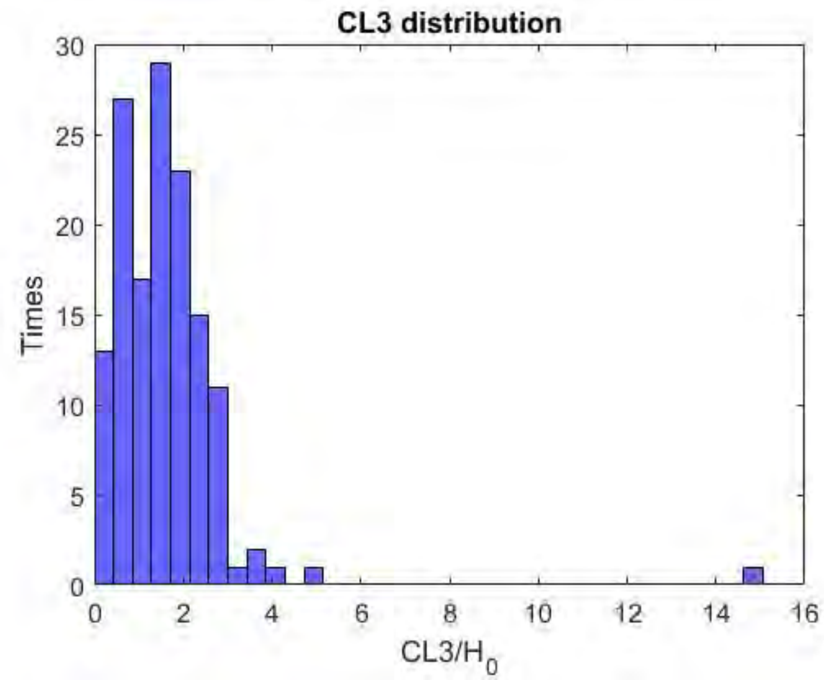

Figure 270: CL3 distribution of W3 web corrosion pattern for beams with a diaphragm - MassDOT

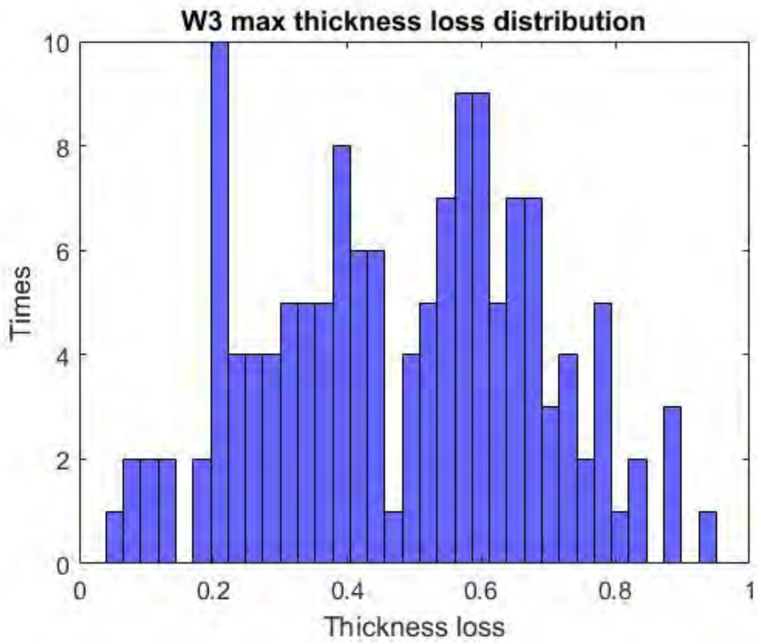

Figure 271: Ma web thickness loss distribution of W3 web corrosion pattern for beams with a diaphragm - MassDOT

From the CH2 histogram, two main trends are noticed, either a) full height corrosion, or b) corrosion up to 50% of H_0.

$$CH_2 = H_0 \; or \; 0 < CH_2 \leq 0.5H_0$$

For full height corrosion:

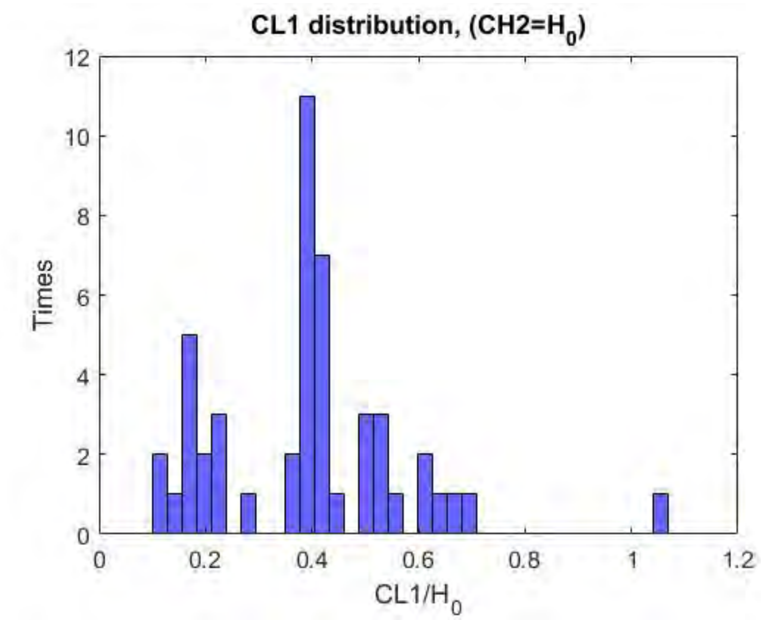

Figure 272: CL1 distribution of W3 web corrosion pattern with full height corrosion for beams with a diaphragm - MassDOT

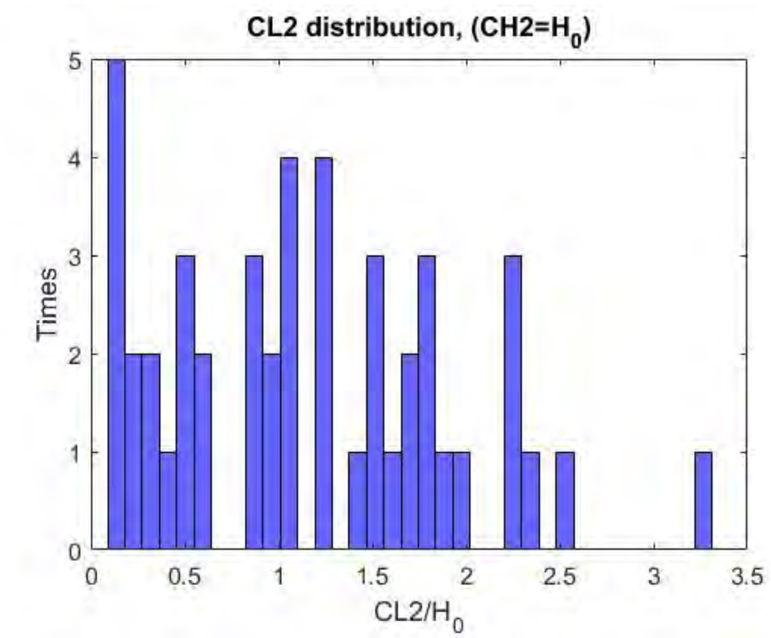

Figure 273: CL2 distribution of W3 web corrosion pattern with full height corrosion for beams with a diaphragm - MassDOT

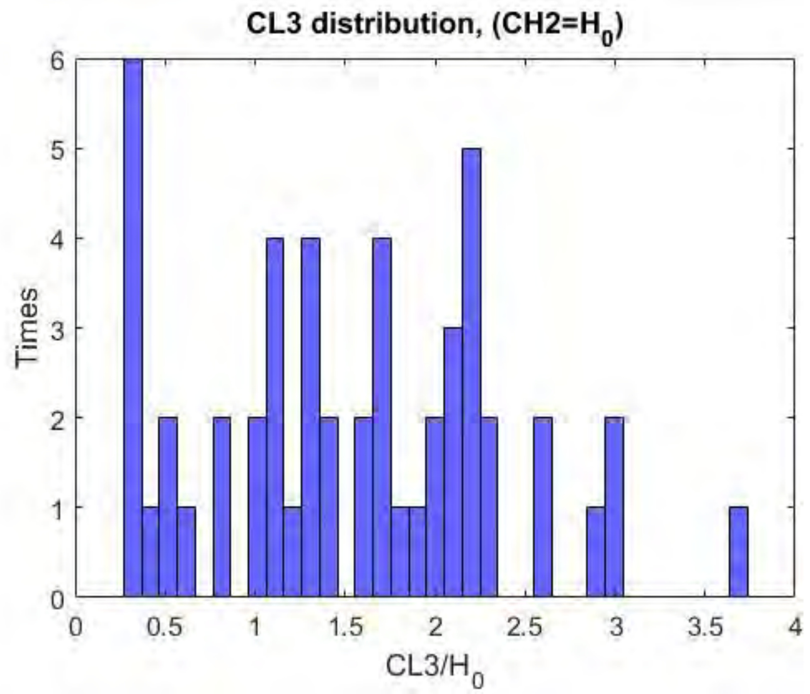

Figure 274: CL3 distribution of W3 web corrosion pattern with full height corrosion for beams with a diaphragm - MassDOT

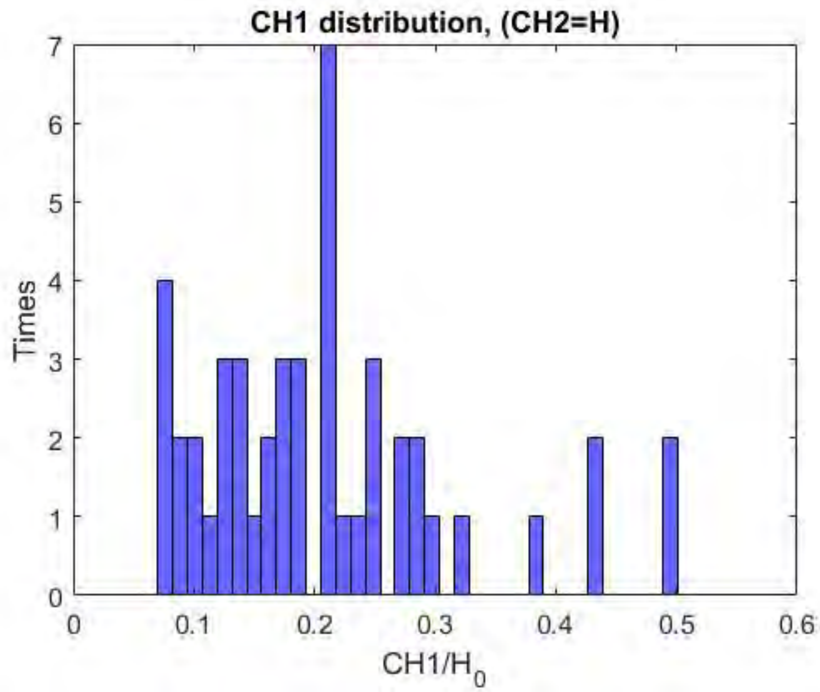

Figure 275: CH1 distribution of W3 web corrosion pattern with full height corrosion for beams with a diaphragm - MassDOT

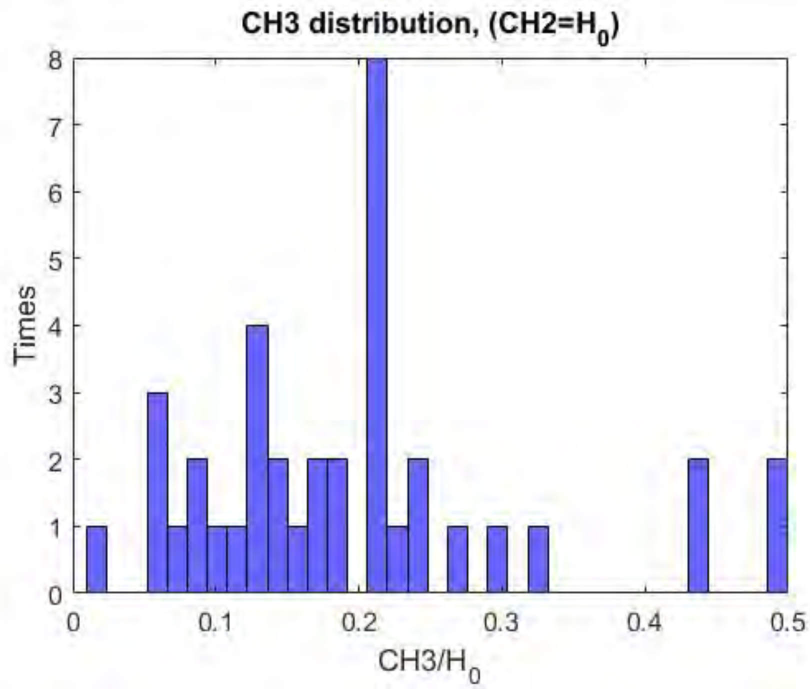

Figure 276: CH3 distribution of W3 web corrosion pattern with full height corrosion for beams with a diaphragm - MassDOT

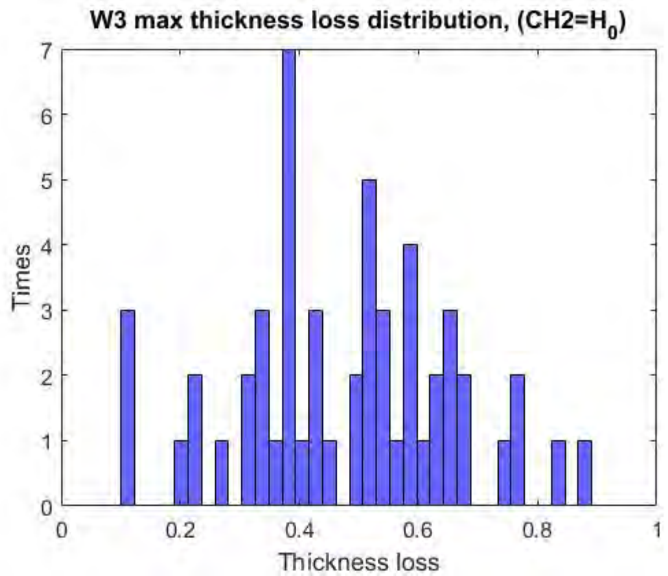

Figure 277: Max web thickness loss distribution of W3 web corrosion pattern with full height corrosion for beams with a diaphragm - MassDOT

From the CL3 histogram, two main trends were noticed:

$$0.25H_0 < CL_3 \leq 0.6H_0 \; and \; 0.6H_0 < CL_3 \leq 2.25H_0$$

For full height corrosion and $0.25H_0$< CL3 ≤ $0.6H_0$

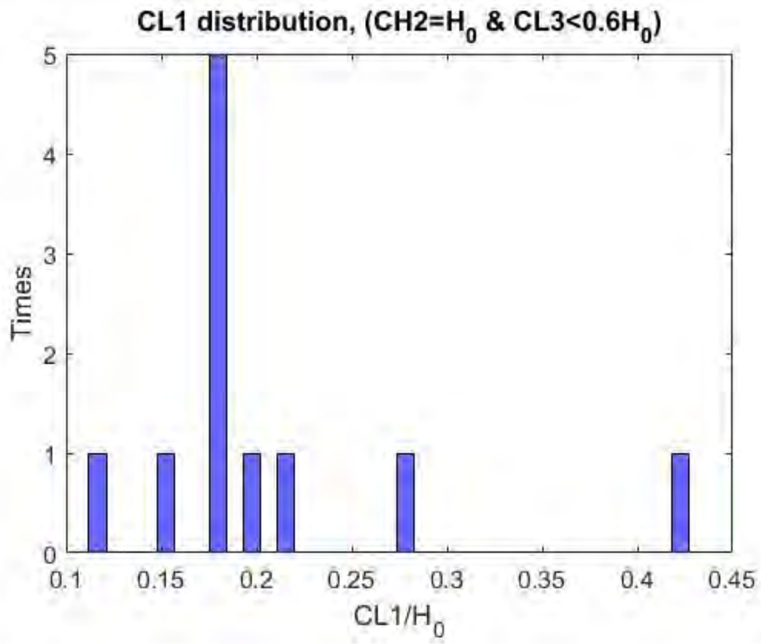

Figure 278: CL1 distribution of W3 web corrosion pattern with full height corrosion and deteriorated length up to 60% of H_0 for beams with a diaphragm - MassDOT

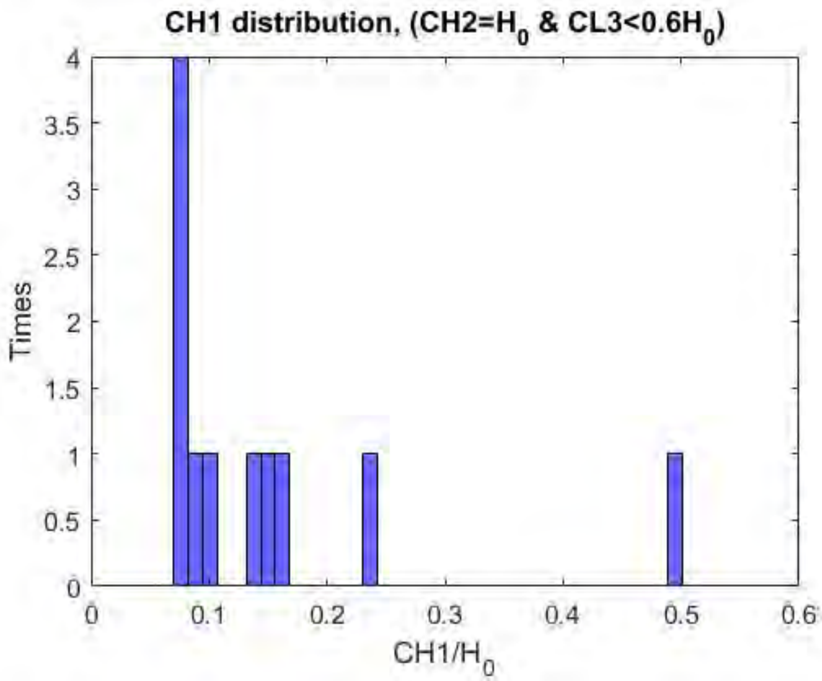

Figure 279: CH1 distribution of W3 web corrosion pattern with full height corrosion and deteriorated length up to 60% of H_0 for beams with a diaphragm - MassDOT

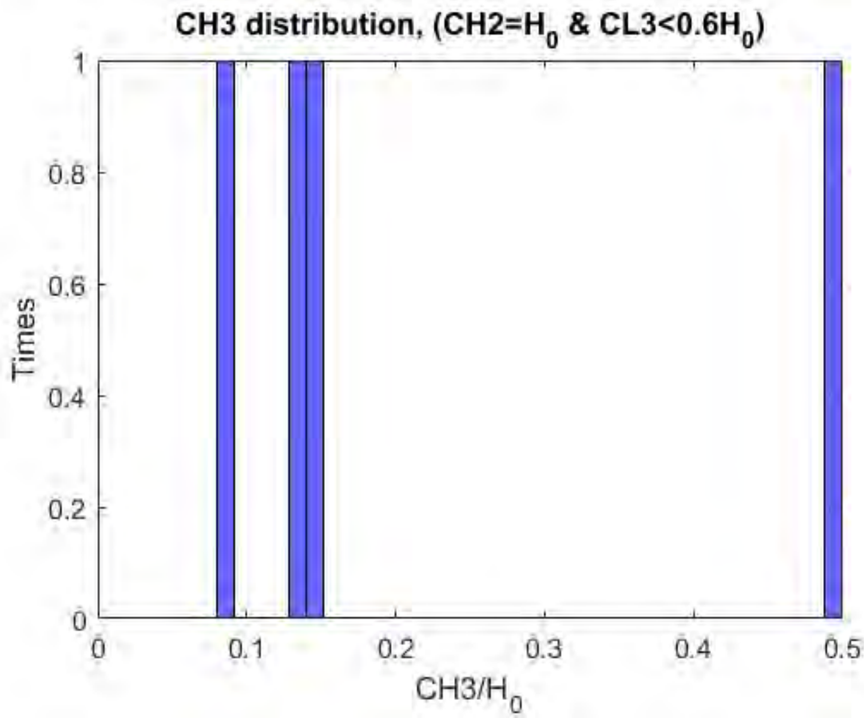

Figure 280: CH3 distribution of W3 web corrosion pattern with full height corrosion and deteriorated length up to 60% of H_0 for beams with diaphragm a - MassDOT

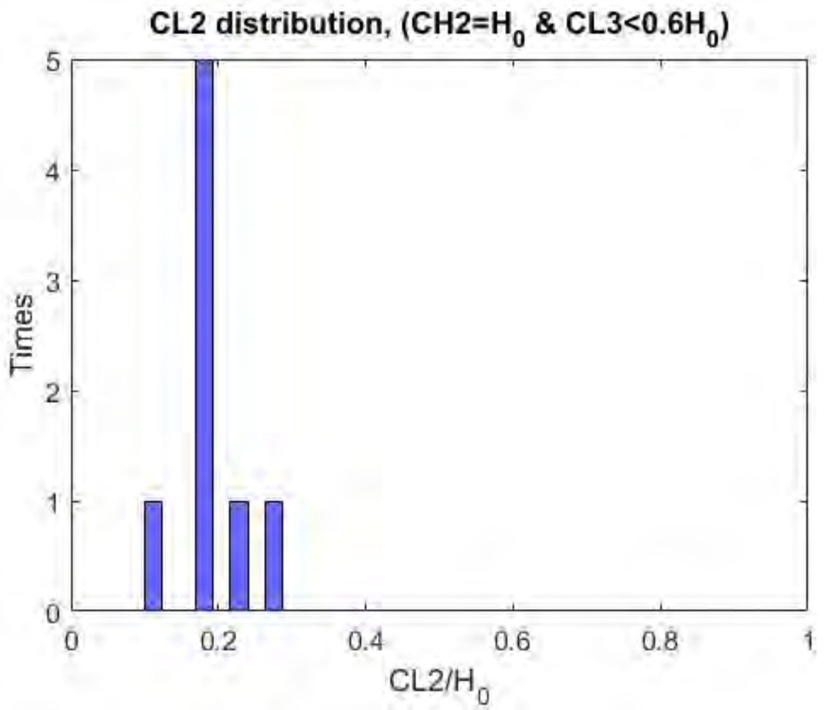

Figure 281: CL2 distribution of W3 web corrosion pattern with full height corrosion and deteriorated length up to 60% of H_0 for beams with a diaphragm - MassDOT

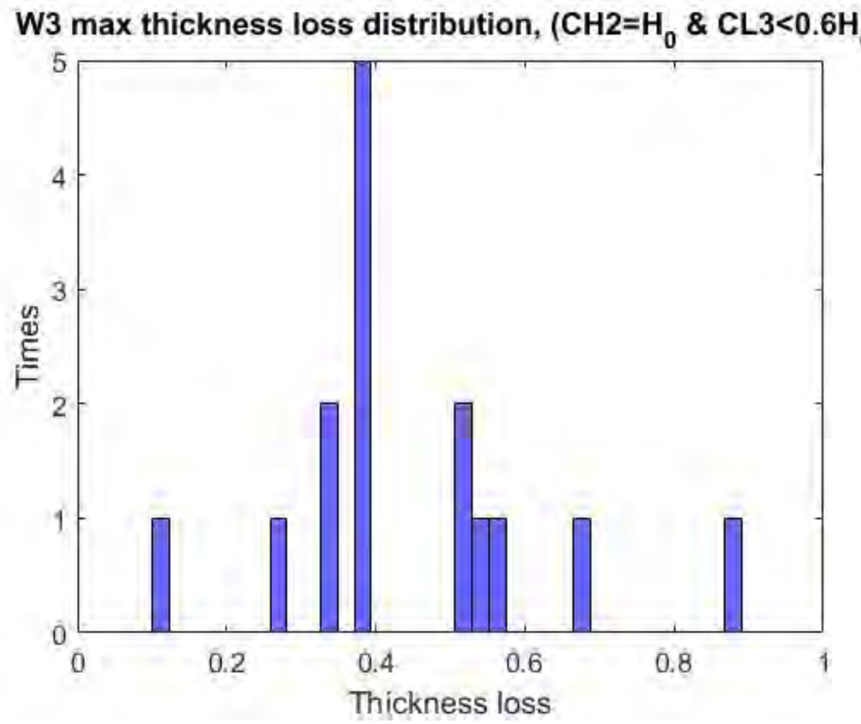

Figure 282: Max web thickness loss distribution, of W3 web corrosion pattern, with full height corrosion and deteriorated length up to 60% of H_0 for beams with a diaphragm - MassDOT

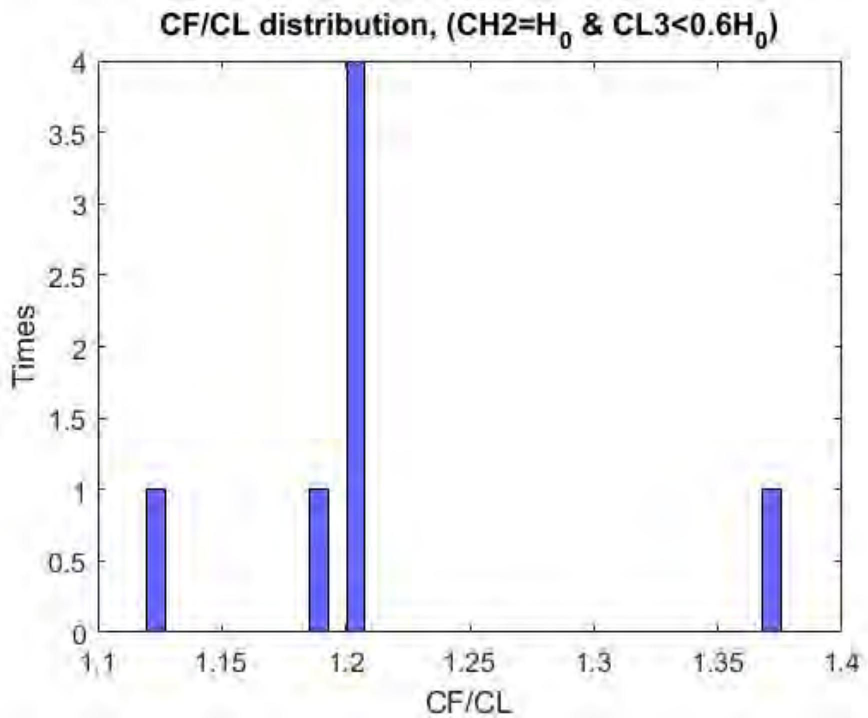

Figure 283: Ratio of flange to web corrosion length distribution, of W3 web corrosion pattern, with full height corrosion and deteriorated length up to 60% of H_0 for beams with a diaphragm - MassDOT

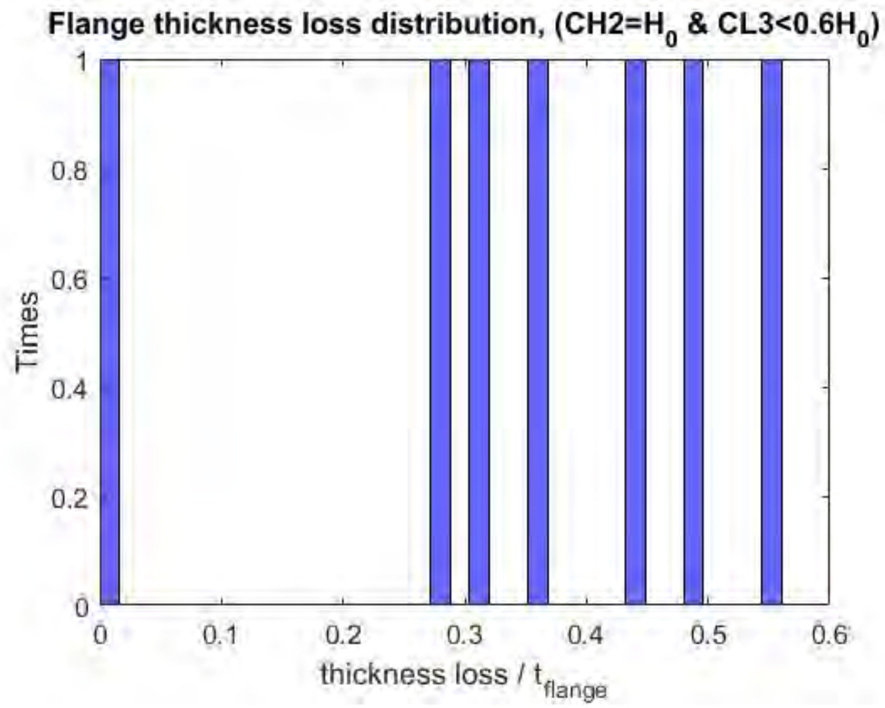

Figure 284: Max flange loss thickness distribution, for beams with W3 web corrosion pattern, with full height corrosion, deteriorated length up to 60% of H_0 and with a diaphragm - MassDOT

$$0.25H_0 < CL_3 \leq 0.6H_0$$

$$0.1H_0 < CL_1 \leq 0.2H_0$$

$$0.06H_0 < CH_1 = CH_3 \leq 0.16H_0$$

$$\frac{t_{loss}}{t_{web}} \ takes\ values\ of\ \{0.4, 0.6\}$$

$$\frac{Cf}{Cl} = 1.2 \text{ and}$$

$$\frac{t_{loss}}{t_{flange}} takes\ values\ of \{0.3, 0.6\}$$

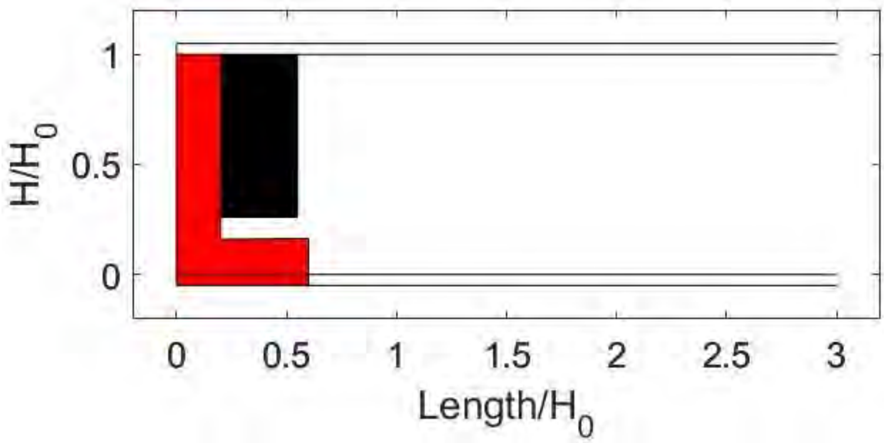

Figure 285: First extreme flange and W3 web corrosion scenario for beams with a diaphragm. - MassDOT

For full height corrosion and CL3<=2.3

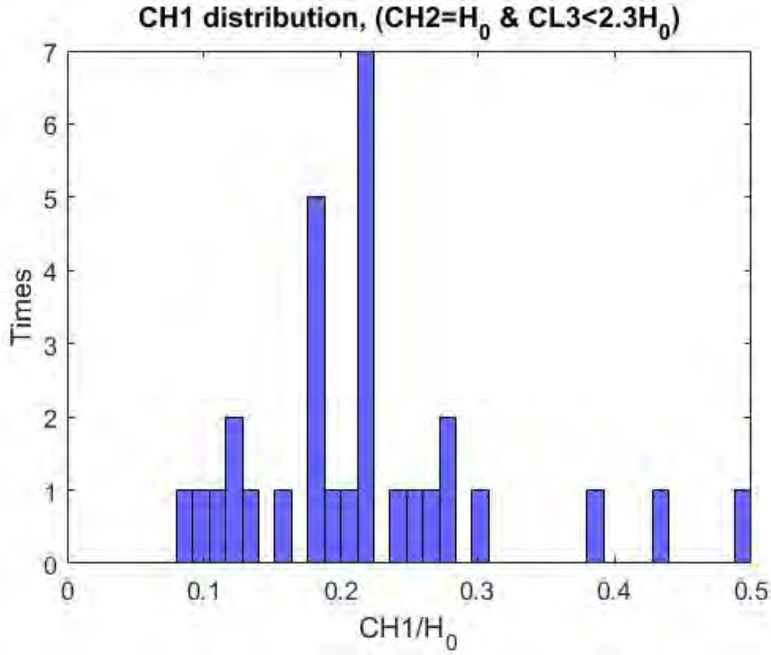

Figure 286: CH1 distribution of W3 web corrosion pattern, with full height corrosion and deteriorated length up to 230% of H_0, for beams with a diaphragm - MassDOT

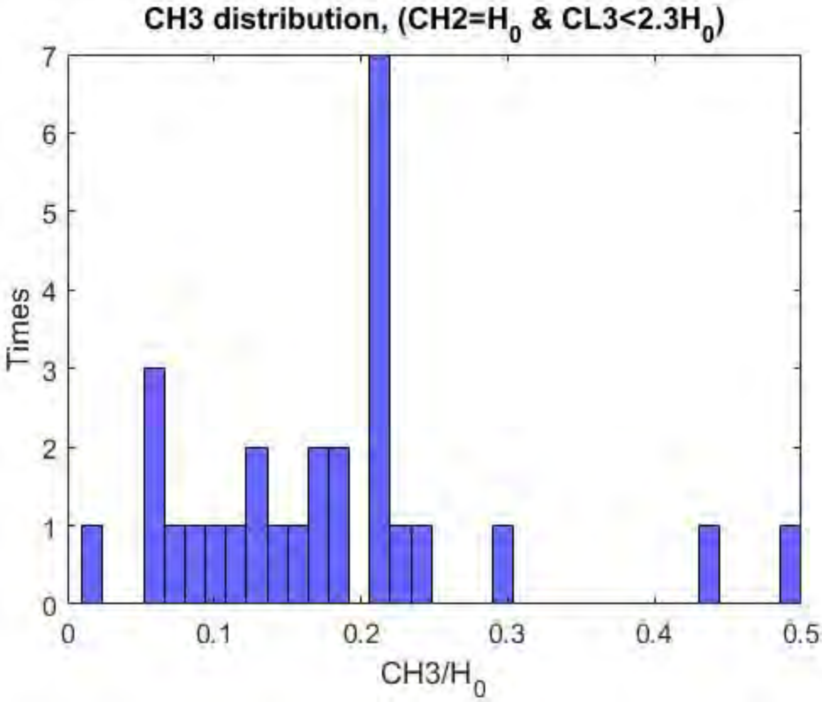

Figure 287: CH3 distribution of W3 web corrosion pattern, with full height corrosion and deteriorated length up to 230% of H_0, for beams with a diaphragm - MassDOT

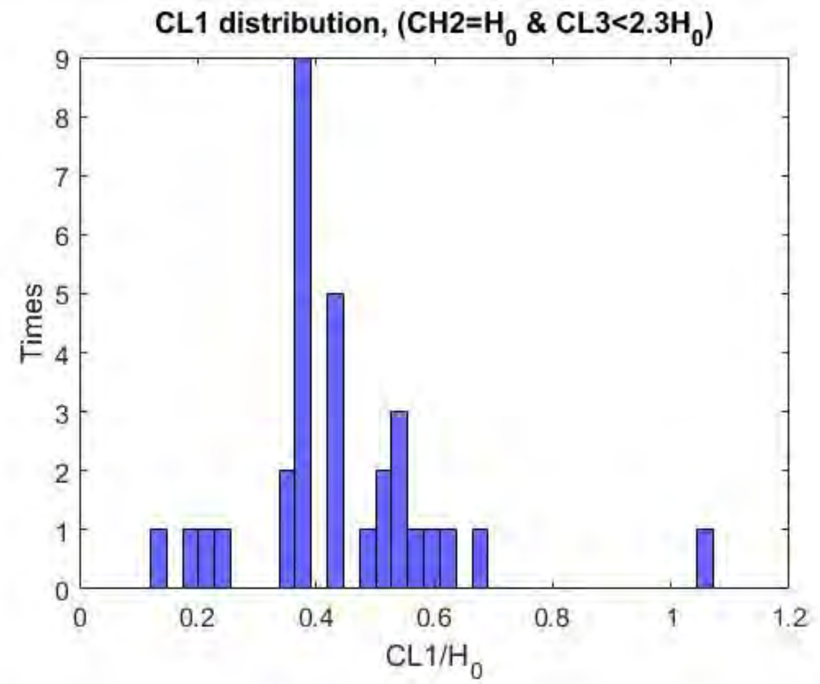

Figure 288: CL1 distribution of W3 web corrosion pattern, with full height corrosion and deteriorated length up to 230% of H_0, for beams with a diaphragm - MassDOT

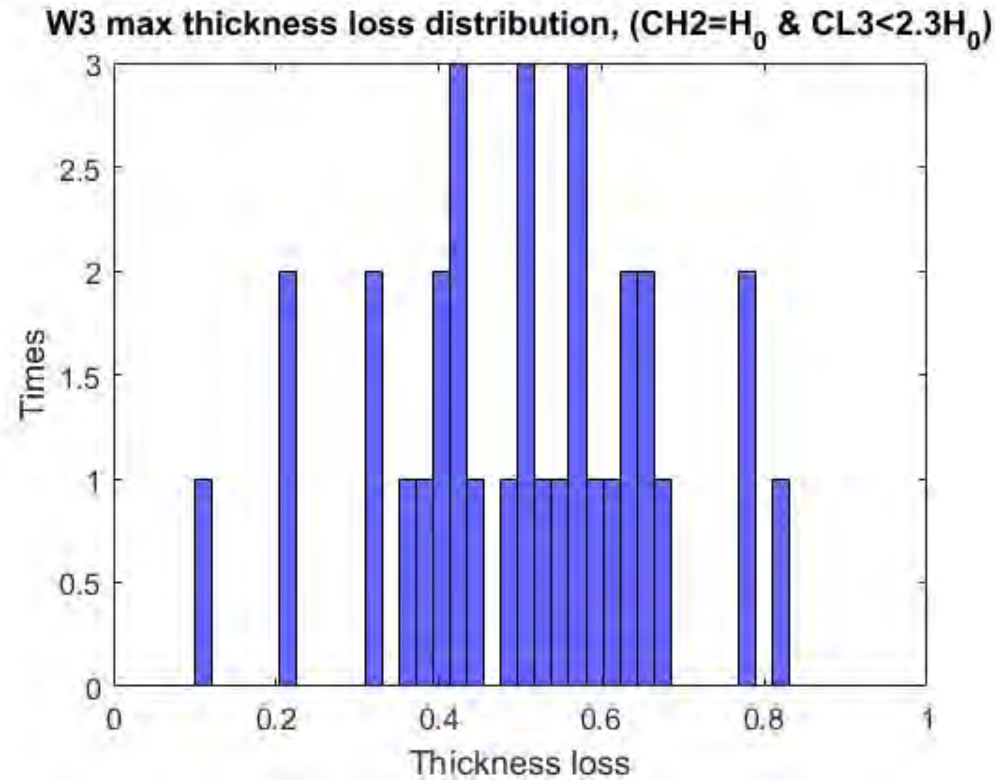

Figure 289: Max web thickness loss distribution, of W3 web corrosion pattern, with full height corrosion and deteriorated length up to 230% of H_0, for beams with a diaphragm - MassDOT

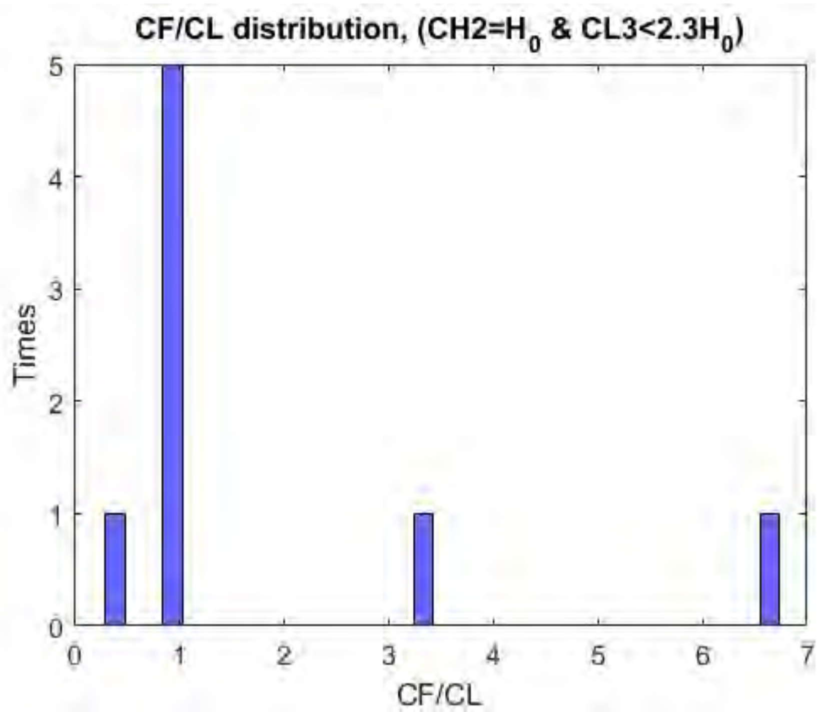

Figure 290: Ratio of flange to web corrosion length distribution, of W3 web corrosion pattern, with full height corrosion and deteriorated length up to 230% of H_0 for beams with a diaphragm - MassDOT

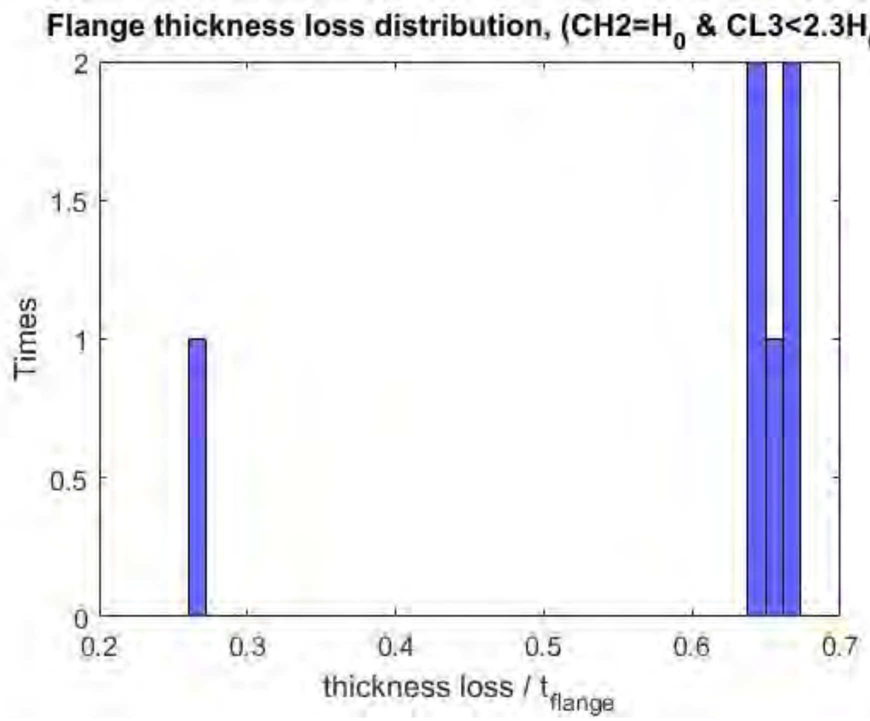

Figure 291: Max flange loss thickness distribution, for beams with W3 web corrosion pattern, with full height corrosion, deteriorated length up to 230% of H_0 and with a diaphragm - MassDOT

$$0.6H_0 < CL_3 \leq 2.3H_0$$

$$0.2H_0 < CL_1 \leq 0.6H_0$$

$$0.05H_0 < CH_1 = CH_3 \leq 0.30H_0$$

$$\frac{t_{loss}}{t_{web}}\,takes\ the\ values\ of\ \{0.4, 0.6, 0.8\}$$

$$\frac{Cf}{Cl} = 1 \text{ and}$$

$$\frac{t_{loss}}{t_{flange}}\,takes\ the\ value\ of\ \{0.65\}$$

Below depicts the second extreme corrosion scenario for the flange and W3 corrosion pattern combination.

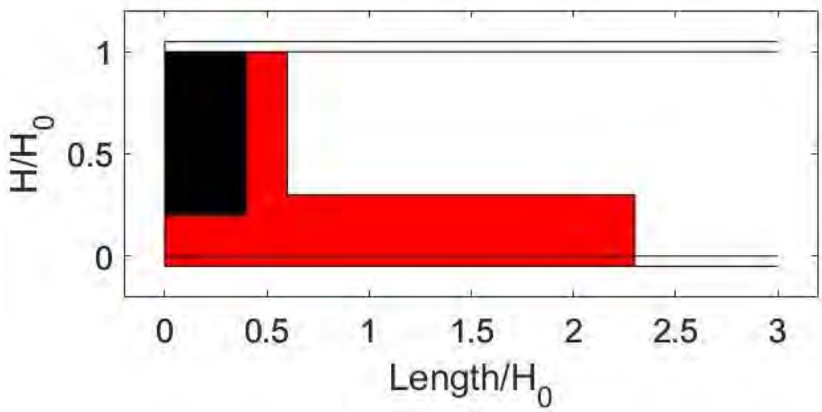

Figure 292: Second extreme flange and W3 web corrosion scenario for beams with a diaphragm - MassDOT

For height <=$0.5H_0$

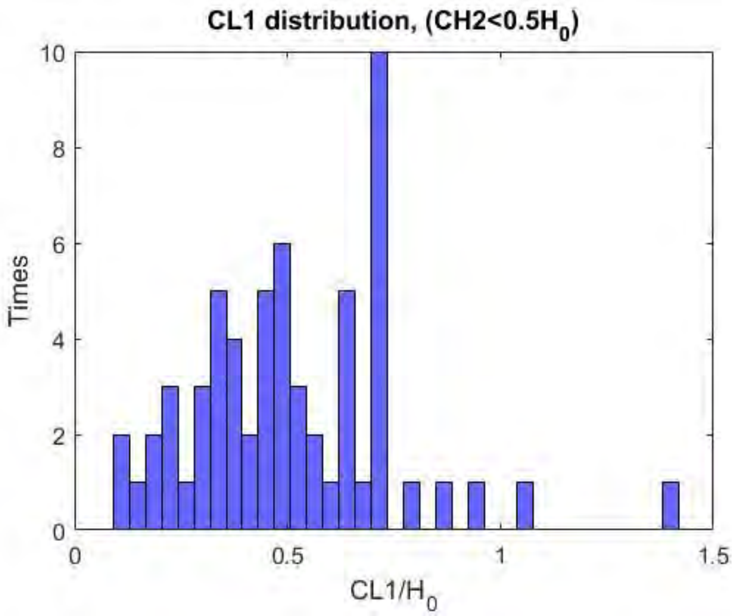

Figure 293: CL1 distribution of W3 web corrosion pattern, with corrosion height up to 50% of H_0, for beams with a diaphragm - MassDOT

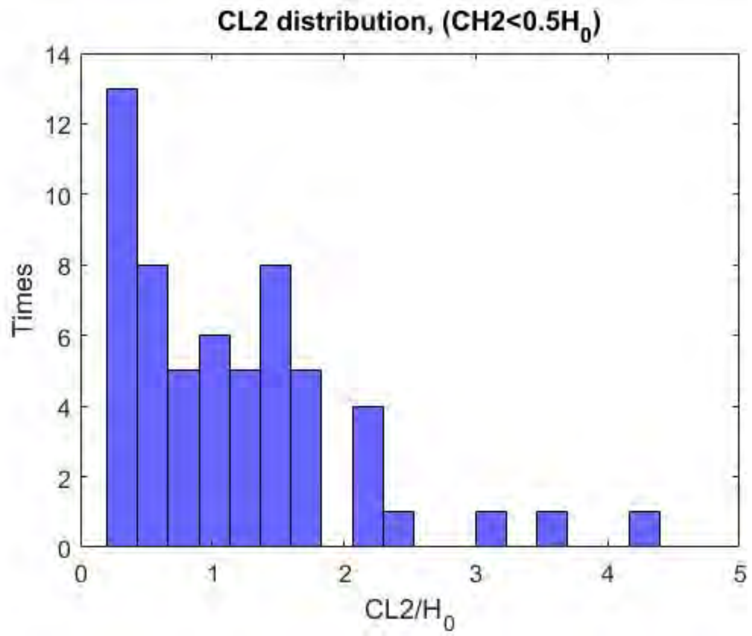

Figure 294: CL2 distribution of W3 web corrosion pattern, with corrosion height up to 50% of H_0, for beams with a diaphragm - MassDOT

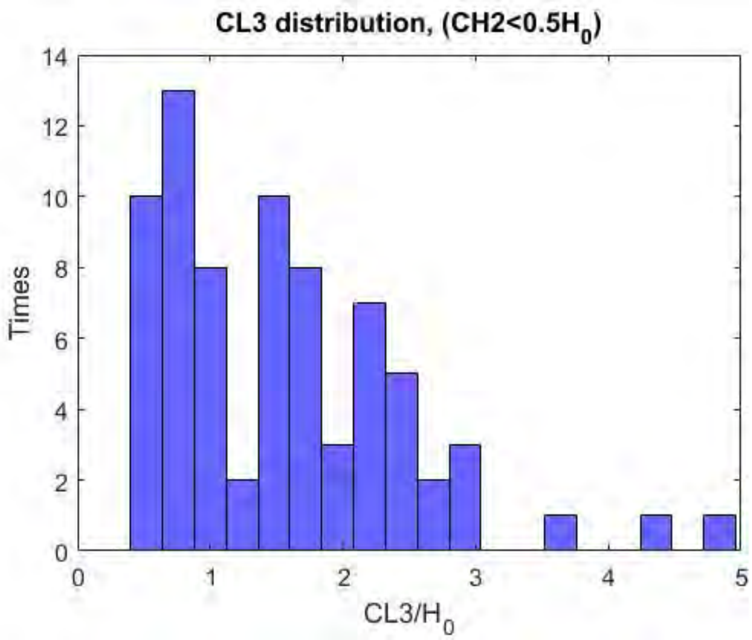

Figure 295: CL3 distribution of W3 web corrosion pattern, with corrosion height up to 50% of H_0, for beams with a diaphragm - MassDOT

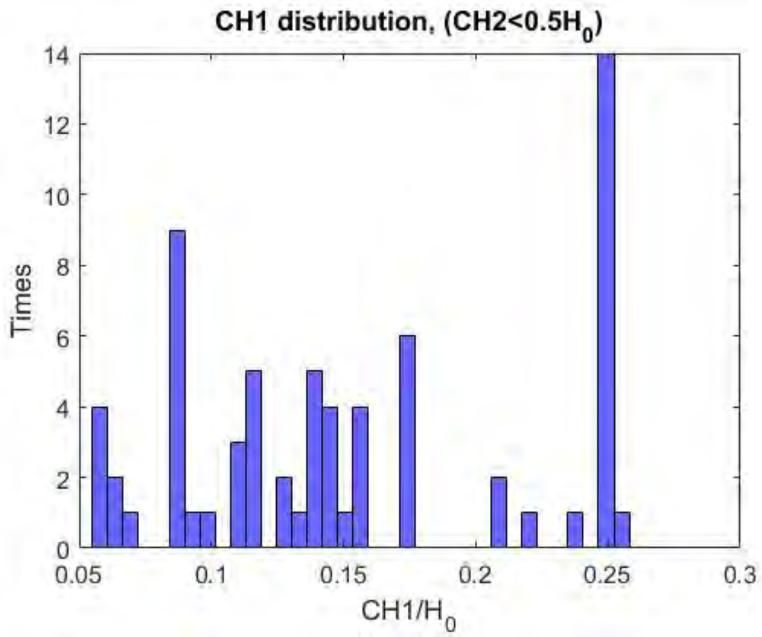

Figure 296: CH1 distribution of W3 web corrosion pattern, with corrosion height up to 50% of H_0, for beams with a diaphragm - MassDOT

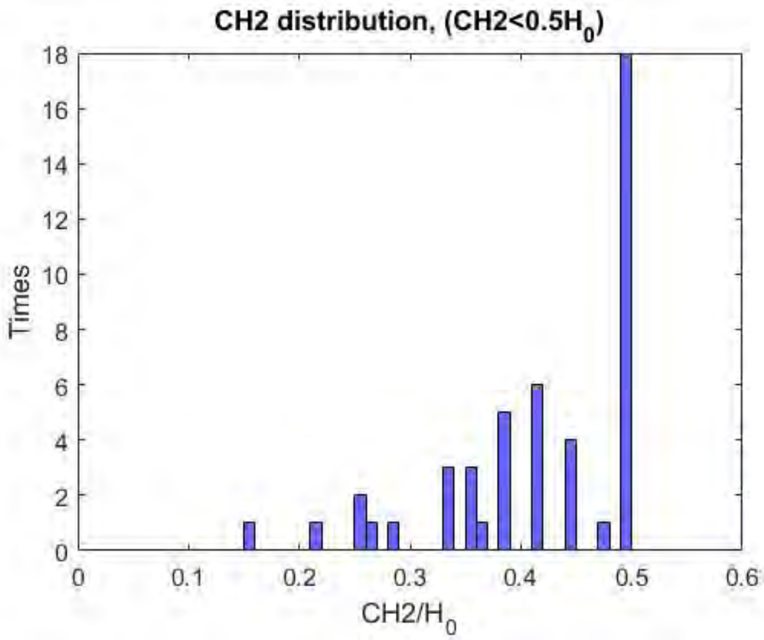

Figure 297: CH2 distribution of W3 web corrosion pattern, with corrosion height up to 50% of H_0, for beams with a diaphragm - MassDOT

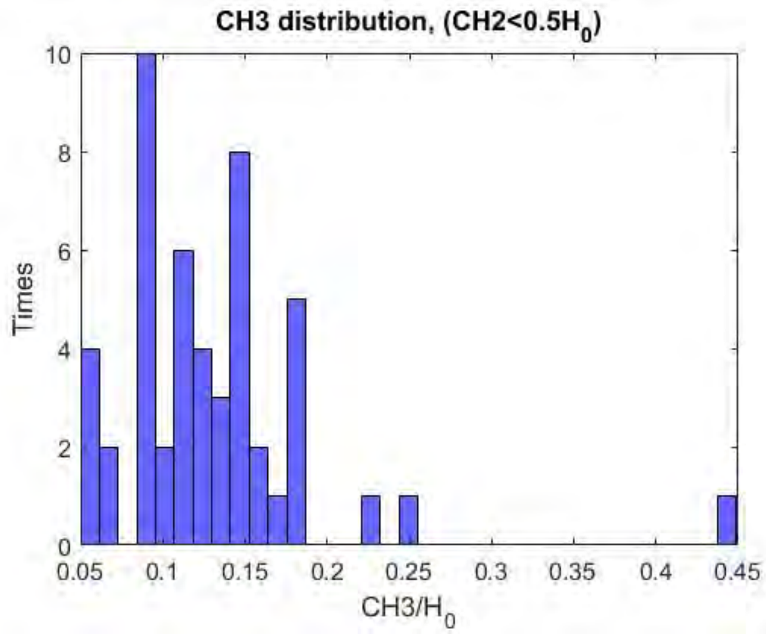

Figure 298: CH3 distribution of W3 web corrosion pattern, with corrosion height up to 50% of H_0, for beams with a diaphragm - MassDOT

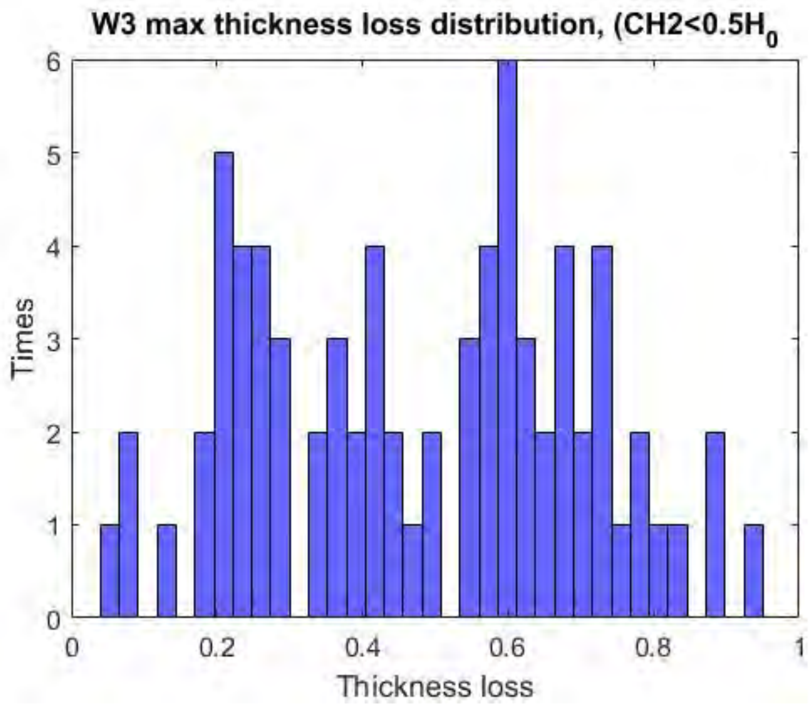

Figure 299: Max web thickness loss distribution of W3 web corrosion pattern, with corrosion height up to 50% of H_0, for beams with a diaphragm - MassDOT

5.2.4.2. Flange Corrosion

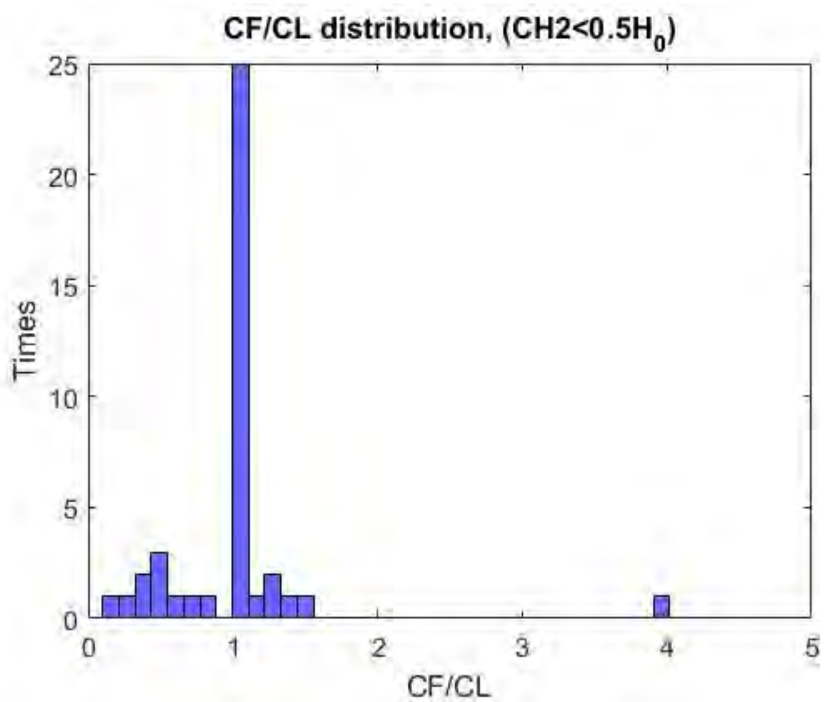

Figure 300: Ratio of flange to web corrosion length distribution, of W3 web corrosion pattern, with corrosion height up to 50% of H_0, for beams with a diaphragm - MassDOT

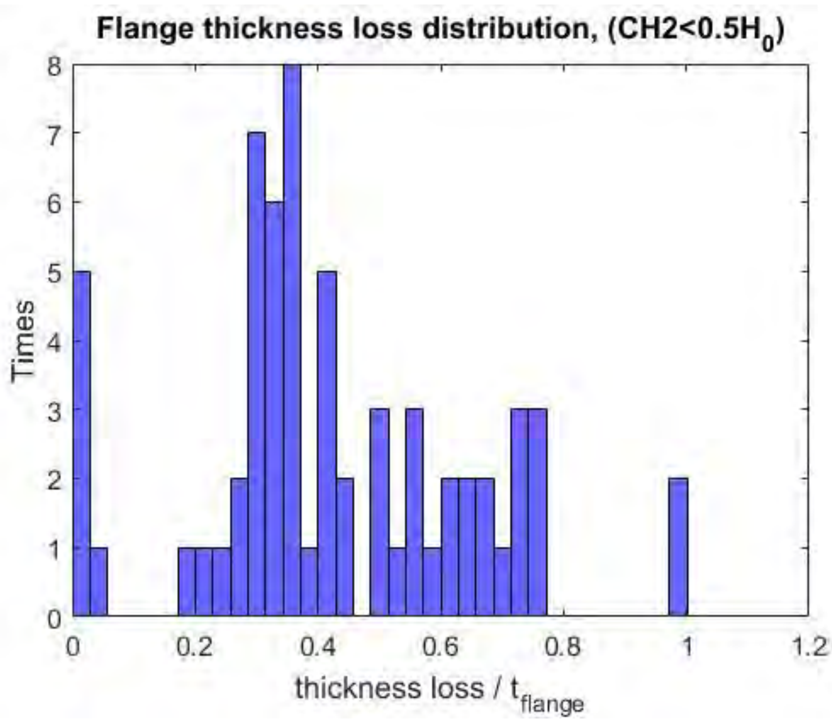

Figure 301: Max flange loss thickness distribution, for beams with W3 web corrosion pattern, with corrosion height up to 50% of H_0, for beams with a diaphragm - MassDOT

$$0.5H_0 < CL_3 \leq 3H_0$$

$$0.1H_0 < CL_1 \leq 0.75H_0$$

$$0.05H_0 < CH_1 \leq 0.25H_0$$

$$0.05H_0 < CH_3 \leq 0.18H_0$$

$$\frac{t_{loss}}{t_{web}}\, takes\ the\ values\ of\ \{0.4, 0.6, 0.8\}$$

$$\frac{Cf}{Cl} = 1 \text{ and}$$

$$\frac{t_{loss}}{t_{flange}}\, takes\ the\ values\ of\ \{\ 0.3, 0.6, 0.8\}$$

Below depicts the third extreme corrosion scenario for the flange and W3 corrosion pattern combination.

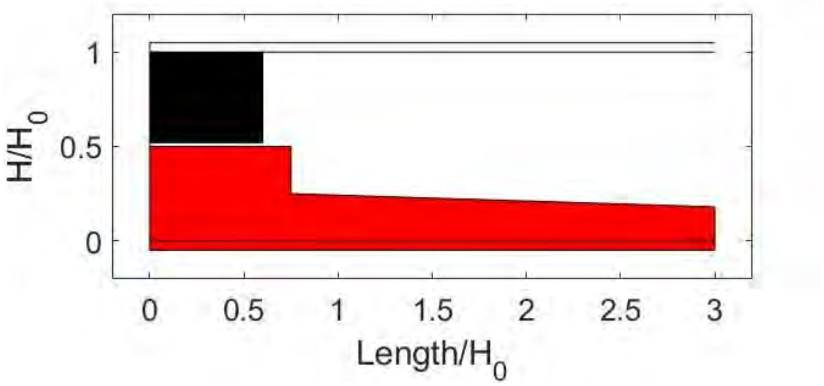

Figure 302: Third extreme flange and W3 web corrosion scenario for beams with a diaphragm - MassDOT

5.2.4.3. Holes

Below, the histogram describes the distribution of holes dimensions for the M1 hole corrosion pattern.

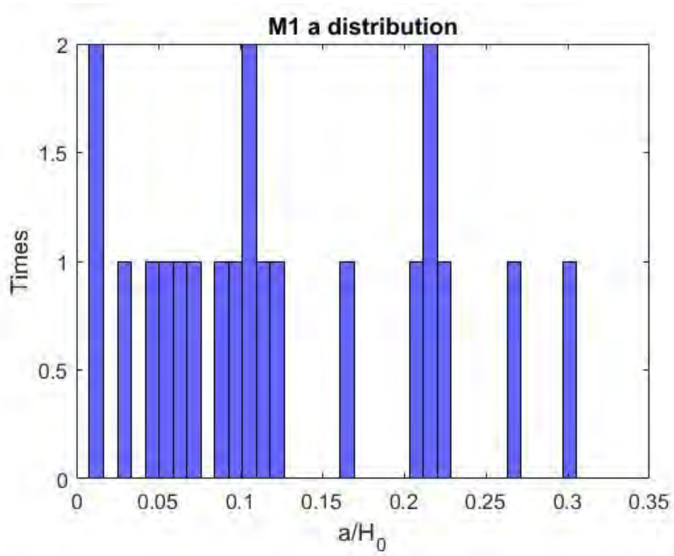

Figure 303: M1 web hole’s pattern height distribution of W3 web corrosion pattern for beams with a diaphragm - MassDOT

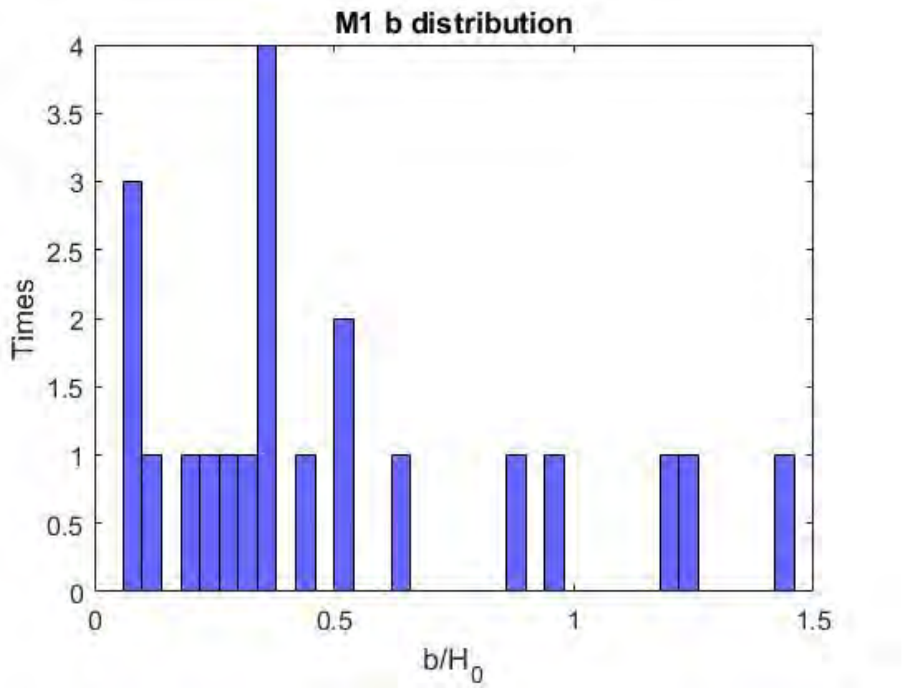

Figure 304: M1 web hole's pattern length distribution of W3 web corrosion pattern for beams with a diaphragm - MassDOT

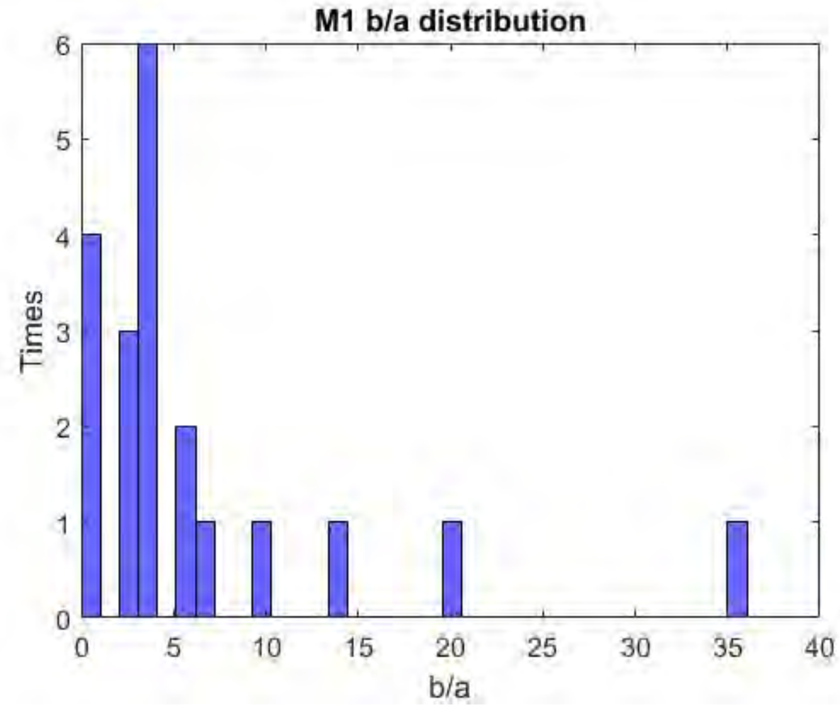

Figure 305: M1 web hole's ratio length to height distribution of W3 web corrosion pattern for beams with a diaphragm - MassDOT

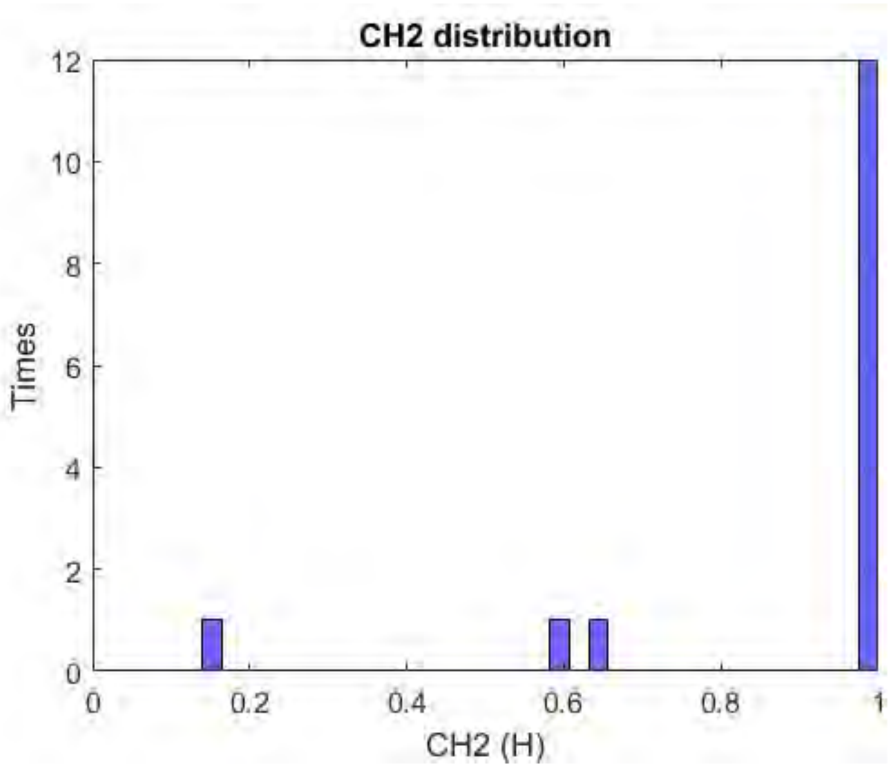

Figure 306: Max corrosion height distribution of W3 pattern with M1 hole, for beams with a diaphragm - MassDOT

From the figure above, it was noticed that holes appear mainly at the full height of the corroded web. The holes observed seem to be mainly thin and long across the web. From Figure 305, most of the cases have ratio of hole's length to height up to 6. From Figure 304, the hole length is up to 50% of H_o. Thus, for the extreme corrosion hole scenario, the hole's height is considered as 0.083.

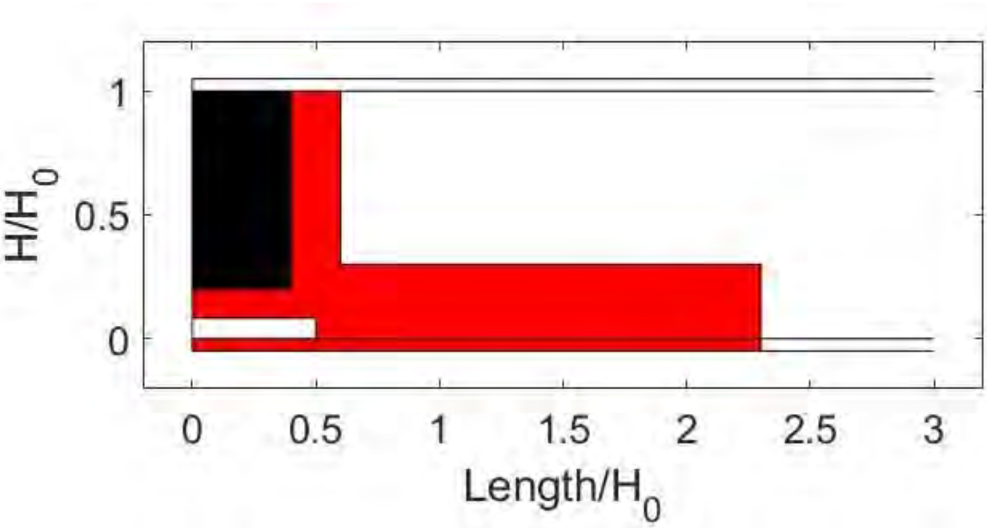

Figure 307: M1 hole pattern projected on the second extreme W3 web corrosion pattern scenario. With black color is illustrated the diaphragm that could be found with these patterns - MassDOT

5.2.5. Pattern W4

The parameters for the corrosion patterns can be found with corresponding diagrams in Section 1.5 *Corrosion Patterns* of this report.

5.2.5.1. Web Corrosion

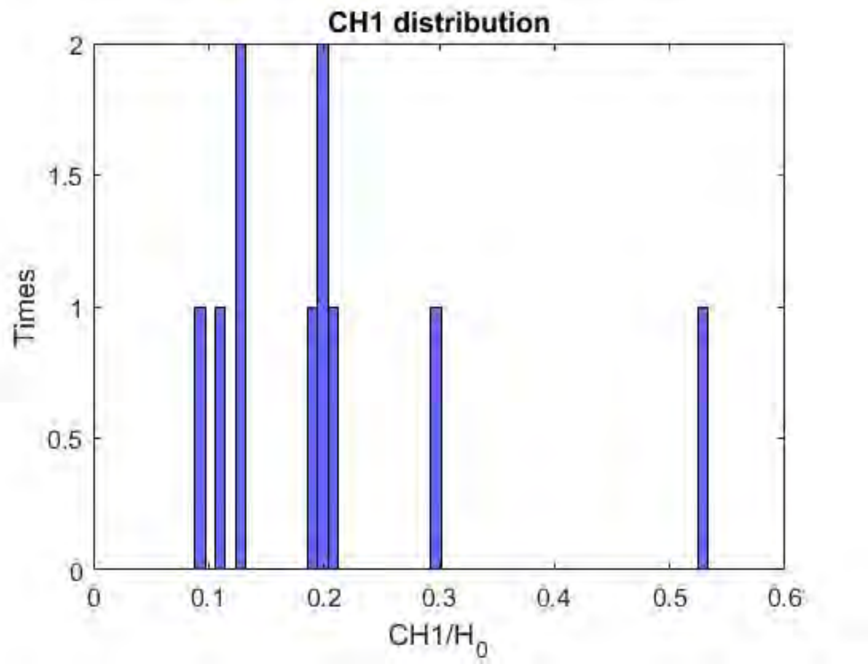

Figure 308: CH1 distribution of W4 web corrosion pattern for beams with a diaphragm - MassDOT

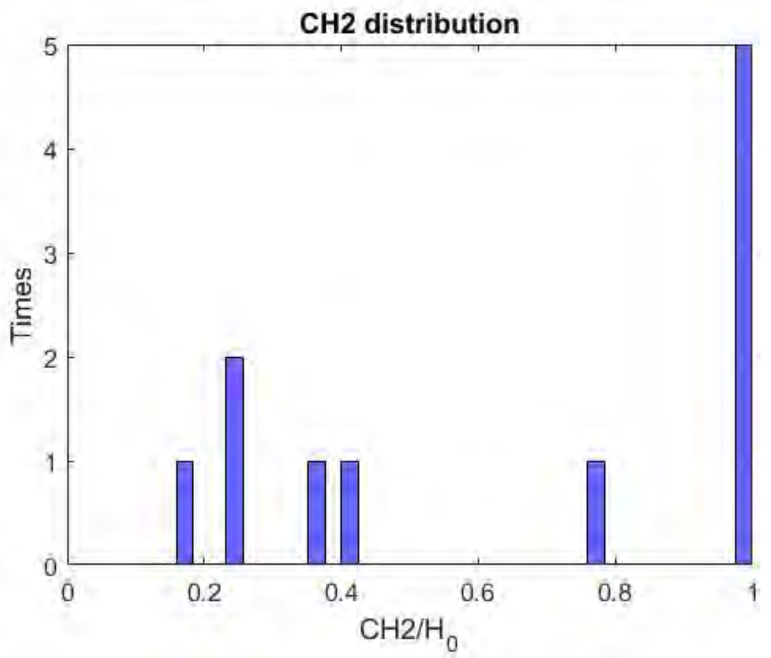

Figure 309: CH2 distribution of W4 web corrosion pattern for beams with a diaphragm - MassDOT

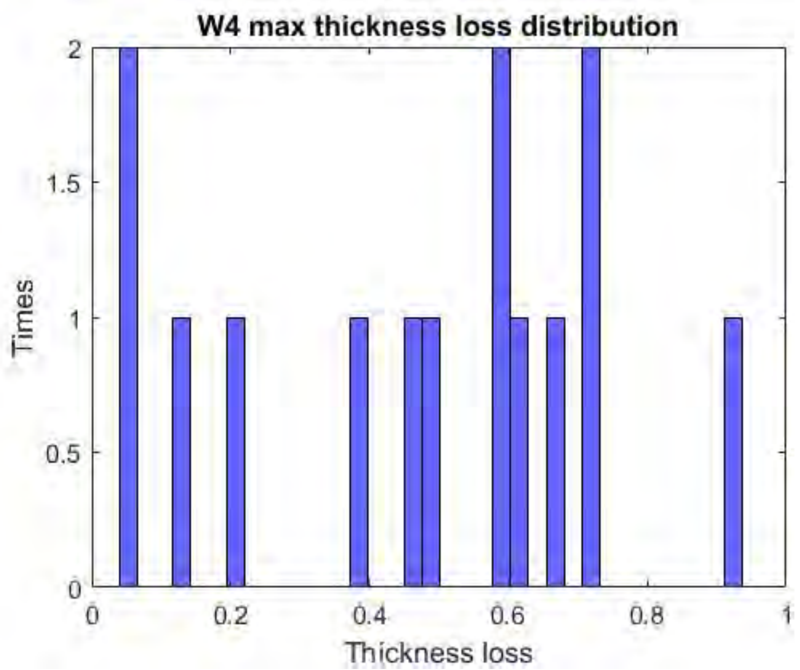

Figure 310: Max web thickness loss distribution of W4 web corrosion pattern for beams with a diaphragm - MassDOT

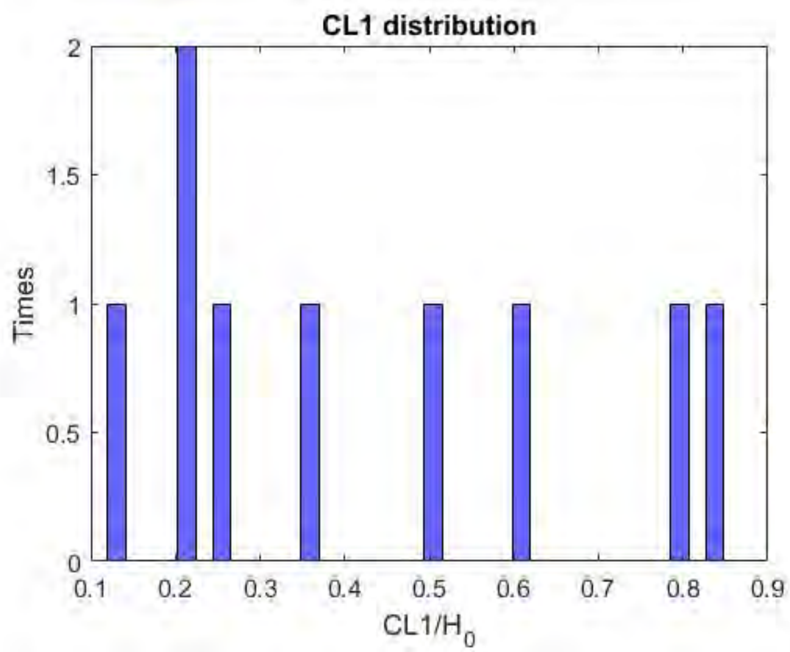

Figure 311: CL1 distribution of W4 web corrosion pattern for beams with a diaphragm - MassDOT

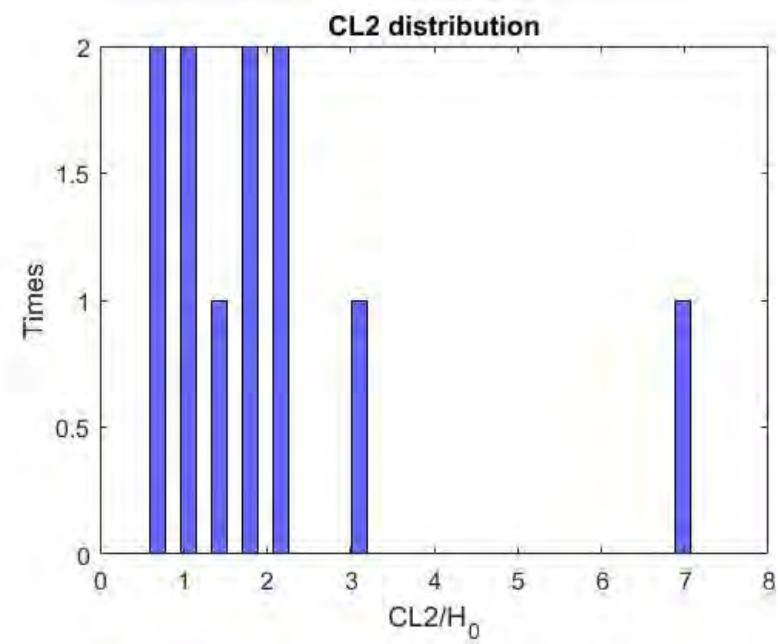

Figure 312: CL2 distribution of W4 web corrosion pattern for beams with a diaphragm - MassDOT

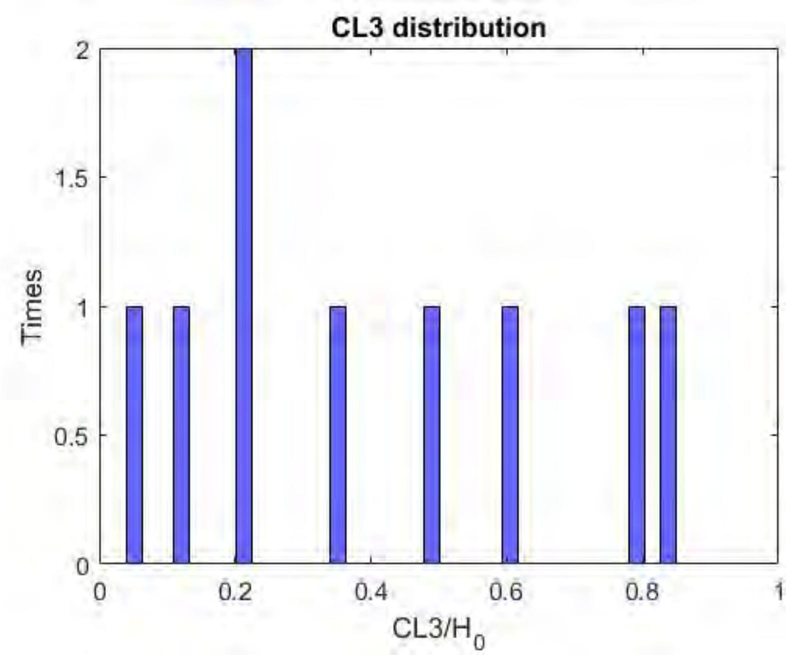

Figure 313: CL3 distribution of W4 web corrosion pattern for beams with a diaphragm - MassDOT

Like in W3 patterns there are observed two trends a) full height corrosion and b) up to 40%H_o. For full height corrosion:

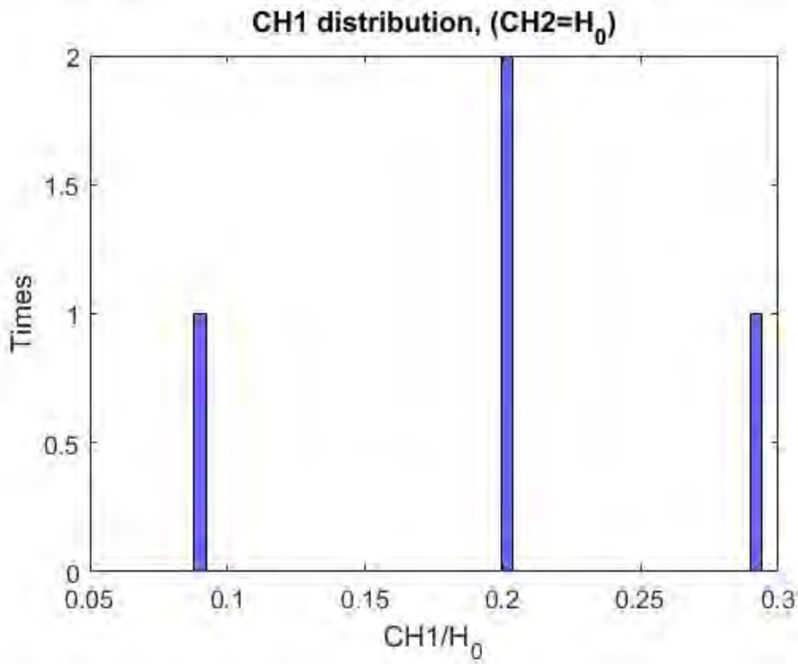

Figure 314: CH1 distribution of W4 web corrosion pattern with full height corrosion for beams with a diaphragm - MassDOT

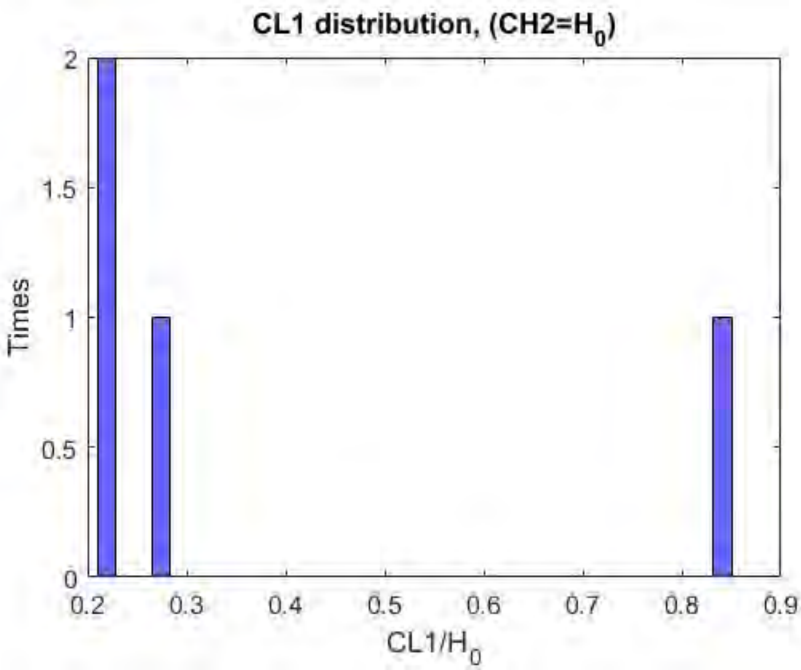

Figure 315: CL1 distribution of W4 web corrosion pattern with full height corrosion for beams with a diaphragm - MassDOT

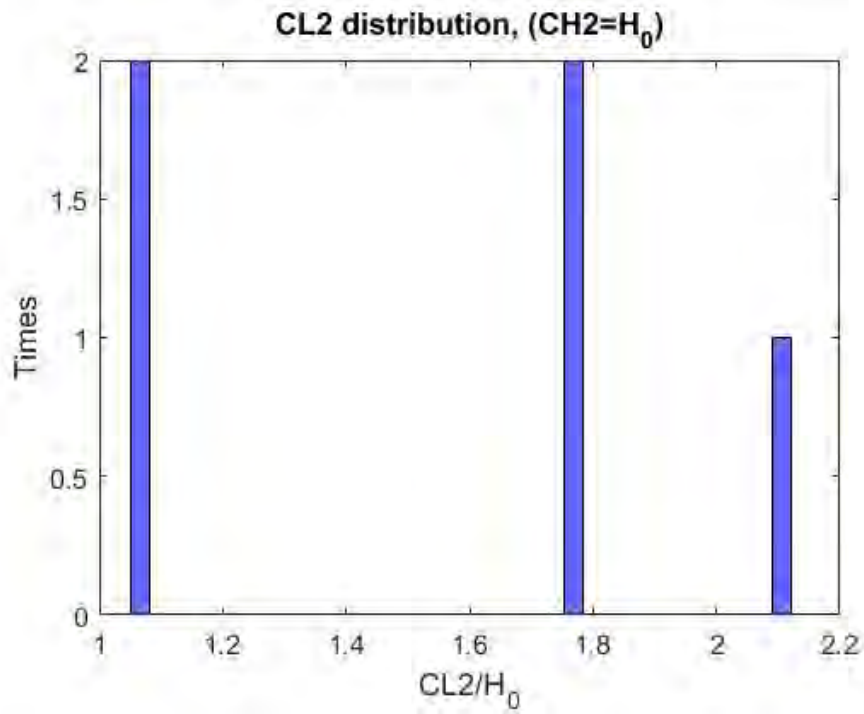

Figure 316: CL2 distribution of W4 web corrosion pattern with full height corrosion for beams with a diaphragm - MassDOT

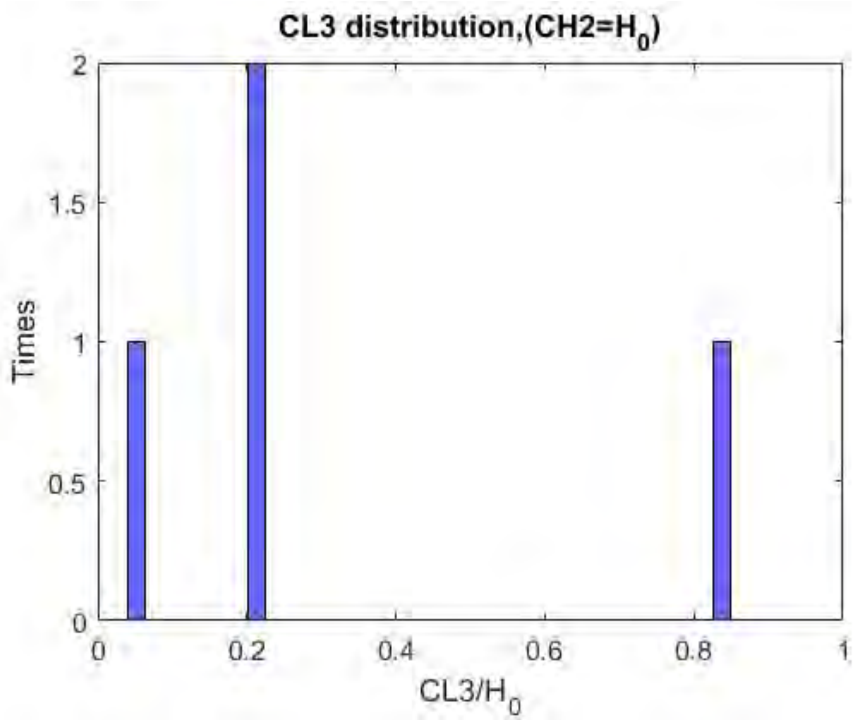

Figure 317: CL3 distribution of W4 web corrosion pattern with full height corrosion for beams with a diaphragm - MassDOT

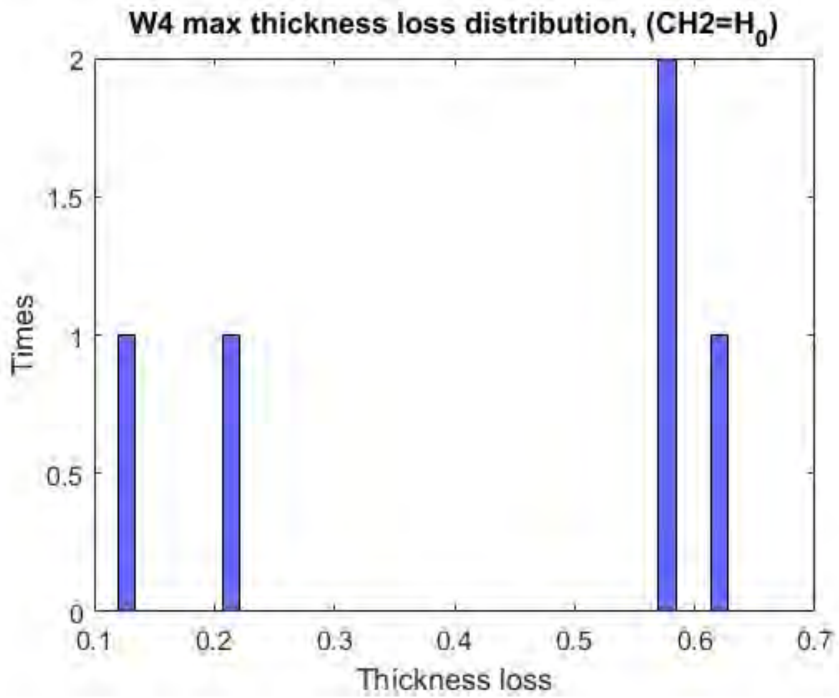

Figure 318: Max web thickness loss distribution of W4 web corrosion pattern with full height corrosion for beams with a diaphragm - MassDOT

Given that the sample of data is small:

$$0.2H_0 < CL_1 < 0.8H_0$$

$$1H_0 \leq CL_2 \leq 2.1H_0$$

$$0.2H_0 < CL_3 < 0.8H_0$$

$$0.1H_0 < CH_1 \leq 0.3H_0$$

$$\frac{t_{loss}}{t_{web}} \, takes \, values \, of \, \{0.1, 0.2, 0.6\}$$

the extreme scenario:

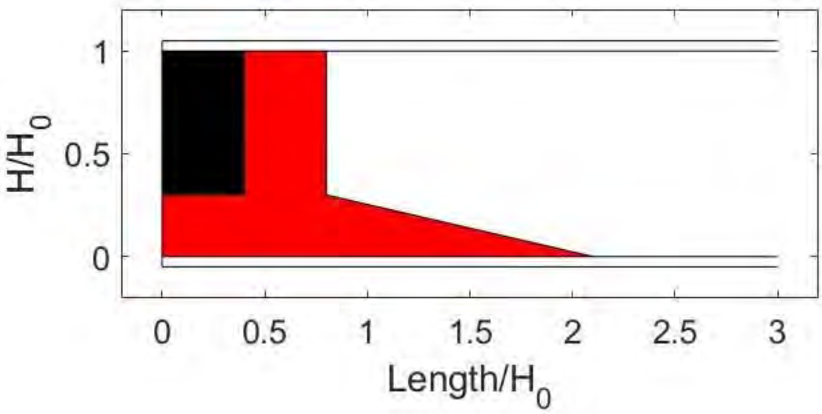

Figure 319: First extreme W4 web corrosion scenario for beams with a diaphragm - MassDOT

Even when considering the small sample, the W4 corrosion pattern with full height corrosion seems to follow the corresponding W3 corrosion pattern.

For Ch2<=0.4H

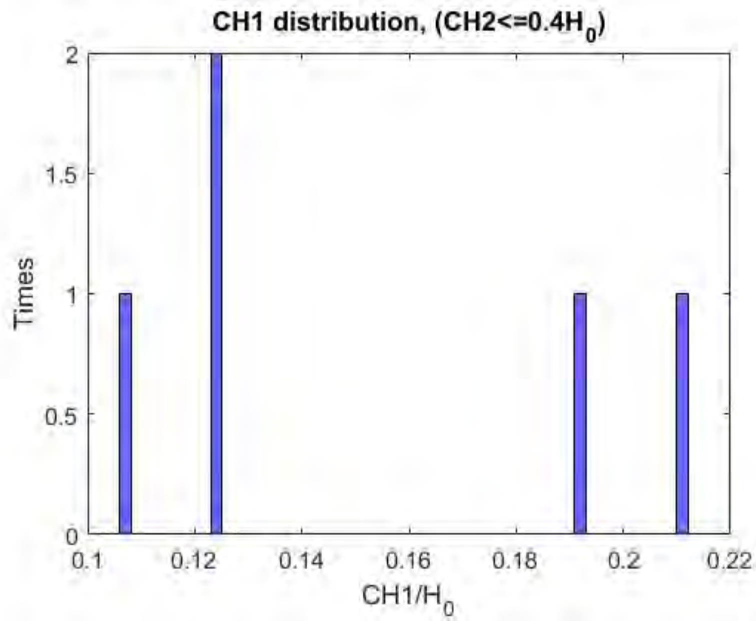

Figure 320: CH1 distribution of W4 web corrosion pattern, with corrosion height up to 40% of H_0, for beams with a diaphragm - MassDOT

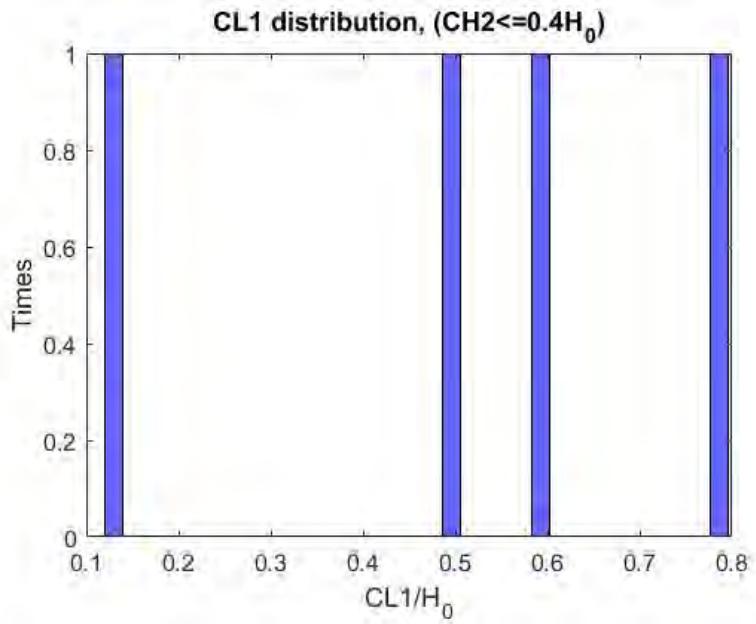

Figure 321: CL1 distribution of W4 web corrosion pattern, with corrosion height up to 40% of H_0, for beams with a diaphragm - MassDOT

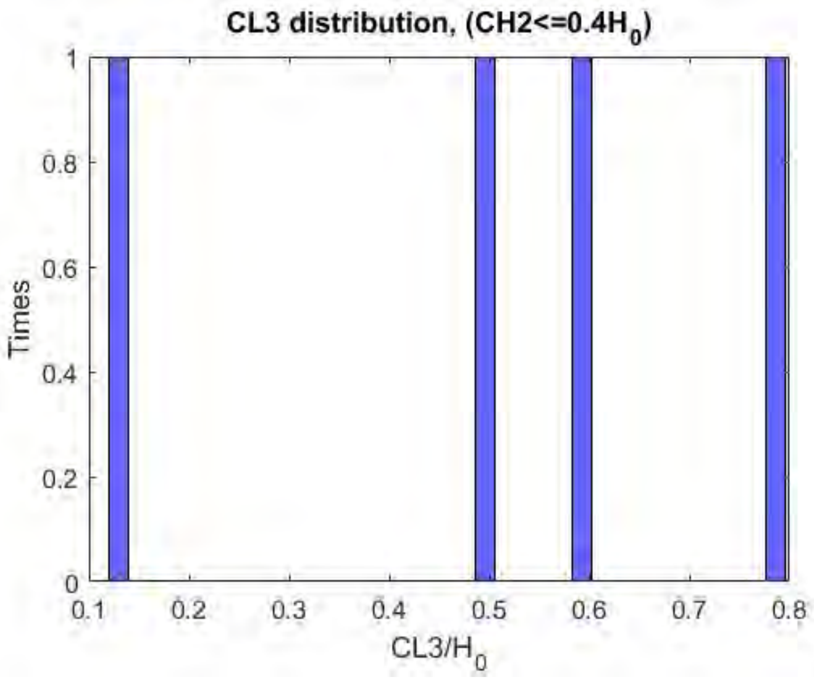

Figure 322: CL3 distribution of W4 web corrosion pattern, with corrosion height up to 40% of H_0, for beams with a diaphragm - MassDOT

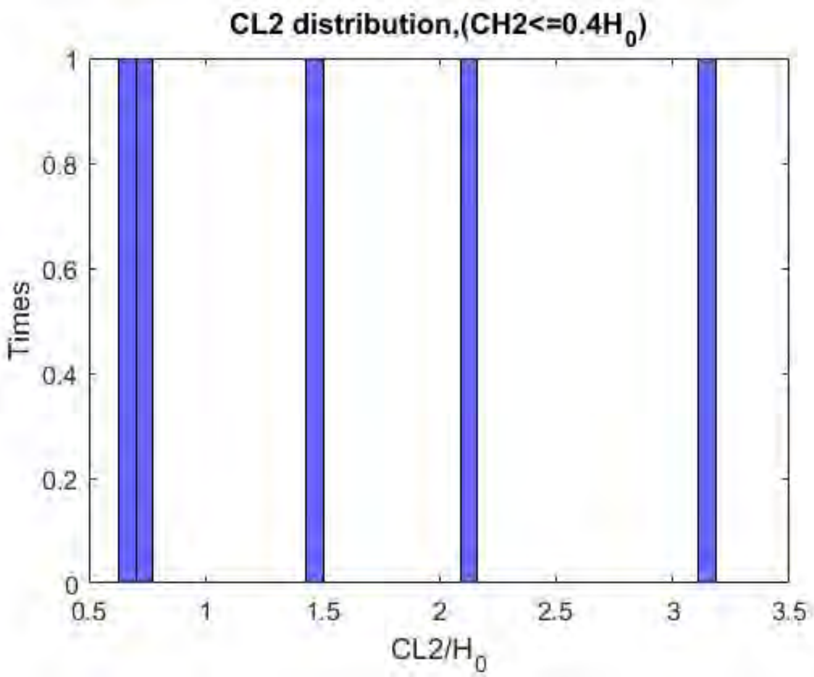

Figure 323: CL2 distribution of W4 web corrosion pattern, with corrosion height up to 40% of H_0, for beams with a diaphragm - MassDOT

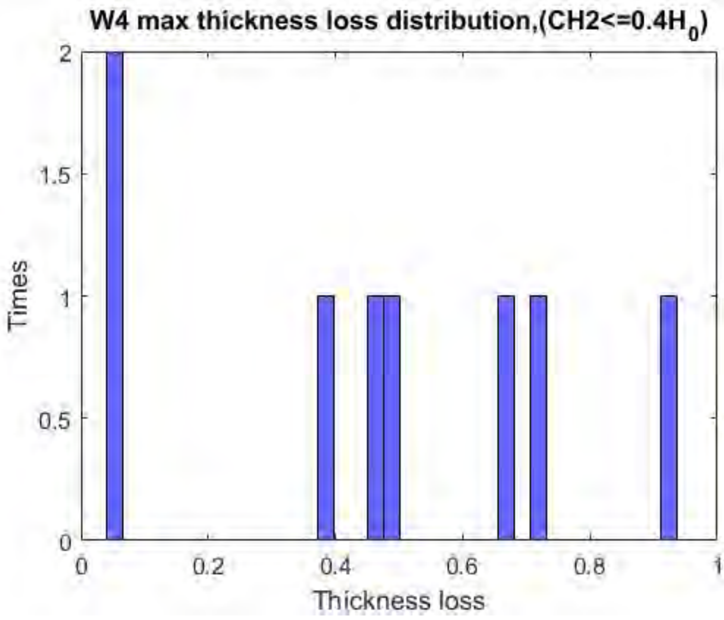

Figure 324: Max web thickness loss distribution of W4 web corrosion pattern, with corrosion height up to 40% of H_0, for beams with a diaphragm - MassDOT

$$0.1H_0 < CL_1 \leq 0.8H_0$$

$$0.6H_0 < CL_2 \leq 3.1H_0$$

$$0.1H_0 < CL_3 \leq 0.8H_0$$

$$0.1H_0 < CH_1 \leq 0.2H_0$$

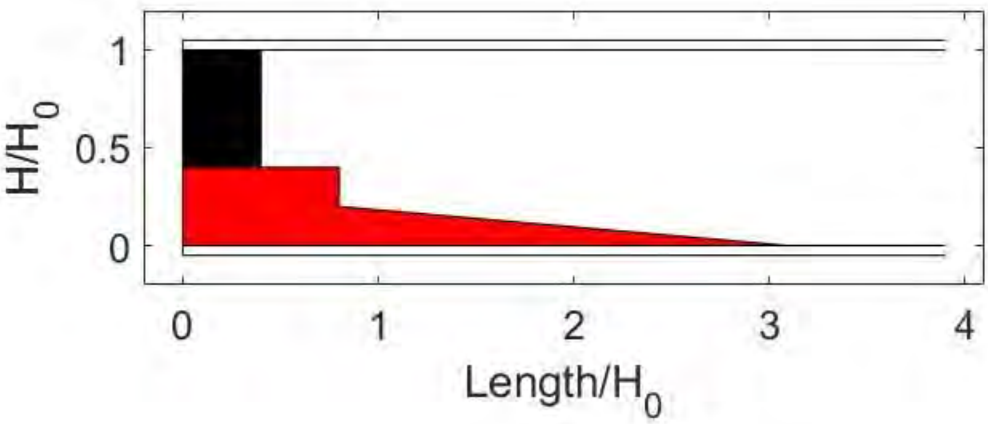

Figure 325: Second extreme W4 web corrosion scenario for beams with a diaphragm - MassDOT

Upon inspection, the W3 corrosion pattern seems to follow the corresponding W4 corrosion pattern.

5.2.5.2. Holes

The M1 corrosion hole pattern is found only once, and it presents itself as pit hole (0.0044*0.0044). The M2 hole corrosion pattern is combined with the W3 M2 pattern combination.

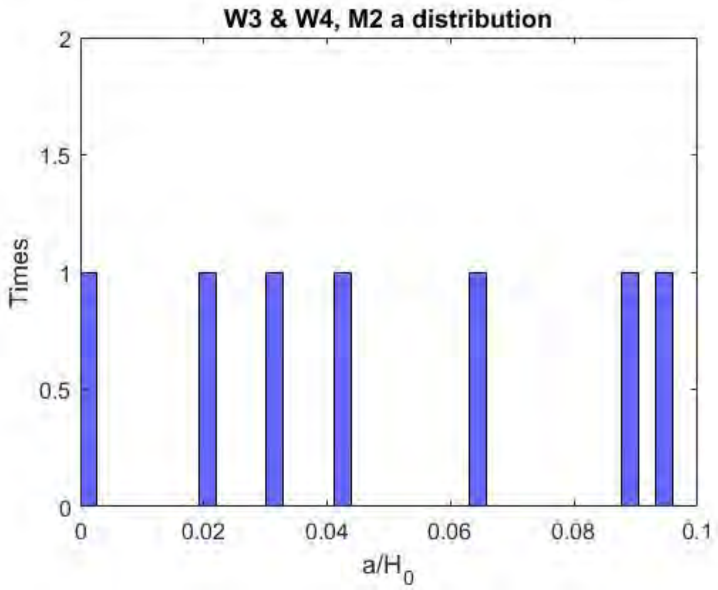

Figure 326: M2 web hole's pattern height distribution of W3 and W4 web corrosion pattern for beams with a diaphragm - MassDOT

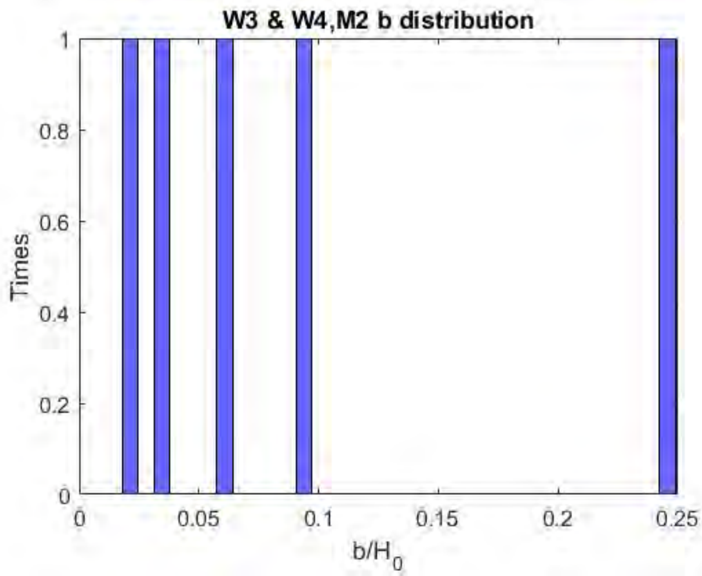

Figure 327: M2 web hole's pattern length distribution of W3 and W4 web corrosion pattern for beams with a diaphragm - MassDOT

The worst case scenario for the M2 hole corrosion pattern was projected on an extreme W4 corrosion pattern with the following parameters: a=0.1 b=0.25

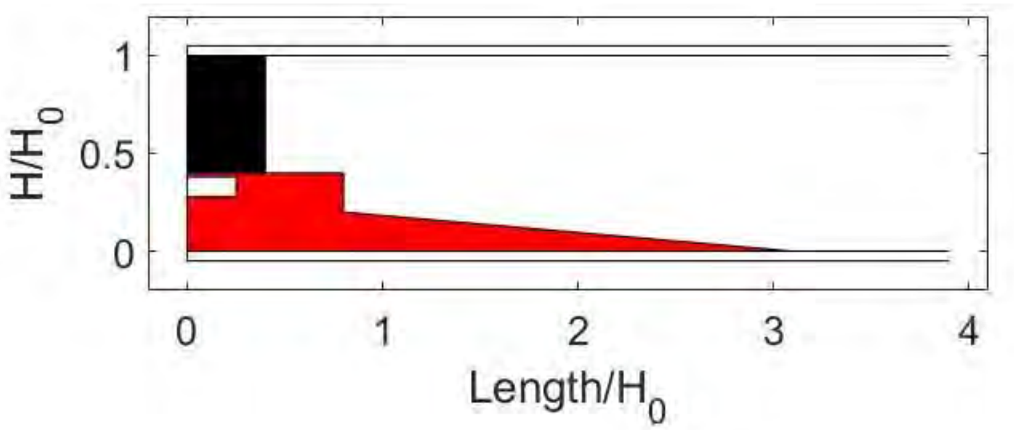

Figure 328: Extreme M2 hole pattern scenario projected on second extreme W4 web corrosion scenario for beams with a diaphragm - MassDOT

5.2.6. Pattern W5

The parameters for the corrosion patterns can be found with corresponding diagrams in Section 1.5 *Corrosion Patterns* of this report.

5.2.6.1. Web Corrosion

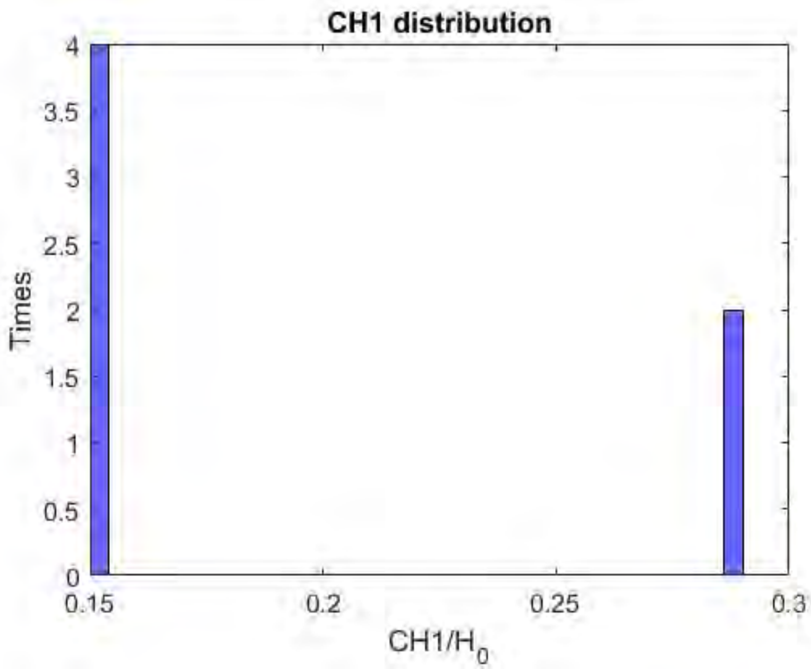

Figure 329. CH1 distribution of W5 web corrosion pattern for beams with a diaphragm - MassDOT

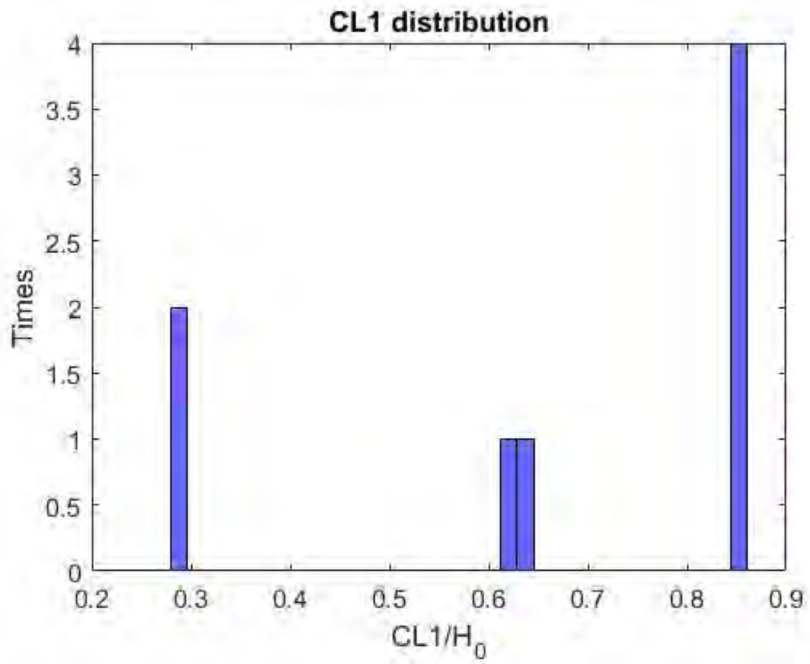

Figure 330: CL1 distribution of W4 web corrosion pattern for beams with a diaphragm - MassDOT

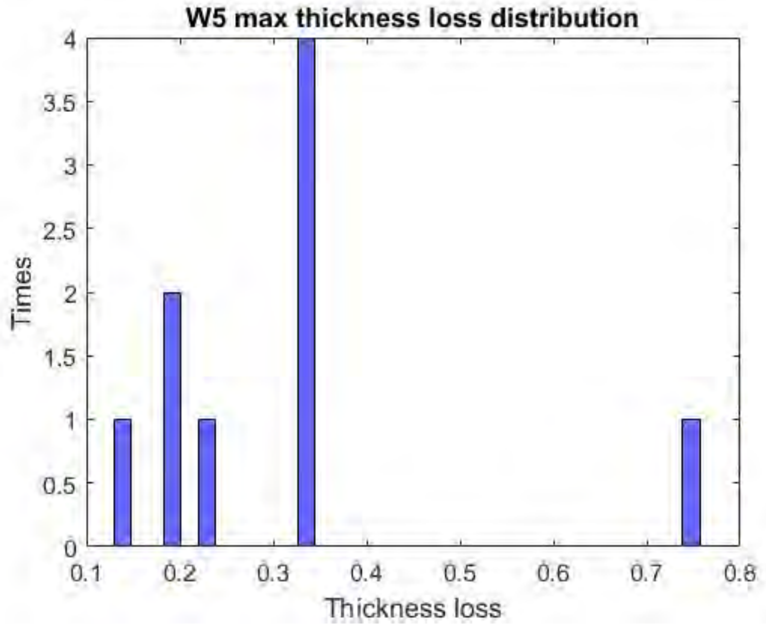

Figure 331: Max web thickness loss distribution of W5 web corrosion pattern for beams with a diaphragm - MassDOT

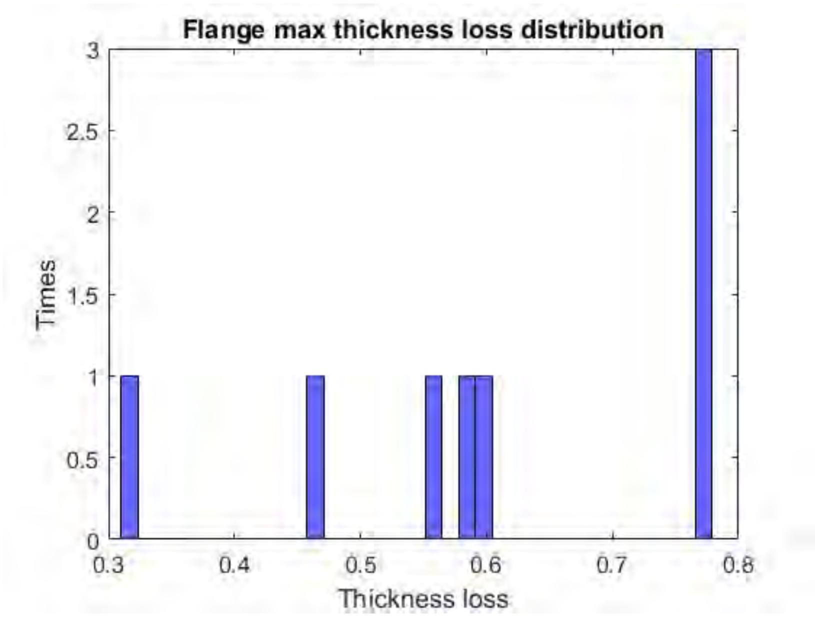

Figure 332: Max flange thickness loss of beams with W5 web corrosion pattern for beams with a diaphragm - MassDOT

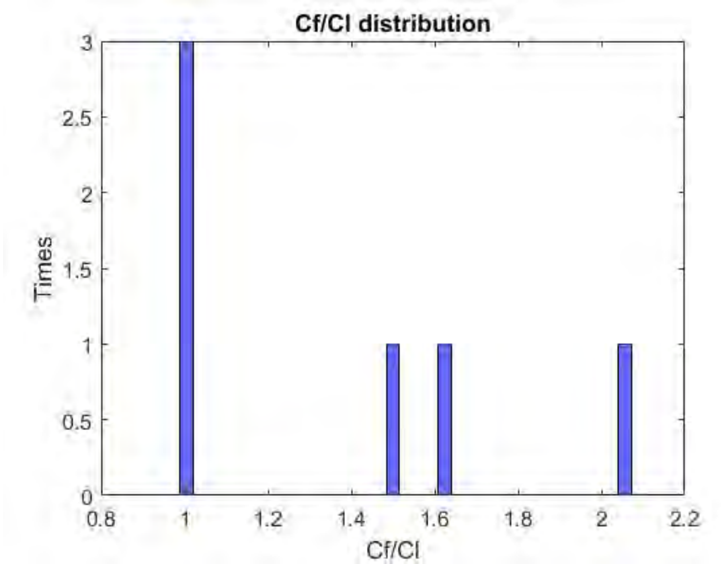

Figure 333: Ratio of flange to web corrosion length distribution, of W5 web corrosion pattern for beams with a diaphragm - MassDOT

$$0.3H_0 \leq CL_1 \leq 0.85H_0$$

$$0.15H_0 < CH_1 \leq 0.30H_0$$

$$\frac{t_{loss}}{t_{web}} \, takes \, the \, value \, of \, \{0.35\}$$

$\frac{t_{loss}}{t_{flange}}$ $takes\ the\ values\ of$ $\{0.3,0.6,0.8\}$ with $\frac{C_f}{C_l}$ $taking\ the\ values\ of$ $\{1,1.6\}$

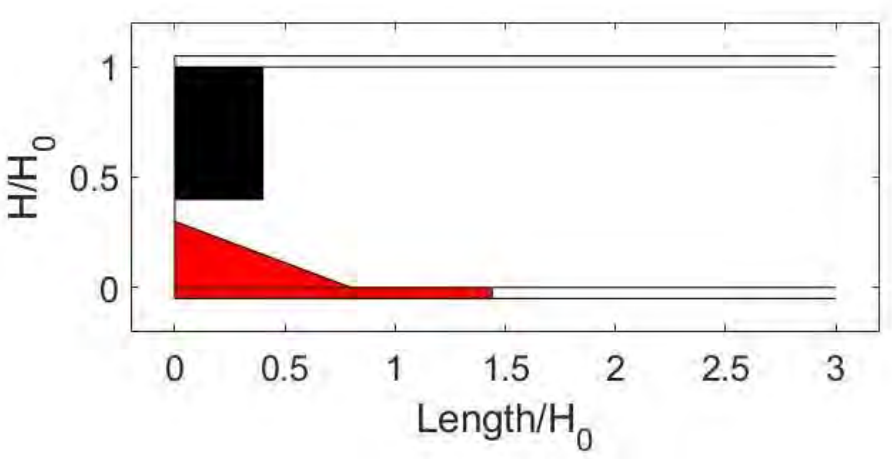

Figure 334: Extreme W5 web corrosion scenario for beams with a diaphragm - MassDOT

5.3.Rhode Island

5.3.1. Introduction

As discussed in the previous sections, the data was divided into two groups: (i) beams without diaphragm and (ii) beams with diaphragm. Additionally, due to significantly differences in the amount of data provided by each state, the results are also divided into groupings by state. Therefore, in this section only beam ends with diaphragms from Rhode Island are considered.

Figure 335 depicts the frequency of corrosion patterns for beam ends with a diaphragm system from Rhode Island. This also means that the graph denotes the total amount of times each pattern appears in the reports.

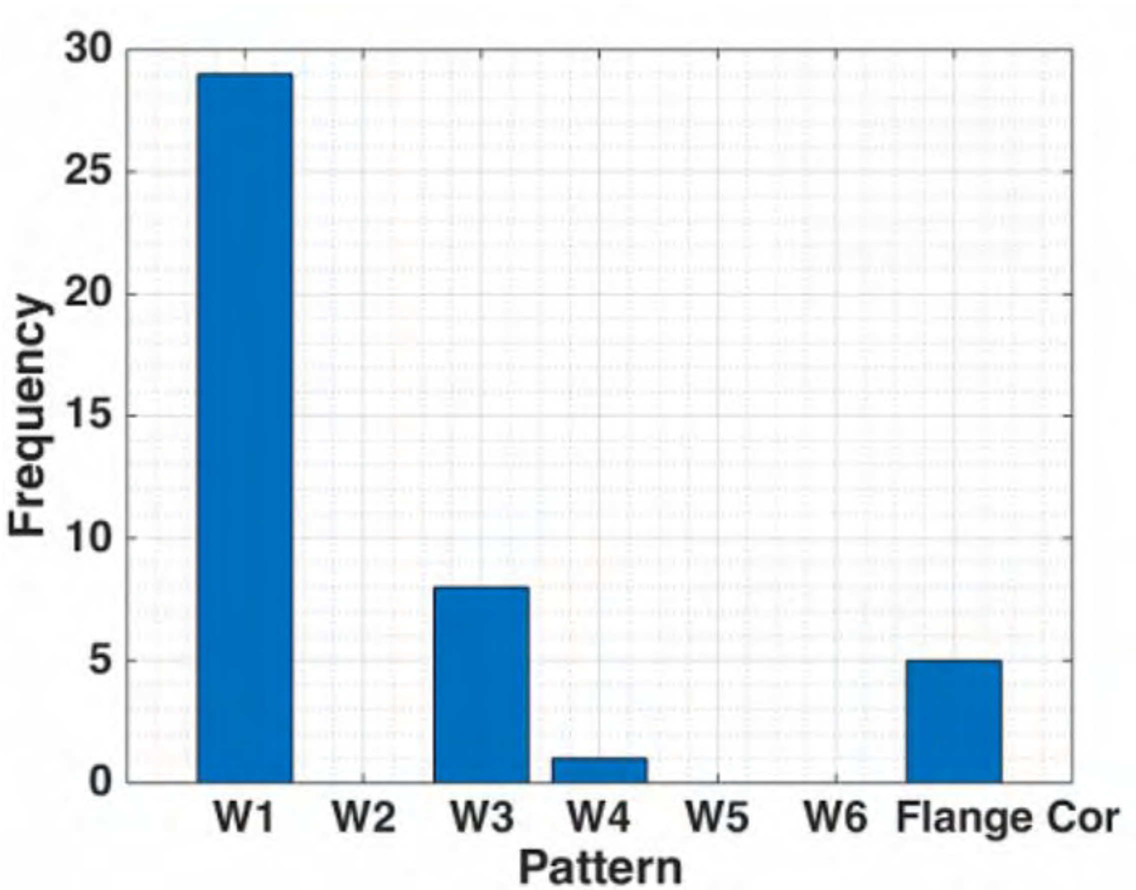

Figure 335: Web corrosion patterns distribution for beams ends with a diaphragm – RIDOT

It is imperative to note that the parameters defined for each corrosion pattern (CH1, CH2, CH3, CL1, CL2, CL3) have been normalized by the web height, H0, defined as H0=H-2tf.

5.3.2. Pattern W1

5.3.2.1. Web corrosion

Similar to the beams without a diaphragm system, the study of trends in the data began with the analysis for the distribution of the total height of corrosion. The parameters for the corrosion patterns can be found with corresponding diagrams in Section 1.5 *Corrosion Patterns* of this report. This resulted in the data presented in Figure 336, which depicts the histogram of CH1 combined with pattern W1. This was obtained from the bridge inspection reports provided by RIDOT.

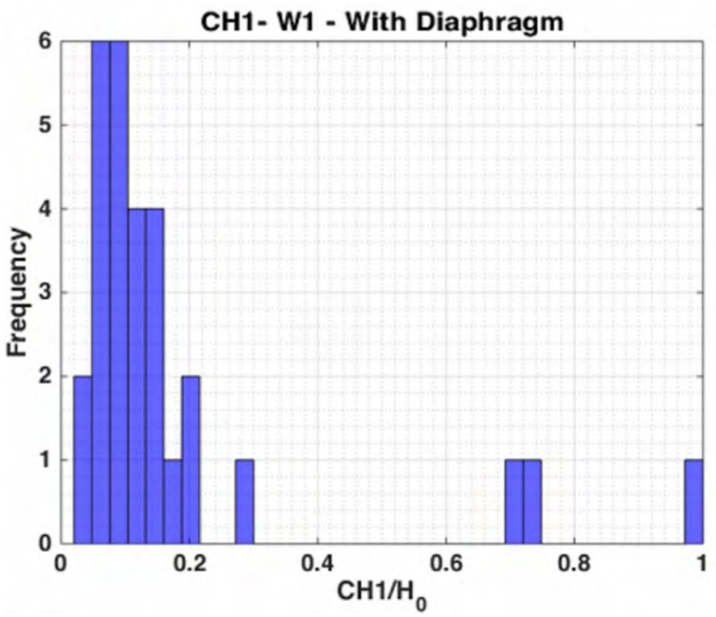

Figure 336: CH1 distribution for beams with diaphragm and W1 corrosion pattern – RIDOT

Figure 336 clearly depicts that $0 < CH_1 \leq 0.2H_0$. With the goal of understanding the relationship between the other parameters of corrosion and the corrosion height, our team had to analyze the behavior of the other parameters given that CH1<0.2H0. Figure 337 and Figure 338 depict the length of corrosion and the web thickness loss for this case.

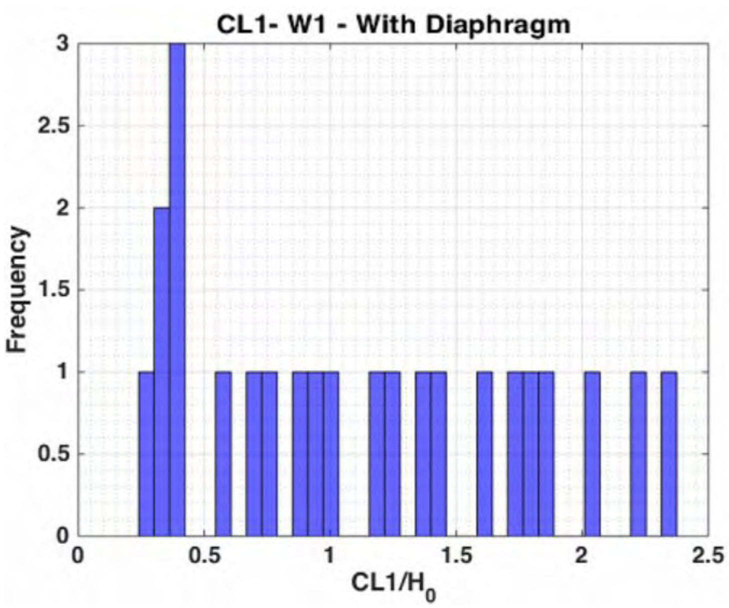

Figure 337: CL1 distribution for beams with diaphragm and W1 corrosion pattern – RIDOT

Although no clear trend is observed from Figure 337, the graph lead our team to state that the length can span 0.25H0 up to 2.5H0. That is, $0.25H_0 \leq CL_1 \leq 2.5H_0$.

Figure 338 depicts the distribution of web thickness loss given that CH1<0.2H0.

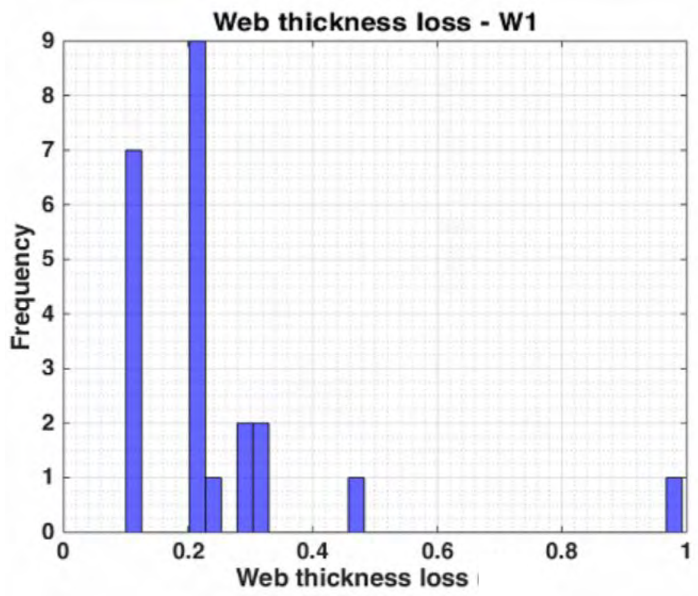

Figure 338: Web thickness loss distribution for beams with diaphragm and W1 corrosion pattern – RIDOT

From Figure 338, our team assumed that most of the beams have web thickness loss found in the following interval:

$$0.1 \leq \frac{t_{loss}}{t_{web}} \leq 0.3$$

Therefore, it is possible to define an extreme case of corrosion for beam ends with a diaphragm system, as depicted in Figure 339.

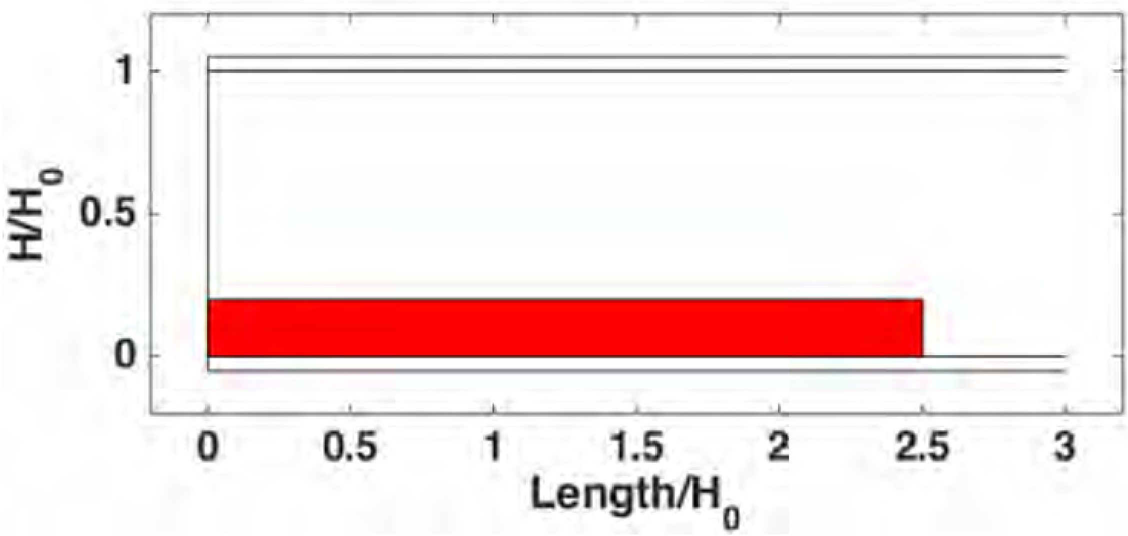

Figure 339: Extreme corrosion case of W1 pattern for beams with a diaphragm – RIDOT

Figure 340 describes the comparison between the extreme corrosion case pattern for the W1 corrosion pattern of beam ends with and without a diaphragm system.

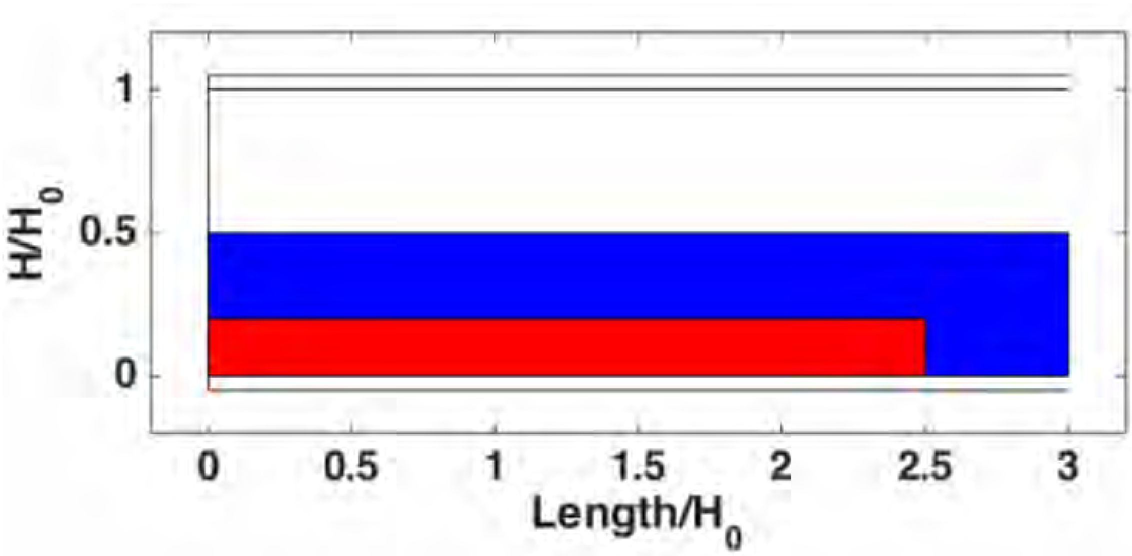

Figure 340: Comparison between extreme corrosion scenarios. Blue represents the extreme scenario for beams without diaphragm, whereas the region in red depicts extreme corrosion scenario for beams with a diaphragm – RIDOT

5.3.2.2. Flange corrosion

Only three cases of flange corrosion were recorded combined with W1 corrosion pattern for beam ends with a diaphragm system. As the amount of data was not sufficient for the research team to draw conclusions, Figure 341, Figure 342, Figure 343 depict only the statistics the research team was able to record from the bridge inspection reports.

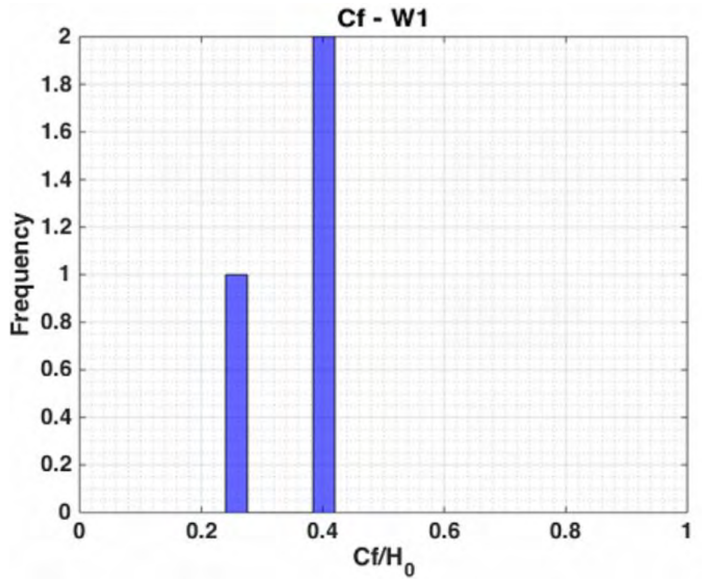

Figure 341: Flange corrosion length for beam ends with diaphragm for W1 pattern – RIDOT

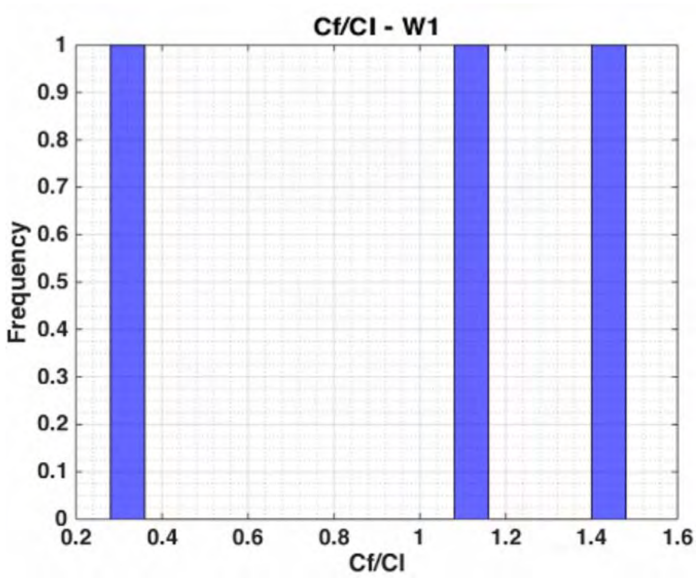

Figure 342: Ratio between flange corrosion length and web corrosion length for W1 pattern – RIDOT

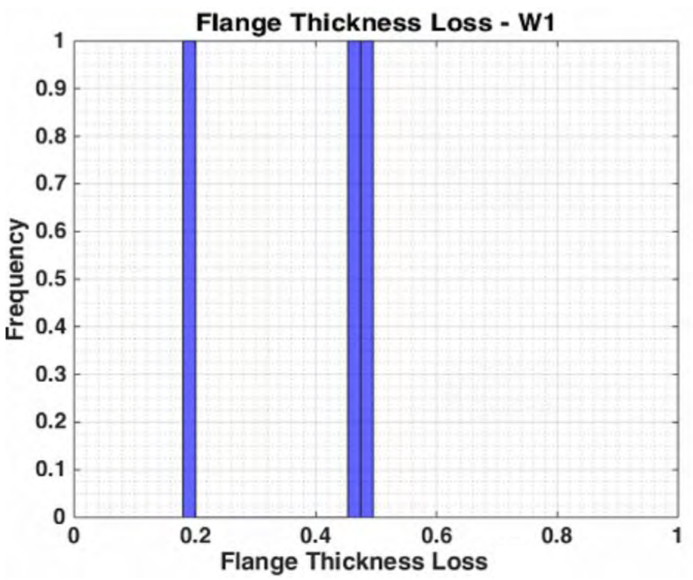

Figure 343: Flange thickness loss distribution for W1 pattern – RIDOT

5.3.2.3. Holes

Table 56 portrays the frequency of corrosion patterns and holes recorded from the bridge inspection reports provided by RIDOT.

Table 56: Holes and patterns for beams ends with diaphragm from RIDOT

	Number	No Hole	M1	M2	M3	M4	M1 and M2	M1 and M3	M2 and M4
W1	29	27	2	0	1	0	0	0	0
W2	0	0	0	0	0	0	0	0	0
W3	8	7	0	0	0	1	0	0	0
W4	1	1	0	0	0	0	0	0	0
W5	0	0	0	0	0	0	0	0	0
W6	0	0	0	0	0	0	0	0	0

As showed in Table 56, just three holes were recorded combined with the W1 corrosion pattern. Due to the small amount of available data, it was not possible to detect any trends. For this reason, Figure 344 and Figure 345 depict the dimensions of the M1 corrosion holes. Figure 346 and Figure 347 depict the dimensions of the M3 corrosion hole.

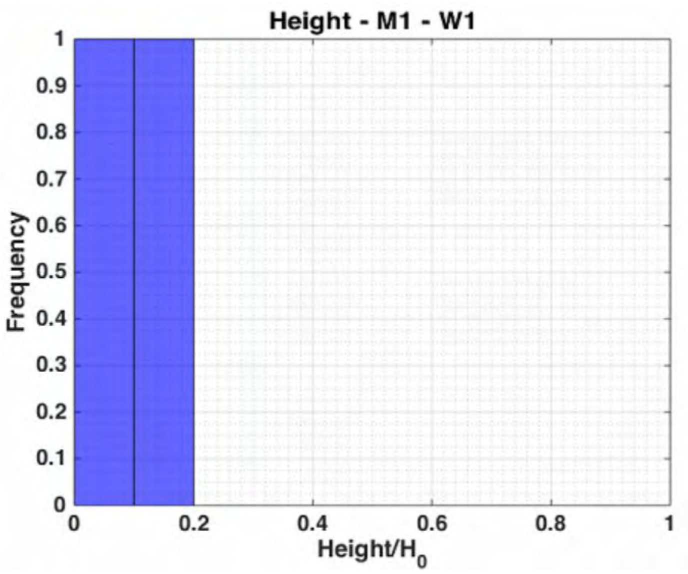

Figure 344: Height of M1 holes combined with W1 pattern – RIDOT

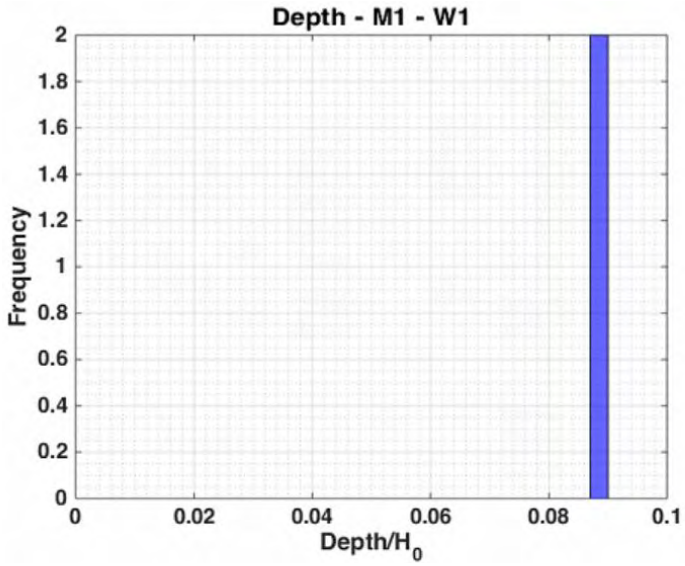

Figure 345: Depth of M1 holes combined with W1 pattern – RIDOT

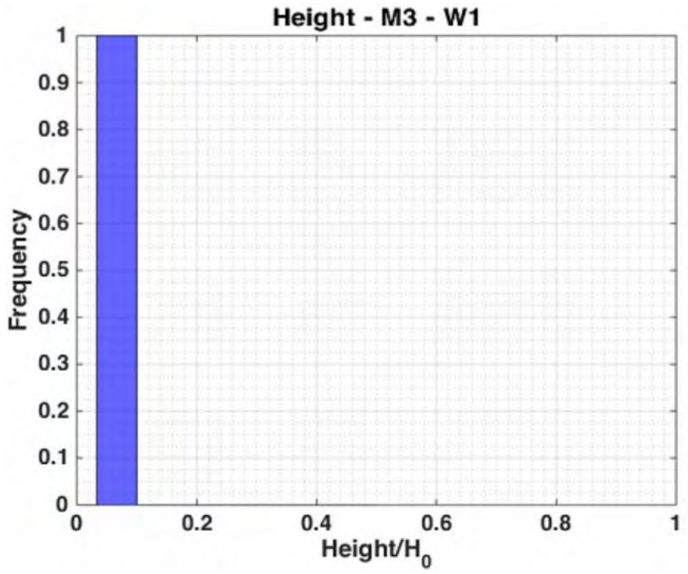

Figure 346: Height of M3 holes combined with W1 pattern – RIDOT

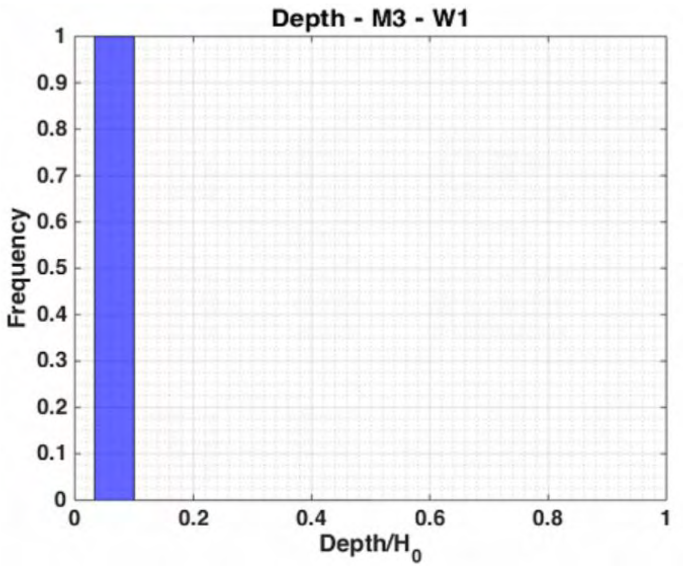

Figure 347: Depth of M3 holes combined with W1 pattern – RIDOT

5.3.3. Pattern W3

5.3.3.1. Web corrosion

Only eight cases of the W3 corrosion pattern were recorded by the research team. The parameters for the corrosion patterns can be found with corresponding diagrams in Section 1.5 *Corrosion Patterns* of this report. Similar to the other cases, the study began by analyzing the distribution of the total height of corrosion, depicted in Figure 348.

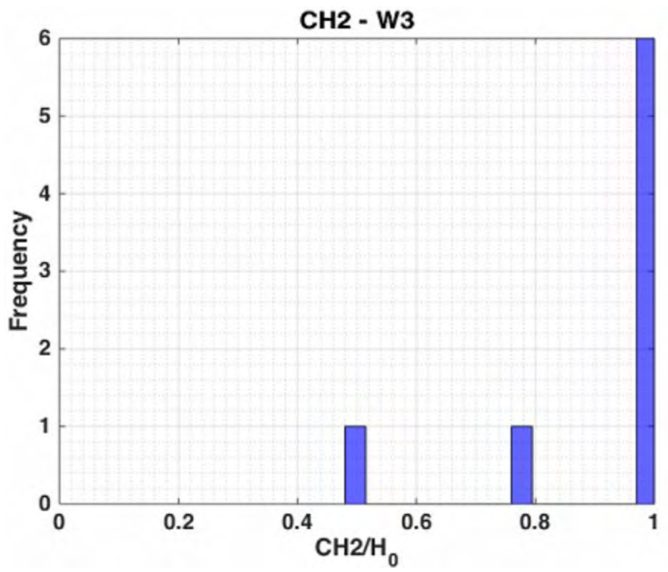

Figure 348: CH2 distribution for W3 pattern – RIDOT

Although Figure 348 clearly depicts that most of the beam ends have the height fully corroded, it was not possible to detect other major trends. The reason for that can be found in Figure 349, Figure 350, Figure 351, Figure 352 and Figure 353. These figures depict scatter among the histograms of the corrosion shape parameters. This limited our team in being able to detect trends in the corrosion data.

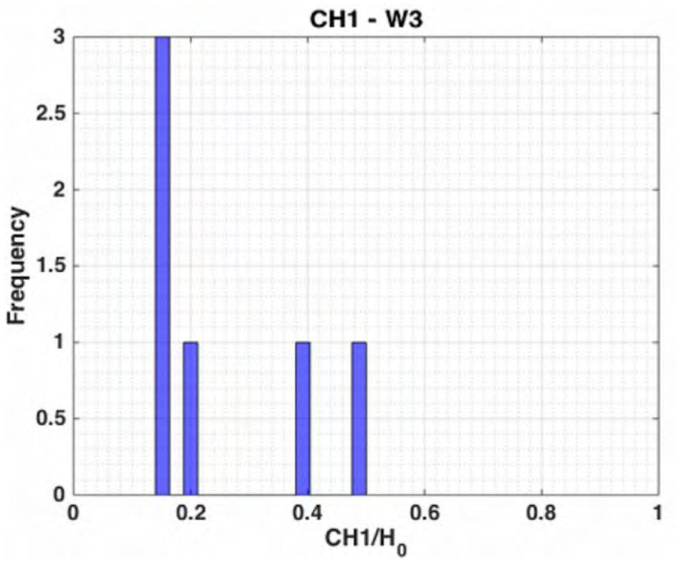

Figure 349: CH1 distribution for W3 pattern – RIDOT

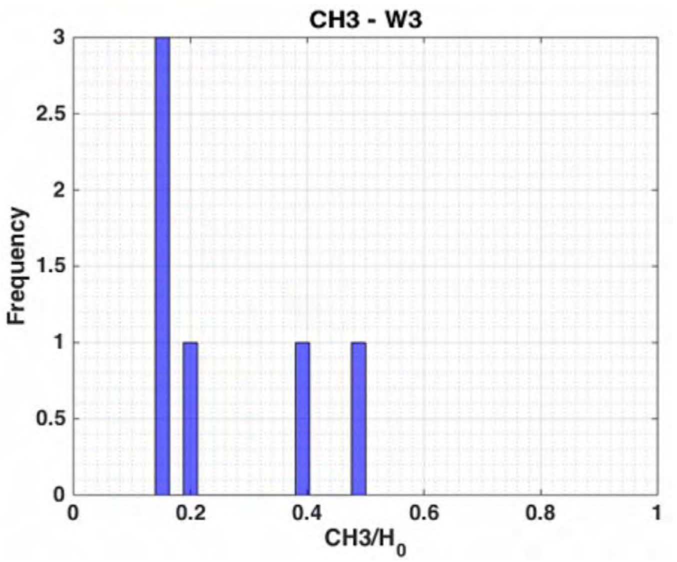

Figure 350: CH3 distribution for W3 pattern – RIDOT

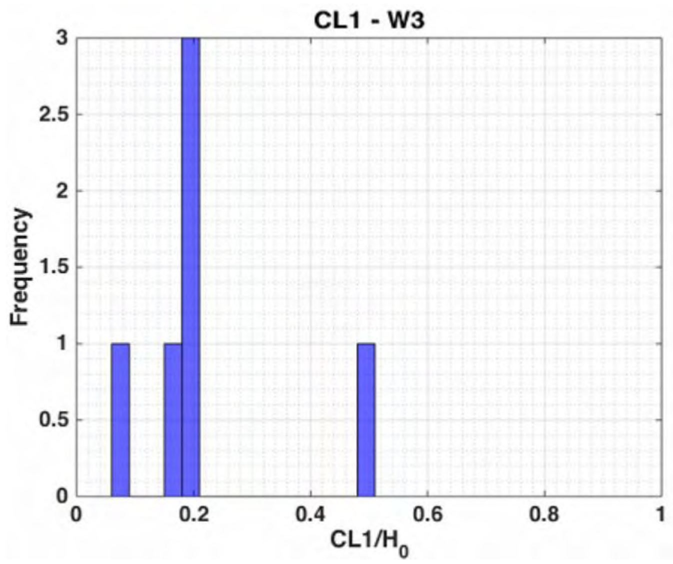

Figure 351: CL1 distribution for W3 pattern – RIDOT

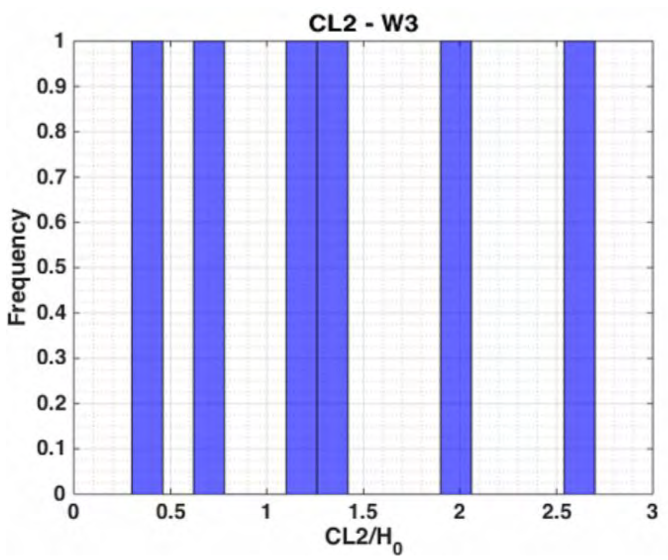

Figure 352: CL2 distribution for W3 pattern – RIDOT

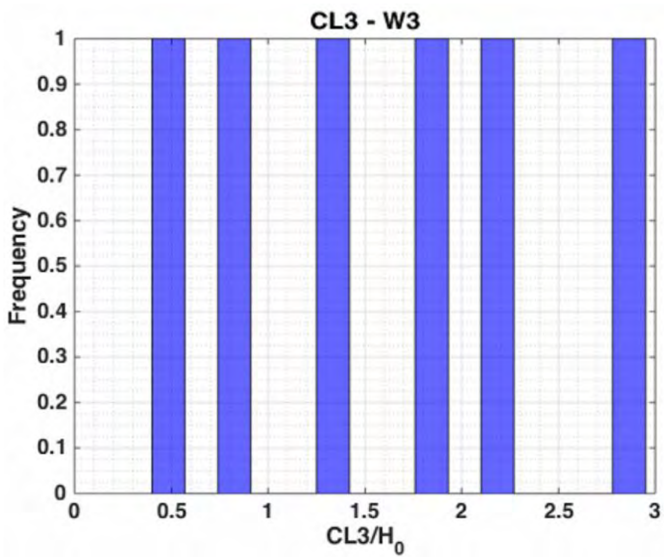

Figure 353: CL3 distribution for W3 pattern – RIDOT

Figure 354 depicts the web thickness loss for beams whose CH2=1H0.

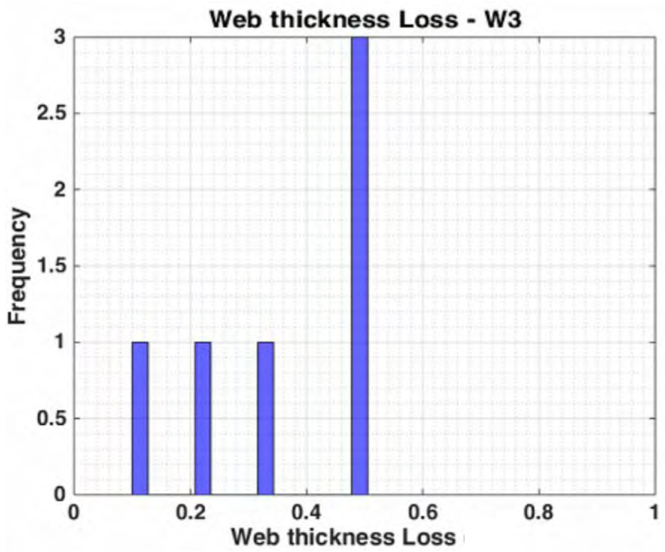

Figure 354: Web thickness loss distribution for W3 pattern – RIDOT

5.3.3.2. Flange corrosion

The research team was able to record information regarding the combination of flange corrosion and the W3 corrosion pattern for two cases. This meant that, due to the small amount of data available, the research team was not able to detect any trend in the data. Figure 355, Figure 356 and Figure 357 depict the statistics the research team was able to obtain from the compiled data.

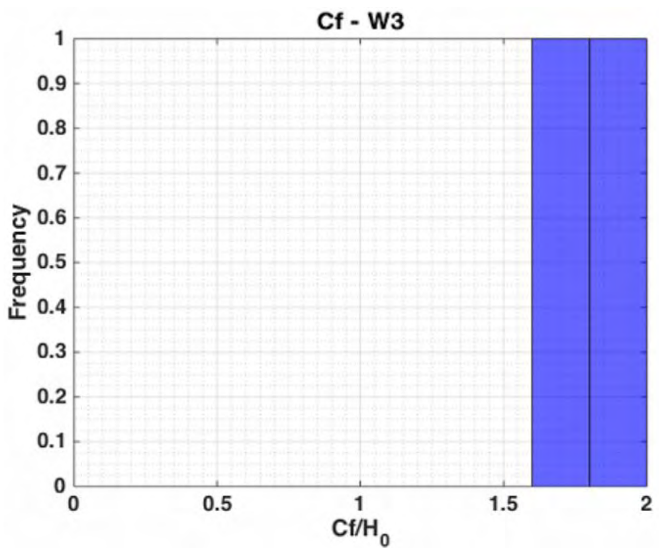

Figure 355: Flange corrosion length for W3 pattern – RIDOT

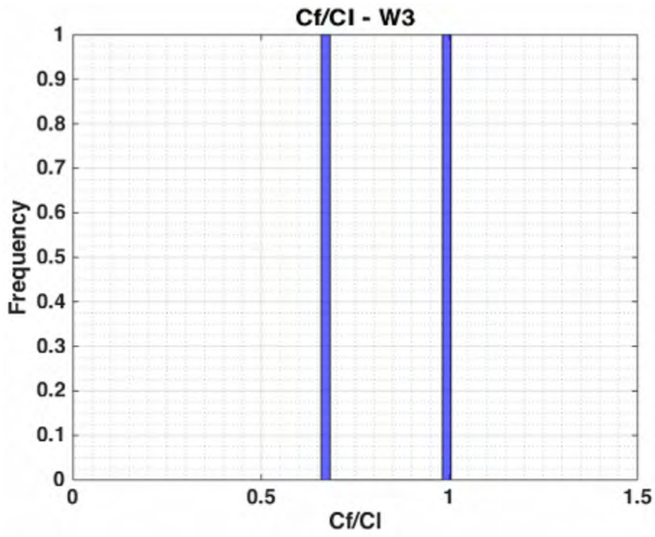

Figure 356: Ratio between flange corrosion length and web corrosion length for W3 pattern – RIDOT

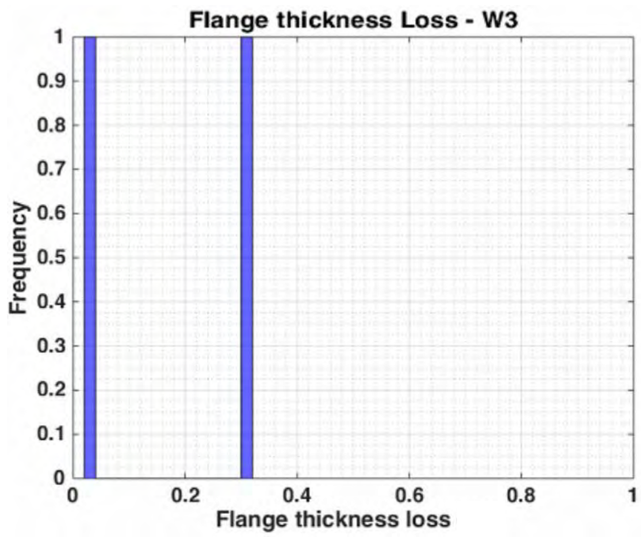

Figure 357: Flange thickness loss distribution for W3 pattern – RIDOT

5.3.3.3. Holes

Only a single hole was recorded combined with the W3 corrosion pattern, as shown in Table 56. This one hole does not constitute enough data for depicting trends. For this reason, the research team was not able to draw any conclusion. Finally, Table 57 shows the dimensions of the M4 corrosion hole normalized by H0.

Table 57: Dimensions of M4 hole combined with W3 pattern – RIDOT

Hole topology	Length	Deep	Distance from the end of the beam
M4	6%	3%	42%

6. References

1. "Bridges." *ASCE's 2017 Infrastructure Report Card*, American Society of Civil Engineers, 2020, www.infrastructurereportcard.org/cat-item/bridges/. Accessed May 5, 2021.
2. Sugimoto, I., Kobayashi, Y., Ichikawa, A. (2006). Durability evaluation based on buckling characteristics of corroded steel deck girders. *QR of RTPI*, 47(3).

3. Roberts, T.M. (1981). Slender plate girders subjected to edge loading. *Proceedings of the Institution of Civil Engineers Part B*, 71:805-819.

4. Johansson, B., Lagerqvist, O. (1995). Resistance of plate edges to concentrated forces. *Journal of Constructional Steel Research, 32:69-105.*

5. Roberts, T.M., Shahabian, F. (2001). Ultimate resistance of slender web panels to combined bending shear and patch loading. *Journal of Constructional Steel Research*, 57:779-790.

6. Chacón, R., Mirambell, E., Real, E. (2009). Influence of designer-assumed initial conditions on the numerical modelling of steel plate girders subjected to patch loading, *Thin-Walled Structures,* 47: 391-402.

7. Hajdin, N., Markovic, N. (2012). Failure mechanism for longitudinally stiffed I girders subjected to patch loading. *Archive of Applied Mechanics,* 82:1377-1391.

8. Salkar, R., Salkar, A., Davids W. (2015). Crippling of webs with partial-depth stiffeners under patch loading. *Engineering Journal,* 221-231.

9. Kayser, J.R., Nowak, A.S. (1989). Capacity loss due to corrosion in steel-girder bridges. *Journal of Structural Engineering,* 115(6):1525-1537.

10. van de Lindt, J.W., Pei, S. (2006). Buckling reliability of deteriorating steel beam ends. *Electronic Journal of Structural Engineering,* 6.

11. Liu, C., Miyashita, T., Nagai, M. (2011). Analytical study on shear capacity of steel I-girders with local corrosion nearby supports. *Procedia Engineering, 14:2276-2284.*

12. Ahn, J.H., Kainuma, S., Kim, I.T. (2013). Shear failure behaviors of a web panel with local corrosion depending on web boundary conditions. *Thin-Walled Structures, 73:302-317.*

13. Ahn, J.H., Kainuma, S., Yasuo, F., Takehiro, I. (2013). Repair method and residual bearing strength evaluation of a locally corroded plate girder at support. *Engineering Failure Analysis,* 33:398-418.

14. Ahn, J.H., Kim, I.T., Kainuma, S., Lee, M.J. (2013). Residual shear strength of steel plate girder due to web local corrosion. *Journal of Constructional Steel Research,* 89:198-212.

15. Kim, I.T., Lee, M.J., Ahn, J.H., Kainuma, S. (2013). Experimental evaluation of shear buckling behaviors and strength of locally corroded web. *Journal of Constructional Steel Research,* 83:75-89.

16. Usukura, M., Yamaguchi, T., Suzuki, Y., Mitsugi, Y. (2013). Strength evaluation for a corroded damaged steel girder end considering its collapse mechanism. *Proceedings of*

the 13th East Asia-Pacific Conference on Structural Engineering and Construction (EASEC), Sapporo, Japan.

17. Yamaguchi, T., Akagi., T. (2013). Degradation of load-carrying capacity of steel I-girders and due to corrosion. *Proceedings of the 13th East Asia-Pacific Conference on Structural Engineering and Construction (EASEC),* Sapporo, Japan.

18. Khurram, N., Sasaki, E., Katsuchi., H., Yamada, H. (2014). Experimental and numerical evaluation of bearing capacity of steel plate girder affected by end panel corrosion. *International Journal of Steel Structures*, 14(3):659-676.

19. Gheitasi, A., Harris, D. (2015). Redundancy and operational safety of composite stringer bridges with deteriorated girders. *Journal of Performance of Constructed Facilities.*

20. Miyashita, T., Nagai, M., Wakabayashi, D., Hidekuma, Y., Kobayashi, A., Okuyama, Y., Koide, N., Horimoto, W. (2015). Repair method for corroded steel girder ends using CFRP sheet. *IABSE-JSCE Joint Conference on Advances in Bridge Engineering-III*, Dhaka, Bangladesh.

21. Ogami, H., Fujii, K., Yamada, T., Iwasaki H. (2015). Renovation of corroded girder end in plate girder bridge with resin and rebars. *Implementing Innovative Ideas in Structural Engineering and Project Management.*

22. Zmetra, K.M., McMullen, K.F., Zaghi, A.E., Wille, K. (2017). Experimental study of UHPC repair for corrosion-damaged steel girder ends. *Journal of Bridge Engineering,* 22(8).

23. McGovern, J. B., Randall, E.A. Connecticut Department of Transportation: Bridge Inspection Manual, 2001, https://portal.ct.gov/-/media/DOT/documents/dpublications/inspection_manual_2019-11-15rev.pdf. Accessed March 15, 2021.
24. FHWA, U. (1995). Recording and coding guide for the structure inventory and appraisal of the nation's bridges. *Recording and coding guide for the structure inventory and appraisal of the nation's bridges. US Department of Transportation, Bridge Management Branch, FHWA, Washington, DC.*
25. NHDOT Bridge Inspection Manual, 2017, https://www.nh.gov/dot/org/projectdevelopment/bridgedesign/documents/NHDOTBridgeInspectionManual.pdf. Accessed March 30, 2021
26. RIDOT Bridge Inspection Manual, 2013, http://www.dot.ri.gov/documents/doingbusiness/RIDOT_Bridge_Inspection_Manual.pdf. Accessed March 30,2021
27. VTRans Inspection Manual, 1997, http://vtransmaps.vermont.gov/Maps/Publications/Maps/Inventory/BC_inspection/VTransInspectionManual.pdf. Accessed March 30,2021
28. Tzortzinis, Georgios, et al. Massachusetts Department of Transportation Office of Transportation Planning, 2019, *Development of Load Rating Procedures for Deteriorated Steel Beam Ends*, www.mass.gov/files/documents/2019/11/13/BeamEndsFinalReportOct_2019.pdf. Accessed May 7, 2021.